

ADVENTURES IN HETEROtic STRING PHENOMENOLOGY

DISSERTATION

Presented in Partial Fulfillment of the Requirements for the Degree Doctor of
Philosophy in the Graduate School of The Ohio State University

By

George Benjamin Dundee, B.S., M.S.

Graduate Program in Physics

The Ohio State University

2010

Dissertation Committee:

Stuart A. Raby, Advisor

Samir D. Mathur

John F. Beacom

Richard Kass

© Copyright by
George Benjamin Dundee
2010

ABSTRACT

In this Dissertation, we consider three topics in the study of effective field theories derived from orbifold compactifications of the heterotic string.

In Chapter 2 we provide a primer for those interested in building models based on orbifold compactifications of the heterotic string.

In Chapter 3, we analyze gauge coupling unification in the context of heterotic strings on anisotropic orbifolds. This construction is very much analogous to effective five dimensional orbifold GUT field theories. Our analysis assumes three fundamental scales, the string scale, M_S , a compactification scale, M_C , and a mass scale for some of the vector-like exotics, M_{EX} ; the other exotics are assumed to get mass at M_S . In the particular models analyzed, we show that gauge coupling unification is not possible with $M_{EX} = M_C$ and in fact we require $M_{EX} \ll M_C \sim 3 \times 10^{16}$ GeV. We find that about 10% of the parameter space has a proton lifetime (from dimension six gauge exchange) 10^{33} yr $\lesssim \tau(p \rightarrow \pi^0 e^+) \lesssim 10^{36}$ yr, which is potentially observable by the next generation of proton decay experiments. 80% of the parameter space gives proton lifetimes below Super-K bounds.

In Chapter 4, we examine the relationship between the string coupling constant, g_{STRING} , and the grand unified gauge coupling constant, α_{GUT} , in the models of Chapter 3. We find that the requirement that the theory be perturbative provides a non-trivial constraint on these models. Interestingly, there is a correlation between the proton decay rate (due to dimension six operators) and the string coupling constant in this class of models. Finally, we make some comments concerning the extension of these models to the six (and higher) dimensional case.

In Chapter 5, we discuss the issues of supersymmetry breaking and moduli stabilization within the context of $E_8 \otimes E_8$ heterotic orbifold constructions and, in particular, we focus on the class of “mini-landscape” models. These theories contain a non-Abelian hidden gauge sector which generates a non-perturbative superpotential leading to supersymmetry breaking and moduli stabilization. We demonstrate this effect in a simple model which contains many of the features of the more general construction. In addition, we argue that

once supersymmetry is broken in a restricted sector of the theory, then all moduli are stabilized by supergravity effects. Finally, we obtain the low energy superparticle spectrum resulting from this simple model.

Let him who seeks not cease seeking until he finds; and when he finds he shall be troubled; and having been troubled he shall marvel.

The Gospel of Thomas

I do not know what I may appear to the world; but to myself I seem to have been only like a boy playing on the seashore, and diverting myself in now and then finding a smoother pebble or a prettier shell than ordinary, whilst the great ocean of truth lay all undiscovered before me.

Isaac Newton

ACKNOWLEDGMENTS

Whatever successes I have had in life are due, in no small part, to those around me. The first acknowledgment is ostensibly reserved for one’s advisor, and I can not recognize mine enough. I am eternally grateful to Stuart Raby for his patience in passing on his expertise—I will hold his advice closely: “Don’t talk, just think!”. Other faculty at Ohio State have been instrumental in my development as well: I would like to specifically thank John Beacom (for teaching me how to read papers), and Samir Mathur (for teaching me to break difficult concepts down to their rudiments), who have helped me develop insight at two very opposite ends of physics. And I must also acknowledge my former advisor, Gerald Cleaver, for his support and encouragement when I decided to leave Baylor with a Master’s degree.

I have had the pleasure to collaborate with Alex Westphal (who knows about everything from supercavitation to the iPad) and Akin Wingerter. Though we have never worked together, I would like to thank Konstantin Bobkov for happy hours on Fridays, and for trying to teach me inflation.

I would also like to thank Steve Avery, Tassos Taliotis, Yogesh Shrivastava (whose last name, appropriately enough, means “the guru”), Borun Chowdhury and Jeremy Michelson for numerous discussions about string theory, and physics in general—from fuzzballs to nuclear physics, from Dirac brackets to superconformal symmetry, I could always count on someone to answer my questions.

A special place in this section is also reserved for Matt Kistler and Hasan Yüksel, who taught me to think outside of the theoretical physics box—I will miss our meetings, talking about scale invariant animals (“unimals”), social behavior of monkeys, mean bicep size of South Indians and the subtleties of ant communities.

My other colleagues at Ohio State have helped me understand everything from graphene to microlensing: Sheldon Bailey, Jim Davis, Kevin Driver, Mike Fellinger, Dave Gohlke, Rob Guidry, Alex Mooney, James Stapleton, Jeff Stevens, Rakesh Tiwari, Greg Viera and Julia Young for evenings at the Scholar and the Library, summer softball, and barbecues at Greg’s place. At Stanford University, I had the pleasure to sit in lectures by Savas Dimopoulos (who taught me that truly understanding something meant that one could

write down the answer without having to do any calculation) and Eva Silverstein. I consider myself fortunate to know Nathaniel Craig, Dan Greene, Kassa Haileyesus, Dan Harlow, Bart Horn, Eder Izaguirre, Jon Maltz, Siavosh Rezvan Behbahani, Tomas Rube, Dusan Simic and Daniele Spier Moreira Alves.

I am lucky to count Josh Friess, Nadir Jevanjee and Amanda Weltman as friends. I would like to especially thank Josh for advice regarding my graduate school applications, and for advice about careers outside of *academia*.

On a more personal level, I'd like to thank Bryanne Bornstein (for making the hard times easier to live through), and her parents (Dr. and Mrs. Bornstein) for always supporting me.

During my time at Ohio State, I have had the pleasure to speak many times with Professor Emeritus Walter Wada, who passed away shortly before I began preparing this Dissertation. Professor Wada's love of physics never dissipated, and even in the last weeks of his life he was trying to convince me that right-handed neutrinos were viable dark matter candidates. I am sorry that he will not be in attendance at my Defense, and I regret that he will never see this work completed, but I do feel privileged to have known him.

Most importantly, I must acknowledge the role of my parents and my grandmother in my education. It is only by their support that I am here today, and everything that I have accomplished has only been with their love and support.

VITA

| | |
|-----------------------------|--|
| Aug 26, 1979 | Born—Galveston, Texas |
| May, 2002 | B.S., Chemistry, Baylor University, Waco, Texas |
| Sept 2004 - Sept 2007 | Texas Space Grant Consortium Graduate Fellow |
| Dec, 2006 | M.S., Physics, Baylor University, Waco, Texas |
| Sept 2006 - present | Graduate Research, Dept. of Physics, The Ohio State University, Columbus, Ohio |

Publications

K. Busch, O. Soyemi, D. Rabbe, K. Humphrey, B. Dundee, and M. Busch, "Wavelength Calibration of a Dispersive Near-Infrared Spectrometer Using Trichloromethane as a Calibration Standard," *Appl. Spect.* **54** 9 (2000).

O. Soyemi, D. Rabbe, B. Dundee, M. Busch, and K. Busch "Design of a Modular, Dispersive Spectrometer for Fundamental Studies in NIR Spectroscopy," *Spect.* **16** 12 (2001).

B. Dundee, J. Perkins and G. Cleaver, "Observable / hidden broken symmetry for symmetric boundary conditions," *Int. J. Mod. Phys.* **A21**, 3367 (2006), hep-ph/0506183.

J. Perkins *et al.*, "Stringent Phenomenological Investigation into Heterotic String Optical Unification," *Phys. Rev. D* **75**, 026007 (2007) hep-ph/0510141.

B. Dundee and G. B. Cleaver, "Randall-Sundrum and flipped SU(5)," *Int. J. Mod. Phys. A* **23**, 2915 (2008) hep-ph/0609129.

B. Dundee, S. Raby, and A. Wingerter, "Reconciling Grand Unification with Strings by Anisotropic Compactifications," *Phys. Rev. D* **78** 066006 (2008) , 0805.4186

B. Dundee, S. Raby, and A. Wingerter, “*Addendum* to “reconciling grand unification with strings by anisotropic compactifications”,” *Phys. Rev. D* **79** 047901 (2009), 0811.4026.

B. Dundee and S. Raby, “On the string coupling in a class of stringy orbifold GUTs,” *Submitted to Phys. Lett. B* 0808.0992.

B. Dundee, S. Raby, and A. Westphal, “Moduli stabilization and SUSY breaking in heterotic orbifold string models,” *Submitted to Phys. Rev. D* 1002.1081.

Fields of Study

Major Field: Physics

Studies in Heterotic String Phenomenology: Stuart A. Raby

Contents

| | Page |
|----------------------------------|------|
| Abstract | ii |
| Dedication | iv |
| Acknowledgments | v |
| Vita | vii |
| List of Tables | xii |
| List of Figures | xiii |

Chapters

| | | |
|----------|---|-----------|
| 1 | Introduction | 1 |
| 1.1 | The Standard Model and the Effective Field Theory Paradigm | 1 |
| 1.1.1 | Fermi Theory: An Example | 3 |
| 1.2 | Supersymmetry: A First Step | 7 |
| 1.3 | Unification | 11 |
| 1.4 | String Theory as a Playground | 15 |
| 1.5 | Outline with an Emphasis on Original Work | 17 |
| 2 | Orbifold Compactifications of the Heterotic String: A How-To Guide | 20 |
| 2.1 | The Heterotic String | 20 |
| 2.1.1 | The Right-moving Sector | 21 |
| 2.1.2 | The Left-moving Sector | 23 |
| 2.1.3 | The Massless Spectrum | 24 |
| 2.1.4 | Toroidal Compactification | 25 |
| 2.2 | General Aspects of Orbifold Compactification | 27 |
| 2.2.1 | The Orbifold Action | 27 |
| 2.2.2 | Fixed Points of the Orbifold | 29 |
| 2.2.3 | Twists and Shifts | 30 |
| 2.3 | Building Orbifold-Invariant States | 31 |
| 2.3.1 | Invariant States in the Untwisted Sector | 32 |
| 2.3.2 | Invariant States in the Twisted Sector | 33 |
| 2.4 | The \mathbb{Z}_6 -II Orbifold Geometry | 35 |
| 2.5 | Orbifold Compactification: The Untwisted Sector of \mathbb{Z}_6 -II | 37 |
| 2.5.1 | Identifying Gauge Groups and Matter Representations | 40 |
| 2.6 | Orbifold Compactification: The Twisted Sectors of \mathbb{Z}_6 -II | 41 |
| 2.6.1 | Constructing the Centralizer | 42 |

| | | |
|----------|--|------------|
| 2.6.2 | The First and Fifth Twisted Sectors | 43 |
| 2.6.3 | The Second and Fourth Twisted Sector | 44 |
| 2.6.4 | The Third Twisted Sector | 47 |
| 2.6.5 | The Complete Spectrum | 49 |
| 3 | Gauge Coupling Unification in a Class of Stringy Orbifold GUTs | 50 |
| 3.1 | Motivation | 50 |
| 3.2 | Orbifold GUTs from String Theory | 52 |
| 3.2.1 | The Mini-Landscape in a Nutshell | 53 |
| 3.2.2 | The Orbifold GUT Picture | 54 |
| 3.3 | Gauge Coupling Unification in Orbifolds | 55 |
| 3.3.1 | Unification in Heterotic String Theory in 10 Dimensions | 55 |
| 3.3.2 | The RGEs for Anisotropic Orbifold Compactifications | 56 |
| 3.3.3 | Gauge Coupling Unification: An Effective Field Theory Calculation | 59 |
| 3.3.4 | Results | 60 |
| 3.4 | Unification, Decoupling of Exotics and Supersymmetry | 63 |
| 3.4.1 | Model 1A | 65 |
| 3.4.2 | Model 2 | 69 |
| 3.5 | Conclusions | 69 |
| 4 | The String Coupling in a Class of Stringy Orbifold GUTs | 72 |
| 4.1 | Motivation | 72 |
| 4.2 | The Starting Point | 72 |
| 4.3 | The String Coupling | 73 |
| 4.4 | Are We Perturbative? | 75 |
| 4.5 | Conclusion | 77 |
| 5 | Moduli Stabilization in Orbifold Compactifications of the Heterotic String | 79 |
| 5.1 | Motivation | 79 |
| 5.2 | General structure | 81 |
| 5.2.1 | Anomalous $U(1)_A$ and Fayet-Illiopoulos D -term | 82 |
| 5.2.2 | Target space modular invariance | 83 |
| 5.2.3 | Gauge kinetic function and sigma model anomaly | 86 |
| 5.2.4 | Non-perturbative superpotential | 87 |
| 5.3 | Moduli stabilization and supersymmetry breaking in the bulk | 90 |
| 5.4 | Moduli stabilization continued - the twisted sector and blow-up moduli | 96 |
| 5.4.1 | Singlets with polynomial Yukawa couplings | 97 |
| 5.4.2 | Singlet directions which are F - and D -flat in global supersymmetry | 99 |
| 5.5 | SUSY spectrum | 102 |
| 5.5.1 | Contributions to the soft terms | 102 |
| 5.5.2 | Relevant details from the “mini-landscape” | 105 |
| 5.5.3 | Hierarchy of F -terms | 107 |
| 5.5.4 | Weak scale observables | 108 |
| 5.6 | Conclusions | 110 |
| 6 | Conclusion | 116 |

Appendices

| | |
|---|------------|
| A The Mode Expansion in the Twisted Sector | 119 |
| A.1 The Mode Expansion in the Twisted Sector | 119 |
| A.2 Fractionally Moded Oscillators | 120 |
| A.3 An Explicit Example | 122 |
| B Some Results from 5d Field Theory | 125 |
| B.1 The Kaluza-Klein Mode Expansion of a Gauge Field | 125 |
| B.2 Something Like the Higgs Mechanism | 127 |
| B.3 A New Contribution to the Beta Functions | 130 |
| C Comparing two SU(6) Orbifold GUTs | 135 |
| D Some (Updated) Constraints on Proton Decay in Orbifold GUTs | 139 |
| D.1 Dimension 6 Operators | 139 |
| D.2 Dimension 5 Operators | 141 |
| E The Role of Holomorphic Gauge Invariant Monomials | 142 |
| F A Different Racetrack | 145 |
| G Some Tricks for Minimizing Potentials Using Mathematica | 146 |
| G.1 My Potential has Spurious Imaginary Parts | 146 |
| G.2 Mathematica Fails to Find a Minimum | 148 |
| G.2.1 The Konstantin Trick: Invent Something Small | 148 |
| G.2.2 The Alex Trick: Step, Step, Decrease, Repeat | 150 |
| G.3 Using the UNIX Terminal from Mathematica | 150 |
| H Miscellany | 152 |

List of Tables

| Table | Page |
|---|-------------|
| 1.1 The Standard Model. | 2 |
| 1.2 The Minimal Supersymmetric Standard Model. | 9 |
| 2.1 The action of the orbifold twists on Γ for the \mathbb{Z}_6 -II orbifold. | 36 |
| 2.2 The transformation of the states in the second twisted sector. | 45 |
| 2.3 The transformation of the states in the third twisted sector. | 47 |
| 5.1 Charge assignments for the fields in a generic hidden sector. | 88 |
| 5.2 Modular weights of the MSSM states in the “mini-landscape” model 1A. . | 106 |
| H.1 Spectrum of Model 1 of the mini-landscape search [38]. | 153 |
| H.2 Spectrum of Model 2 of the mini-landscape search [38]. | 154 |
| H.3 The full (five dimensional) spectrum of the models that we analyze [36]. . | 155 |
| H.4 Exotic matter content in Models 1A/B and 2 from [38]. | 155 |
| H.5 Values of the β -function coefficients for the <i>brane-localized</i> exotic matter. . | 155 |
| H.6 Values of the β -function coefficients for matter living in the bulk. | 156 |
| H.7 Comparison of proton lifetime to M_S , M_C , and M_{EX} | 156 |
| H.8 Comparison of proton lifetime to M_S , M_C , and M_{EX} | 157 |
| H.9 Models listed in Tables H.7 and H.8 with moderate hierarchies. | 158 |
| H.10 Subset of models listed in Reference [30] which exhibit $g_{\text{STRING}} \lesssim 1$ | 159 |
| H.11 Input values for the superpotential parameters for three different cases. . | 160 |
| H.12 The values for field VEVs and soft SUSY breaking parameters. | 160 |
| H.13 The hierarchy of F terms. | 161 |
| H.14 Boundary conditions at the string scale. | 161 |
| H.15 Weak scale observables, with no contribution from gauge mediation. | 162 |
| H.16 Scan over $\tan \beta$ and $\text{sgn}(\mu)$ | 163 |

List of Figures

| Figure | Page |
|--|------|
| 1.1 The Fermi Theory as the prototypical effective field theory. | 4 |
| 1.2 A process which is not accounted for in Fermi's theory. | 5 |
| 1.3 Inverse muon decay. | 6 |
| 1.4 The one loop correction to the Higgs mass in the Standard Model. | 7 |
| 1.5 A contribution to the Higgs mass in the MSSM. | 8 |
| 1.6 MSSM contribution to SM FCNC at one loop. | 10 |
| 1.7 The coupling "constants" in the Standard Model. | 11 |
| 1.8 The coupling "constants" in the Minimal Supersymmetric Standard Model. | 12 |
| 1.9 Unification of gauge bosons in a typical Grand Unified Theory. | 12 |
| 1.10 Unification of leptons in the $SO(10)$ grand unified theory. | 13 |
| 1.11 Proton decay at dimension 6 in a typical Grand Unified Theory | 14 |
| 1.12 Graviton-graviton scattering in string theory. | 16 |
| 2.1 The geometry of the compact dimensions. | 37 |
| 3.1 Setup of the 5d orbifold GUT. | 54 |
| 3.2 Histogram of solutions with $M_S > M_C \gtrsim M_{\text{EX}}$ | 61 |
| 3.3 An example of gauge coupling evolution. | 62 |
| 3.4 The correlation between the hierarchies in the problem. | 64 |
| 4.1 Histogram of the string coupling of the 252 solutions of Reference [30]. | 75 |
| 5.1 The potential along $\text{RE}[T]$ for $b > 0$ and $b < 0$ | 114 |
| 5.2 The scalar potential in the $\text{RE}[S]$ direction for Case 2. | 115 |
| 5.3 The one loop Coleman-Weinberg potential (Case 4) for ϕ_2 | 115 |

Chapter 1

INTRODUCTION

When you can measure what you are speaking about, and express it in numbers, you know something about it; but when you cannot measure it, when you cannot express it in numbers, your knowledge is of a meagre and unsatisfactory kind; it may be the beginning of knowledge, but you have scarcely in your thoughts advanced to the state of *Science*, whatever the matter may be.

Lord William Thompson Kelvin

1.1 The Standard Model and the Effective Field Theory Paradigm

The twentieth century has played witness to the birth and maturation of particle physics as both a theoretical and experimental science—from Dirac’s early attempts to build a covariant wave equation, resulting in the prediction of anti-particles [1, 2] to Anderson’s remarkable experimental confirmation of the “positive electron” [3]; from Pauli’s “desperate” invention of a new, massless fermion to reconcile beta decay with conservation of spin [4], to the discovery of the neutrino by Reines and Cowan [5]; from the prediction of the charm quark by Glashow, Iliopoulos and Maiani [6] to the near-simultaneous discovery of the J/ψ by two groups [7, 8]; from Glashow [9], Weinberg [10] and Salam’s [11] description of the electro-weak force to the experimental observation of the W and Z bosons at CERN [12, 13], the last hundred years should be classed as nothing short of a Golden Age for high energy physics. This theoretical and experimental triumph culminates in an elegant and concise description of Nature called the Standard Model of particle physics.

The Standard Model consists of three forces and 58 particles, laid out in a repeating “generation” structure: three families consisting of two quarks and two leptons, with each quark coming in three colors. There are six anti-quarks (coming in three “anti-colors”) and three anti-leptons. The strong nuclear (or “color”) force is mediated by 8 gluons, and the electro-weak force is mediated by four vector bosons: three W ’s and a B . The fundamental Higgs scalar breaks the electro-weak force to electromagnetism and the weak nuclear force by giving mass to three of these four vector bosons—the W^\pm ($\sim W_1 \pm iW_2$)

| Fermions | Quarks | Q | Matter | | | Forces | | Bosons |
|----------|--------|---------|-----------|------------|-----|---------------|----------|--------|
| | | +2/3 | u | c | t | $g(\times 8)$ | | |
| Leptons | -1/3 | d | s | b | | EW | WN + EM | |
| | -1 | e | μ | τ | | W_1 | W^+ | |
| | 0 | ν_e | ν_μ | ν_τ | | W_2 | W^- | |
| | | | | | | W_3 | Z^0 | |
| | | | | | | B | γ | |
| Higgs | 0 | | h | | | | | |

Table 1.1: The matter content and force carriers of the Standard Model. The six varieties of quarks (called “flavors”) are the (u)p, (d)own, (c)harm, (s)trange, (t)op and (b)ottom, each of which comes in three different “colors”. The “up-type” quarks all have electric charge +2/3, while the “down-type” quarks all have electric charge -1/3. The six leptons are the (e)lectron, the muon (μ), the tau (τ), and their associated neutrinos—the electron, μ and τ have charge -1, while all three neutrinos are neutral. The strong nuclear (or color) force is mediated by the gluon (of which there are eight). The electro-weak force is mediated by the $W_{1,2,3}$ and B bosons, but is broken to the weak nuclear (WN) force and electromagnetism (EM) by the Higgs. The WN force is mediated by W^\pm and Z^0 , while EM is mediated by the photon, γ . We have highlighted the Higgs boson, in the last row, as the only piece of the Standard Model which has not been confirmed by experiment.

and Z^0 ($\sim W_3 - B$) carry the (short range) weak nuclear force, and a massless, chargeless photon ($\sim W_3 + B$) mediates electromagnetism. The matter content of the Standard Model is listed in Table 1.1. Ignoring neutrino mixing, there are 18 parameters which are required by the Standard Model. The phenomenology that can be derived from these five sentences of text cannot be summarized in 1000 pages of tables [14].

For all of its utility, however, the Standard Model is not a fundamental theory—this is evidenced by the fact that the Standard Model does not explain the origin of any of its 18 parameters, nor does it make any attempt to describe gravity. There are a host of other aesthetic and experimental questions for which the Standard Model offers no rejoinder: Why three families? Why three forces? Why is the Higgs boson the only fundamental scalar? How can we reconcile questions of cosmology, notably dark matter, dark energy, and inflation, with the Standard Model? Why is it that some particles (like neutrinos) are very light, yet other particles (like the top quark) are very heavy? Why are the electric charges of the quarks and leptons rational numbers? Why should the weak nuclear force be the only short range force, and what sets the scale?

Today, we understand the Standard Model as an effective description of Nature above some characteristic length scale¹ ℓ_{NP} : the theory is an approximate description of all physics at long distances relative to that scale, but has nothing to say about physics at shorter length scales. The Standard Model emerges from some fundamental (but unknown) physics, and one can understand all of the aesthetic and experimental issues with the Standard Model in terms of this more fundamental theory. The modern interpretation of quantum field theory says that questions of the type listed above are misguided: they are the relics of short distance physics, and are of limited importance when one only cares about *measuring* something. The fact that we have never measured a significant deviation from the predictions of the Standard Model affirms that short distance physics plays, at most, a very limited role in the effective theory. Conversely, non-observation of violations of the predictions of the Standard Model will allow one to set limits on the scale of new physics, ℓ_{NP} .

1.1.1 Fermi Theory: An Example

As an example of the effective theory paradigm, we will consider Enrico Fermi’s theory of weak interactions [16]. The weak nuclear force is mediated by exchange of W^\pm and Z^0 bosons. The force is short range because the W and Z bosons can only travel a finite distance ($\sim \ell_{\text{EW}}$) before decaying. At distances much larger than ℓ_{EW} , Fermi’s theory describes an interaction between four fermions, approximating the physics of the W and Z bosons with a point-like interaction, which we schematically depict in Figure 1.1. The four fermions interact with a strength characterized by G_F , the Fermi coupling constant, which is the only parameter in the effective theory, and may be derived from the underlying weak nuclear physics. As we probe shorter and shorter distance scales, the physics of the W and Z bosons becomes non-negligible—the “point-like” approximation fails, as it should, when we begin to probe distance scales of the order ℓ_{EW} .

In the figure, we have shown the decay of a muon into an electron and two neutrinos in both Fermi’s theory (top) and the weak theory (bottom). Using Fermi’s theory, we can calculate the lifetime of a muon at rest and find $\tau_\mu \approx 2.188 \times 10^{-6}$ s. The experimentally measured (average) lifetime of the muon is $\tau_\mu^{\text{EXP}} \approx 2.198 \times 10^{-6}$ s [14], corresponding to a difference of less than 1%.

For simple calculations Fermi’s theory gives very accurate results, providing an empirical justification for neglecting corrections due to short distance physics; however, short distance physics *does* play some role in the processes which we observe in experiments. Occasionally, the muon will decay into two neutrinos, an electron, and a photon, as in Figure 1.2. This is a decay which is unaccounted for in Fermi theory. In the weak theory, the

¹We use the symbol ℓ_{NP} as the defining scale of the Standard Model as we typically expect New Physics—physics not described by the Standard Model—to appear at that length scale.

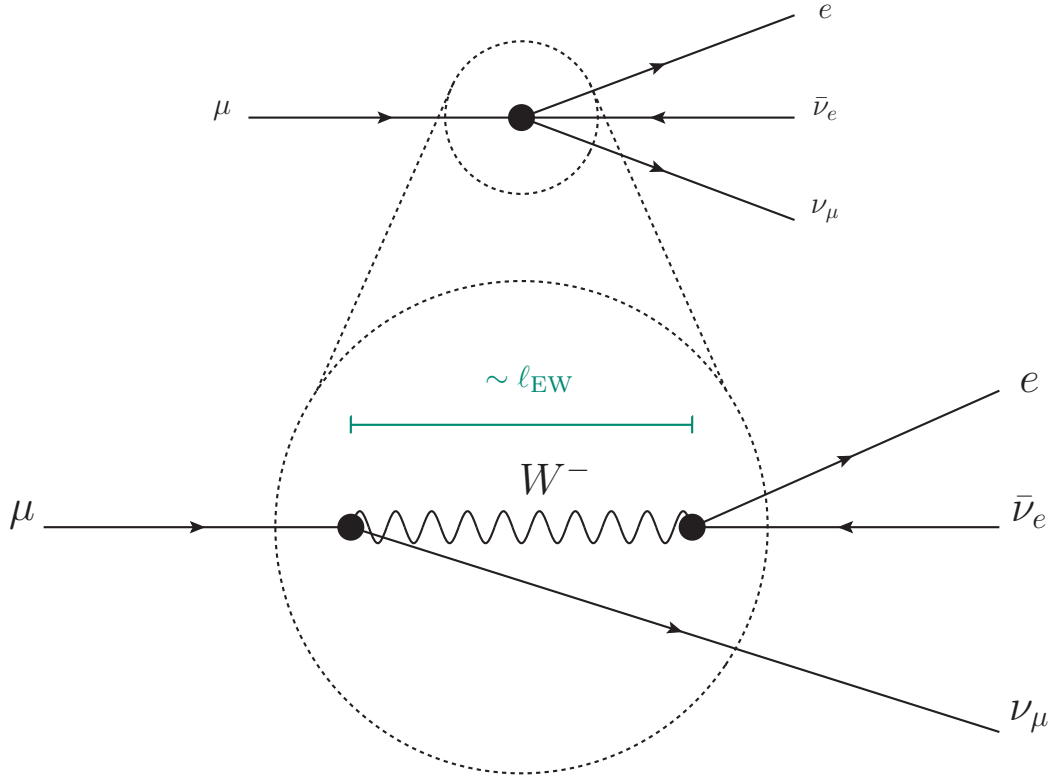


Figure 1.1: Enrico Fermi’s theory of weak interactions can be understood as the effective field theory that one obtains by decoupling the W^\pm and Z bosons from the weak nuclear theory. In this case, a muon decays into a muon neutrino, an electron and an electron anti-neutrino—in the Fermi theory, this interaction occurs at a single point in space-time. We can “zoom in” to see the fundamental (i.e., short distance) physics which is going on: a W^- boson is being exchanged. Deviations from the prediction of Fermi theory only occur when one can accurately measure physics near the length scale associated with the W boson, ℓ_{EW} . If we only ever measure processes occurring at large distances, we will never notice the short distance physics. All figures involving Feynman diagrams were generated with [15].

W bosons carry electric charge, thus they may emit and absorb photons. In Fermi theory the interaction does not couple to the photon, and processes as in Figure 1.2 give us a hint of the physics from which Fermi theory emerges².

We can consider other processes using Fermi’s theory. For example, we may scatter muon neutrinos off of electrons at high energies³, producing muons and electron neutrinos in a process called “inverse muon decay” [17], as in Figure 1.3. Using Fermi theory, we

²We note that a much more common process is for the muon or electron to emit an additional photon.

³Historically, measuring this interaction was crucial to establishing the $V - A$ nature of charged weak interactions in the Standard Model.

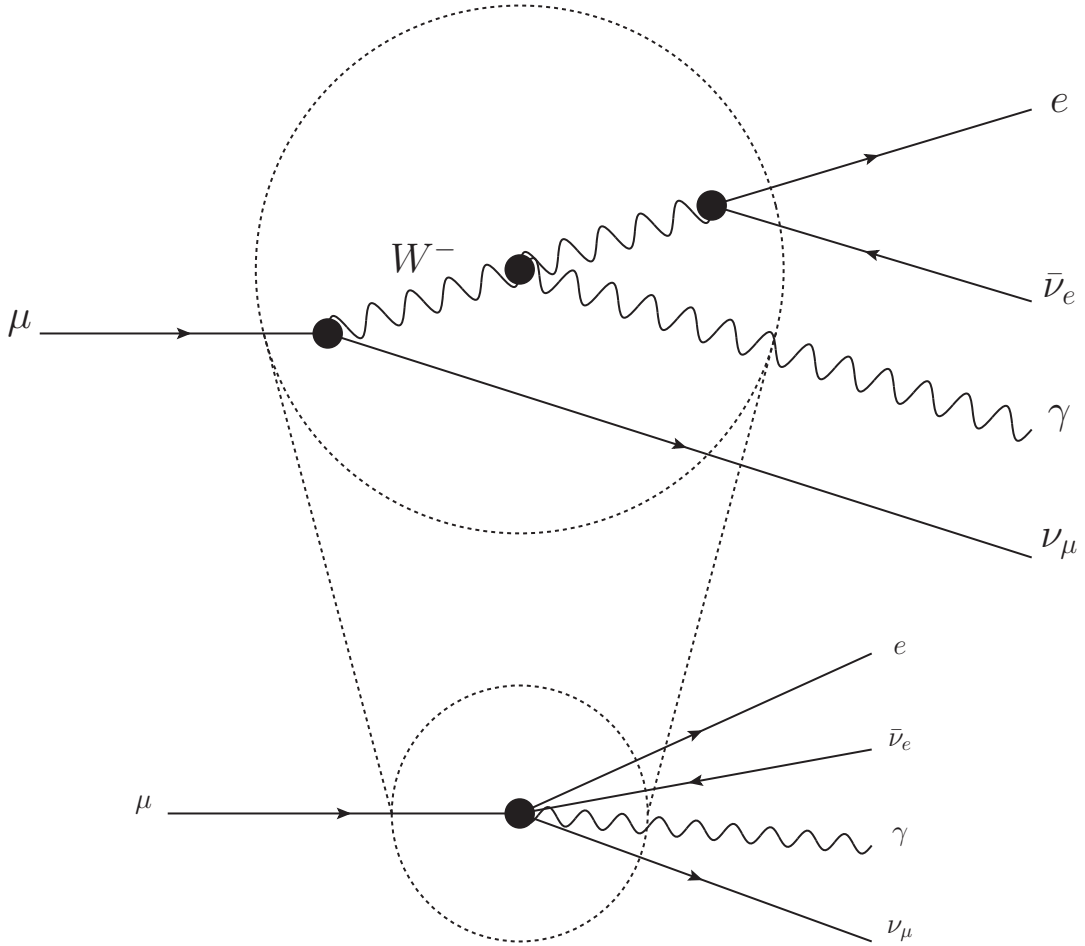


Figure 1.2: Fermi’s theory fails to account for some processes, such as this one. About 1% of the time, the muon emits a neutrino and a W^- boson, and the W boson emits a photon (γ), before decaying into an electron and an electron neutrino. This process is highly suppressed relative to the process in Figure 1.1—a much more common process is for the incoming muon or the outgoing electron to emit a photon.

can estimate the cross section (σ , which has units of area) for this process on dimensional grounds, and find $\sigma \sim s G_F^2$, where \sqrt{s} is the center of mass energy of the collision and G_F is the strength of the Fermi interaction. If we perform this experiment using incident neutrinos with arbitrarily large energies (that is, we consider taking $s \rightarrow \infty$), the cross section clearly diverges ($\sigma \rightarrow \infty$). Cross sections which diverge indicate an interaction which occurs with probability greater than one—the prediction from Fermi’s theory breaks down, as it should, when $\sqrt{s} \sim 1/\ell_{EW}$. Physically, the electro-weak theory becomes important, and Fermi theory fails, when we probe the length scale associated with the W boson.

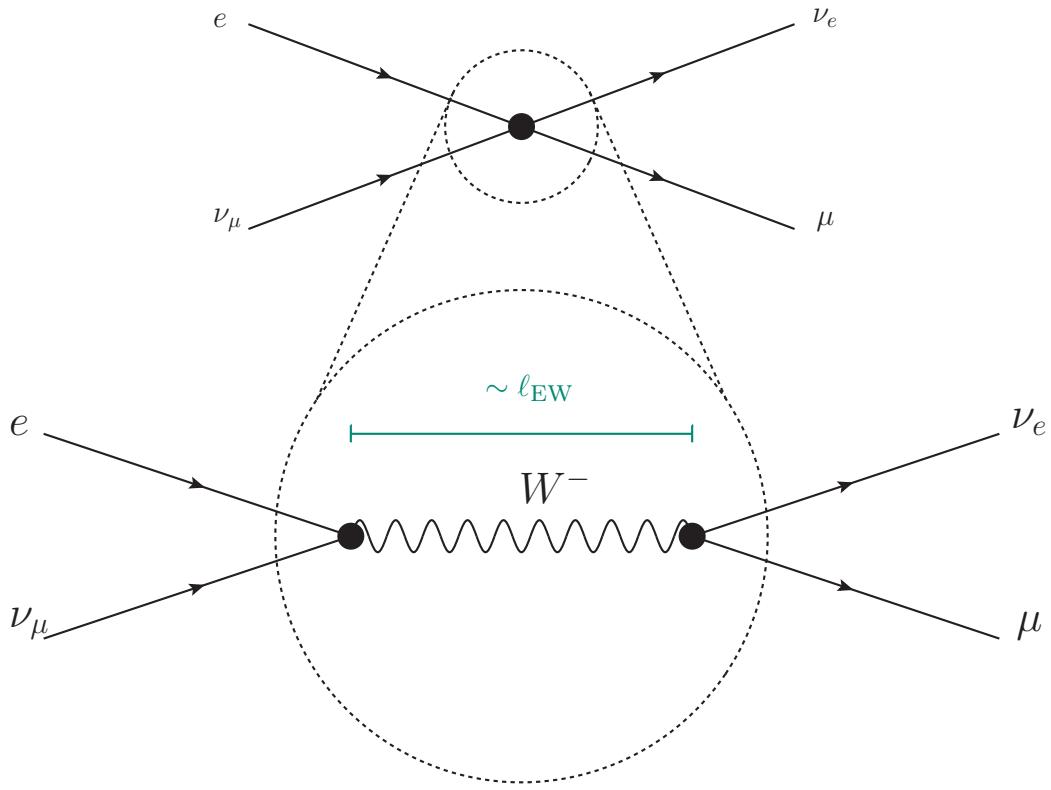


Figure 1.3: The scattering of muon neutrinos off of electrons in Fermi theory and in the electro-weak theory, a process called inverse muon decay.

Because we understand both the effective description and the physics from which it emerges, Fermi theory provides a complete example of how an effective theory works. For example, the coupling constant in the Fermi theory may be derived from the parameters of the underlying weak nuclear physics—likewise, we might expect any theory which gives rise to the Standard Model to *explain* why the coupling constants take the values that they do. This theory could *explain* the scale of the weak force, and it might *explain* the differences in particle masses. We might also hope that this fundamental theory would *explain* the reason that we have the forces that we do, and it may *explain* why we have three families of quarks and leptons.

Moreover, Fermi theory gives us some intuition about how we might observe the physics underlying the Standard Model: we may either increase the energy of our experiments or we may increase the precision of our results. In the former case, the inverse muon decay in Figure 1.3 has a cross section which grows as the center of mass energy of the collision, which implies a breakdown of probabilities. Because this is a clearly unphysical situation, it must be that the predictions of the Fermi theory are wrong in that regime, and indeed

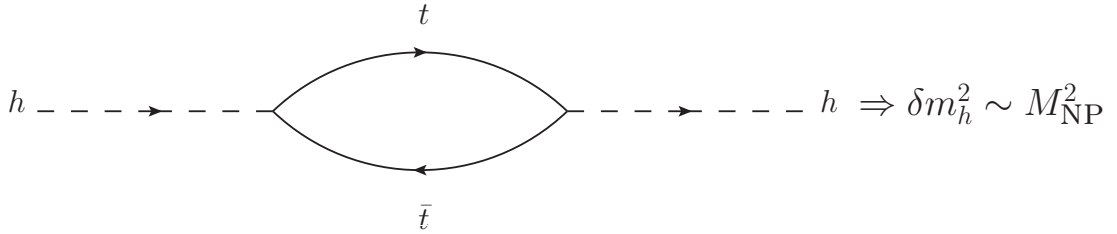


Figure 1.4: Of all the particles in the Standard Model, the Higgs couples most strongly to the top quark (t and \bar{t}), which are fermions. This is the dominant contribution to the correction to the Higgs mass, and is proportional to M_{NP}^2 .

they are. Increasing the energy of the incident neutrino allows us to directly probe the physics of the underlying weak theory. Conversely, we can work to increase the precision of our experiments. Most of the allowed interactions in the Standard Model are known very precisely, and there are many experiments performing precision measurements of Standard Model processes. Deviations from the expected results, or the observation of forbidden processes (in analogy to Figure 1.2) gives us another window into the physics from which the Standard Model emerges.

1.2 Supersymmetry: A First Step

Once we view the Standard Model as an effective field theory, we expect that many of its apparent shortcomings may be understood as manifestations of short distance physics. The most dramatic of these problems is an issue with the stability of the Standard Model, called the Hierarchy Problem. As we have already mentioned, the weak force is a short range force whose range is set by the mass of the W boson, which in turn is set by the mass parameter of the Higgs boson: roughly (up to a conversion factor), $m_h \sim 1/\ell_{\text{EW}} \sim 100 \text{ GeV}$. As with all parameters in the Standard Model, we define the Higgs mass parameter at some scale ℓ_{NP} . If we are interested in physics at long distances relative to that scale, we must compute corrections to our parameters which take into account this difference in scales. Typically, the corrections are small, but in the case of the Higgs mass, these corrections are large and uncontrolled.

The dominant correction to the Higgs mass comes from its coupling to top quarks, as illustrated in Figure 1.4. One can calculate this contribution, and find that it goes as $\delta m_h^2 \sim M_{\text{NP}}^2$, where $M_{\text{NP}} \sim 1/\ell_{\text{NP}}$ up to some conversion factor. As the scale of new physics becomes shorter, the correction to the Higgs mass becomes larger. Let us, for the moment, make the naive assumption that the Standard Model emerges directly from some quantum theory of gravity, whose characteristic length scale is the Planck length (ℓ_{PL}). In

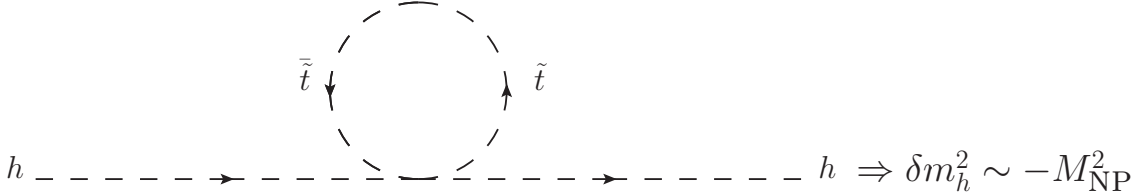


Figure 1.5: In the Minimal Supersymmetric Standard Model (MSSM), top quarks have supersymmetric scalar partners, called top *squarks* (\tilde{t} and $\tilde{\bar{t}}$). The top squarks couple in a similar manner as the top quarks, but the top squark loop contributes to the Higgs mass with a negative sign relative to the top quark loop. Thus, the one loop corrections to the Higgs mass cancel in a supersymmetric gauge theory.

particular, this implies that the effective field theory will be valid at energies below the Planck energy, which (in turn) implies the identification $M_{\text{NP}} = M_{\text{PL}} \sim 10^{19} \text{ GeV}$. Under these assumptions, the corrections to the Higgs mass are 17 orders of magnitude larger than the the initial value, and we see that the Higgs mass in the Standard Model is tuned very precisely. Thus we arrive at the stability issue: what physics can tune the Higgs mass so precisely?

Surely, we must ensure that $M_{\text{NP}} \ll M_{\text{PL}}$. In other words, we can control the corrections to the Higgs mass by postulating some new physics at an energy scale smaller than the Planck scale by requiring that the Standard Model emerge from some physics other than quantum gravity. Of course, this new physics will come with some new effective interactions, and we must ensure that those interactions do not disagree with what we have already measured. Requiring consistency with experiments is a very tight constraint on solutions to the stability problem.

An elegant way to assure that $M_{\text{NP}} \ll M_{\text{PL}}$ is to ensure that the large corrections due to the top quark *mostly* vanish. Here we note a fundamental difference between bosons and fermions: it is a curious property of quantum field theory that fermion loops (as in Figure 1.4) and boson loops (as in Figure 1.5) come with a relative minus sign. The top quarks in Figure 1.4 are fermions (cf Table 1.1). Thus, if we suppose that a freely propagating Higgs boson could emit and absorb a pair of bosonic particles with the same properties as the top quark, the large corrections ($\sim M_{\text{NP}}^2$) to the Higgs mass parameter would cancel against each other.

The fact that the large corrections cancel provides motivation for supersymmetry [18–21]. In short, all particles in the Standard Model get partners: fermions get bosonic partners (called “sfermions”), gauge bosons get fermion partners (called “gauginos”), and the Higgs gets a fermionic partner, called a “Higgsino”. Each Standard Model state gets one

| | | Q | Matter | | | Gaugino | Fermions |
|---------|----------|------|-----------------|-------------------|--------------------|---------------|----------|
| Scalars | Squarks | +2/3 | \tilde{u} | \tilde{c} | \tilde{t} | \tilde{g} | |
| | Sleptons | -1/3 | \tilde{d} | \tilde{s} | \tilde{b} | \tilde{w}_1 | |
| | | -1 | \tilde{e} | $\tilde{\mu}$ | $\tilde{\tau}$ | \tilde{w}_2 | |
| | | 0 | $\tilde{\nu}_e$ | $\tilde{\nu}_\mu$ | $\tilde{\nu}_\tau$ | \tilde{w}_3 | |
| | Higgsino | 0 | | | \tilde{h} | \tilde{b} | |

Table 1.2: The new content of the Minimal Supersymmetric Standard Model. The “squarks” are the supersymmetric partners of the quarks. The top quark’s partner is the “stop” (\tilde{t}), the electron’s partner is the “selectron” (\tilde{e}), etc. The electric charges of the new particles are the same as their supersymmetric partners’, see Table 1.1. Note that there is a degeneracy in the table: the partner of the B (the “bino”) has the same symbol (\tilde{b}) as the partner for the bottom quark (the “sbottom”). In practice, context always distinguishes the two.

superpartner and each super-particle has exactly one partner in the Standard Model—this is called $\mathcal{N} = 1$ supersymmetry. The particle content is listed in Table 1.2.

From experiments, however, we know that Nature is not supersymmetric—if supersymmetry were a good symmetry, we would expect to see the supersymmetric partners of the Standard Model particles. Indeed, if supersymmetry has anything to do with Nature, then we should understand how the Standard Model emerges from some underlying supersymmetric physics, which we call the Minimal Supersymmetric Standard Model (MSSM). Aside from the new particles, the MSSM contains a myriad of new parameters which tell us (indirectly) about how supersymmetry breaks down. As in the case of Fermi Theory, we fully expect that all of these new parameters will be explained by any theory from which the MSSM can be derived.

If the Standard Model does indeed emerge from the MSSM, then we expect to see some traces of supersymmetry as we increase the energy of our experiments and probe shorter length scales. Such experimental evidence might include the direct production of the supersymmetric partners at colliders. Conversely, we may increase the statistics of our experiments: in Figure 1.6 we show a process which receives corrections from MSSM particles. In the Standard Model, the W bosons change quark flavor *and* electric charge—thus, a bottom quark ($Q = -1/3$) may turn into an up, charm, or top quark ($Q = 2/3$) by emitting a W^- boson, but cannot change (directly) into a strange quark. While direct transitions between quark flavors of the same charge (called flavor changing neutral currents) are forbidden, *indirect* transitions are possible. For example, the bottom quark may change

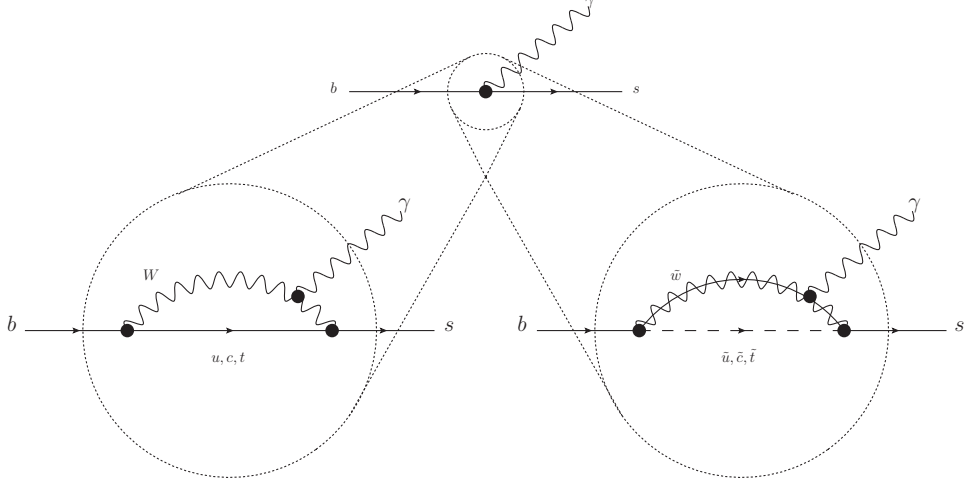


Figure 1.6: Flavor changing neutral currents in the Standard Model (left) and the MSSM (right). In the Standard Model, the W bosons change quark flavor *and* electric charge. In this process, the bottom quark changes into an up, charm, or top quark by emitting a W boson; the internal quark subsequently reabsorbs the W^- boson and transitions into a strange quark. In the MSSM, the bottom quark may emit a \tilde{w} gaugino and an up, charm or top squark. The gaugino and squark are reabsorbed by a strange quark.

into an up, charm, or top quark by emitting a W boson. If the up, charm or top quark subsequently reabsorbs the W^- boson, it may transition into a strange quark, as we have demonstrated in Figure 1.6. We can measure the rate of transitions between bottom and strange quarks in experiments (top), and compare this result to our expectations from the Standard Model (bottom, left). If the Standard Model emerges from the MSSM, we expect new contributions to the transition rate, such as those in the bottom right of Figure 1.6, with the internal quarks replaced with their scalar partners. Indeed, at the time of writing, experiments [22] seem to measure a small excess in the $b \rightarrow s\gamma$ rate as predicted by the Standard Model [23], in line with what is expected in the MSSM.

As we have already pointed out, the parameters in any quantum field theory receive corrections which account for the difference between the scale at which the theory is defined and the scale at which measurements are performed. This applies not only to the Higgs mass, but also to the coupling constants which parametrize the relative strengths of the strong and electro-weak forces [24, 25]. The coupling constants α_i determine the strength of interaction between fermions and bosons—the color force is mediated by gluons, which couple to quarks with a strength set by α_3 . The $W_{1,2,3}$ bosons couple to matter with strength α_2 , and the B couples to matter with strength α_1 . Assuming that no new physics occurs between the weak scale M_{EW} and the Planck scale, we have shown how

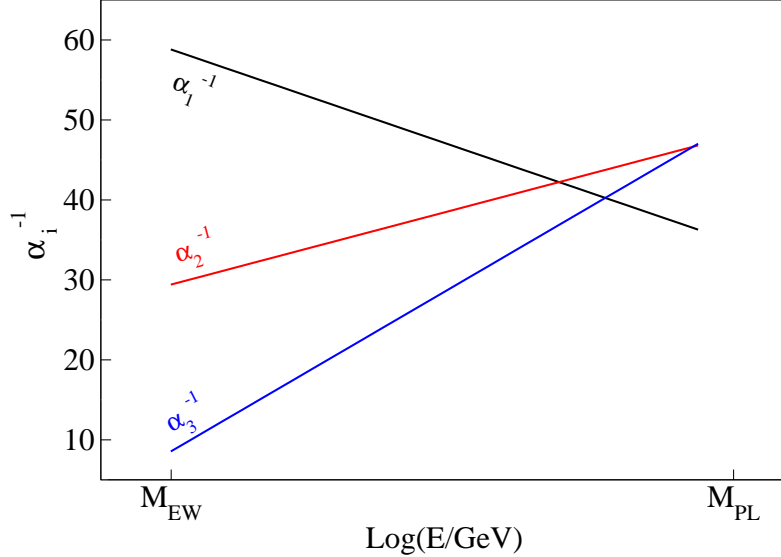


Figure 1.7: The strengths of the forces in the Standard Model depend on the energy at which one measures them. Extrapolating these strengths across many decades in energy, we see that they tend to roughly the same value. This gave an early indication that there may be some more fundamental “grand unified theory” which gives rise to the Standard Model.

these strengths depend on energy scale in the Standard Model in Figure 1.7. There is nothing particularly noteworthy in Figure 1.7, however, if we perform the same calculation in the MSSM, we find a very striking result. As Figure 1.8 shows, the three forces become comparable in strength at an energy scale $M_{\text{GUT}} \approx 3 \times 10^{16}$ GeV. This is one of the most inspiring qualitative features of the MSSM: it seems to predict that the three forces are unified at some large energy scale.

1.3 Unification

The tendency of the gauge coupling constants in the MSSM towards a common value motivates us to explore the possibility that the three forces are the descendants of a single “grand” unified force [26, 27]. It is hard to imagine that this unification⁴ is an accident: the couplings in the effective theory (the MSSM) have no relationship to each other. In calculating the corrections to these values we have assumed only the matter content of the MSSM, which mirrors the matter content in the Standard Model. We are left with three

⁴Unified descriptions of (seemingly) disparate phenomena are not new in physics: James Maxwell unified electric and magnetic phenomena in 1861. In the twentieth century, Glashow, Weinberg and Salam showed how the weak force and electromagnetism were unified in the electro-weak theory.

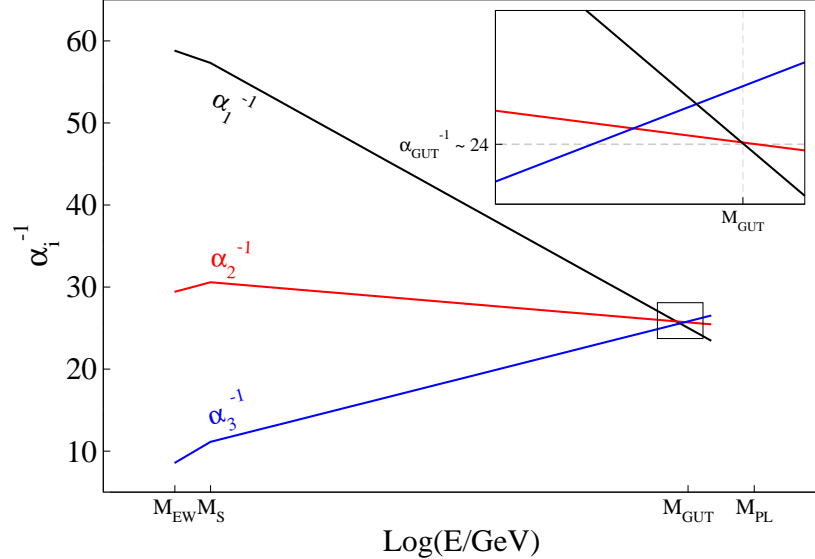


Figure 1.8: In the Minimal Supersymmetric Standard Model, the unification of forces is no longer approximate, contrary to the case in the Standard Model—in fact, we have to magnify the intersection to see that the lines do not meet (inset). Note that we have assumed that the supersymmetric particles all have the same mass in drawing this figure, $M_{\text{SUSY}} \approx 1$ TeV.

$$\begin{pmatrix} g \\ W_1 & W_2 \\ W_3 & B \end{pmatrix} \implies \begin{pmatrix} \begin{pmatrix} g \\ X \end{pmatrix} & X \\ X & \begin{pmatrix} W_1 & W_2 \\ W_3 & B \end{pmatrix} \end{pmatrix}$$

Figure 1.9: The gauge bosons of the MSSM are unified into a representation of the grand unified theory. There are new gauge bosons (which we call, collectively, X) in the grand unified theory which are not present in the low energy effective field theory.

unrelated lines which (up to a small correction) meet at a single point—in the absence of a grand unified theory, this would be a quite spectacular coincidence.

If the three forces are unified at some large scale as Figure 1.8 seems to indicate, the force carriers in the MSSM (the eight gluons g , and the four electro-weak gauge bosons $W_{1,2,3}$ and B) must be related to the gauge bosons of the new force. Figure 1.9 shows how this works schematically: the gauge bosons of the Standard Model can be represented as sets of matrices. These matrices are components of the larger set of matrices which represent the set of grand unified gauge bosons—all MSSM gauge bosons are also gauge

$$\begin{array}{c}
 \left(\begin{array}{c} u \\ d \\ u^c \\ d^c \\ e \\ \nu_e \\ e^c \end{array} \right) \quad \Rightarrow \quad \left(\begin{array}{c} u \\ d \\ u^c \\ d^c \\ e \\ \nu_e \\ e^c \\ \nu_e^c \end{array} \right) \\
 \end{array}$$

Figure 1.10: One generation of 15 quarks and leptons unify completely in the SO(10) grand unified theory. (There are two flavors of quarks (u and d) and their anti-partners (u^c and d^c), each coming in three colors, an electron and its anti-partner (e^c), and a neutrino.) The one new lepton predicted by the SO(10) grand unified theory is the anti-neutrino (ν^c , or “right-handed” neutrino), and may be responsible for giving the neutrinos in the Standard Model small but non-zero masses.

bosons of the grand unified theory, however, there are some gauge bosons of the grand unified theory which are not present in the MSSM, called collectively X .

While unification of the gauge bosons requires several extra degrees of freedom, the MSSM quarks and leptons (and, equivalently, the squarks and sleptons) unify more economically. In the SO(10) grand unified theory, in fact, only one extra particle (per generation) is predicted. Coincidentally, these three new particles (called “right-handed” neutrinos— $\nu_e^c, \nu_\mu^c, \nu_\tau^c$) may be instrumental in explaining why we observe a small (but non-zero) neutrino mass: the “right-handed” neutrinos are seen as more of an asset than a liability.

We stress that Figures 1.9 and 1.10 do not represent a mathematical sleight of hand. The statement that gauge bosons and leptons can be represented as matrices and vectors can be made mathematically rigorous: historically, the idea that Nature can be described by abstract algebraic structures is one of the cornerstones of modern physics [28], and is surely one of the most beautiful results in theoretical science. The fact that a single generation of Standard Model particles can be fully embedded into a single representation of SO(10) (as in Figure 1.10) is nothing short of remarkable, and would represent another astounding coincidence.

One of the generic predictions of grand unified theories is the decay of the proton: there exist no decay channels for the proton in the Standard Model or the MSSM⁵, thus we expect it to have an infinite lifetime. In a typical grand unified theory, however, quarks can change into leptons by emitting an X boson, causing the proton to decay into a positron

⁵As a technical aside, we define the MSSM such that it preserves R parity.

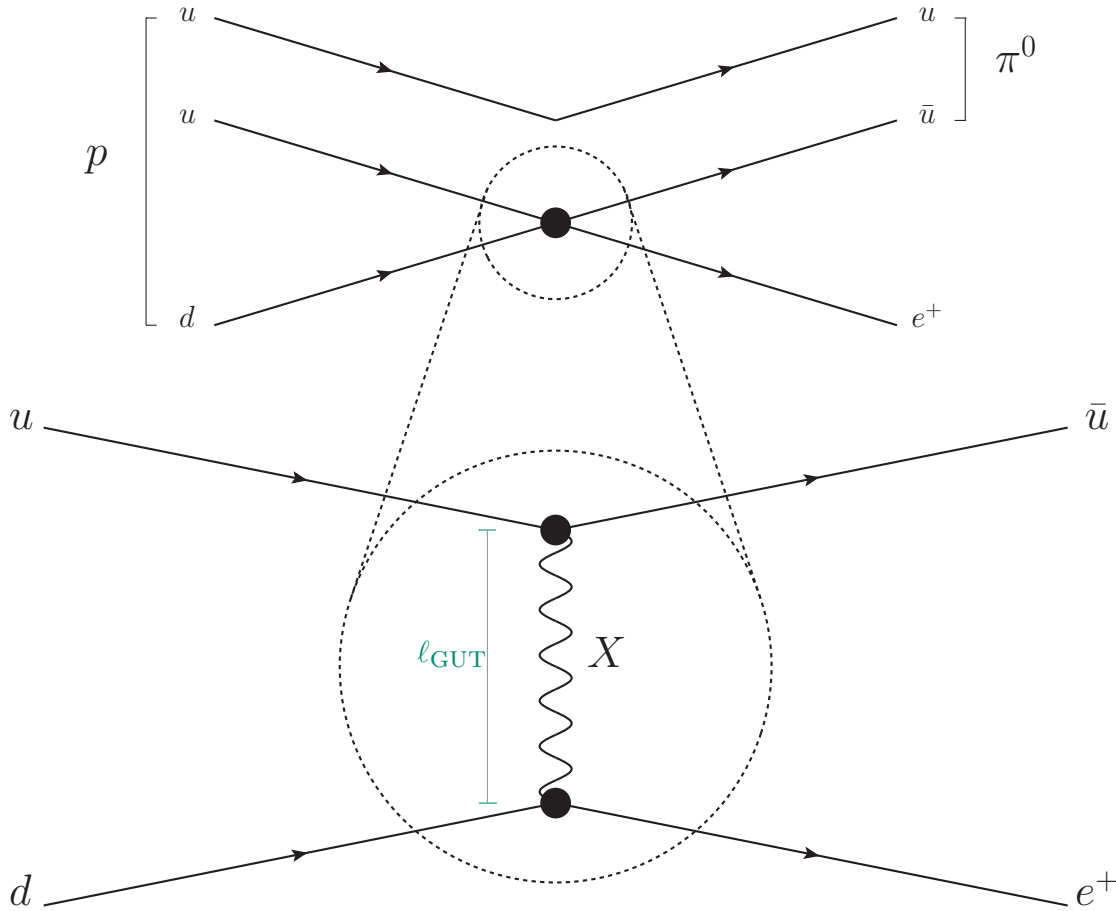


Figure 1.11: The proton becomes unstable in a typical grand unified theory, and can decay when the quarks inside the proton exchange X bosons. In this process, an up quark emits an X boson turning into an anti-up quark. The X boson is absorbed by a down quark, turning it into a positron (anti-electron).

and a pion as in Figure 1.11. The experiments to detect proton decay rely on large statistics: because it is not feasible to perform scattering experiments to directly probe GUT scale physics, searches involve watching a lot of protons and waiting for one of them to decay⁶. Observation of proton decay would be a clear signal of the physics underlying the Standard Model, much like the process in Figure 1.2 is a clear indication of the weak physics from which the Fermi theory emerges.

⁶A dedicated experiment in Japan (super-Kamiokande) has put a lower bound on the lifetime of the proton of 8.2×10^{33} years [29] using 50,000 tons of ultra-pure water.

1.4 String Theory as a Playground

In the preceding discussion, any mention of gravity has been conspicuously absent—gravity seems to be *different* from the other forces. In particular, treating gravity as “just another gauge field” leads to terrible inconsistencies. Typically, we would assume that gravity is mediated by a point particle (called a graviton). Quantizing a theory based on a point-like graviton proves to be impossible: if we treat gravity in the same way that we treat the other forces, we find that the description breaks down at energies comparable to the Planck scale. Of course, if we view gravity as just another effective field theory, we are not surprised at all by this result—Fermi theory gave very good results when we calculated the lifetime of a muon at rest, just as Einstein’s gravity does an exceptional job in describing the dynamics of galaxies and planets. But Fermi theory falls apart when we probe the electro-weak scale, just as gravity falls apart when we probe the Planck scale. If we are interested in learning about physics at very short length scales, it is abundantly clear that the canonical approach is inadequate.

Loosely, string theory is the result of generalizing quantum theory such that the fundamental excitations are one dimensional, extended “string-like” objects rather than zero dimensional “point-like” particles. In describing the quantum string, much of the intuition gained from studying classical strings is retained: for example, a closed string may have a center of mass momentum, but may also carry internal momentum in the form of oscillations. As in the classical string, the right-moving and left-moving oscillation modes of a closed string may be decoupled, and the wave equation can be applied to the two sets of modes independently. Closed strings may wind around compact dimensions, and open strings may have Dirichlet or Neumann boundary conditions.

Once the string is quantized, we can calculate all of the possible states and find one with the exact properties of a graviton. That string theory contains a graviton candidate is remarkable by itself: the quantum theory was derived without any reference to gravity, thus there was no reason to expect the theory to contain a state with the same properties as a graviton. Even more remarkable is the fact that we can calculate the amplitude for two gravitons to scatter off of each other in string theory and recover *exactly* the answer given by Einstein’s theory—this correspondence is shown schematically in Figure 1.12. We stress that this is entirely unexpected—there is no reason that string theory should reduce to General Relativity. Many find this result the most basic motivation for studying string theory as a theory of quantum gravity.

One of the most beautiful implications of string theory is that it *explains* the dimensionality of space-time. Einstein’s gravity works in an arbitrary number of space-time dimensions, however, string theory is *only* consistent in one time-like and nine spatial dimensions. This is a unique feature of string theory: if we perform scattering experiments

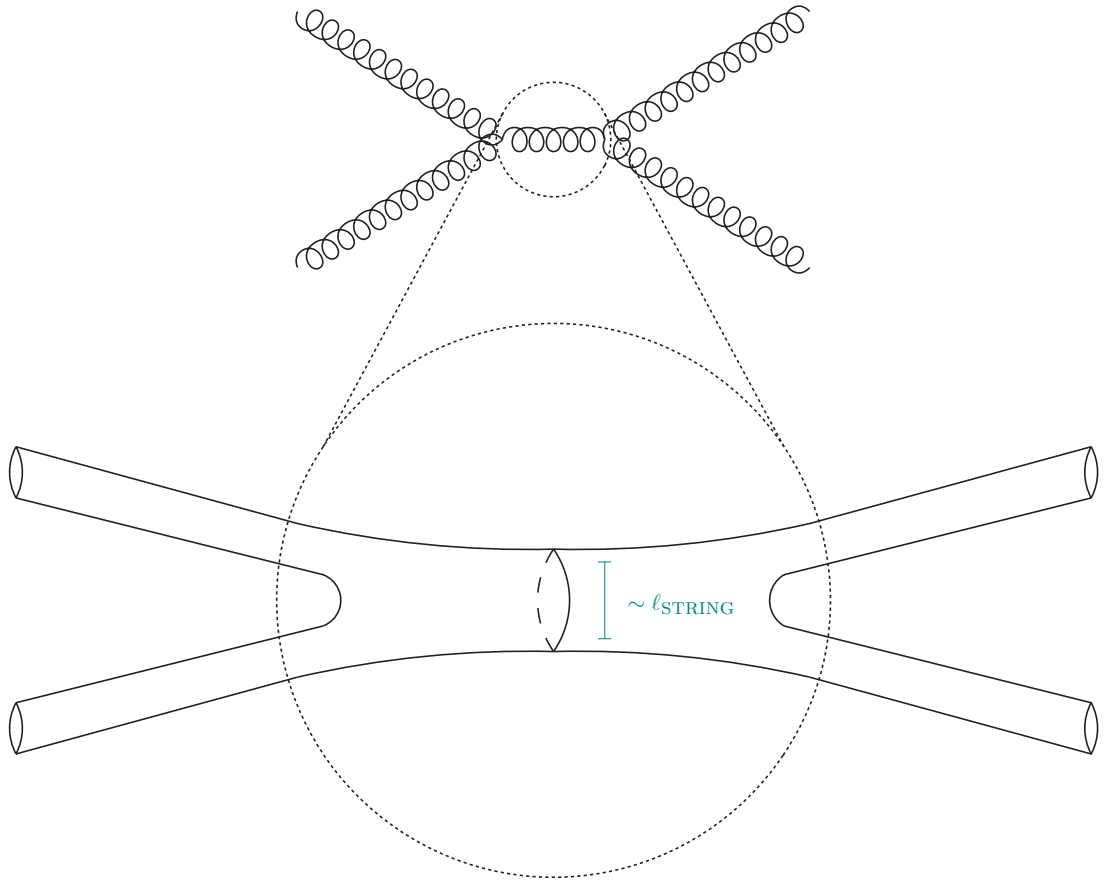


Figure 1.12: In string theory, gravitons are closed strings: as we probe the string scale (ℓ_{STRING}) in graviton-graviton scattering experiments (top), string theory postulates that we should begin notice the extended character of the string (bottom).

to probe the string scale, it is an unambiguous prediction of the theory that we should observe the effects of the extra dimensions.

Of course, low energy physics is not ten dimensional, so to make contact with reality we must “compactify” six of the nine spatial dimensions. What we are left with is a four (3+1) dimensional effective field theory, whose parameters and particle content are determined by the sizes and shapes of the six compact dimensions. The hope is that one can choose the details of the six compact directions in such a way as to reproduce the 18 “free” parameters in the Standard Model, or the myriad of parameters in the MSSM. In the following chapters, we will describe positive steps toward that end, however, at the time of writing there exists no exact realization of the MSSM in string theory.

Obtaining a stringy completion of the MSSM seems to be the equivalent of looking for a needle in a haystack. Even though the mathematical structures needed to describe Nature

can be found in nearly all classes of string compactifications, there is simply no unique way to determine the sizes or shapes of the compact dimensions. From the perspective of string theory all solutions seem to be equally likely—there are an uncountable (and possibly infinite) number of possible compactifications, informally called the “landscape”. We are left to differentiate the vacua on their ability to give models consistent with observation, with no guiding principle for our search.

In the absence of direction from string theory, we will follow the guidance that low energy physics seems to provide us—the biggest issue with the Standard Model seems to be the stability of the Higgs mass parameter, which is elegantly solved by supersymmetry. Supersymmetry seems to suggest unification of forces into a grand unified theory. Thus, our problem of finding the Standard Model in the unassailable “landscape” of vacua is reduced to looking for some grand unified theory. In this vein, our chief interest in string theory is as a tool for producing effective field theories which incorporate the paradigm of supersymmetric grand unification, which also happen to be consistent theories of quantum gravity. Addressing some issues in the effective field theory may necessitate knowledge of the underlying “stringy” dynamics; however, if our experience with effective field theories has taught us anything, it is that those details are largely irrelevant.

1.5 Outline with an Emphasis on Original Work

In this Dissertation, we are specifically interested in the low energy physics which emerges from general heterotic string compactifications. Chapters 3, 4 and 5 all represent original work to this end [30–33]. For concreteness, we will focus our attention on the so-called “mini-landscape” models [34–38].

Chapter 2 serves as background for the mini-landscape models. We will discuss all of the relevant details of the underlying string theory in this chapter, with an emphasis on constructing the \mathbb{Z}_6 -II orbifold models. While the prime-ordered orbifold models (T^6/\mathbb{Z}_3 , for example) have been studied extensively in the literature, there is relatively few references available which describe the massless spectra of the non-prime ordered orbifolds, like \mathbb{Z}_6 -II. After a brief discussion of the heterotic string, we describe the method by which these models may be constructed.

In Chapter 3, we examine how the idea of gauge coupling unification in these models may be addressed in a precise manner, using a “bottom-up” approach [30]. In particular, we will be interested in anisotropic compactifications, where one of the six compact dimensions is larger than the other five [39–41], and has characteristic length $1/M_C$. The gauge couplings get large corrections from the tower of Kaluza-Klein modes in the large extra dimension [42, 43], a result which is derived in Appendix B. In addition to the corrections to the gauge couplings coming from the Kaluza-Klein modes, we also introduce

exotic matter at an intermediate scale, M_{EX} . In the particular models analyzed, we show that gauge coupling unification is not possible with $M_{\text{EX}} = M_{\text{C}}$ and in fact we require $M_{\text{EX}} \ll M_{\text{C}} \sim 3 \times 10^{16}$ GeV. We find that about 10% of the parameter space has a proton lifetime (from dimension 6 gauge exchange) 10^{33} yr $\lesssim \tau(p \rightarrow \pi^0 e^+) \lesssim 10^{36}$ yr, while 80% of the parameter space gives proton lifetimes below Super-K bounds.

The corrections coming from the exotic matter and the “large” extra dimensions require us to examine the consistency of our approach in Chapter 4. The idea in Chapter 3 was to perform all of our calculations in the effective field theory, essentially ignoring the microscopic details of the underlying string theory [32]. It is clear, however, that any calculation done in the effective approach cannot be inconsistent with the requirements of the short distance physics. One way to check this consistency is to ensure that the conclusions of Chapter 4 are not at odds with the assumption that our string theory is weakly coupled. We examine the relationship between the effective field theory parameters and the string coupling g_{STRING} . More interestingly, perhaps, is a relationship we derive between the lifetime of the proton and the string coupling constant. This gives an experimental probe of the parameter space of the underlying string theory.

In Chapter 5, we address the issue of moduli stabilization within the context of the heterotic string in the effective field theory [33]. The issue of moduli stabilization has been an open question within the context of the heterotic string models, stalling progress for roughly 15 years. Using a simple one condensate model, we show how one may stabilize the dilaton and all geometric moduli in a typical heterotic string compactification with a near zero cosmological constant in a vacuum with spontaneously broken (local) supersymmetry. We further show how one can stabilize the large number of non-Abelian singlet fields (some of which correspond to blow-up modes of the orbifold) once supersymmetry is broken. This work represents one of the last and most crucial steps towards a fully stringy realization of the MSSM.

The moduli stabilization mechanism which we propose gives a low energy effective field theory with broken supersymmetry. We make some general assumptions about the details of the underlying string construction in order to get an idea about the weak scale observables [33]. Mediation of supersymmetry breaking to the visible sector come primarily from supergravity (SUGRA) effects, however, we allow for other sources of mediation as well. The anomaly mediation effects are estimated, and (given the results of Chapter 3) we allow for the possibility that some intermediate scale matter can play the role of messenger, resulting in a hybrid gauge-gravity-anomaly mediation scheme. Assuming only the MSSM matter content in the effective theory, we derive the spectrum of soft parameters which one might measure at the Large Hadron Collider.

In Chapter 6, we offer some concluding remarks, and suggest some future directions for investigation.

We reserve some longer tables and calculations for the appendices. In Appendix A, we derive (from first principles) the mode expansion of the heterotic string in the twisted sector. In particular, we show how twisted sector states may have fractional oscillator number. In Appendix B we present some results for five dimensional field theories. We calculate the Kaluza-Klein [44, 45] mode expansion for a gauge field in the $S_1/\mathbb{Z}_2 \times \mathbb{Z}'_2$ orbifold, and show how each mode in the tower is higgsed. Finally, we calculate the contribution of a five dimensional fermion to the vacuum polarization, giving a power law correction to the coupling constant renormalization. In Appendix C, we compare our $SU(6)$ orbifold GUT to an example appearing in the literature, noting some key differences. Specifically, we prove that the threshold corrections coming from the Kaluza-Klein modes of the MSSM matter do not allow for unification. Appendix D contains some constraints on the relationship between the string scale, the compactification scale and the proton lifetime for the models described in Chapter 3. We have updated these results to reflect the current experimental constraints [29]. Appendix E serves as an *addendum* to Chapter 3, in which we demonstrate the role of holomorphic, gauge invariant monomials (HIMs) in proving $D = 0$. We then use this result to show that the results of Chapter 3 are consistent with this constraint, completing the proof that the mini-landscape models exhibit gauge coupling unification in globally supersymmetric ($F = D = 0$) vacua. In Appendix G we outline some of the tricks that we learned for dealing with the complicated potentials in Chapter 5. There is certainly nothing which could be published in this appendix, however, we hope that it might provide some useful hints to anyone having trouble using `Mathematica` to find SUGRA scalar potentials. In Appendix H contains longer tables with results from Chapters 3, 4 and 5.

Chapter 2

ORBIFOLD COMPACTIFICATIONS OF THE HETEROtic STRING: A HOW-TO GUIDE

Aεί ο Θεὸς ο Μέγας γεωμετρεῖ

Plato

In this chapter, we will demonstrate the general method for constructing the massless spectrum of the heterotic string [46, 47], compactified on an orbifold. We will review the details of the heterotic string mainly to set the notation—readers interested in a more rigorous development should consult the canonical references [48–52]. Our ultimate goal is to describe how one may obtain the massless spectrum in both the untwisted and twisted sectors of the \mathbb{Z}_6 -II orbifold. As a final note, we have erred on the side of *too many* details, which (we hope) newcomers to the field will find refreshing.

2.1 The Heterotic String

d'Alembert proved that the oscillations of a closed string may be separated into left moving modes and right moving modes. In other words, suppose $X^\mu(\sigma, \tau)$ is a solution to the closed string equations of motion:

$$\square X^\mu(\sigma, \tau) = 0, \tag{2.1}$$

where $\square \equiv \eta^{\alpha\beta} \partial_\alpha \partial_\beta$, and $\eta^{\sigma\sigma} = -\eta^{\tau\tau} = -1$ while $\eta^{\sigma\tau} = \eta^{\tau\sigma} = 0$. Note that μ is a label for X , while σ, τ are world-sheet coordinates. We can define “left-moving” coordinates (σ_+) and “right-moving” coordinates (σ_-) by

$$\sigma^\pm = \tau \pm \sigma. \tag{2.2}$$

We now suppose that $X^\mu(\sigma, \tau) \equiv X_L^\mu(\sigma^+) + X_R^\mu(\sigma^-)$, where $X_{L,R}^\mu$ are arbitrary functions of their argument. If we define appropriate derivatives ($\partial_\pm \equiv \frac{1}{2}(\partial_\tau \pm \partial_\sigma)$), it follows immediately that

$$\partial_+ \partial_- (X_L^\mu(\sigma^+) + X_R^\mu(\sigma^-)) = 0. \quad (2.3)$$

Thus *any solution* to the closed string wave equation may be decomposed into left-moving and right-moving pieces.

Equation (2.3) tells us that the left-moving modes and right-moving modes of the string decouple, thus we are free to treat them independently. Quantum mechanically, this becomes a statement about the Hilbert space of physical closed string states. A physical state ($|\phi\rangle$) is composed of a state from the left-moving space of states ($|p\rangle \in \mathcal{H}_L$) and a state from the right-moving space of states ($|q\rangle \in \mathcal{H}_R$):

$$|\phi\rangle = |p\rangle \otimes |q\rangle. \quad (2.4)$$

The important point is that \mathcal{H}_L and \mathcal{H}_R may be completely unrelated. For example, in the heterotic string theory, the right-moving sector is composed of a superstring (in ten dimensions), while the left-moving sector is composed of a bosonic string (in twenty-six dimensions). We will see that the extra dimensions in the left-moving sector give rise to internal gauge degrees of freedom, and the massless spectrum of the heterotic string is exactly a Yang-Mills gauge theory coupled to $\mathcal{N} = 1$ supergravity (SUGRA) in ten dimensions.

In what follows, we will use the following notation: μ labels coordinates $0, \dots, 9$, and I labels the (left-moving) coordinates $10, \dots, 25$. We will work in the “light-cone gauge” where directions $0, 9$ are taken along the world-sheet—in that case, we will use i which labels coordinates $1, \dots, 8$. When we discuss compactification, we will always work in the light-cone gauge, and use $\mu = 1, 2$ for non-compact dimensions, and $i = 3, \dots, 8$ for compact dimensions.

2.1.1 The Right-moving Sector

The right-moving (superstring) sector of the heterotic string can be separated into bosonic degrees of freedom and fermionic degrees of freedom. The right-moving bosons are described by

$$X_R^\mu(\sigma^-) = \frac{1}{2}x^\mu + \sqrt{\frac{\alpha'}{2}}p^\mu\sigma^- + i\sqrt{\frac{\alpha'}{2}}\sum_{n \neq 0} \frac{\alpha_n^\mu}{n}e^{-in\sigma^-}. \quad (2.5)$$

x^μ and p^μ are the center-of-mass coordinates of the string, and are shared between left-movers and right-movers. α' is a parameter with dimensions of mass squared, and serves as the intrinsic scale in string theory. We will set $\alpha' = \frac{1}{2}$ temporarily, and restore it below.

α_n^μ are operators which create and destroy oscillators on the string—note that $(\alpha_n^\mu)^\dagger = \alpha_{-n}^\mu$ because X_R^μ must be hermitian.

The fermions in the right-moving sector are solutions to

$$\partial_+ \psi_R^\mu(\sigma^-) = 0, \quad (2.6)$$

and obey either periodic (Ramond) or anti-periodic (Neveu-Schwarz) boundary conditions. The solutions to Equation (2.6) are given by

$$\psi_R^\mu(\sigma^-) = \sum_{n \in \mathbb{Z}} d_n^\mu e^{-in\sigma^-} \quad (\text{Ramond}), \quad (2.7)$$

$$\psi_R^\mu(\sigma^-) = \sum_{r \in \mathbb{Z} + \frac{1}{2}} b_r^\mu e^{-ir\sigma^-} \quad (\text{Neveu-Schwarz}). \quad (2.8)$$

The creation/annihilation operators obey anti-commutation relations:

$$\{d_n^\mu, d_m^\nu\} = \eta^{\mu\nu} \delta_{n,-m}, \quad (2.9)$$

$$\{b_r^\mu, b_s^\nu\} = \eta^{\mu\nu} \delta_{r,-s}. \quad (2.10)$$

Consider first the Neveu-Schwarz sector. The lowest lying state is given by

$$b_{-1/2}^\mu |0\rangle. \quad (2.11)$$

The index structure suggests that this state corresponds to a vector in 10 dimensions.

The lowest lying states in the Ramond sector are a bit more interesting. Upon proper normalization, the lowest lying Fourier coefficients can be seen to obey the Dirac algebra:

$$\left\{ i\sqrt{2}d_0^\mu, i\sqrt{2}d_0^\nu \right\} = -2\eta^{\mu\nu}. \quad (2.12)$$

This implies that it is impossible to choose a unique, non-degenerate ground state in this sector of the theory. Let us choose a basis of the Lorentz generators⁷ where

$$|s\rangle = \left| \pm\frac{1}{2}, \pm\frac{1}{2}, \pm\frac{1}{2}, \pm\frac{1}{2}, \pm\frac{1}{2} \right\rangle. \quad (2.13)$$

Note that this gives a **32** dimensional representation of the ten dimensional Lorentz group, which decomposes as **32** = **16** ⊕ **16'**. Because chirality can be defined in an even number of dimensions, the **16**, **16'** may be labeled by their quantum numbers under $\gamma_{11} \equiv \prod_\mu \gamma^\mu$.

Let us now count degrees of freedom of the lowest lying states. The NS sector furnishes a massless ten dimensional vector, which has $10 - 2 = 8$ degrees of freedom. Equation (2.12)

⁷See Appendix B of [52], for example.

suggests that the lowest lying states in the Ramond sector are spinors. Spinors in ten dimensions have $2^{10/2} = 32$ complex components. In ten dimensions, one can impose simultaneously the Majorana and Weyl constraints—the former can be shown by constructing a basis in which all ten of the Dirac matrices are imaginary, while the latter follows from the fact that chirality can always be defined in an even number of dimensions, as we can always define an analogue of γ^5 which anti-commutes with all of the other γ^μ [48]. This leaves us with 16 real degrees of freedom. We further note that the lowest lying state obeys the (massless) Dirac equation: $\gamma^\mu \partial_\mu \chi = 0$, cutting the number of degrees of freedom in half again. This gives us a total of 8 real degrees of freedom. Thus we see that the lowest lying states in the Ramond and Neveu-Schwarz sectors can be consistently paired to form a $D = 10$, $\mathcal{N} = 1$ vector multiplet if (and only if) we impose Majorana and Weyl conditions on the fermions. One can ensure that the entire spectrum, including the massive sectors, obeys $D = 10$, $\mathcal{N} = 1$ supersymmetry by defining the GSO projections. At the massless level, the projections are tantamount to the Majorana-Weyl conditions.

In the light-cone gauge, the lowest lying states in the NS (R) sector correspond to the $\mathbf{8}_v$ ($\mathbf{8}_s$) representations of $\text{SO}(8)$. We will denote the right-moving ground state by $|q\rangle_R$, and in the Cartan-Weyl basis we have

$$|q\rangle_R = \begin{cases} |\pm 1, 0, 0, 0\rangle & \Rightarrow \mathbf{8}_v \quad \text{NS} \\ |\pm \frac{1}{2}, \pm \frac{1}{2}, \pm \frac{1}{2}, \pm \frac{1}{2}\rangle & \Rightarrow \mathbf{8}_s \quad \text{R} \end{cases} . \quad (2.14)$$

The line beneath the Neveu-Schwarz states means that we should take all permutations, and the GSO projection demands that we take only states in the Ramond sector with an even number of + signs. Both NS and R states fulfill

$$\alpha' M_R^2 = q^2 - 1 = 0, \quad (2.15)$$

where we have restored the units on the left hand side.

2.1.2 The Left-moving Sector

In the left-moving sector, we work with a bosonic string, living in 26 dimensions. We imagine compactifying the left-moving string on a sixteen torus, T^{16} . This gives sixteen internal degrees of freedom, denoted with the index I , and 10 space-time degrees of freedom, denoted with the index μ :

$$X_L^\mu(\sigma^+) = \frac{1}{2}x^\mu + \frac{1}{2}p^\mu\sigma^+ + \frac{i}{2}\sum_{n \neq 0} \frac{\tilde{\alpha}_n^\mu}{n} e^{-in\sigma^+}, \quad (2.16)$$

$$X_L^I(\sigma^+) = x^I + p^I\sigma^+ + \frac{i}{2}\sum_{n \neq 0} \frac{\tilde{\alpha}_n^I}{n} e^{-in\sigma^+}. \quad (2.17)$$

The massless degrees of freedom satisfy

$$\alpha' M_L^2 = p^2 + 2\tilde{N} - 2 = 0, \quad (2.18)$$

where \tilde{N} counts the number of left-moving oscillators. In the light-cone gauge, the lowest lying states are:

$$\tilde{\alpha}_{-1}^i |0\rangle_L \quad i = 1, \dots, 8; \quad (2.19)$$

$$\tilde{\alpha}_{-1}^I |0\rangle_L \quad I = 1, \dots, 16; \quad (2.20)$$

$$|p^I\rangle_L \quad \text{such that } p^2 = 2. \quad (2.21)$$

Equation (2.21), together with the one loop partition function, implies that the lattice representing the internal sixteen torus must be even and self-dual [50]. Only two such lattices are known: $E_8 \otimes E_8$ and $SO(32)$, both of which have rank 16⁸. The weights of both are given by

$$\Lambda_{E_8 \otimes E_8} \Rightarrow p^I \in \begin{cases} (\pm 1, \pm 1, 0^6) (0^8) \oplus (0^8) (\pm 1, \pm 1, 0^6) \oplus \\ \frac{1}{2} ([\pm 1]^8) (0^8) \oplus (0^8) \frac{1}{2} ([\pm 1]^8) \end{cases}, \quad (2.22)$$

$$\Lambda_{SO(32)} \Rightarrow p^I \in (\underline{\pm 1, \pm 1, 0^{14}}). \quad (2.23)$$

Again, an underline denotes permutation, and an exponent denotes a repeated entry⁹. The $E_8 \otimes E_8$ lattice vectors which are written in terms of $\pm \frac{1}{2}$ contain an even number of $\pm \frac{1}{2}$.

2.1.3 The Massless Spectrum

Now that we have the lowest lying states in the left-moving and right-moving sectors, we can construct the entire massless spectrum of the heterotic string in ten dimensions. Physical states must obey the level matching condition:

$$M_L^2 = M_R^2. \quad (2.24)$$

We combine the massless right-movers in Equation (2.14) with the massless left-movers in Equations (2.19)-(2.21) to find the following massless states (in the light-cone gauge):

- a $D = 10$, $\mathcal{N} = 1$ supergravity (SUGRA) multiplet:

$$\tilde{\alpha}_{-1}^j |0\rangle_L \otimes |q\rangle_R. \quad (2.25)$$

⁸Note that there are 16 states in Equation (2.20), corresponding exactly to the roots (uncharged gauge bosons) of $E_8 \otimes E_8$ or $SO(32)$.

⁹For example, the $SO(32)$ weight lattice is sixteen dimensional. Each weight has two factors of ± 1 and fourteen zeroes.

- the 16 roots (uncharged gauge bosons) of $E_8 \otimes E_8$ or $SO(32)$:

$$\tilde{\alpha}_{-1}^I |0\rangle_L \otimes |q\rangle_R; \quad (2.26)$$

- and the 480 weights (charged gauge bosons) of $E_8 \otimes E_8$ or $SO(32)$:

$$|p^I\rangle_L \otimes |q\rangle_R. \quad (2.27)$$

It is worthwhile to examine this spectrum a bit more closely.

The $D = 10, \mathcal{N} = 1$ SUGRA Multiplet

Let us restrict our attention to the NS right movers. In the light cone gauge, we have

$$|q\rangle_R \Big|_{NS} = b_{-1/2}^i |0\rangle_R, \quad (2.28)$$

where i is a space-time index. The SUGRA multiplet can then be formed by

$$b_{-1/2}^i |0\rangle_R \otimes \tilde{\alpha}_{-1}^j |0\rangle_L, \quad (2.29)$$

where j is also a space-time index. Note that we can decompose any tensor into a symmetric piece, and anti-symmetric piece, and a trace: we symmetrize over i, j to obtain the graviton, we anti-symmetrize over i, j to obtain B^{ij} , and trace over the indices to see the dilaton ϕ . By supersymmetry, the states in the Ramond sector should decompose in a similar manner, furnishing the super-partners of each of these states.

The $D = 10, \mathcal{N} = 1$ Vector Multiplet

As before, let us consider the NS right movers, which carry a space-time index. Clearly the states in Equations (2.26) and (2.27) have the correct Lorentz structure to be considered gauge bosons. Moreover, the internal degrees of freedom ($|p^I\rangle$) also have the correct gauge structure. The fact that there are 496 states, which is exactly the dimension of the adjoint representation of both $E_8 \otimes E_8$ and $SO(32)$, is suggestive of this fact. Note that the gauginos come from the Ramond sector.

2.1.4 Toroidal Compactification

We have shown that the massless spectrum of the heterotic string furnishes $D = 10, \mathcal{N} = 1$ SUGRA, coupled to either $E_8 \otimes E_8$ or $SO(32)$ gauge theory. In and of itself, this is a rather remarkable feature. To this point, we have really only demanded consistency of the underlying quantum theory: in essence, we get this $D = 10, \mathcal{N} = 1$ SUGRA theory “for free”. This can be seen as a prediction of string theory: namely, at the string scale, the

massless spectrum is exactly that of $D = 10$, $\mathcal{N} = 1$ SUGRA in the weakly coupled limit. It is likely that string theory itself furnishes a consistent theory of quantum gravity, thus we have (in some sense) a “theory of everything” in ten dimensions.

But we don’t live in ten dimensions, so we need to compactify six of the dimensions. This amounts to manifestly breaking the ten dimensional Lorentz invariance, a process for which very few mechanisms exist. We will ignore this technicality, and try to choose the shapes of the internal dimensions in as simple a manner as possible. We take the six internal degrees of freedom (along $i = 3, \dots, 6$) to be periodic, and (recalling that two dimensions are large by default) leave two dimensions ($\mu = 1, 2$) large.

The problem with toroidal compactification can be seen by examining the SUGRA multiplet. Taking the right-movers from the Ramond sector, we have

$$\left| \underbrace{\pm \frac{1}{2} \pm \frac{1}{2}}_{\text{spin}} \pm \underbrace{\frac{1}{2} \pm \frac{1}{2}}_{\text{internal}} \right\rangle \otimes \tilde{\alpha}_{-1}^j |0\rangle_L \quad (2.30)$$

The first entry of the $| \dots \rangle$ describes what is happening in the large dimensions, while the next three entries are purely internal degrees of freedom. If we must have an even number of plus signs, we have both polarizations of four gravitino. This corresponds to $\mathcal{N} = 4$ supersymmetry in four dimensions, which is non-chiral, and thus has no chance of modeling Nature.

We can see the same problem in the gauge sector. If we consider the $E_8 \otimes E_8$ or $SO(32)$ roots, the dimensional reduction gives us

$$|\pm 1, 0, 0, 0\rangle \otimes \tilde{\alpha}_{-1}^I |0\rangle_L \Rightarrow 2 \text{ vector d.o.f.}, \quad (2.31)$$

$$|0, \pm 1, 0, 0\rangle \otimes \tilde{\alpha}_{-1}^I |0\rangle_L \Rightarrow 6 \text{ real scalar d.o.f.}, \quad (2.32)$$

$$\left| \underbrace{\pm \frac{1}{2} \pm \frac{1}{2}}_{\text{spin}} \pm \underbrace{\frac{1}{2} \pm \frac{1}{2}}_{\text{internal}} \right\rangle \otimes \tilde{\alpha}_{-1}^I |0\rangle_L \Rightarrow 8 \text{ real fermion d.o.f.} \quad (2.33)$$

In Equation (2.31), we see the two helicities (± 1) of a (massless) four dimensional gauge boson, in Equation (2.32) there are six internal degrees of freedom of a state which is a Lorentz singlet (as the first entry is 0), and in Equation (2.33) we have eight real fermion degrees of freedom. These states complete the $D = 4$, $\mathcal{N} = 4$ vector multiplet.

Why $\mathcal{N} = 4$?

It is important to understand *why* we get $\mathcal{N} = 4$ supersymmetry from the toroidal compactification, if we are to understand how to get $\mathcal{N} = 1$ supersymmetry from some other compactification. As we have remarked, compactification means that we have broken the ten dimensional Lorentz invariance down to a subgroup. The fact that the torus is flat means

that the internal dimensions have a trivial holonomy¹⁰. Because the holonomy group is trivial, all spinors are invariant under group rotations, thus all of the states in Equation (2.33) survive the projection. It is clear, then, that we need to find some manifolds with non-trivial holonomy on which to compactify our theory.

2.2 General Aspects of Orbifold Compactification

We have seen that the heterotic string gives $D = 10$, $\mathcal{N} = 1$ SUGRA coupled to $E_8 \otimes E_8$ or $SO(32)$ Yang-Mills theory, and that toroidal compactification of this theory gives $D = 4$, $\mathcal{N} = 4$ SUGRA coupled to $E_8 \otimes E_8$ or $SO(32)$. In order to model our universe, however, we must find a way to break the supersymmetries as well as the gauge symmetries in the low energy effective field theory.

What sorts of compactifications give $\mathcal{N} = 1$ SUSY in the low energy limit? Let us suppose that we compactify on some manifold with holonomy group $SO(6) \cong SU(4)$. Let the generators of $SU(4)$ be denoted by U . The requirement of $\mathcal{N} = 1$ SUSY in $D = 4$ is tantamount to the requirement that one find exactly one spinor ϵ which obeys $U\epsilon = \epsilon$ —in other words, we need to find some ϵ which is invariant upon parallel transport around a closed path in the compact space¹¹. Without loss of generality, we can assume that ϵ is in the 4 (as opposed to the $\bar{4}$) of $SU(4)$, and by an $SU(4)$ transformation, we may always write

$$\epsilon = \begin{pmatrix} 0 \\ 0 \\ 0 \\ \epsilon_0 \end{pmatrix}. \quad (2.34)$$

It is clear that an $SU(3)$ subgroup of $SU(4)$ always leaves exactly one ϵ invariant, which motivates us to consider manifolds of $SU(3)$ holonomy. The $U(1)$ subgroup, which acts on ϵ , corresponds to the $U(1)_R$ of $\mathcal{N} = 1$ SUSY in $D = 4$.

2.2.1 The Orbifold Action

The simplest manifolds of $SU(3)$ holonomy are torii moded out by a discrete symmetry, \mathcal{P} . \mathcal{P} is called the point group of the torus, and to ensure that the low energy spectrum respect $\mathcal{N} = 1$ SUSY, we require that $\mathcal{P} \subset SU(3)$. This is actually a surprisingly strict requirement, and there exist only a few consistent choices of \mathcal{P} , which can be found in the literature [53–55]. Of this subset, we will limit our discussion to those orbifolds which

¹⁰The holonomy group of a manifold tells one how tangent vectors behave under transportation around closed loops on the manifold.

¹¹This requirement can be seen from the supersymmetry transformations. In order that the supersymmetry transformations leave the vacuum invariant, we need an unbroken SUSY generator ϵ . For each ϵ we find, there is a conserved supercharge Q . $\mathcal{N} = 1$ supersymmetry implies that we want exactly one ϵ .

can be factorized into a product of three two-tori: $T^6 \cong T^2 \otimes T^2 \otimes T^2$, though this is not a necessary requirement. The resulting orbifold may be described by a lattice in the complex plane, which we denote Γ . We consider two classes of point groups:

- \mathbb{Z}_N : Cyclic groups of order N describe rotations of the lattice by multiples of $2\pi/N$. More formally:

$$\mathbb{Z}_N \equiv \left\{ \Theta = \theta^k \mid k = 0, \dots, N-1 \right\}; \quad (2.35)$$

- $\mathbb{Z}_N \times \mathbb{Z}_M$: Each factor corresponds to an independent rotation of the lattice, θ_1 and θ_2 .

$$\mathbb{Z}_N \times \mathbb{Z}_M \equiv \left\{ \Theta = \theta_1^k \theta_2^\ell \mid k = 0, \dots, N-1; \ell = 0, \dots, M-1 \right\}. \quad (2.36)$$

Note that the orbifold is also invariant under translations along the lattice (i.e., steps around the torus along one of its cycles), thus we define the space group, S :

$$S \equiv \left\{ g = (\Theta, n_\alpha e_\alpha) \mid \Theta \in \mathcal{P}, n_\alpha \in \mathbb{Z} \right\}. \quad (2.37)$$

Modular invariance (see Section 2.2.3) requires that we embed the space S into the gauge degrees of freedom¹²:

$$S \hookrightarrow G, \quad (2.38)$$

where G is the analogue of the point group in the $E_8 \otimes E_8$ or $SO(32)$ lattice. (Recall, the gauge degrees of freedom come from compactifying sixteen (bosonic) directions on a torus.) Under each of the two classes of point groups, we have

- $\mathbb{Z}_N : (\theta_1^k, n_\alpha e_\alpha) \mapsto (kV, n_\alpha A_\alpha)$, and
- $\mathbb{Z}_N \times \mathbb{Z}_M : (\theta_1^k \theta_2^\ell, n_\alpha e_\alpha) \mapsto (kV_1 + \ell V_2, n_\alpha e_\alpha)$,

for $k, \ell, n_\alpha \in \mathbb{Z}$. The $V_{(1,2)}$ are shifts in the $E_8 \otimes E_8$ or $SO(32)$ lattice, and the A_α are (sixteen component) Wilson lines wrapping the e_α , which also act as shifts in the gauge lattice. Under the action of the gauge twist G ,

$$X^I \rightarrow X^I + kV^I + n_\alpha A_\alpha \quad \text{for } \mathbb{Z}_N, \quad (2.39)$$

$$X^I \rightarrow X^I + kV_1^I + \ell V_2^I + n_\alpha A_\alpha \quad \text{for } \mathbb{Z}_N \times \mathbb{Z}_M. \quad (2.40)$$

Let us close this subsection by formally defining an orbifold as

$$\mathcal{O} = \mathbb{R}^6 / S \otimes T^{16} / G, \quad (2.41)$$

¹²This is the well-known requirement (for vanishing H flux) that any string compactification obey: $\text{TR } R \wedge R = \text{TR } F \wedge F$, where R is the Riemann curvature tensor and F is the Yang-Mills field strength, see [49].

and the orbifold group $S \otimes G$ as

$$\left(\theta^k, n_\alpha e_\alpha ; kV, n_\alpha A_\alpha \right) \in S \otimes G. \quad (2.42)$$

2.2.2 Fixed Points of the Orbifold

The development thus far has been completely general. Let us now specialize to the case where the T^6 is factorizable. Under this assumption, it is sometimes more convenient to represent the torus in terms of complex coordinates:

$$\begin{aligned} Z^a &\equiv \frac{1}{\sqrt{2}} (X^{2a+2} + iX^{2a+3}), \\ Z^{\bar{a}} &\equiv \frac{1}{\sqrt{2}} (X^{2a+2} - iX^{2a+3}). \end{aligned} \quad (2.43)$$

We will also specialize to the case of $\mathcal{P} \sim \mathbb{Z}_N$, as our ultimate goal is to describe the massless spectrum of the \mathbb{Z}_6 -II models.

We define a fixed point as a point which is left invariant by the action of the orbifold group. Each fixed point on the orbifold can be described by that element of the orbifold group which leaves it invariant, called the constructing element $g \equiv (kv, n_\alpha e_\alpha ; kV, n_\alpha A_\alpha) \in S \otimes G$. A fixed point z on the orbifold obeys

$$z = gz = \theta^k z + n_\alpha e_\alpha. \quad (2.44)$$

A string which lives at the fixed point g need only be closed up to orbifold twists and lattice steps:

$$Z(\sigma^+ + 2\pi) = gZ(\sigma^+) = \theta^k Z(\sigma^+) + n_\alpha e_\alpha. \quad (2.45)$$

Physically, this describes a string which is stuck at a fixed point z of the orbifold, with non-zero winding number (if $n_\alpha \neq 0$). This can be seen, for example, by considering the mode expansion in the twisted sector as in Appendix A—one finds that the center of mass coordinate of the twisted string is always localized at a fixed point. We will define the untwisted sector by those points for which $k = 0$. Likewise, a point with a non-zero value of k is said to lie in the k^{th} twisted sector.

Equation (2.45) implies

$$(\mathbb{1} - \theta^k) z \in \Gamma. \quad (2.46)$$

In other words, the space group element g takes the fixed point back to itself, up to shifts of the lattice Γ . The number of fixed points is given by

$$\# \text{ of fixed points} = \det(\mathbb{1} - \Theta). \quad (2.47)$$

Given the constructing element g , we can define the notion of “equivalent” and “in-equivalent” fixed points. Two fixed points z_1 and z_2 , described by the constructing elements g_1 and g_2 , will be considered equivalent if g_1 and g_2 are in the same conjugacy class:

$$g_1 = hg_2h^{-1}, \quad h \in S \otimes G. \quad (2.48)$$

One can show that equivalence of g_1 and g_2 in general implies¹³

$$z_1 = hz_2. \quad (2.49)$$

Thus, under the action of the orbifold, the points z_1 and hz_2 are the same point.

2.2.3 Twists and Shifts

The action (Θ) of the point group in the complexified coordinates (2.43) is specified by a four component vector, v , which acts on the three (complex) compact directions:

$$Z^a \rightarrow e^{2\pi i k v_a} Z^a, \quad a = 1, 2, 3. \quad (2.50)$$

As we have remarked previously, it is clear that Θ corresponds to a rotation in the complex plain. Under the full space group we have

$$Z^a \rightarrow \Theta Z^a = e^{2\pi i k v_a} Z^a + n_a \hat{e}_a, \quad a = 1, 2, 3 \quad (2.51)$$

where $n_a \in \mathbb{Z}$ and the \hat{e}_a are related to the e_α as in Equations (2.43)¹⁴. The requirement of SU(3) holonomy is ensured by

$$\sum_{a=1}^3 v_a = 0 \pmod{2}. \quad (2.52)$$

Below, we will show that this condition projects out exactly three of the gravitino states in Equation (2.30), leading to a massless spectrum which respects $\mathcal{N} = 1$ SUSY in $D = 4$.

The embedding of the spatial degrees of freedom into the gauge degrees of freedom implies a set of constraints on v , V , and A_α . These constraints can be obtained from the one loop partition function of the heterotic string, and we will state (without proof) the

¹³A simple case to prove is the case where h is a pure shift: $h = (\mathbb{1}, n_\alpha e_\alpha)$. Note that if $h = (\theta, n_\alpha e_\alpha)$, $h^{-1} = (\theta^{-1}, -\theta^{-1} n_\alpha e_\alpha)$. See [56], for example.

¹⁴Note that we will switch between the \hat{e}_a and e_α when it is convenient.

result [53, 57]:

$$N(V^2 - v^2) \equiv 0 \pmod{2}, \quad (2.53)$$

$$NV \cdot A_\alpha \equiv 0 \pmod{1}, \quad (2.54)$$

$$NA_\alpha \cdot A_\beta \equiv 0 \pmod{1}, (\alpha \neq \beta), \quad (2.55)$$

$$NA_\alpha^2 \equiv 0 \pmod{2}, \quad (2.56)$$

where N is the order of the orbifold. These conditions are called the *weak* modular invariance constraints, and are sufficient when working with the generalized GSO projectors, see Appendix A of [39]. The advantage of the generalized GSO projectors seems to be that they are easier to automate, but are conceptually more difficult to understand. Below we will describe the “centralizer” method of constructing orbifold states. The advantage of this approach is that it is somewhat easier to understand, but more difficult to automate. In this case, one must require that v, V and A satisfy the *strong* modular invariance constraints:

$$(V^2 - v^2) \equiv 0 \pmod{2}, \quad (2.57)$$

$$V \cdot A_\alpha \equiv 0 \pmod{1}, \quad (2.58)$$

$$A_\alpha \cdot A_\beta \equiv 0 \pmod{1}, (\alpha \neq \beta), \quad (2.59)$$

$$A_\alpha^2 \equiv 0 \pmod{2}. \quad (2.60)$$

Note that we can bring any v, V, A satisfying Equations (2.53)-(2.56) into strong modular invariant form by simply adding $\text{SO}(8)$, $E_8 \otimes E_8$ or $\text{SO}(32)$ lattice vectors, as appropriate.

2.3 Building Orbifold-Invariant States

In order to motivate the following, consider the Hilbert space of states of a free particle living in \mathbb{R} , $\mathcal{H}_{\mathbb{R}}$. We mod \mathbb{R} by the translation group \mathbb{Z} , obtaining S^1 . Now consider translations v in \mathbb{Z} , which are generated by $e^{ip \cdot v}$. Clearly, all states in $\mathcal{H}_{\mathbb{R}}$ do not survive the compactification—the geometry imposes the requirement that the wave-function of the free particle be periodic. States which *do* survive the compactification obey $\Phi(x + 2\pi) = \Phi(x)$. Thus, in order to construct the massless spectrum of this theory, we must project onto states which are invariant under the action of the translation operator.

This example can be extended to a closed string living on the D torus, $T^D = \mathbb{R}^D / \mathbb{Z}^D$ [57]. In that case we project onto those states for which the translation operator acts trivially on the string’s wave-function. But the string can also wrap one of the cycles of the torus, so we must also take into account those states which come back to themselves up to a lattice shift, which define new sectors of the theory \mathcal{H}_v . When we have an orbifold

(or more generally, fixed points), we must further consider only those strings which come back to themselves up to an element of the space group.

After constructing the spectrum of the heterotic string, we were left with some Hilbert space of physical states $|\phi\rangle = |p\rangle_L \otimes |q\rangle_R \in \mathcal{H}$. As in the examples above, we want to know how these states transform under the orbifold group $S \otimes G$, and what subset of states in \mathcal{H} appear in the massless spectrum. As we discovered in the example above, we must be careful to include *all* massless states—the presence of stringy degrees of freedom above led to additional states in the physical spectrum. We will find that this is indeed the case in the twisted sector of the theory.

2.3.1 Invariant States in the Untwisted Sector

In the untwisted sector, states must be invariant under the entire orbifold group $S \otimes G$. We first consider the generators of translation, and their action on the states in the untwisted sector. Under some element $h \in S \otimes G$, we have

$$|p\rangle_L \xrightarrow{h} e^{-2\pi i p \cdot X} |p\rangle_L, \quad p \cdot X \equiv p^I X^I, \quad (2.61)$$

where we explain the sign in the exponent below. Under the action of $S \otimes G$ we have

$$X^I \xrightarrow{h} X^I + kV + n_\alpha A_\alpha, \quad (2.62)$$

which implies that states in the left-moving sector transform as

$$|p\rangle_L \xrightarrow{h} e^{-2\pi i p \cdot (kV + n_\alpha A_\alpha)} |p\rangle_L. \quad (2.63)$$

Similarly, the right-movers transform as

$$|q\rangle_R \xrightarrow{h} e^{2\pi i q \cdot (kv)} |q\rangle_R. \quad (2.64)$$

We note the minus sign difference between the transformation of the left movers and the right movers. This minus sign comes from the fact that the momentum lattice is Lorentzian [58, 59]¹⁵. The oscillators with indices (μ, i) transform as follows:

$$\tilde{\alpha}_{-1}^{I,\mu} \xrightarrow{h} \tilde{\alpha}_{-1}^{I,\mu}, \quad \mu = 1, 2 \quad I = 1, \dots, 16 \quad (2.65)$$

$$\tilde{\alpha}_{-1}^a \xrightarrow{h} e^{2\pi i k v_a} \tilde{\alpha}_{-1}^a, \quad a = 1, 2, 3, \quad (2.66)$$

$$\tilde{\alpha}_{-1}^{\bar{a}} \xrightarrow{h} e^{-2\pi i k v_a} \tilde{\alpha}_{-1}^{\bar{a}}, \quad \bar{a} = 1, 2, 3. \quad (2.67)$$

¹⁵We have chosen to take the left movers to transform with a minus sign, but one could equally take the right movers to transform with a minus sign. The effect of changing this convention in the massless spectrum is superficial: the k^{th} and $(N - k)^{\text{th}}$ twisted sectors will be exchanged.

Equations (2.63), (2.64) and (2.65)-(2.67), a physical state transforms as

$$|\phi\rangle \xrightarrow{h} e^{2\pi i [R \cdot kv - p \cdot (kV + n_\alpha A_\alpha)]} |\phi\rangle. \quad (2.68)$$

We have defined the R charge to take into account both the right moving momentum and the oscillator number:

$$R^a \equiv q^a + N^a - \bar{N}^{\bar{a}}. \quad (2.69)$$

Clearly, invariant states in the untwisted sector must obey

$$R \cdot kv - p \cdot (kV + n_\alpha A_\alpha) = 0 \pmod{1}, \quad (2.70)$$

for all k, n_α .

2.3.2 Invariant States in the Twisted Sector

Constructing states invariant under $S \otimes G$ in the twisted sector is a bit more subtle than in the untwisted case—this stems from the presence of additional states, localized at fixed points, which appear in the massless spectrum. We would like to understand what conditions these states must obey.

In general, there are $N - 1$ twisted sectors, labeled by k . In Appendix A, we derive the mode expansion of the twisted sector states, and address some subtleties regarding the (fractionally moded) oscillators. The mode expansions are qualitatively different, which results in a deformation of both the $SO(8)$ and $E_8 \otimes E_8$ weight lattices. One can show that the right-movers in the k th twisted sector come from a shifted $SO(8)$ lattice:

$$\hat{q}^a \equiv q^a + kv^a, \quad (2.71)$$

where k is determined by the constructing element, g , of the fixed point. The mass equation also changes:

$$\alpha' M_R^2 = \hat{q}^2 - 1 - 2\delta, \quad (2.72)$$

where δ is the new zero point energy, and is defined as

$$\delta = \frac{1}{2} \sum_{a=1}^3 \eta^a (1 - \eta^a), \quad (2.73)$$

where $\eta^a = kv^a \pmod{1}$ such that $0 \leq \eta^a < 1$. Note that this contribution to the massless condition is clearly different for each twisted sector k .

Likewise, in the left-moving sector, the $E_8 \otimes E_8$ lattice is shifted at each fixed point:

$$\hat{p}^I = p^I + kV^I + n_\alpha A_\alpha^I, \quad (2.74)$$

where k and n_α are determined by the constructing element. The new mass equation for the left-movers is given by

$$\alpha' M_L^2 = \hat{p}^2 + 2\tilde{N} - 2 + 2\delta. \quad (2.75)$$

Solving Equations (2.72) and (2.75) is a non-trivial problem, however, a clever algorithm to do so is presented in [60].

At each fixed point g , Equations (2.72) and (2.75) define a Hilbert space of states \mathcal{H}_g . But we are not guaranteed that all of the states in \mathcal{H}_g will be invariant under the orbifold group $S \otimes G$. The states \mathcal{H}_g are confined at g , and only “know about” the orbifold in their neighborhood. But the orbifold itself is invariant under a larger set of orbifold operations. To construct the subset of \mathcal{H}_g which survives into the massless spectrum, we consider some element of the orbifold group $h \equiv (\kappa v, m_\alpha e_\alpha ; \kappa V, m_\alpha A_\alpha) \in S \otimes G$. We have one of two possibilities: either $[h, g] = 0$ or $[h, g] \neq 0$.

If $[h, g] = 0$, then one may write

$$hZ(\sigma^+ + 2\pi) = hgZ(\sigma^+) = ghZ(\sigma^+). \quad (2.76)$$

Thus the state hZ is periodic up to the action of g , and must be a state in the Hilbert space \mathcal{H}_g . The crucial point is that the action of the orbifold *identifies* the points Z and hZ because $[g, h] = 0 \Rightarrow g = hgh^{-1}$. Equation (2.49) then implies that h acts trivially on the state Z , and thus must act trivially on the entire Hilbert space \mathcal{H}_g . Moreover, any element of \mathcal{H}_g which is not invariant under the action of any h which commutes with g *must* be projected out from the space of physical states.

In principle, the number of possible hs is infinite, as we can always find another equivalent h at another place on the lattice by taking a few steps¹⁶. In practice, we can simply generate a large set of states h which commute with g (which is known). The set of hs which satisfy $[h, g] = 0$ is known as the “centralizer”, and is denoted with $\mathcal{Z}(g)$.

Practically, this means that physical states in the twisted sector transform as

$$\tilde{\alpha} |\hat{p}\rangle_L \otimes |\hat{q}\rangle_R \xrightarrow{h} e^{2\pi i [\kappa R \cdot v - \hat{p} \cdot (\kappa V + m_\alpha A_\alpha)]} \tilde{\alpha} |\hat{p}\rangle_L \otimes |\hat{q}\rangle_R. \quad (2.77)$$

Note that we have included the possibility of oscillator states, which transform as

$$\begin{aligned} \tilde{\alpha}_{n-\eta_a}^a &\rightarrow e^{2\pi i \kappa v_a} \tilde{\alpha}_{n-\eta_a}^a, \\ \tilde{\alpha}_{n+\eta_a}^{\bar{a}} &\rightarrow e^{-2\pi i \kappa v_a} \tilde{\alpha}_{n+\eta_a}^{\bar{a}}. \end{aligned} \quad (2.78)$$

We define R in terms of the *integer* oscillator number and \hat{q} :

$$R^a \equiv \hat{q}^a + N^a - \bar{N}^{\bar{a}}. \quad (2.79)$$

¹⁶If $[h, g] = 0$, then $[h^2, g] = 0$. It is clear, though, that any state invariant under h should also be invariant under h^2 , thus h^2 can imply no new projection conditions.

The state is invariant under the action of h if and only if

$$R \cdot \kappa v - \hat{p} \cdot (\kappa V + m_\alpha A_\alpha) = 0 \pmod{1}. \quad (2.80)$$

Alternatively, it could be that $[h, g] \neq 0$. In this case

$$hZ(\sigma^+ + 2\pi) = hgZ(\sigma^+) = hgh^{-1}hZ(\sigma^+), \quad (2.81)$$

where the action of h maps a state in \mathcal{H}_g to $\mathcal{H}_{hgh^{-1}}$. Likewise, the action of h maps a state in $\mathcal{H}_{hgh^{-1}}$ to $\mathcal{H}_{h^2gh^{-2}}$, etc. In order to construct a physical state, then, one must combine states in each of the $\mathcal{H}_{h^ngh^{-n}}$. We emphasize that no states are projected out by this condition, rather, this tells us how to build interaction eigenstates (in the sense of four dimensional physics) from “orbifold eigenstates” [38].

This last case is important when counting the states on the orbifold. For example, if three fixed points (g_1 , g_2 , and g_3) are in the same conjugacy class, the massless spectrum *will not include* all of the states which are invariant under $\mathcal{Z}(g_1)$, $\mathcal{Z}(g_2)$, and $\mathcal{Z}(g_3)$ independently. Rather, invariant states from \mathcal{H}_{g_1} , \mathcal{H}_{g_2} , and \mathcal{H}_{g_3} must be combined (with the appropriate phases) to form interaction eigenstates. The phases are determined by the action of h on the states at the g_1 , g_2 , and g_3 . Each linear combination of states will be comprised of a state from each of \mathcal{H}_{g_1} , \mathcal{H}_{g_2} , and \mathcal{H}_{g_3} , giving an overall reduction in the number of states in the massless spectrum. We will encounter an explicit example of this point in Chapter 2.6.3.

2.4 The \mathbb{Z}_6 -II Orbifold Geometry

For the remainder of this Chapter, we will specialize our discussion to the case of the \mathbb{Z}_6 -II orbifold. The \mathbb{Z}_6 -II orbifold is defined by the twist vector

$$v \equiv \frac{1}{6} (0, 1, 2, -3), \quad (2.82)$$

corresponding to a rotation by $2\pi \times 1/6$ in the first torus, a rotation by $2\pi \times 1/3$ in the second torus, and a rotation by $2\pi \times (-1/2)$ in the third torus. We choose the compact dimensions (consistent with v) to be the root lattice (Γ) of

$$\Gamma \equiv G_2 \otimes \text{SU}(3) \otimes \text{SO}(4). \quad (2.83)$$

We note that this choice is not unique, however, it is the only lattice which factorizes as $T^6 \cong T^2 \otimes T^2 \otimes T^2$.

We note a peculiar feature of this particular orbifold. If we consider $k = 1, \dots, 5$, then

$$2 \cdot v = \frac{1}{3} (0, 1, 2, 0), \quad 4 \cdot v = \frac{1}{3} (0, 2, 1, 0) \quad 3 \cdot v = \frac{1}{2} (0, 1, 0, -1). \quad (2.84)$$

| | e_1 | e_2 | e_3 | e_4 | e_5 | e_6 |
|------------|---------------|----------------|--------------|--------------|--------|--------|
| θ^1 | $-e_1 + e_2$ | $-3e_1 + 2e_2$ | e_4 | $-e_3 - e_4$ | $-e_5$ | $-e_6$ |
| θ^2 | $-2e_1 + e_2$ | $-3e_1 + e_2$ | $-e_3 - e_4$ | e_3 | e_5 | e_6 |
| θ^3 | $-e_1$ | $-e_2$ | e_3 | e_4 | $-e_5$ | $-e_6$ |
| θ^4 | $e_1 - e_2$ | $3e_1 - 2e_2$ | e_4 | $-e_3 - e_4$ | e_5 | e_6 |
| θ^5 | $2e_1 - e_2$ | $3e_1 - e_2$ | $-e_3 - e_4$ | e_3 | $-e_5$ | $-e_6$ |

Table 2.1: The action of the orbifold twists on Γ . Note that θ^2 and θ^4 leave the third torus fixed, while θ^3 leaves the second torus fixed. The first torus is rotated by θ^k for $1 \leq k \leq 5$.

Notice that the third torus is left invariant by $2 \cdot v$ and $4 \cdot v$, while the second torus is left invariant by $3 \cdot v$. In the second/fourth twisted sector, the third torus is “fixed”, while the second torus is fixed in the third twisted sector. The implication is that strings living in the second/fourth or third twisted sectors are free to move in six dimensions, while strings in the first and fifth twisted sector are confined to move only in the four large space-time dimensions¹⁷.

In the case where no torii are left un-rotated by the action of some particular g , it is straightforward to evaluate Equation (2.46) directly, however, when dealing with the non-prime orbifolds, subtleties arise. To demonstrate these subtleties directly, we offer an example. Without loss of generality, let us consider the second twisted sector. If we solve Equation (2.47) directly, we find that there should be nine fixed points in the second twisted sector: three in the first torus, three in the second torus, and none in the third torus. However, the three fixed points in the first twisted sector (g_1 , g_2 , and g_3) are not independent. They are given by

$$\begin{aligned} g_1 &= (\theta^2, 0), \\ g_2 &= (\theta^2, e_1), \\ g_3 &= (\theta^2, 2e_1). \end{aligned} \tag{2.85}$$

If we define

$$h \equiv (\theta, e_1), \tag{2.86}$$

then using Table 2.1 one can check that $g_3 = hg_2h^{-1}$, and g_2 and g_3 are in the same conjugacy class, see Equation (2.81). One can check that the same behavior occurs in the fourth twisted sector. The third twisted sector also exhibits similar behavior.

¹⁷If we imagine “blowing up” one of the fixed torii, we are left with a six dimensional model, with some matter confined to four dimensional hypersurfaces in the six dimensional space, and some matter free to propagate in all six dimensions. See Chapter 3.

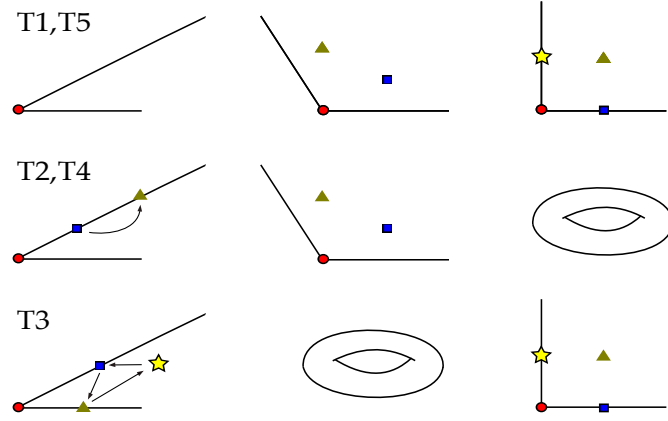


Figure 2.1: The geometry of the compact dimensions. In the first (fifth) twisted sector, there are 12 fixed points. The second (fourth) twisted sector has six fixed points, and in the third twisted sector there are 8 fixed points. We denote this lattice by Γ .

The geometry of the \mathbb{Z}_6 -II orbifold is pictured in Figure 2.1. The first twisted sector has $12 = 1 \times 3 \times 4$ fixed points and no fixed torii, while the second (fourth) twisted sector has $6 = 2 \times 3$ fixed points and the third twisted sector has $16 = 4 \times 4$ fixed points.

2.5 Orbifold Compactification: The Untwisted Sector of \mathbb{Z}_6 -II

We will choose the gauge lattice to be $E_8 \otimes E_8$, and work with the so-called “standard embedding”:

$$\begin{aligned} v &\equiv \frac{1}{6} (0, 1, 2, -3), \\ V &\equiv \frac{1}{6} (1, 2, -3, 0^{13}) (0^{16}), \\ A_\alpha &\equiv 0. \end{aligned} \tag{2.87}$$

This choice of V corresponds to a direct embedding of the space degrees of freedom v into the gauge degrees of freedom V , and is a common starting point for string model builders from every corner of the landscape.

The untwisted sector of any orbifold model is straightforward to compute. First, consider the transformation of the SUGRA multiplet. For oscillators with indices labeled by μ we have:

$$\tilde{\alpha}_{-1}^\mu |0\rangle_L \otimes |q\rangle_R \rightarrow e^{2\pi i k(R \cdot v - 0 \cdot V)} \tilde{\alpha}_{-1}^\mu |0\rangle_L \otimes |q\rangle_R \tag{2.88}$$

The left mover transforms trivially, thus it must be that $k(R \cdot v) = 0 \pmod{1}$ for every value of k . Note that this can be ensured only for

$$|q\rangle_R = \begin{cases} |\pm 1, 0, 0, 0\rangle & \text{NS} \\ \pm |\frac{1}{2} \frac{1}{2} \frac{1}{2} \frac{1}{2}\rangle & \text{R} \end{cases} \quad (2.89)$$

The two states in the NS sector correspond to the two polarizations of a (massless) graviton in four dimensions, while the two states in the R sector give the two chiralities of a gravitino. Thus we conclude that the low energy spectrum should exhibit $\mathcal{N} = 1$ supersymmetry.

There are also states in the SUGRA multiplet which have indices in the internal directions:

$$\tilde{\alpha}_{-1}^a |0\rangle_L \otimes |q\rangle_R \rightarrow e^{2\pi i k(R \cdot v - 0 \cdot V) + 2\pi i v^a} \tilde{\alpha}_{-1}^a |0\rangle_L \otimes |q\rangle_R. \quad (2.90)$$

These correspond to *former* gravitons, which (after compactification) live in chiral multiplets and are (of course) gauge singlets: these states are the chiral singlet moduli which parametrize the sizes and shapes of the internal dimensions. In terms of the NS right movers, we have:

$$\begin{cases} \tilde{\alpha}_{-1}^1 |0\rangle_L \otimes |0, -1, 0, 0\rangle, \\ \tilde{\alpha}_{-1}^2 |0\rangle_L \otimes |0, 0, -1, 0\rangle, \\ \tilde{\alpha}_{-1}^3 |0\rangle_L \otimes |0, 0, 0, 1\rangle, \end{cases} \quad (2.91)$$

with similar expressions for the $\tilde{\alpha}_{-1}^{\bar{a}}$. Their fermionic partners come from the NS sector:

$$\begin{cases} \tilde{\alpha}_{-1}^1 |0\rangle_L \otimes |-\frac{1}{2} - \frac{1}{2} + \frac{1}{2} + \frac{1}{2}\rangle, \\ \tilde{\alpha}_{-1}^2 |0\rangle_L \otimes |-\frac{1}{2} + \frac{1}{2} - \frac{1}{2} + \frac{1}{2}\rangle, \\ \tilde{\alpha}_{-1}^3 |0\rangle_L \otimes |-\frac{1}{2} + \frac{1}{2} + \frac{1}{2} - \frac{1}{2}\rangle, \end{cases} \quad (2.92)$$

We can symmetrize their indices, for example, and get the metric of the internal dimensions:

$$G_{ij} = e_i \cdot e_j, \quad (2.93)$$

where i, j are internal indices, and the $e_{i,j}$ are the basis vectors of the internal torii. One may write the T and U moduli in terms of the components of G_{ij} , see Chapter 5.

Next, we consider the adjoint $(248, 1) \oplus (1, 248)$ representation of $E_8 \otimes E_8$. All of the states in the untwisted sector are subsets of this representation. The uncharged gauge bosons transform as

$$\tilde{\alpha}_{-1}^I |0\rangle_L \otimes |q\rangle_R \rightarrow e^{2\pi i k(R \cdot v - 0 \cdot V)} \tilde{\alpha}_{-1}^I |0\rangle_L \otimes |q\rangle_R. \quad (2.94)$$

As before, the right-movers consistent with this transformation are

$$|q\rangle_R = \begin{cases} |\pm 1, 0, 0, 0\rangle & \text{NS} \\ \pm |\frac{1}{2} \frac{1}{2} \frac{1}{2} \frac{1}{2}\rangle & \text{R} \end{cases} \quad (2.95)$$

These correspond to sixteen massless vector bosons (in four dimensions) and their supersymmetric partners (gauginos). Because we end up with sixteen uncharged gauge bosons, the rank of the resulting gauge group will be sixteen, as will always be the case when breaking the gauge symmetry using discrete shifts (V or A) in the $E_8 \otimes E_8$ lattice.

Finally, we consider the charged $E_8 \otimes E_8$ gauge bosons. These states will give the charged gauge bosons of the surviving gauge symmetry in the low energy theory, as well as the charged matter present after compactification. We note that the charged gauge bosons in the low energy theory should have the same right-movers as the *uncharged* gauge bosons, Equation (2.95). Clearly, we wish to find all p consistent with

$$k(p \cdot V) = 0 \pmod{1}. \quad (2.96)$$

We find 72+240 states consistent with this condition (72 from the first E_8 factor and 240 from the second). As it turns out, the representation of the gauge bosons is

$$(78, 1) \oplus (1, \mathbf{248}) \oplus (1, 1) \oplus (1, 1). \quad (2.97)$$

The unbroken gauge symmetry can only be

$$E_6 \otimes U(1)^2 \otimes E_8. \quad (2.98)$$

To determine the charged matter content of the model, we first realize that the right-movers from the NS sector should be given by

$$|q\rangle_R = |0, \pm 1, 0, 0\rangle. \quad (2.99)$$

These states correspond to the scalar degrees of freedom living in the chiral multiplets. As an example, let us consider $|q\rangle_R = |0, -1, 0, 0\rangle$. We find

$$\begin{array}{cccccc} k & = & 1 & 2 & 3 & 4 & 5 \\ \Rightarrow R \cdot kv & = & -\frac{1}{6} & -\frac{1}{3} & -\frac{1}{2} & -\frac{2}{3} & -\frac{5}{6} \end{array} \quad (2.100)$$

In order to form a chiral multiplet, however, we must find the state from the Ramond sector with the same transformation properties. One can check that the left chiral $|q\rangle_R = |-\frac{1}{2}, -\frac{1}{2}, +\frac{1}{2}, +\frac{1}{2}\rangle$ transforms appropriately. Next, we find the subset of lattice vectors $|p\rangle_L$ which give us invariant states. We find a total of 29 states $|p\rangle_L$ which transform correctly. We know that the smallest representation of E_6 is 27 dimensional, thus we must have that

these states correspond to a $\mathbf{27} \oplus \mathbf{1} \oplus \mathbf{1}$ under¹⁸ $E_6 \otimes U(1)^2$. Note that no charged matter remains in the second E_8 . The entire charged matter spectrum of the untwisted sector contains

$$3 \times [(\overline{\mathbf{27}}, 1) + (1, 1)] + (\mathbf{27}, 1). \quad (2.101)$$

Dealing with $U(1)$ Charges

In what follows, we will neglect the two $U(1)$ factors, simply noting that every state has some charge under both of the $U(1)$ factors. The task of calculating the charges under the $U(1)$ factors is straightforward but tedious: we know that $E_6 \otimes E_8$ has 14 simple roots and we know what those simple roots are. We can project these 14 simple roots (α_i) onto the 16 simple roots of $E_8 \otimes E_8$ (ε_j), giving us a matrix $[\mathbb{B}]_{ij} = \alpha_i \cdot \varepsilon_j$. If we multiply every entry in \mathbb{B} by 4, we can be assured that $[\mathbb{B}]_{ij} \in \mathbb{Z}$. We then seek solutions ξ such that

$$\mathbb{B}\xi = 0, \quad (2.102)$$

where the elements of ξ are integers¹⁹. This is a system of Diophantine equations, and algorithms can be found in the mathematical literature for solving them [62]. The $U(1)$ charges can then be determined by taking the dot product of ξ with the highest weight of each representation.

We are interested in the $U(1)$ charges for several reasons. First, we must be able to construct hypercharge in order to be able to claim that we can construct the standard model. Other $U(1)$ charges, like $U(1)_{B-L}$ are also of interest to model builders, and we would like to be able to incorporate such features into our string models. From the stringy perspective, the Green-Schwarz [63, 64] mechanism implies that one or both of these $U(1)$ factors is anomalous²⁰. Determining the anomalies, then, just amounts to tracing over the $U(1)$ charges of all of the states in the spectrum. Some methods for dealing with these issues are described in [56].

2.5.1 Identifying Gauge Groups and Matter Representations

When working with more complicated shift vectors V and non-trivial Wilson lines, the gauge symmetries obtained are much smaller than E_6 and E_8 . In these cases, it is much more difficult, if not impossible, to uniquely determine the charged matter representations by inspection. In this subsection, we wish to describe how one may unambiguously determine the representations of the charged matter.

In order to calculate the gauge group, the process goes as follows:

¹⁸Generally, determining the $U(1)$ charges of the states on the orbifold is non-trivial, however, in the untwisted sector, one can simply look up the branching rules in [61], for example.

¹⁹Requiring $\xi \in \mathbb{Z}$ ensures that the $U(1)$ charges will be rational.

²⁰We can always “rotate” to a basis where only a single $U(1)$ factor is anomalous.

- Determine the $E_8 \otimes E_8$ roots which transform as $k(p \cdot V) = 0 \pmod{1}$, and find a set of basis vectors.
- Identify the positive roots. A positive root is a root whose first entry is positive.
- Identify the simple roots, α_i . A simple root may not be expressed as the sum of two other positive roots.
- Count $U(1)$ factors. The number of $U(1)$ factors is sixteen minus the number of simple roots. This gives the dimension of the Cartan matrix.
- Calculate the Cartan matrix:

$$[\mathbb{A}]_{ij} = \frac{2\alpha_i \cdot \alpha_j}{\alpha_j^2}. \quad (2.103)$$

The Cartan matrix for each gauge group is unique (see [61]), and thus allows one to (uniquely) determine the resulting gauge group.

In order to identify the surviving gauge group, it is advantageous to reorder the roots so that the Cartan matrix has factors of 2 along the main diagonal.

Once one has a set of simple roots, it is then easy to determine the representations of the surviving charged matter:

- Determine the Dynkin labels of each weight. The i th Dynkin label of a weight is the dot product of the weight with the i th simple root.
- Identify the highest weights. The highest weights are those whose entries are all positive or zero. Each charged matter representation has a highest weight, thus it is sufficient to keep only the highest weights from this point forward.
- The dimensions of the representations can be identified using the tables in [61], or one can compute them directly: see Equation (5.5) of [61], for example.

2.6 Orbifold Compactification: The Twisted Sectors of \mathbb{Z}_6 -II

In this section, we will construct the twisted sector the the standard embedding in great detail. In addition to listing the centralizers for several fixed points, we will also list several of the solutions to the mass equations. The hope is that this will provide those who wish to automate this procedure an important sanity check in their calculations. At the time of writing, no publicly available code to perform these calculations exists, however, at least one collaboration (see [56, 65]) is working to this end.

2.6.1 Constructing the Centralizer

The development in Section 2.3.2 was rather formal. We will pause here and demonstrate how one actually might go about constructing the centralizer. We first note, that without doing any calculation, we can find two elements of the centralizer right out. Clearly, $g\mathbb{1} = \mathbb{1}g$. Moreover, g commutes with itself. Thus $\mathcal{Z}(g)$ must contain at least $\mathbb{1}$ and g itself.

Consider the fixed point \star in the $\text{SO}(4)$ torus, but at the origin of the other two torii of the \mathbb{Z}_6 -II orbifold (see Figure 2.1). The constructing element for this fixed point is

$$g_{\bullet\bullet\star} = (\theta, e_6). \quad (2.104)$$

In other words, \star transforms into itself if we rotate the lattice by π radians and step back along e_6 . In order to construct the centralizer for this fixed point, we need to find some set of h such that $[g, h] = 0$. Consider $h = (\theta^3, e_6)$. This corresponds to a rotation of the lattice by 3π radians, and a translation along e_6 . Because a rotation by 3π is equivalent to a rotation by π , clearly $[(\theta, e_6), (\theta^3, e_6)] = 0$.

Let's try a less trivial example. Consider the fixed point \blacksquare in the second ($\text{SU}(3)$) torus, and at the origin of the other two torii, whose constructing element is

$$g_{\bullet\blacksquare\bullet} = (\theta, e_3). \quad (2.105)$$

Consider $h = (\theta^2, e_3 + e_4)$. Then, for some point x , we have (using Table 2.1)

$$(\theta, e_3) (\theta^2, e_3 + e_4) x = (\theta, e_3) (\theta^2 x + e_3 + e_4) = \theta^3 x + e_4 - e_3 - e_4 + e_3 = \theta^3 x. \quad (2.106)$$

Similarly,

$$(\theta^2, e_3 + e_4) (\theta, e_3) x = (\theta^2 x + e_3 + e_4) (\theta x + e_3) = \theta^3 x + \theta^2 e_3 + e_3 + e_4 = \theta^3 x. \quad (2.107)$$

As a final example, consider the fixed point at \blacksquare in the second ($\text{SU}(3)$) torus and at \star in the $\text{SO}(4)$ torus. The constructing element for this fixed point is given by

$$g_{\bullet\blacksquare\star} = (\theta, e_3 + e_6). \quad (2.108)$$

One can check using Table 2.1 that the following choices of h all commute with g :

$$h = \begin{cases} (\theta, e_3, e_6), \\ (\theta^2, e_3, e_4), \\ (\theta^3, e_6), \\ (\theta^4, e_3), \\ (\theta^5, e_3, e_4, e_6) \end{cases} \quad (2.109)$$

Given the multiplication rules in Table 2.1, one can then either construct the centralizers for each fixed point by hand, or automate the process to generate the centralizers.

2.6.2 The First and Fifth Twisted Sectors

In the first twisted sector, the (right-moving) massless condition is satisfied by

$$\eta = \left(0, \frac{1}{6}, \frac{1}{3}, \frac{1}{2} \right). \quad (2.110)$$

Two right-movers satisfy the massless condition (2.72):

$$|\hat{q}\rangle_R = \begin{cases} |0, \frac{1}{6}, \frac{1}{3}, \frac{1}{2}\rangle, \\ |\frac{1}{2}, -\frac{1}{3}, -\frac{1}{6}, 0\rangle \end{cases}. \quad (2.111)$$

Note that these two states correspond to half of an $\mathcal{N} = 1$ chiral multiplet in four dimensions. The other real scalar and real fermion degree of freedom are in the fifth twisted sector. This is a general feature of orbifold models: the conjugate partners of the states in the k th twisted sector are always found in the $(N - k)$ th twisted sector. Under the action of the twist, the right movers transform as

$$|\hat{q}\rangle_R \rightarrow e^{2\pi i R \cdot v} |\hat{q}\rangle = e^{2\pi i \left(\frac{-1}{9}\right)} |\hat{q}\rangle. \quad (2.112)$$

The massless condition (2.75) yields 27 solutions at each of the (12) fixed points, all of which transform as (recall the relative minus sign in the transformation between the left movers and the right movers)

$$|\hat{p}\rangle \rightarrow e^{-2\pi i k \hat{p} \cdot V} |\hat{p}\rangle = e^{-2\pi i \left(-\frac{1}{9}\right)} |\hat{p}\rangle. \quad (2.113)$$

For example, at $g_{\bullet \blacksquare \blacktriangle}$ we find

$$\begin{aligned} & \left(\frac{1}{6}, \frac{1}{3}, \frac{1}{2}, \pm 1, 0, 0, 0, 0 \right) (0^8) \times 10, \\ & \left(-\frac{1}{3}, -\frac{1}{6}, 0, \left[\text{odd } \# + \frac{1}{2} \right] \right) (0^8) \times 16, \\ & \left(-\frac{5}{6}, -\frac{2}{3}, -\frac{1}{2}, 0^5 \right) (0^8) \times 1. \end{aligned} \quad (2.114)$$

In general, if there are no Wilson lines, the centralizer implies no new projection conditions. We will list here the centralizers for three fixed points, and one can check explicitly that

this is indeed the case.

$$\begin{aligned}\mathcal{Z}(g_{\bullet\bullet\bullet}) &= \{\mathbf{1}, (\theta^\kappa, 0)\}, \quad \kappa = 1, 2, 3, 4, 5 \\ \mathcal{Z}(g_{\bullet\bullet\star}) &= \{\mathbf{1}, (\theta, e_6), (\theta^2, 0), (\theta^3, e_6), (\theta^4, 0), (\theta^5, e_6)\}, \\ \mathcal{Z}(g_{\bullet\blacksquare\star}) &= \{\mathbf{1}, (\theta, e_3 + e_6), (\theta^2, e_2 + e_3), (\theta^3, e_6), (\theta^4, e_3), (\theta^5, e_3 + e_4 + e_6)\}\end{aligned}\quad (2.115)$$

The easy way to see that all \mathcal{Z} in Equation (2.115) imply the same projection condition is to note that, for $A_\alpha = 0$, the phase of the left movers under translations becomes

$$\hat{p} \cdot (\kappa V + m_\alpha A_\alpha) \rightarrow \hat{p} \cdot \kappa V. \quad (2.116)$$

Because there is no dependence on m_α , all of the centralizers imply the same projection conditions—from Equation (2.115) we see that all three centralizers imply $\kappa = 1, 2, 3, 4, 5$. One can then check by hand that all of the solutions in Equation (2.114) survive.

Counting oscillator states (see Appendix A for the explicit calculation) gives an additional 4 singlets at each fixed point. The left-chiral pieces (which complete the supermultiplets) are found in the fifth twisted sector. In summary, in the first twisted sector, we find

$$12 \times (\mathbf{27}, 1)_r + 12 \times 4 \times (1, 1)_r, \quad (2.117)$$

where r denotes the chirality of the state.

We close this section by noting that the spectrum at each of the fixed points is identical. The reason for this stems from the fact that we have turned all of the Wilson lines off. This is a common occurrence in the orbifold models in this limit: the Wilson lines serve not only to break the gauge group and representations to smaller sizes, but can also serve to distinguish between otherwise identical points on the orbifold, see Equation (??) for example. This idea of using Wilson lines to split the spectra at various fixed points is the cornerstone of the “local GUT” picture that emerges from the heterotic string models, and provides a successful embedding of the orbifold GUT picture into string theory, see Chapter 3.

2.6.3 The Second and Fourth Twisted Sector

In the second and fourth twisted sectors, there are nine fixed points. Six of the fixed points are related by a symmetry of the orbifold, and the third torus is left unaffected by the action of the twist vector:

$$2v = \frac{1}{3} (0, 1, 2, 0), \quad 4v = \frac{1}{3} (0, 2, 1, 0). \quad (2.118)$$

| | θ^1 | θ^2 | θ^3 | θ^4 | θ^5 |
|---|----------------|------------|----------------|------------|----------------|
| $(27\rangle + 1\rangle) \otimes \frac{1}{2}, \dots\rangle$ | 0 | 0 | 0 | 0 | 0 |
| $(27\rangle + 1\rangle) \otimes -\frac{1}{2}, \dots\rangle$ | $-\frac{1}{2}$ | 0 | $\frac{1}{2}$ | 0 | $-\frac{1}{2}$ |
| $(\overline{27}\rangle + 1\rangle) \otimes \frac{1}{2}, \dots\rangle$ | $\frac{1}{2}$ | 0 | $-\frac{1}{2}$ | 0 | $\frac{1}{2}$ |
| $(\overline{27}\rangle + 1\rangle) \otimes -\frac{1}{2}, \dots\rangle$ | 0 | 0 | 0 | 0 | 0 |

Table 2.2: The transformation of the states in the second twisted sector.

There are two solutions to the (right-moving) massless condition for the R states in the second twisted sector. They are given by

$$|\hat{q}\rangle = \begin{cases} \left| -\frac{1}{2}, -\frac{1}{6}, \frac{1}{6}, \frac{1}{2} \right\rangle, \\ \left| \frac{1}{2}, -\frac{1}{6}, \frac{1}{6}, -\frac{1}{2} \right\rangle \end{cases}, \quad (2.119)$$

with corresponding states in the NS sector:

$$|\hat{q}\rangle = \begin{cases} \left| 0, -\frac{2}{3}, -\frac{1}{3}, 0 \right\rangle, \\ \left| 0, \frac{1}{3}, \frac{2}{3}, 0 \right\rangle \end{cases}, \quad (2.120)$$

First, we concentrate on the three fixed points at the origin of the G_2 torus: (\bullet, \bullet, T^2) , $(\bullet, \blacksquare, T^2)$, and $(\bullet, \blacktriangle, T^2)$. The constructing element of the latter point is

$$g_{(\bullet, \blacktriangle, T^2)} = (\theta^2, e_3 + e_4). \quad (2.121)$$

The centralizer for $g_{(\bullet, \blacktriangle, T^2)}$ is

$$\mathcal{Z}(g_{(\bullet, \blacktriangle, T^2)}) = \{(\theta^{0 \text{ or } 3}, ae_5 + be_6), (\theta^{1 \text{ or } 4}, e_3 + ae_5 + be_6), (\theta^{2 \text{ or } 5}, e_3 + e_4 + ae_5 + be_6)\}, \quad (2.122)$$

where $a, b = 0, 1$. The centralizers for the other two fixed points are similar, and we will not list them here. The massless conditions (2.75) have 28 solutions at each fixed point. We find (at $g_{(\bullet, \blacktriangle, T^2)}$):

$$\begin{aligned} & \left(\frac{1}{3}, \frac{2}{3}, 0, \pm 1, 0, 0, 0, 0 \right) (0^8) \times 10, \\ & \left(\frac{1}{6}, -\frac{1}{6}, 0, \left[\text{odd } \# + \frac{1}{2} \right] \right) (0^8) \times 16, \\ & \left(-\frac{2}{3}, -\frac{1}{3}, \pm 1, 0^5 \right) (0^8) \times 2. \end{aligned} \quad (2.123)$$

After constructing the invariant states, we find

$$3 \times [(27, 1)_r + (\overline{27}, 1)_l + (1, 1)_r + (1, 1)_l] \quad (2.124)$$

where l and r denote the chirality of the state, defined by the first entry in the Ramond right-movers in Equation (2.119). The conjugate states come from the fourth twisted sector.

The remaining six fixed points are related in the sense of Equation (2.81), thus we must build interaction eigenstates by taking appropriate linear combinations of states at each fixed point. To see how this works, first note that the \mathbb{Z}_2 subgroup is generated by θ^3 , so we expect that any linear combinations of states should also be invariant under this operation. Moreover, $g_{\blacksquare\dots}$ and $g_{\blacktriangle\dots}$ are in the same conjugacy class (see Equation (2.81)). Under the action of $h \equiv (\theta, e_1)$

$$\mathcal{H}_{g_{\blacksquare}} \xrightarrow{h} \mathcal{H}_{g_{\blacktriangle}} \xrightarrow{h} \mathcal{H}_{g_{\blacksquare}}. \quad (2.125)$$

That is, h maps a state in the Hilbert space at the fixed point $g_{\blacksquare\dots}$ to a state in the Hilbert space at the fixed point $g_{\blacktriangle\dots}$. Thus we must form linear combinations of the two states.

Let us concentrate on the fixed point whose constructing element is $g_{\blacksquare\blacktriangle T^2}$, which is given by

$$g_{\blacksquare\blacktriangle T^2} = (\theta^2 + e_4). \quad (2.126)$$

The centralizer is given by

$$\mathcal{Z}(g_{\blacksquare\blacktriangle T^2}) = \{(\mathbb{1}, ae_b + be_6) (\theta^2, ae_b + be_6)\}, \quad (2.127)$$

where (as before), $a, b = 0, 1$. Note, in contrast to Equation (2.122), the centralizer only depends on even powers of θ . There are 28 solutions to the mass equation (2.75), which are the same as in Equation (2.114). As before, however, the centralizer implies no new projection conditions. The Hilbert space of states is the same at every fixed point because there are no Wilson lines to distinguish the points.

Next, we must build invariant states. The transformation properties of the states in the second twisted sector are given in Table 2.2. We then have

$$(\mathbf{27})_l^{\blacksquare} \xrightarrow{h} -(\mathbf{27})_l^{\blacktriangle} \xrightarrow{h} (\mathbf{27})_l^{\blacksquare}. \quad (2.128)$$

where (as before) $\mathbf{27}_l \equiv |\mathbf{27}\rangle \otimes |-\frac{1}{2}, \dots\rangle$, and we have labeled the state with its fixed point in the first (G_2) torus. We can now build the invariant states:

$$\begin{aligned} (\mathbf{27})_r^{\blacksquare} &+ (\mathbf{27})_r^{\blacktriangle} \sim \mathbf{27}_r, \\ (\mathbf{27})_l^{\blacksquare} &- (\mathbf{27})_l^{\blacktriangle} \sim \mathbf{27}_l, \\ (\overline{\mathbf{27}})_r^{\blacksquare} &- (\overline{\mathbf{27}})_r^{\blacktriangle} \sim \overline{\mathbf{27}}_r, \\ (\overline{\mathbf{27}})_l^{\blacksquare} &+ (\overline{\mathbf{27}})_l^{\blacktriangle} \sim \overline{\mathbf{27}}_l, \end{aligned} \quad (2.129)$$

| | θ^1 | θ^2 | θ^3 | θ^4 | θ^5 |
|--|----------------|----------------|------------|----------------|----------------|
| $ \mathbf{27}\rangle \otimes \frac{1}{2}, \dots\rangle$ | 0 | 0 | 0 | 0 | 0 |
| $ \mathbf{27}\rangle \otimes -\frac{1}{2}, \dots\rangle$ | $\frac{2}{3}$ | $\frac{1}{3}$ | 0 | $-\frac{1}{3}$ | $-\frac{2}{3}$ |
| $ \overline{\mathbf{27}}\rangle \otimes \frac{1}{2}, \dots\rangle$ | $-\frac{2}{3}$ | $-\frac{1}{3}$ | 0 | $\frac{1}{3}$ | $\frac{2}{3}$ |
| $ \overline{\mathbf{27}}\rangle \otimes -\frac{1}{2}, \dots\rangle$ | 0 | 0 | 0 | 0 | 0 |

Table 2.3: The transformation of the states in the third twisted sector.

with similar linear combinations for the singlet fields. The total matter content at these six fixed points, not counting oscillators, is then

$$3 \times [(\mathbf{27}, 1)_l + (\mathbf{27}, 1)_r + (\overline{\mathbf{27}}, 1)_l + (\overline{\mathbf{27}}, 1)_r] + 6 \times ((1, 1)_l + (1, 1)_r). \quad (2.130)$$

The additional singlets come from the oscillator states. In closing, we note that the states conjugate to those in Equation (2.130) come from the fourth twisted sector.

2.6.4 The Third Twisted Sector

In the third twisted sector, we find 16 fixed points with 12 related by an orbifold symmetry. We note that the second (SU(3)) torus is invariant under the action of the twist vector:

$$3v = \frac{1}{2} (0, 1, 0, -1). \quad (2.131)$$

The massless right-movers are given by

$$|\hat{q}\rangle = \begin{cases} |-\frac{1}{2}, 0, \frac{1}{2}, 0\rangle, \\ |\frac{1}{2}, 0, -\frac{1}{2}, 0\rangle \end{cases}, \quad (2.132)$$

with corresponding states in the NS sector:

$$|\hat{q}\rangle = \begin{cases} |0, -\frac{1}{2}, 0, -\frac{1}{2}\rangle, \\ |0, \frac{1}{2}, 0, \frac{1}{2}\rangle \end{cases}. \quad (2.133)$$

The centralizer for $g_{\blacksquare T^2 \bullet}$ is given by

$$\mathcal{Z}_{g_{\blacksquare T^2 \bullet}} = \{(\mathbb{1}, ae_3 + be_4), (\theta^3, a3_3 + be_4)\}, \quad (2.134)$$

where $a, b = 0, 1$. The left movers at $g_{\blacksquare T^2 \bullet}$ are given by

$$\begin{aligned} \left(-\frac{1}{2}, 0, -\frac{1}{2}, \frac{\pm 1, 0, 0, 0, 0}{2} \right) (0^8) &\times 10, \\ \left(0, \frac{1}{2}, 0, \left[\text{odd } \# - \frac{1}{2} \right] \right) (0^8) &\times 16, \\ \left(\frac{1}{2}, 1, \frac{1}{2}, 0^5 \right) (0^8) &\times 1. \end{aligned} \quad (2.135)$$

There is one slight difference between the results in the second twisted sector, and those in the third twisted sector. In the third twisted sector, the points $g_{\blacksquare \dots}$, $g_{\blacktriangle \dots}$ and $g_{\star \dots}$ are all in the same conjugacy class. This means, for example, that

$$(\mathbf{27})_l^{\blacksquare} \xrightarrow{h} e^{2\pi i(1/3)} (\mathbf{27})_l^{\blacktriangle} \xrightarrow{h} e^{2\pi i(2 \times 1/3)} (\mathbf{27})_l^{\star} \xrightarrow{h} (\mathbf{27})_l^{\blacksquare}. \quad (2.136)$$

To build invariant states, then, Table 2.3 tells us that we should take the following linear combinations:

$$\begin{aligned} (\mathbf{27})_l^{\blacksquare} + e^{2\pi i(1/3)} (\mathbf{27})_l^{\blacktriangle} + e^{2\pi i(2/3)} (\mathbf{27})_l^{\star} &\sim \mathbf{27}_l, \\ (\overline{\mathbf{27}})_r^{\blacksquare} + e^{2\pi i(2/3)} (\overline{\mathbf{27}})_r^{\blacktriangle} + e^{2\pi i(1/3)} (\overline{\mathbf{27}})_r^{\star} &\sim \overline{\mathbf{27}}_r, \\ (\mathbf{27})_r^{\blacksquare} + (\mathbf{27})_r^{\blacktriangle} + (\mathbf{27})_r^{\star} &\sim \mathbf{27}_r, \\ (\overline{\mathbf{27}})_l^{\blacksquare} + (\overline{\mathbf{27}})_l^{\blacktriangle} + (\overline{\mathbf{27}})_l^{\star} &\sim \overline{\mathbf{27}}_l. \end{aligned} \quad (2.137)$$

There are four groups of fixed points (which can be labeled by their location in the third torus), which gives us a total spectrum about the four sets of three equivalent fixed points as

$$4 \times (\mathbf{27}_l + \mathbf{27}_r + \overline{\mathbf{27}}_l + \overline{\mathbf{27}}_r). \quad (2.138)$$

After constructing the invariant states, including oscillators, we find a complete spectrum in the third twisted sector:

$$4 \times \mathbf{27}_l + 8 \times \overline{\mathbf{27}}_l + 8 \times \mathbf{27}_r + 4 \times \overline{\mathbf{27}}_r + 52 \times (1_l + 1_r). \quad (2.139)$$

Note that the third twisted sector is self conjugate.

2.6.5 The Complete Spectrum

To simplify the notation, we list only the left-chiral states. We find

$$\begin{aligned}
 U &: 3 \times \overline{\mathbf{27}} + 1 \times \mathbf{27} + 3 \times 1; \\
 T1 + T5 &: 12 \times \overline{\mathbf{27}} + 48 \times 1; \\
 T2 + T4 &: 12 \times \overline{\mathbf{27}} + 6 \times \mathbf{27} + 18 \times 1; \\
 T3 &: 8 \times \overline{\mathbf{27}} + 4 \times \mathbf{27} + 52 \times 1.
 \end{aligned} \tag{2.140}$$

Note that this model has 35 anti-generations ($\overline{\mathbf{27}}$) and 11 generations ($\mathbf{27}$), giving a net 24 anti-generations of standard model fermions. As is typical of the orbifold compactifications, there are a large number (121) of gauge singlets—these singlets include the “blow-up” modes, which are states with non-zero oscillator number that are localized at fixed points.

Chapter 3

GAUGE COUPLING UNIFICATION IN A CLASS OF STRINGY ORBIFOLD GUTS

The agreement of the results seems to show that light and magnetism are affections of the same substance, and that light is an electromagnetic disturbance propagated through the field according to electromagnetic laws.

James Clerk Maxwell

3.1 Motivation

Supersymmetric grand unification [66–71] is one of the most attractive scenarios for beyond the Standard Model physics. One can simultaneously explain the apparent unification of the electroweak and strong coupling constants around 3×10^{16} GeV, charge quantization, the conservation of B-L, and why quarks and leptons come in families. Nevertheless the simplest four dimensional SUSY GUTs have some notable problems. Spontaneously breaking the GUT symmetry requires scalars in adjoint representations and complicated symmetry breaking potentials. In addition, Higgs doublet-triplet splitting demands special treatment. Neither of these problems is insurmountable but it is difficult to imagine that these special sectors can be derived from a more fundamental theory. In addition, Super-K bounds on the proton lifetime place 4-dimensional SUSY GUTs “under siege” [72, 73]. Finally, in order to understand fermion masses and mixing angles it is likely that additional family symmetries may be needed.

In the early work within the framework of the weakly coupled heterotic string it was argued for string unification, as opposed to grand unification with an independent lower energy GUT breaking scale.²¹ Gauge couplings naturally unify at the string scale with a unification scale²² of around 5×10^{17} GeV [74–76]. Unfortunately the precision low

²¹In fact, it is difficult to get massless adjoints in the string spectrum, needed for GUT symmetry breaking.

²²Assuming $SU(2)$ and $SU(3)$ are represented at Kač-Moody level $k_2 = k_3 = 1$ and the $U(1)$ of hypercharge is normalized with $k_1 = 5/3$.

energy data prefers a lower unification scale, $M_{\text{GUT}} \sim 3 \times 10^{16}$ GeV. This tension between gravity and gauge coupling unification has been termed the “factor of 20” problem with string unification [77]. Nevertheless string theory has some very nice features, i.e. the $E_8 \times E_8$ (or $\text{SO}(32)$) symmetry of the weakly coupled heterotic string is easily broken via an orbifold compactification of the extra 6 spatial dimensions [53, 57]. In addition, Higgs doublet-triplet splitting is also easily accomplished by the same means [78, 79]. Significant progress was made early on in obtaining standard-model-like theories using orbifolding and Wilson lines to break the gauge symmetry [79–83].

More recently, it was realized that some of the problems with SUSY GUTS could be solved by understanding our low energy physics in terms of an effective five or six dimensional field theory in which one or two of the directions is compactified [42, 43, 84–91]. Typically one takes a five (six) dimensional gauge theory, and compactifies one (two) of the directions on an orbifold. The geometry of the orbifold admits solutions for higher dimensional fields which are localized on two or more branes, and fields which are free to propagate in the bulk. The former are called “brane” fields, the latter “bulk” fields. By assigning the bulk fields boundary conditions along the fifth (and sixth) direction(s), one can achieve GUT/SUSY breaking without the large representations and complicated GUT breaking potentials encountered in 4 dimensional constructions. In addition, placing the electroweak Higgs multiplet in the bulk, Higgs doublet-triplet splitting can also be affected via a judicious choice of boundary conditions. Generally, the placement of the matter and the assignment of orbifold parities is done in a bottom up manner; one identifies certain phenomenological features (eg. suppressing dangerous proton decay operators) and then chooses mass scales, matter localization, and orbifold parities accordingly. For example, one can keep $b - \tau$ Yukawa unification by placing the third family on an $\text{SU}(5)$ brane or suppress proton decay by placing the first two families in the bulk [85]. Finally, four dimensional SUSY GUTs require of order 3% threshold correction at the GUT scale in order to precisely fit the low energy data [29]. Given a GUT breaking sector, this correction must come from the spectrum of massive states with mass of order M_{GUT} . In orbifold GUTs this correction comes from the Kaluza-Klein modes between the compactification scale, M_C , and the cut-off scale, M_* , with unification occurring at the cut-off. In fact, the ratio $M_*/M_C \sim 100$ is determined by gauge coupling unification. The problem with orbifold GUT field theories, however, is the necessity for a cut-off.

In Refs. [39–41], it was shown that effective orbifold SUSY GUT field theories can be obtained by orbifold compactifications of the heterotic string. These theories provide an ultraviolet completion of orbifold GUT field theories with a physical cut-off at the string scale. These are so-called anisotropic orbifold theories with one or two large extra dimensions ($R = M_C^{-1} \gg l_S = M_S^{-1}$). At lowest order the gauge couplings unify at M_S . Further, when working within the framework of the weakly coupled heterotic string, there is a

very specific relationship between the strength of the GUT coupling and the strength of gravity (see Equation (3.2)). Viewed in this manner, the factor of 20 turns into a factor of 400 when comparing to the (experimentally measured) value of Newton’s constant. This makes it clear that there needs to be significant threshold corrections (both logarithmic and power law) in order to match the low energy data. In fact, important threshold corrections are provided by Kaluza-Klein modes running in loops. Their spectrum is calculable, and often gives non-trivial corrections to the running of the couplings [42, 43].

In this paper, we investigate ways to solve the “factor of 20” problem with heterotic string unification, within the context of the orbifold GUT picture proposed in references [39–41]²³. In order to make unification work, we find that we generally need to introduce an intermediate scale, M_{EX} , which is typically two or three orders of magnitude below the compactification scale. When we impose the conditions that $M_{\text{S}} > M_{\text{C}} \gtrsim M_{\text{EX}}$, we find a large number of solutions for which unification works. Note the proton lifetime (from dimension six operators) scales as the fourth power of M_{C} . Most solutions are excluded by proton decay, however a small number predict proton lifetimes (from dimension six operators) that can be measured in future experiments.

We begin with a brief review of the stringy embedding of orbifold GUTs [39–41], and a presentation of the models in the “mini-landscape” search [34–38] in Section 3.2. We focus on two “benchmark” models from the mini-landscape search in this analysis, called “Model 1A” and “Model 2” in Reference [38]. Specific details of these models (the full spectrum in four dimensions, etc.) can be found in Appendix H. The main result of our analysis is a detailed examination of the parameter space which allows for unification, and how this parameter space relates to proton decay constraints from dimension six (and possibly dimension five) operators. This work is summarized in Section 3.3. Solutions consistent with gauge coupling unification are found in Tables H.7 - H.10 on pages 156 - 159. In Section 3.4 we check whether any of our solutions are consistent with decoupling of exotics in supersymmetric vacua.

3.2 Orbifold GUTs from String Theory

In exploring gauge coupling unification in orbifold constructions, we focus on a class of models [34–38] that are based on $\text{SU}(6)$ gauge-Higgs unification in five dimensions, and whose low-energy spectrum is exactly that of the MSSM. Similar theories have also been considered in the context of orbifold GUT field theory [93]. We shall comment on the differences in Appendix C.

²³A recent analysis of gauge coupling unification can also be found in Reference [92].

3.2.1 The Mini-Landscape in a Nutshell

We compactify the 6 extra dimensions of the heterotic string on the product of three 2-tori as shown in Figure 2.1. Moding out the discrete \mathbb{Z}_6 -II symmetry given as a 60° , 120° , 180° rotation (“twist” v) in the first, second, and third torus, respectively, defines the orbifold [53, 57]. The geometry of the orbifold allows for no Wilson lines in the first torus, one order-3 Wilson line A_3 in the second torus (e_3 and e_4 are the same direction on the orbifold) and two order-2 Wilson lines A_2, A'_2 along e_5, e_6 , respectively [55]. We take $A'_2 \equiv 0$ to localize 2 identical copies of **16**’s at the fixed points \bullet and \star that will eventually sport a D_4 family symmetry [39, 94, 95].

Modular invariance allows for 61 different gauge embeddings (“shift” V) of the twist. Only 15 of these shifts break $E_8 \times E'_8$ to a gauge group containing $SO(10)$, and only 2 shifts allow for **16**’s in the first/fifth twisted sector (T_1, T_5 , respectively) that are not projected out by the Wilson lines.

The models that come closest to the real world all stem from one shift [34, 35], termed $V^{SO(10),1}$ in Refs. [36, 38]. Switching on all possible Wilson lines consistent with this shift and modular invariance, we obtain $\sim 22,000$ models with different particle spectra. Successively, we impose our phenomenological priors to get as close to the MSSM as we possibly can: (i) Standard Model gauge group, (ii) non-anomalous hypercharge that lies in $SU(5) \subset SO(10)$, (iii) 3 generations of quarks and leptons, 1 pair of Higgs doublets, (iv) all exotic (i.e. non-standard-model) particles are vector-like, (v) trilinear Yukawa coupling for a heavy top, (vi) generalized B-L generator that is eventually broken down to R -parity, (vii) all spurious abelian gauge group factors are broken, (viii) string selection rules allow for all exotics to decouple consistent with the “choice of vacuum” (singlet VEVs must not break SM gauge symmetries and R -parity, and must satisfy $F = D = 0$).

This leaves us with 15 models with promising phenomenology. We use this sample to investigate whether the unification picture in orbifolds is consistent with the measured values of the coupling constants at low energies, or in other words, whether we can fit α_1 , α_2 and α_3 at the electroweak scale with a single coupling constant α_{STRING} at M_S . Specifically, the set of exotics in both Models 1 and 2 of Reference [38] are similar enough to warrant parallel treatment, and are listed in Table H.4 on page 155. As can be seen, the exotic matter which is charged under the MSSM in Model 1 overlaps with the exotic matter in Model 2. Note that we have labeled states with their hypercharge and B-L quantum numbers as subscripts.

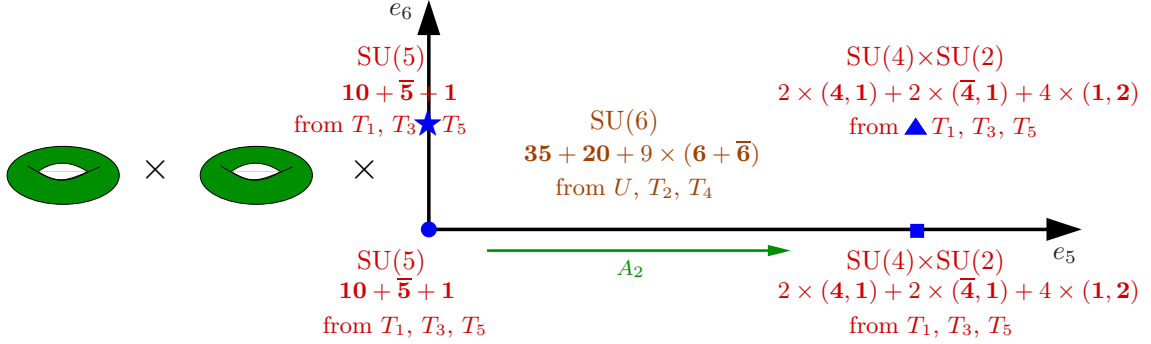


Figure 3.1: Setup of the 5d orbifold GUT, where the 5th dimension (e_5) is large compared to the other compact dimensions.

3.2.2 The Orbifold GUT Picture

The 15 models described in Section 3.2.1 are naturally embedded into a grand unified theory in 5 or 6 dimensions [41]. Consider Model 2 of Section 5.2 of the mini-landscape search [38]. For completeness, the full details of the model have been reproduced in Appendix H.

Instead of moding out the full $\mathbb{Z}_6\text{-II} \simeq \mathbb{Z}_2 \times \mathbb{Z}_3$ symmetry (generated by the twist v) to get the 4-dimensional spectrum, we can mod out the \mathbb{Z}_3 subgroup (generated by $2v$) alone, leaving the $\text{SO}(4)$ torus invariant. The particles from the U, T_2, T_4 sectors are free to move around in the $\text{SO}(4)$ torus and can thus be considered to be the “bulk states” of a 6-dimensional \mathbb{Z}_3 orbifold with twist $2v$, shift $2V$ and Wilson line A_3 .

In this picture, moding out the residual \mathbb{Z}_2 symmetry (generated by $3v$) corresponds to adding “brane states” to the theory. The gauge group at the fixed points is obtained from the bulk symmetry by moding out $V_2 = 3V$ for \bullet and \star and $V_2 + A_2$ for \blacksquare and \blacktriangle . The matter representations follow from the mass equation at the respective fixed points (given in terms of V_2 and A_2), subject to projection conditions from $V_3 = 2V$ and A_3 .

The gauge symmetry in 4 dimensions is the intersection of all gauge groups, and the brane GUT states branch to SM representations of the T_1, T_3, T_5 sectors. This can be understood from an orbifold GUT viewpoint by assigning parities to the brane modes given by

$$P \sim e^{2\pi i p \cdot V_2}, \quad P' \sim e^{2\pi i p \cdot (V_2 + W_2)},$$

where p (the highest weight associated with the state) is a sixteen dimensional vector from the $E_8 \times E_8$ lattice. Then, the setup of Figure 3.1 describes an orbifold $S^1/\mathbb{Z}_2 \times \mathbb{Z}'_2$ where 1 extra dimension is compactified on a circle. The discrete symmetries are realized as a reflection $\mathcal{P} : x^5 \rightarrow -x^5$ and a translation $\mathcal{T} : x^5 \rightarrow x^5 + 2\pi R$. Only the states that are

invariant under

$$\begin{aligned}\mathcal{P} : \Phi(x^5) &\rightarrow \Phi(-x^5) = P\Phi(x^5), \\ \mathcal{PT} : \Phi(x^5) &\rightarrow \Phi(-x^5 + 2\pi R) = P'\Phi(x^5)\end{aligned}\tag{3.1}$$

will be present in the low energy spectrum.²⁴

Orbifold GUTs, when generated from an underlying string theory, are significantly more constrained than orbifold GUT field theories. Whereas the only *real* constraint in an orbifold GUT field theory is that the low energy effective field theory be anomaly free, all anomalies in the string theory are canceled at the string scale by the generalized Green-Schwarz mechanism [63, 64, 96–98], so this condition is automatically satisfied. In string orbifolds, the parities are realized in terms of Wilson lines that must satisfy stringent modular invariance constraints, so we cannot simply assign parities at will. Further, the placement of matter is not an independent degree of freedom in string models. Finally, we are given a value for the coupling constant at the cut-off, see Equation (3.2) on page 55. In a typical orbifold GUT, this is a free parameter. In addition, there may be some assumptions about strong coupling, but the details of the ultraviolet completion are not addressed.

3.3 Gauge Coupling Unification in Orbifolds

3.3.1 Unification in Heterotic String Theory in 10 Dimensions

As a unified framework for particle physics and gravity, string theory predicts Newton's constant G_N and relates it to the gauge coupling constants. Unfortunately, the predicted value for G_N , in the weakly coupled heterotic string, turns out to be too large and needs to be reconciled with the extrapolated running gauge coupling constants at the unification scale.

Throughout this paper we assume that we are in the weakly-coupled regime of the heterotic string. After compactifying the 10-dimensional low-energy effective action on a 6-dimensional manifold, one obtains [74]

$$G_N = \frac{1}{8} \alpha_{\text{STRING}} \alpha'.\tag{3.2}$$

Here, α_{STRING} denotes the common value of the gauge coupling constants at the string scale, $M_s = 1/\sqrt{\alpha'}$.²⁵ Low-energy data suggests $\alpha_{\text{STRING}}^{-1} \simeq \alpha_{\text{GUT}}^{-1} \simeq 24$ and $M_s \simeq M_{\text{GUT}} \simeq 10^{16}$ GeV, so the predicted value for Newton's constant is off by a factor of about 400. Putting it another way, if we use the measured value of the gravitational constant $G_N = 1/(M_{\text{PL}}^2)$ with $M_{\text{PL}} \simeq 1.2 \times 10^{19}$ GeV, the string scale is predicted to be $M_s \simeq 5 \times 10^{17}$ GeV [74], in

²⁴ $P' \equiv P T$ where T corresponds to the discrete gauge transformation due to a Wilson line.

²⁵ The string scale M_s defined here corresponds to the effective cut-off scale in our field theory calculation. This is discussed in more detail in footnote 8, Section 3.3.2.

disagreement with M_{GUT} . These conclusions are based on the assumptions that (i) we are in the weak coupling limit, (ii) there are no new states between the electroweak and the GUT scale that could contribute to the renormalization group equations (RGEs), (iii) the compactification is isotropic, i.e. all compactified dimensions are comparable in size.

In the following, we explore *anisotropic orbifold compactifications* to fit low-energy data with a single coupling constant at M_s .²⁶ Other proposals that have been considered in the literature include exotic matter representations at intermediate scales, large threshold corrections, non-standard hypercharge normalizations from higher-level Kač-Moody algebras, strings without supersymmetry, or the strong coupling regime of the heterotic string [74–76, 92, 102–111]. For a review of grand unification in the context of string theory, see Reference [77].

3.3.2 The RGEs for Anisotropic Orbifold Compactifications

We study gauge coupling unification for the “benchmark” models presented in the mini-landscape search [38]. As has been emphasized in Section 3.2.1, these models are two out of 15 that already satisfy quite a few non-trivial criteria on the road to the MSSM. We are working in the the orbifold GUT limit as outlined in Section 3.2.2. The gauge group geography and the relevant part of its 5-dimensional spectrum for Model 2 are given in Figure 3.1 on page 54. For the full details of the 4-dimensional spectrum, see Tables H.1 and H.2 on pages 153 and 154. The anisotropic compactification singles out the fifth dimension that is assumed to be large and thus introduces a new scale into the theory, the compactification scale M_c . The other 5 compactified dimensions are assumed to be of order the string scale, M_s .

We want to compare our models with low energy data. At the string scale, M_s , we have a unified gauge coupling, α_{STRING} . Below the string scale we have three gauge couplings which renormalize independently down to the weak scale. In general, there are additional small (stringy) corrections to the relationship in Equation (3.2) at the string scale, M_s [74–76]. Because these contributions are expected to be small, we will neglect them in this analysis. In principle we should integrate the three gauge couplings down to the SUSY breaking scale using the two-loop RGEs, including one-loop threshold corrections at the string scale, the compactification scale, the exotic scale, M_{EX} , and the SUSY scale, finally fitting $\alpha_i, i = 1, 2, 3$ at M_Z [112, 113]. However, it is sufficient to compare the orbifold GUT to the four dimensional SUSY GUT running equations, which approximately (and implicitly) correct for SUSY threshold corrections at the weak scale and two-loop renormalization

²⁶For earlier work along this line see, [39, 99–101].

group running from the weak scale to the GUT scale. These are given by the equations:

$$\alpha_i^{-1}(\mu) = \alpha_{\text{GUT}}^{-1} + \frac{b_i}{2\pi} \log \frac{M_{\text{GUT}}}{\mu} + \frac{6}{2\pi} \delta_{i3}, \quad (3.3)$$

The indices $i = 3, 2, 1$ refer to $\text{SU}(3)_c$, $\text{SU}(2)_L$, $\text{U}(1)_Y$, respectively. The b_i are the so-called β -function coefficients and are most conveniently expressed in terms of the Dynkin index²⁷ [61]

$$b_i = -3\ell(\text{vector multiplets}) + \ell(\text{chiral multiplets}). \quad (3.4)$$

For the MSSM we have $b_i = (-3, 1, 33/5)$. Finally, the last term in Equation (3.3) is a 3% threshold correction to α_3^{-1} at the GUT scale that we need to match the precision electroweak data.

The minimal and most elegant way to fit the low-energy data is to arrange for all exotics (i.e. non-standard-model particles) to obtain mass around M_s . Up to the scale M_c , assumed to be not much below M_{GUT} , the evolution of the gauge coupling constants is then governed by the same renormalization group equations as in the usual GUT picture. For energies above M_c , the RGEs receive additional contributions from the Kaluza-Klein tower of those Standard Model particles that live in the bulk, thus giving rise to both logarithmic and power-law running [42, 43]. Unfortunately, this simple setup does not work. Varying the values of α_{STRING} at M_s and of the compactification scale M_c , we cannot fit the gauge coupling constants at the electroweak scale. We elaborate on this point in Appendix C, where we show the difficulties involved with gauge-Higgs unification in five dimensions.

The remaining possibility is to assume that not all exotics obtain mass at M_s , but some are light enough to be relevant for the evolution of the coupling constants. At the same time, of course, the exotics must still be massive enough to decouple from the low-energy theory. We will call this intermediate scale M_{EX} and assume in the following $M_s > M_c \gtrsim M_{\text{EX}}$. Now we can try to fit the low-energy data by varying M_{EX} , M_c , M_s and the multiplicities and quantum numbers of the light exotics. Note that the running of the coupling constants below M_{EX} will be given by the same Equation (3.3) as in the MSSM, since all the exotics are assumed to be heavier than M_{EX} and the first excitation of the Kaluza-Klein tower is of order M_c . Near $\mu \simeq M_{\text{EX}}$, the renormalization group equations

²⁷For hypercharge, we define the Dynkin index to be $\ell = (3/5)Y^2/4$.

read:

$$\begin{aligned}
\alpha_i^{-1}(\mu) = & \alpha_{\text{STRING}}^{-1} + \frac{b_i^{\text{MSSM},++} + b_i^{\text{MSSM},\text{brane}}}{2\pi} \log \frac{M_s}{\mu} \\
& + \frac{b_i^{\text{EX},++} + b_i^{\text{EX},\text{brane}}}{2\pi} \log \frac{M_s}{M_{\text{EX}}} \\
& - \frac{1}{4\pi} \left(b_i^{\text{MSSM},++} + b_i^{\text{MSSM},--} + b_i^{\text{EX},++} + b_i^{\text{EX},--} \right) \log \frac{M_s}{M_c} \\
& + \sum_{P=\pm, P'=\pm} \frac{b_i^{\text{MSSM},PP'} + b_i^{\text{EX},PP'}}{2\pi} \left(\frac{M_s}{M_c} - 1 \right)
\end{aligned} \tag{3.5}$$

These equations are obtained by starting at the highest scale in the theory, M_s , and evolving the gauge couplings α_i down to M_c , taking into account all the particles with mass less than M_s . In the next step, one takes the values obtained for α_i as boundary conditions for the renormalization group equations at M_c and calculates α_i at M_{EX} . In order to compare to experimental values of the coupling constants at M_Z , we apply the two loop RGEs [114]. Note that this involves integrating out SUSY particles at M_{SUSY} . Technically, because the two loop RGEs are good *near* the GUT scale, our approach will be to compare the two equations (Equations (3.3) and (3.5)) at the scale M_{EX} . Provided that M_{EX} is *near* the GUT scale, the error introduced in the analysis should be negligible. In principle, the exotic scale M_{EX} can be small, perhaps a TeV. In all cases we find, however, the exotic scale is larger than 10^9 GeV, and in most cases it is greater than 10^{12} GeV. The error we make by matching Equations (3.3) and (3.5) at $M_{\text{EX}} \sim 10^9$ GeV comes from the difference in the two loop corrections to the RG running from M_{EX} to the GUT scale. This correction is expected to be less than a percent.

Let us look at Equation (3.5) in some more detail. The first term is the tree level boundary condition from the heterotic string. The second and third terms contain loop contributions from MSSM fields and exotic matter, respectively—the zero KK modes and the brane states are kept separate for clarity. The last two terms are due to the massive KK states in the bulk. The logarithmic ($\sim \log \frac{M_s}{M_c}$) and linear terms ($\sim \frac{M_s}{M_c}$) are a consequence of the geometry, i.e. in an equivalent string calculation the factor of $\frac{M_s}{M_c}$ arises from the dependence on the T (volume) and U (shape) moduli of the torus.²⁸ Note, the last term is a universal

²⁸Note, our one loop calculations are performed using an effective field theory approach. In particular the sum over the infinite tower of KK modes follows the regularization scheme of Dienes et al. [42, 43]. Moreover, in the work of Ghilencea and Nibbelink [115] it is shown that if the field theory cut-off Λ^2 is chosen to satisfy the relation $\Lambda^2 = \frac{2e}{3\sqrt{3}} \frac{1}{\alpha'} \approx 1.05/\alpha'$ then the heterotic string loop calculation is approximately equal to the field theory results. Thus we identify the string scale $M_s = \Lambda \approx \frac{1}{\sqrt{\alpha'}}$. We should note that the analysis of [115] was done in the context of toroidal compactification. A more relevant comparison should be done in an orbifold compactification with Wilson lines. The latter approach was taken by the authors of Reference [92] in a T^2/\mathbb{Z}_3 orbifold. Their results, however, are not directly applicable to our situation.

correction due to the $SU(6)$ fields in the bulk. We introduce the following definitions:

$$\begin{aligned} b_i^{\text{MSSM}} &\equiv b_i^{\text{MSSM},++} + b_i^{\text{MSSM},\text{brane}}, & b_i^{\text{EX}} &\equiv b_i^{\text{EX},++} + b_i^{\text{EX},\text{brane}}, & b_i^{++} &\equiv b_i^{\text{MSSM},++} + b_i^{\text{EX},++} \\ b_i^{--} &\equiv b_i^{\text{MSSM},--} + b_i^{\text{EX},--}, & b^{\mathcal{G}} &\equiv \sum_{P=\pm, P'=\pm} b_i^{\text{MSSM},PP'} + b_i^{\text{EX},PP'} \end{aligned}$$

This simplifies Equation (3.5) a bit:

$$\begin{aligned} \alpha_i^{-1}(\mu) &= \alpha_{\text{STRING}}^{-1} + \frac{b_i^{\text{MSSM}}}{2\pi} \log \frac{M_S}{\mu} + \frac{b_i^{\text{EX}}}{2\pi} \log \frac{M_S}{M_{\text{EX}}} \\ &\quad - \frac{1}{4\pi} (b_i^{++} + b_i^{--}) \log \frac{M_S}{M_C} + \frac{b^{\mathcal{G}}}{2\pi} \left(\frac{M_S}{M_C} - 1 \right) \end{aligned} \quad (3.6)$$

3.3.3 Gauge Coupling Unification: An Effective Field Theory Calculation

Before we proceed, we will clear up some notational issues. We will *always* talk about fields in the language of $N = 1$ SUSY in four dimensions. The $N = 1$, 5-dimensional hyper multiplet contains two 4-dimensional chiral multiplets, and a 5-dimensional vector multiplet contains a 4-dimensional vector multiplet and a 4-dimensional chiral multiplet. The 5-dimensional $N = 1$ theory can thus be described in terms of 4-dimensional $N = 1$ fields (or in terms of 4-dimensional $N=2$ hyper multiplets).

In order to check gauge coupling unification, we will equate the values of (i) $1/\alpha_3 - 1/\alpha_2$, (ii) $1/\alpha_2 - 1/\alpha_1$, (iii) α_3 as obtained from Equation (3.3) and Equation (3.6), respectively, at the scale M_{EX} , where both equations are valid. We find:

$$\log \frac{M_S}{M_{\text{GUT}}} = \frac{n_3 - n_2}{4} \log \frac{M_S}{M_{\text{EX}}} - \frac{3}{2}, \quad (3.7a)$$

$$\log \frac{M_S}{M_{\text{GUT}}} = \frac{10n_2 - n_3 - 3n_1}{56} \log \frac{M_S}{M_{\text{EX}}} + \frac{3}{7} \log \frac{M_S}{M_C}, \quad (3.7b)$$

$$\begin{aligned} 48\pi &= \frac{\pi}{4} \left(\frac{M_{\text{PL}}}{M_S} \right)^2 - 6 - 3 \log \frac{M_S}{M_{\text{GUT}}} + n_3 \log \frac{M_S}{M_{\text{EX}}} \\ &\quad + \log \frac{M_S}{M_C} - 4 \left(\frac{M_S}{M_C} - 1 \right), \end{aligned} \quad (3.7c)$$

where the n_i are beta function contributions from the *brane localized* exotics, as defined below. The first two equations describe the *relative* running of the couplings (i.e. their slopes), and the last one gives us information about the *absolute* running (i.e. their intercepts). The coefficients n_i are defined in terms of the set of exotics with mass of order M_{EX} as follows:

$$n_3 \times [(\mathbf{3}, 1)_{1/3,*} + (\bar{\mathbf{3}}, 1)_{-1/3,*}] + n_2 \times [(1, \mathbf{2})_{0,*} + (1, \mathbf{2})_{0,*}] + n_1 \times [(1, 1)_{1,*} + (1, 1)_{-1,*}], \quad (3.8)$$

where “*” for the B-L charge denotes anything. The necessary β -function coefficients b_i , using the numbers in Tables H.5 on page 155 are found to be

$$\vec{b}_{\text{EX}} = (n_3, n_2, \frac{n_3 + 3n_1}{10}). \quad (3.9)$$

Let us now consider those MSSM states located in the bulk. In general, we can find two pairs of $N = 1$ chiral multiplets $\mathbf{6} + \mathbf{6}^c$ which decompose as

$$\begin{aligned} 2 \times (\mathbf{6} + \mathbf{6}^c) \supset & \left[(1, \mathbf{2})_{1,1}^{--} + (\mathbf{3}, 1)_{-2/3,1/3}^{-+} \right] + \left[(1, \mathbf{2})_{-1,-1}^{++} + (\overline{\mathbf{3}}, 1)_{2/3,-1/3}^{--} \right] \\ & + \left[(1, \mathbf{2})_{1,1}^{-+} + (\mathbf{3}, 1)_{-2/3,1/3}^{--} \right] + \left[(1, \mathbf{2})_{-1,-1}^{+-} + (\overline{\mathbf{3}}, 1)_{2/3,-1/3}^{++} \right]. \end{aligned} \quad (3.10)$$

This gives us the the third family \bar{b} and L —the rest of the third family comes from the $\mathbf{10} + \mathbf{10}^c$ of $\text{SU}(5)$ contained in the $\mathbf{20} + \mathbf{20}^c$ of $\text{SU}(6)$, which lives in the untwisted sector. An interesting point is the genesis of the Higgs bosons. We have remarked earlier that the models we look at come from a broader class of models satisfying “gauge-Higgs unification”. Our bulk gauge symmetry is $\text{SU}(6)$, so the $\text{SU}(6)$ gauge bosons (and thus the adjoint representation) necessarily live in the bulk. Under $\text{SU}(5) \times \text{U}(1)$, the adjoint decomposes as

$$\mathbf{35} \rightarrow \mathbf{24}_0 + \mathbf{5}_{+1} + \mathbf{5}_{-1}^c + \mathbf{1}_0. \quad (3.11)$$

Thus the MSSM Higgs sector emerges from the breaking of the $\text{SU}(6)$ adjoint by the orbifold. Including the contributions from the third family and the Higgses, we find using Table H on page 156

$$\vec{b}^{++} = (-7, -3, 13/5), \quad \vec{b}^{--} = (5, 1, 1/5), \quad b^G = -4. \quad (3.12)$$

3.3.4 Results

We find it necessary to introduce an intermediate mass scale M_{EX} , perhaps *near* the compactification scale, and identify a set of exotics with mass M_{EX} consistent with gauge coupling unification. Solving the RG equations numerically, we find 252 versions of Model 2 (of which 82 are also versions of Model 1), where by “versions” we mean inequivalent sets of “light” exotics satisfying gauge coupling unification. Of these 252 (82), only 48 (9) are consistent with the Super-K bounds on the proton lifetime [29] (see Section 3.5). These are found in Tables H.7 and H.8 on pages 156 and 157, where we also calculate the lifetime of the proton due to dimension six operators, see Appendix D and Figure 4.1. The solutions which are applicable to Model 1 are listed in **bold** in both tables. Note that the GUT coupling constant, α_{STRING} , (evaluated at M_s) varies depending on M_s and M_{EX} . For example,

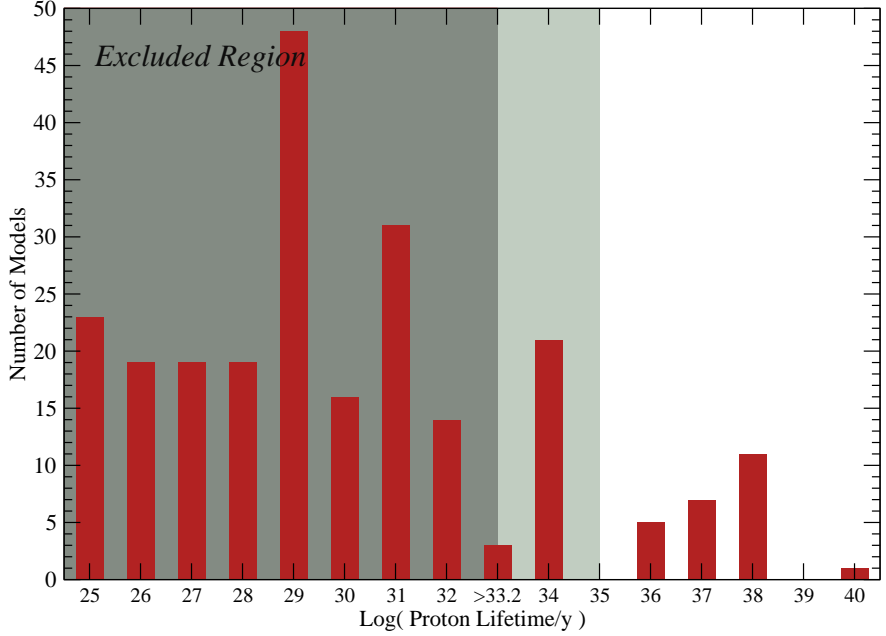


Figure 3.2: Histogram of solutions with $M_S > M_C \gtrsim M_{\text{EX}}$, showing the models which are excluded by Super-K bounds (darker green) and those which are potentially accessible in a next generation proton decay experiment (lighter green). Of 252 total solutions, 48 are not experimentally ruled out by the current experimental bound, and most of the remaining parameter space can be eliminated in the next generation of proposed proton decay searches.

in the last row of Table H.7 on page 156, we find

$$\alpha_{\text{STRING}}^{-1} = \frac{1}{8} \left(\frac{M_{\text{PL}}}{M_S} \right)^2 \simeq \frac{1}{8} \left(\frac{1.22 \times 10^{19} \text{ GeV}}{5.47 \times 10^{17} \text{ GeV}} \right)^2 \simeq 62. \quad (3.13)$$

Near the exotic scale where we match onto the low energy physics, we expect the (inverse) coupling constants to be of order 30-40. Likewise, $\alpha_{\text{STRING}}^{-1}$ is typically *larger* than this, of order 50-60 or so (but sometimes as big as $\mathcal{O}(1000)$). Thus, we *must* have a large and negative contribution from the power-law running, which translates into the requirement that $b^G < 0$. This is evident in Equation (3.6), for example. If $b^G > 0$, we would need a large negative contribution from the other terms, which is hard to reconcile with the logarithmic suppression. For completeness, we plot the β -functions of the last solution in Table H.7 in Figure 3.3. The evolution of the gauge couplings is typical in this class of models, i.e. the power law running between the compactification scale is rather pronounced.

For the 11 models in Table H.7, we keep only the minimum amount of matter in the bulk, i.e. in order to get the MSSM spectrum, it is sufficient to keep $2 \times (\mathbf{6} + \mathbf{6}^c)$ massless below the string scale. Given the constraint that we want $b^G < 0$, however, we are in

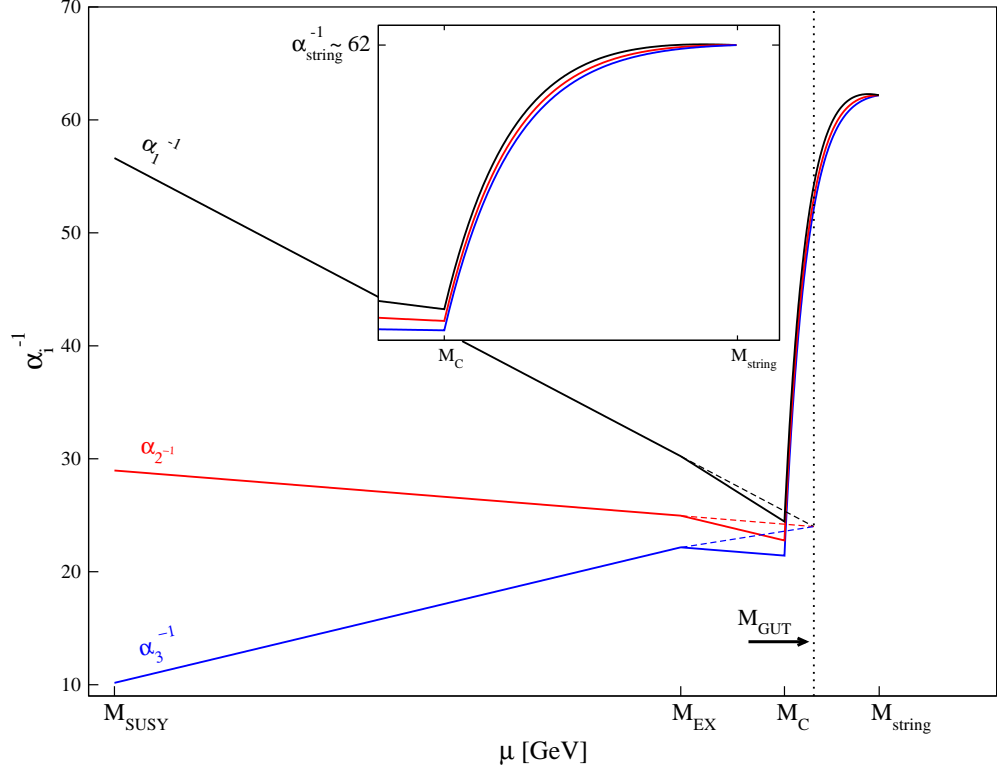


Figure 3.3: An example of the type of gauge coupling evolution we see in these models, versus the typical behavior in the MSSM. The “tail” is due to the power law running of the couplings when towers of Kaluza-Klein modes are involved. Unification in this model occurs at $M_S \simeq 5.5 \times 10^{17}$ GeV, with a compactification scale of $M_C \simeq 8.2 \times 10^{15}$ GeV, and an exotic mass scale of $M_{\text{EX}} \simeq 8.2 \times 10^{13}$ GeV.

principle able to leave $4 \times (\mathbf{6} + \mathbf{6}^c)$ massless below the string scale. This gives $b^G = -2$, and leads to 37 new solutions. These are listed in Table H.8 on page 157. Of the 48 solutions (included in both Models 1 and 2), 22 have proton lifetimes which can potentially be tested by the next generation of proton decay experiments, see Appendix D and Figure 4.1 for more details.

We stress that this analysis is quite general. Of the fifteen models which fit the criteria in the mini-landscape search, all come from a five dimensional SU(6) orbifold, and all of them have the same types of exotics. This means that the analysis preformed here generalizes in a straightforward manner to the other min-landscape models, whose spectra are listed in Reference [116].

In order to try and get a feel for the tunings involved in the above conclusions, we can compare the GUT coupling constant (at the string scale) with the ratio between the string

scale and the compactification scale.²⁹ Further, we will separate the solutions based on the hierarchy between the compactification scale and the exotic scale. We plot the result in Figure 3.4. What we see is the correlation between a long lived proton and a moderate hierarchy between the compactification scale and the string scale, and between the string scale and the Planck scale. However, these moderate hierarchies come at the cost of introducing a smaller and smaller exotic scale, M_{EX} . This means that a long lived proton favors a *large* hierarchy between the compactification scale and the exotic scale. The black diamonds represent those models with a moderate ($< \mathcal{O}(350)$) hierarchy between the compactification scale and the exotic scale. Most of these solutions are already ruled out by proton decay constraints. The gray shaded circles represent those solutions for which there is a large difference between the exotic scale and the compactification scale.

We would also like to point out the small set of solutions in the large red box, for which there are only moderate hierarchies, and which are consistent with the current bounds on dimension six operators³⁰. Specifically, there seems to be a “sweet spot” where all of the hierarchies in the problem are of $\mathcal{O}(100)$ or so. These models are highlighted in Table H.10. In particular, these models can all be eliminated by improving the current bounds on proton decay from dimension 6 operators by a factor of 50-100.

The fact that the data falls approximately on two straight lines is not surprising, and is evidence of a power-law relationship between $\alpha_{\text{STRING}}^{-1}$ and $\frac{M_s}{M_c}$. One can see this relationship as by eliminating $\log \frac{M_s}{M_{\text{EX}}}$ between Equations (3.7a) and (3.7b). We eventually find

$$\log \alpha_{\text{STRING}}^{-1} = A \log \frac{M_s}{M_c} + B, \quad (3.14)$$

where A and B are given in terms of the beta function coefficients and $\log \frac{M_{\text{PL}}}{M_{\text{GUT}}}$. It is not surprising to find that the actual values for A and B are roughly the same for all of the solutions, and that many solutions give *identical* values for A and B .

3.4 Unification, Decoupling of Exotics and Supersymmetry

Now that we understand what exotic matter we need to accommodate unification, we can ask if an intermediate scale, M_{EX} , is consistent with decoupling of the other exotics. The potential difficulty can be summarized as follows: all of the (200,000+) mass terms in the superpotential come from giving various MSSM singlets VEVs. Above, we have shown that unification depends on some exotics receiving mass at the string scale, and some exotics receiving mass at an intermediate scale. This means that some singlets need to have VEVs on the order of the string scale, M_s , while other singlets need to have VEVs

²⁹The proton decay rate $\Gamma(p \rightarrow \pi^0 e^+)$ is proportional to the fourth power of the GUT coupling constant, see Appendix D.

³⁰See Appendix D for more details.

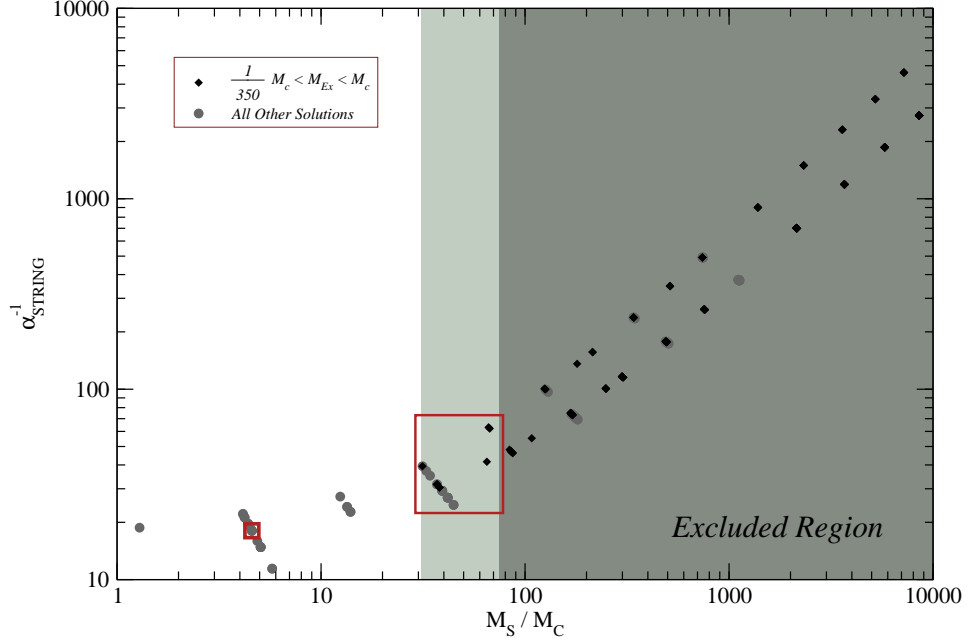


Figure 3.4: Here we show the correlation between the hierarchies in the problem. Quite generally, a small value of $\alpha_{\text{STRING}}^{-1}$ requires a large hierarchy between the compactification scale and the exotic scale. Again we show the excluded (darker green) and possibly testable (lighter green) models. The exact relationship between the ratio of $M_{\text{S}}/M_{\text{C}}$ and the proton lifetime is given in Appendix D. In particular, note the “nice” models (black diamonds) in the large red box, characterized by moderate hierarchies between all scales. These models are collected in Table H.10. Finally, note the one point in the small red box—this model is described in Section 3.4.

on the order of the exotic mass scale, M_{EX} . It is not obvious, *a priori*, that we can do this in a consistent way. That is, decoupling with $D = F = 0$ was checked in Reference [38], but only for the case where all of the singlet VEVs were of order the string scale. In light of gauge coupling unification, we are motivated to revisit the previous conclusions.

As we will show, there is a very nice way to accommodate unification in Model 1A, which relies only on moderate tunings. The tunings will be apparent when we address the question of $F = 0$ in Section 3.4.1. In that section we will see how some numbers of order the string scale must conspire to cancel some numbers of order the exotic scale.

While Model 1A and Model 2 have similar sets of exotics, *they have different super potentials*. So while it is possible to find nice ways to accommodate unification within Model 1A, we find that there *does not* seem to be an easy way to assign singlet VEVs in Model 2 such that we can accommodate unification. This does not mean that it is impossible to accommodate unification in Model 2, but it does make the process of assigning singlet VEVs an exercise in fine tuning.

In what follows, we use the notation defined in Reference [38] concerning the MSSM singlets. In short, the states labeled s_i are singlets under the hidden sector and visible sector gauge groups, while the states labeled h_i transform as (hidden sector) SU(2) doublets. Some subset of the s_i and h_i are expected to get non-zero VEVs, which defines a vacuum configuration. Again, we refer the reader to Reference [38] for more details.

3.4.1 Model 1A

Let us first consider the issue of unification in Model 1A, where we can solve the $F_i = 0$ equations exactly, giving us conditions on the singlet VEVs to ensure that mass terms for the exotics do not break supersymmetry at some high scale. We must check that we can consistently give some exotics intermediate scale mass, while maintaining supersymmetry.

It turns out that giving only *brane localized* exotic matter intermediate scale mass will not give gauge coupling unification in this model. This can be seen as follows: in order to get unification, we need $b_3^{\text{EX}} - b_2^{\text{EX}} > 0$, otherwise the prediction for the string scale is $M_S \lesssim 10^{15}$ GeV. The states which contribute to this difference are (see Table H.4, for example)

$$v \equiv (\mathbf{3}, 1)_{1/3, -2/3}, m \equiv (1, \mathbf{2})_{0,*} \text{ and } y \equiv (1, \mathbf{2})_{0,0}. \quad (3.15)$$

The mass matrices for the y and v turn out to be the same, which means that we always get an equal number $v + \bar{v}$ and $y + \bar{y}$ with the same mass. One can check in Table H.7 that there are no solutions in which the number of $v + \bar{v}$ is less than or equal to the number of $y + \bar{y}$. Conversely, one can see this from Equation (3.7a). If $n_2 \geq n_3$, the string scale must be smaller than the GUT scale (assuming $M_S > M_{\text{EX}}$), which (as we have previously argued) is not physical. Thus we *must* give some bulk exotic matter intermediate scale mass as well.

In giving bulk matter mass, we are severely limited in our options. For one, the requirement that $b^G < 0$ means that we can only keep two extra pair of $\mathbf{6} + \mathbf{6}^c$ light. Further, there is only one pair of extra down quarks and the states $\delta + \bar{\delta}$. In the first case, the extra $d + \bar{d}$ pair comes in an SU(6) multiplet with an extra $\ell + \bar{\ell}$, both of which have $(++)$ boundary conditions, and both of which couple in the same way to the singlet fields (to sixth order, and likely to all orders). This means that they must get the same mass, and we cannot get $b_3^{\text{EX}} - b_2^{\text{EX}} > 0$ in this manner. The remaining option is that we find an assignment of singlet VEVs to give one pair of $\delta + \bar{\delta}$ intermediate scale mass.

Let us be a bit more explicit about how one would accomplish this, starting with a brief examination of the δ s. The mass matrix for the δ s looks like

$$\mathcal{M}_{\delta\bar{\delta}} = \begin{pmatrix} 0 & B_1 & B_2 & 0 & 0 & 0 \\ B_3 & A_1 & A_2 & 0 & 0 & 0 \\ B_4 & A_3 & A_4 & 0 & 0 & 0 \\ 0 & 0 & 0 & C_1 & C_2 & D_1 \\ 0 & 0 & 0 & C_3 & C_4 & D_2 \\ 0 & 0 & 0 & D_3 & D_4 & 0 \end{pmatrix}, \quad (3.16)$$

where A_i, B_i, C_i and D_i are functions of singlet fields. Let us concentrate on the upper left block of this matrix, which involves only A_i and B_i . (The expressions for C_i and D_i are long and unenlightening, and not essential for the discussion here.) In general, the entries in the matrix have the following form:

$$A_i \sim \frac{1}{M_S^5} s_1 \cdot s_5 \cdot s_6 \cdot s_{18} \cdot (h_1 \cdot h_{10} + h_2 \cdot h_9), \quad (3.17)$$

$$B_i \sim \frac{1}{M_S^5} s_5 \cdot s_6 (h_{10} \cdot h_1 + h_9 \cdot h_2) \cdot (h_1 \cdot h_2 + s_{17} \cdot s_{18}). \quad (3.18)$$

Naively, diagonalizing this block gives one zero eigenvalue, which means that there are two linear combinations of the δ s that are massless. However, one must remember that the string selection rules only give us the *form* of the Yukawa couplings, and not their exact magnitudes. In general, this means that we should be calculating N point correlation functions on the orbifold in order to get the *exact* Yukawa couplings in the theory. In particular, it is important to remember that the δ s live at *different* orbifold fixed points, and the interaction eigenstates are a linear superposition of these “orbifold eigenstates”. Returning to Equation (3.17), we see that if we require

$$\begin{aligned} \langle s_1 \rangle &\sim M_{\text{EX}}, \\ \text{All other singlets} &\sim M_S, \end{aligned} \quad (3.19)$$

we naturally get one eigenstate with mass of order M_{EX} , and five heavy ($\sim M_S$) eigenstates. We note that there is some dependence on $\langle s_1 \rangle$ in the C_i and D_i at fifth order in the singlets, however, there is *no* dependence at sixth order, suggesting that these terms (in general) dominate the much smaller fifth order terms.

Next we consider the the $v + \bar{v}$ and $y + y$. The mass matrices for these states are 2×2 and identical, and after they are diagonalized we find (ignoring constants of order one)

$$m \sim s_{25} \left\{ 1 + \frac{1}{M_S^2} (s_{26} \cdot s_{15} + s_{26} \cdot s_{16}) + \frac{1}{M_S^4} (s_{26}^2 \cdot s_{15} \cdot s_{16} + s_{26}^2 \cdot s_{16}^2 + s_{26}^2 \cdot s_{15}^2) + \frac{1}{M_S^5} (s_4 \cdot s_6 \cdot s_9 \cdot s_{30} \cdot s_{18}) \left(\frac{s_{11} \pm s_5}{s_{25}} \right) \right\}. \quad (3.20)$$

It is clear that the following set of singlet VEVs is consistent with giving $2 \times (v + \bar{v}) + 2 \times (y + y)$ a mass at M_{EX} :

$$\begin{aligned} \langle s_1 \rangle \sim \langle s_{25} \rangle &\sim M_{\text{EX}}, \\ \text{All other singlets} &\sim M_S. \end{aligned} \quad (3.21)$$

Note that we do rely here on some suppression in the sixth order term, so that it does not give an overwhelming (i.e., $\mathcal{O}(M_S)$) contribution to the mass term. This may be viewed as an additional tuning in the singlet VEVs, on the order of one part in ten or twenty.

Finally we check whether the VEV assignment (3.21) is consistent with having some number of $(1, 1)_{1,*} + (1, 1)_{-1,*}$ pairs with mass $\sim M_{\text{EX}}$. In general, the charged singlet mass matrix (if we ignore the possibility of intermediate scale mass for the $\bar{f}^+ + f^-$) is 14×14 with equally complicated eigenvalues, so we will omit the details of this analysis. Nevertheless, if we proceed in the same manner, we do find two linear combinations of singlets (s^+ and s^-) whose mass terms depend *explicitly* on the VEV $\langle s_{25} \rangle$, giving them naturally small mass terms.

We conclude that unification is possible *in principle* in Model 1A. Specifically, in the absence of accidental cancellations, and assuming that higher order terms in the superpotential are negligible (such that the light linear combination of the δ s remains light), we have found one version of Model 1A that gives us gauge coupling unification. Namely, if we assume order one coefficients in the mass matrices, and that

$$\langle s_1 \rangle \sim \langle s_{25} \rangle \sim M_{\text{EX}}, \quad \text{All other singlets} \sim M_S, \quad (3.22)$$

we have exactly the following matter content in the theory with mass on the order of M_{EX} :

$$2 \times [v + \bar{v}] + 1 \times [y + y] + 2 \times [s^+ + s^-] + [\delta + \bar{\delta}].$$

This corresponds to the solution marked with an arrow (\Rightarrow) in Table H.8 on page 157³¹. This gives us a prediction for the intermediate scale, the compactification scale, the string

³¹Note that the states y are doublets under a hidden sector $SU(2)$, so that $1 \times [y + y] \sim 2 \times [(1, \mathbf{2})_{0,*} + (1, \mathbf{2})_{0,*}]$

scale, and proton decay coming from dimension six operators:

$$\begin{aligned}
M_{\text{EX}} &\sim 1.9 \times 10^9 \text{ GeV}, \\
M_{\text{C}} &\sim 2.2 \times 10^{17} \text{ GeV}, \\
M_{\text{S}} &\sim 1.0 \times 10^{18} \text{ GeV}, \\
\tau(p \rightarrow e^+ \pi^0) &\sim 1.2 \times 10^{38} \text{ y}.
\end{aligned} \tag{3.23}$$

It is worth pointing out that this solution is not yet ruled out by the current bounds on proton decay, a fact which was not guaranteed. This model is pictured in the small red box in Figure 3.4 on page 64.

We note that the other option that one may try is, for example

$$\langle s_{11} \rangle + \langle s_5 \rangle \sim M_{\text{S}}, \quad \langle s_{11} \rangle - \langle s_5 \rangle \sim M_{\text{EX}}, \quad \langle s_{25} \rangle \sim \langle s_1 \rangle \sim M_{\text{EX}}. \tag{3.24}$$

This is a tuning to one part in $M_{\text{S}}/M_{\text{EX}}$, and is consistent with $F = 0$, which is discussed below. This gives us one pair of $v + \bar{v}$ and one y , and one pair of $\delta + \bar{\delta}$ with exotic scale mass, assuming that we *can't* neglect the sixth order term in Equation (3.20). The problem that one may encounter is with the charged singlets. Taking $\langle s_{25} \rangle \sim M_{\text{EX}}$ generally gives one at least *two* charged singlets with mass at the intermediate scale, so one may need an additional tuning in that sector of the theory in order to realize one of the solutions in Table H.8.

$F = 0$

Let us now comment on the compatibility of these solutions with the constraint of $F = 0$ in the case of Model 1A. If we set all of the coefficients in the superpotential to one, the F flatness conditions can be solved exactly in this model. In units where $M_{\text{S}} \equiv 1$, we find the following relationships among the singlet VEVs:

$$s_{22} = -\frac{1}{s_{20} + s_{21}} (h_1 h_2 + s_{17} s_{18}) - s_{23}, \tag{3.25}$$

$$s_{26} = -\frac{1}{s_{15} + s_{16}}, \tag{3.26}$$

$$\begin{aligned}
s_1 &= \frac{s_{15} + s_{16}}{s_{18}} \left\{ h_1 h_{10} + h_2 h_9 + s_{17} s_{25} + s_{18} s_{27} \right. \\
&\quad \left. + (s_{15} + s_{16}) s_{30} + (s_{20} + s_{21}) s_{31} \right\}.
\end{aligned} \tag{3.27}$$

The task is to now assign arbitrary VEVs to everything *except* s_{22} , s_{26} , and s_1 , and look for solutions where $s_1 \sim s_{25} \sim M_{\text{EX}}$. The tuning in this model is evident in Equation (3.27). It is clear that there must be a cancellation on the right hand side of the equation to one part

in M_S/M_{EX} . In general, one has no trouble finding numerical solutions to these equations such that $s_1 \sim s_{25} \sim M_{\text{EX}}$, while all other singlets have VEVs near the string scale.

One may object to the fact that we did not include superpotential coefficients in Equation (3.25) - (3.27), as it is clear that decoupling depends on these coefficients *not* being set to one. Solving the F flatness conditions with arbitrary superpotential coefficients is a computationally intensive problem. However, we expect that the inclusion of such coefficients will not significantly alter our conclusions.

3.4.2 Model 2

The exotic matter content of Model 2 is listed in Table H.4. The *brane localized* states which contribute to the differential running $\alpha_3^{-1} - \alpha_2^{-1}$ are

$$v \equiv (\mathbf{3}, 1)_{1/3, -4/3}, m \equiv (1, \mathbf{2})_{0,*} \text{ and } y \equiv (1, \mathbf{2})_{0,0}. \quad (3.28)$$

In Model 2 we have

$$4 \times (v + \bar{v}) + 2 \times (y + y) + 2 \times (m + m) + 20 \times (s^+ + s^-) + 2 \times (x^+ + x^-), \quad (3.29)$$

where x^\pm are defined in Table H.4.

The mass matrix for the v is a 4×4 block diagonal matrix. The blocks are both 2×2 , and the upper block turns out to be equivalent to the (2×2) mass matrix for the ys . By choosing

$$\langle h_2 \rangle \sim \langle s_{43} \rangle \sim M_{\text{EX}}, \quad \text{All other singlets} \sim M_S, \quad (3.30)$$

we find $4 \times (v + \bar{v}) + 2 \times (y + y)$. The problem with the VEV assignment in Equation (3.30) is that we get too many charged singlets, so we will need to rely (heavily) on tuning arguments. Thus we conclude that for Model 2 to be consistent with gauge coupling unification, we must arrange a conspiracy among the singlet VEVs, such that we get intricate cancellations in the charged singlet sector.

3.5 Conclusions

We have addressed the question of gauge coupling unification in a class of 15 “mini-landscape” models [38] with properties very similar to the MSSM. We analyze these $E_8 \times E_8$ weakly coupled heterotic string models compactified on an anisotropic orbifold with one large (R) and five small (l_S) extra dimensions, where $R \gg l_S$ and l_S is the string length. All of these theories can then be described in terms of an effective 5D $SU(6)$ orbifold GUT field theory with compactification scale $M_C = 1/R$ and cut-off scale $M_S = 1/l_S$. $SU(6)$ is broken to the MSSM gauge group by orbifold boundary conditions at M_C and gauge couplings must unify at the cut-off scale, M_S . Moreover, in an orbifold GUT field theory, this

is accomplished with the aid of Kaluza-Klein modes which contribute to the RG running above the compactification scale, M_C .

In all 15 models the electroweak Higgs doublets reside in the (effective 4D, $N = 2$) vector multiplet, hence the models satisfy “gauge-Higgs unification.” In addition the third family of quarks and leptons are “bulk” modes, while the two lighter families are “brane” states. Although “gauge-Higgs unification” may be well-motivated by aesthetics, we prove in Appendix C that gauge coupling unification is not possible if one only includes MSSM states and their KK towers. Thus it is necessary to also include the possible contribution of vector-like exotics to the RG running. To simplify the analysis, we assume a small set of exotics obtain mass at a scale $M_{\text{EX}} < M_C$ with the remainder obtaining mass at M_S . Using an effective field theory analysis, we find many solutions to gauge coupling unification labeled by the different inequivalent sets of exotics with mass at M_{EX} . These solutions are found in Tables H.7 - H.10, on pages 156 - 159.

We have analyzed two models in more detail (Models 1A and 2 [38]), since for these models we have the superpotential up to order 6 in MSSM singlets. In this case, we have shown that one of our solutions (in Model 1A) is consistent with string theory in a supersymmetric vacuum with $F = 0$, if we tune the singlet VEVs appropriately in Equation (3.27). On the other hand, for the case of Model 2, although there are many effective field theory solutions, we have not been able to demonstrate the existence of a simple string vacuum solution with $F = 0$. In this case, a solution may still be possible, however, it would require more fine-tuning.

Since quarks and leptons of the first two families are located on an effective $SU(5)$ brane, they are subject to proton decay processes mediated by gauge exchange at the compactification scale M_C . Moreover, since M_C is generically less than the 4D GUT scale, the proton decay rate for the process $p \rightarrow e^+ \pi^0$ is enhanced. Thus 80% of the models satisfying gauge coupling unification are excluded by Super-K bounds on proton decay. Most of the other models can be tested at a future proton decay detector.

All of the “mini-landscape” models have an exact R parity, so they do not suffer from dimension 3 or 4 baryon and/or lepton number violating processes. Moreover, the LSP is stable and a possible dark matter candidate. However, unlike 5D or 6D orbifold GUT field theories studied in the literature, these models suffer from uncontrolled dimension 5 operator contributions to proton decay. In particular, some of the vector-like exotics have quantum numbers of color triplet Higgs multiplets. When given mass at M_S or M_{EX} they induce dimension 5 proton decay operators. Although it may be possible to fine-tune the coefficients of these operators to be small, it would be preferable to have a symmetry argument. This problem needs to be addressed in any future string model building.

As noted, all of the models studied in this analysis have a 5D (or 6D) $SU(6)$ orbifold GUT limit. The complete spectrum of the 6D model (prior to the final \mathbb{Z}_2 orbifold and

Wilson line, A_2) is given in Table H.3. It is very interesting to note that the spectrum is identical with the spectrum found in an $E_8 \times E'_8$ heterotic string compactified on a smooth $K_3 \times T^2$ manifold with instantons embedded in the $E_8 \times E'_8$ gauge groups [117]. This suggests that these models may be obtained by the final \mathbb{Z}_2 orbifolding of these smooth manifolds.

In conclusion, we have shown that gauge coupling unification may be accommodated in the present class of string models. However, a simple solution, without including vector-like exotics below the string scale, was not possible. This appears to be a general conclusion stemming from the particular implementation of “gauge-Higgs unification” in these models. Finally, any future string model building needs to address the general problem of uncontrolled dimension 5 baryon and lepton number violating operators.

Chapter 4

THE STRING COUPLING IN A CLASS OF STRINGY ORBIFOLD GUTS

4.1 Motivation

In Chapter 3 it was shown how the mini-landscape models [34–38] could accommodate gauge coupling unification in the 5D orbifold GUT limit. Given the exotic matter content of the two benchmark models outlined in Reference [38], we found (using an effective field theory analysis) 252 ways to achieve unification by varying the cutoff M_s in the effective field theory, the compactification scale M_C , and (most importantly) the spectrum of “light” exotics with mass M_{EX} . Of the 252 different solutions found, 48 were not already ruled out by current (dimension six) proton decay bounds. By assigning VEVs to MSSM singlets, we were able to show how one could realize one of these solutions in the “Model 1A” of Reference [38]. In addition, the solution described in [30] satisfies the constraints for unbroken low energy supersymmetry: $F = D = 0$. This latter feature is essential if we are to understand the origin of the hierarchy between the electroweak and Planck scales.

In this Chapter we address the important question of whether any of these constructions are consistent with a perturbative string expansion. We find a simple formula for the 10D string coupling g_{STRING} (see Eqn. 4.6) and show that the constraint $g_{\text{STRING}} < 1$ is correlated with the longevity of the proton. Of course, this result applies only to a very small, even minuscule, portion of the string landscape; however, the relevant question is whether or not it is applicable to those very constrained portions of the string landscape where the minimal supersymmetric standard model can be shown to reside.

4.2 The Starting Point

The models of Reference [38] are derived from an orbifold compactification of the weakly coupled heterotic string: formally $T^6/\mathbb{Z}_6\text{-II}$, which can be parameterized by the root lattice $G_2 \times \text{SU}(3) \times \text{SO}(4)$. By varying the VEVs of the T (size) and U (shape) moduli associated

with the $SO(4)$ lattice, it was shown in References [39–41] that one can achieve a stringy embedding of the highly successful orbifold GUT picture [84–86, 90]. In the literature, this has been called “anisotropic” string compactification [39, 41, 99–101, 118]. The problem, of course, is that the GUT coupling constant in the effective four dimensional theory is proportional to the ten dimensional Yang-Mills coupling (and thus the string coupling, g_{STRING}) by a factor of one over the volume of the six-dimensional compactification. The requirement of acceptable unification in the low energy effective field theory may be inconsistent with the requirement that the underlying string theory be weakly coupled ($g_{\text{STRING}} \lesssim 1$), depending on the precise relationship between the two parameters.

By demanding that the underlying heterotic string theory still be perturbative (i.e., weakly coupled), we show how one can further constrain the parameter space of our models—in fact, of the 252 solutions which were found in Reference [30], only 28 of them turn out to have $g_{\text{STRING}} < 1$, see Table H.10 on page 159. Moreover, all of these 28 models have a long lived proton, with $\tau(p \rightarrow \pi^0 e^+) \gtrsim 10^{34}$ y. Because the proton lifetime is proportional to the fourth power of the compactification scale, and the string coupling g_{STRING} is inversely proportional to the volume of the compact space, there is a correlation between M_C , g_{STRING} and M_S , which we make explicit. This means that the question of weak string coupling is not entirely decoupled from the low energy phenomenology in these models. In fact, for a reasonable choice of parameters, a long lived proton seems to be *synonymous with* weak string coupling. A particularly interesting detail is that the same example which we constructed in Section 4 of Reference [30] will survive this round of scrutiny, with $g_{\text{STRING}} \sim 0.5$. In addition, all but one of the nine models which were categorized as “interesting” (see Table 9 in Reference [30]) are eliminated when we require the string coupling to be small. Thus the requirement that we be in a perturbative regime of the underlying string theory gives a new, non-trivial constraint on the “mini-landscape” models. In light of this requirement, we comment on the ability to interpret the models of References [34–38] as six (and higher) dimensional orbifold GUTs.

4.3 The String Coupling

In a given string compactification, the string coupling is set by the VEV of a scalar field, called the dilaton. In general, one has $g_{\text{STRING}}^2 \sim e^{2\phi}$. In order to find the exact relationship, one must start from the ten dimensional effective action for the weakly coupled heterotic string and compactify on some six dimensional manifold. The four dimensional effective action is [119]

$$\mathcal{S}_{\text{eff}} = - \int d^4x \sqrt{g} e^{-2\phi} V_6 \left\{ \frac{4}{\alpha'^4} R + \frac{1}{\alpha'^3} \text{TR} F^2 + \dots \right\}. \quad (4.1)$$

where ϕ is the (ten dimensional) dilaton, V_6 is the volume of the compactification, and α' is the parameter which sets the string tension. We can identify the coefficient of the gravity term with Newton's constant:

$$\frac{4e^{-2\phi}V_6}{\alpha'^4} \equiv \frac{1}{16\pi G_N} \Rightarrow G_N \equiv \frac{\alpha'^4 e^{2\phi}}{64\pi V_6}, \quad (4.2)$$

and the coefficient of the gauge kinetic term with the (four dimensional) Yang-Mills coupling constant³²:

$$\frac{e^{-2\phi}V_6}{\alpha'^3} \equiv \frac{1}{2g_{\text{GUT}}^2} \Rightarrow \alpha_{\text{GUT}} \equiv \frac{\alpha'^3 e^{2\phi}}{8\pi V_6}. \quad (4.3)$$

The parameter α' is related to the cutoff in the effective field theory [30, 120]: $\Lambda^{-2} \equiv M_s^{-2} \approx \alpha'$. Note that this parameter was chosen in such a way as to capture the maximum amount of stringy (threshold) effects in the low energy effective field theory without actually calculating them [120]. Of course, the exact relationship between α' and M_s depends on the regularization scheme (see for example [74]). In particular, we will take the standard definition of the *string length* ℓ_s , such that it is related to the cutoff by $\ell_s \equiv \frac{\sqrt{\alpha'}}{2} \approx \frac{1}{2M_s}$. Finally, the compactification scale is given in terms of the radius of the fifth dimension: $\ell_c = R \equiv \frac{1}{M_c}$.

By exploiting the duality between the $E_8 \otimes E_8$ heterotic theory and heterotic-M theory, Hebecker and Trapletti argued [101] that the proper relationship between the 10D dilaton and the string coupling constant is given by³³

$$g_{\text{STRING}}^2 \equiv \frac{8e^{2\phi}}{(2\pi)^7}. \quad (4.4)$$

This gives us a relationship between the (four dimensional) GUT coupling constant at the string scale and the string coupling. By eliminating the dilaton dependence between Equations (4.3) and (4.4) we find

$$\alpha_{\text{GUT}} = \frac{\alpha'^3 (2\pi)^6}{2^5 V_6} g_{\text{STRING}}^2 \quad (4.5)$$

Taking five directions compactified at the string length, ℓ_s , and one direction compactified at ℓ_c , we find

$$g_{\text{STRING}}^2 = \alpha_{\text{GUT}} \frac{M_s}{M_c}. \quad (4.6)$$

³²Note that we have normalized the gauge fields such that in the fundamental representation of $SU(N)$ we have $\text{TR}(T_a T_b) = \frac{1}{2} \delta_{ab}$, which is the standard normalization used for phenomenology. In addition the GUT coupling α_{GUT} is evaluated at the string scale M_s .

³³They showed that for $g_{\text{STRING}} < 1$, the lowest lying massive state is a perturbative heterotic string state, while for $g_{\text{STRING}} > 1$ it is a Kaluza-Klein mode of M theory. At the present time, this is the best estimate we know of for defining the perturbative heterotic string regime.

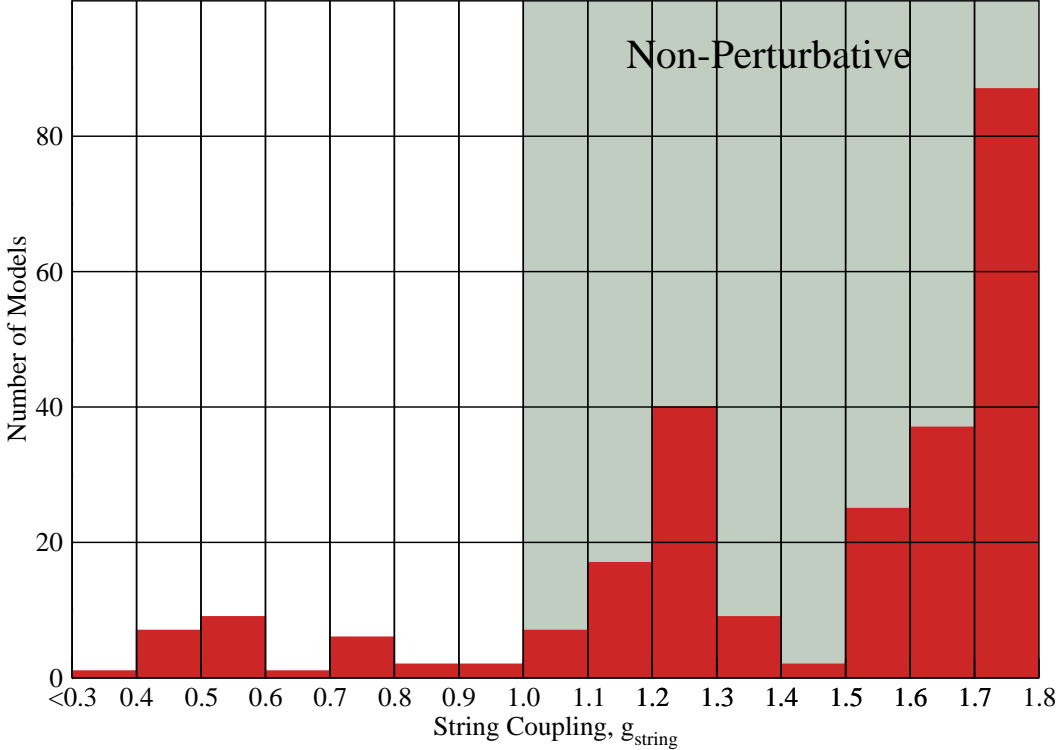


Figure 4.1: Histogram of the string coupling of the 252 solutions of Reference [30]. Of the 48 models which were not eliminated previously because of dimension six proton decay, 28 have $g_{\text{STRING}} \lesssim 1$.

Note that it is entirely possible that the effective field theory be weakly coupled, but that the underlying string theory be strongly coupled.

4.4 Are We Perturbative?

Using the relationship in Equation (4.6), we can examine the 252 different solutions found in Reference [30]. The results of this analysis are shown in Figure 4.1. Of the 48 models which were not eliminated previously because of dimension six proton decay, 28 have $g_{\text{STRING}} \lesssim 1$. There is certainly a preference for strong coupling in these models: this is a competing effect between the ratio of the string scale to the Planck scale (which sets α_{GUT}) and the ratio of the string scale to the compactification scale (which sets g_{STRING}).

In general, however, it is significant that only the models with long lived protons have small string coupling. As discussed in [30] the proton lifetime scales as $(M_C/4\pi^2)^2/\alpha_{\text{GUT}}^2$. Then using the relation between α_{GUT} and the Planck scale

$$\alpha_{\text{GUT}}^{-1} = \frac{1}{8} \left(\frac{M_{\text{PL}}}{M_{\text{S}}} \right)^2 \quad (4.7)$$

obtained by combining Equations (4.2) and (4.3), and the dimension 6 operator contribution to the proton decay rate (see Reference [30]), we obtain the following useful formula for the proton lifetime:

$$\tau(p \rightarrow \pi^0 e^+) \cong 5.21 \times 10^{40} \left(\frac{M_C}{M_S} \right)^4 \text{ yr.} \quad (4.8)$$

We can then re-write Equation (4.6) as

$$g_{\text{STRING}}^2 = \alpha_{\text{GUT}} \left(\frac{5.21 \times 10^{40} \text{ yr}}{\tau(p \rightarrow \pi^0 e^+)} \right)^{1/4}. \quad (4.9)$$

The current (published) limit on the proton lifetime [?]

$$\tau(p \rightarrow e^+ + \pi^0) > 1.6 \times 10^{33} \text{ yr} \quad (4.10)$$

implies that

$$g_{\text{STRING}}^2 \lesssim 600 \frac{M_S^2}{M_{\text{PL}}^2}, \quad (4.11)$$

where we have inserted the definition of α_{GUT} in terms of the Planck scale, Equation (4.7). If we take a typical value for the string scale $\sim 5.0 \times 10^{17} \text{ GeV}$ and the Planck scale $\sim 1.2 \times 10^{19} \text{ GeV}$, we find that

$$g_{\text{STRING}}^2 \lesssim 1. \quad (4.12)$$

Another interesting point is that the model described in Section 4 of Reference [30] has a small string coupling. There, we found $M_C \sim 2.2 \times 10^{17} \text{ GeV}$ and $M_S \sim 1.0 \times 10^{18} \text{ GeV}$. We find $g_{\text{STRING}} \sim 0.5$. This is encouraging because we were able to show that that model is consistent with $F = D = 0$ and the decoupling of unwanted exotics from the low energy spectrum.

Of the 48 solutions which we found in Reference [30], we isolated a handful (9) which exhibited only moderate hierarchies between the scales in the problem. When we look at the string coupling using Equation (4.6), however, we see that only one of them can be derived from a model at weak coupling. Unsurprisingly, this is also the model with the largest value of M_C and thus the longest lived proton.

Note that in all of the models with $g_{\text{STRING}} < 1$, the compactification scale M_C is above or equal the 4D GUT scale: see Table H.10 on page 159. Hence the threshold corrections in these models, which focus the 3 low energy couplings, come predominantly from the contribution of the exotics with mass M_{EX} . This result is particularly model dependent. While the KK modes contribute the universal power law running which allows the theory to satisfy the weakly coupled heterotic string boundary condition, Equation (4.7), they also contribute to the differential running in a way which does not focus the 3 gauge couplings. It is the exotic matter at the intermediate scale which furnishes a contribution to

the differential running, allowing for $M_C \gtrsim M_{\text{GUT}}$. However, it is possible that in other string models the KK modes alone would be sufficient to both satisfy the weakly coupled heterotic string boundary condition and focus the 3 gauge couplings.

Finally, we note that the models described in Reference [38] can be interpreted as six dimensional orbifold GUTs. If this is the case, then the relationship in Equation (4.6) will be amended:

$$g_{\text{STRING}}^2 = 2 \frac{M_s^2}{M_5 M_6} \alpha_{\text{GUT}} = 16 \frac{M_s^4}{M_5 M_6 M_{\text{PL}}^2}, \quad (4.13)$$

where $\ell_{5(6)} \equiv M_{5(6)}^{-1}$ is the radius of the fifth (sixth) direction. In this case, it seems equally likely that a weakly coupled model can be constructed. If we take, for example, $M_5 \sim M_6 \sim M_C$, and the typical value of $M_s \sim 5 \times 10^{17}$ GeV, we find $g_{\text{STRING}} \lesssim 1$ requires $M_C \gtrsim 8 \times 10^{16}$ GeV.

Taking more directions larger than the string length pushes us toward stronger and stronger coupling, and it seems likely that if this is the case then some other directions would have to be *smaller* than the string length. This can be seen by looking at the general relationship between g_{STRING} and the other scales in the problem. If we take n extra dimensions to be large, we find

$$g_{\text{STRING}}^2 = 2^{n+2} \frac{M_s^{n+2}}{M_C^n M_{\text{PL}}^2}. \quad (4.14)$$

If we take $n = 3$, and a typical string scale, we find that $M_C \gtrsim 3 \times 10^{17}$ GeV.

4.5 Conclusion

In this Chapter, we have analyzed the string coupling in a class of highly successful models based on anisotropic compactifications of the weakly coupled heterotic string. Of the 252 different solutions consistent with gauge coupling unification found in Reference [30], 48 were not already ruled out by current (dimension six) proton decay bounds. In this paper, out of the 48 solutions (not eliminated by the non-observation of proton decay) we find 28 which are consistent with a weakly coupled heterotic string, $g_{\text{STRING}} < 1$ (see Figure 4.1).

We also pointed out an interesting correlation between the string scale, the Planck scale, and the compactification scale (which sets the proton lifetime). Specifically, a proton lifetime consistent with current bounds on dimension six operators seems to require weak coupling, for a reasonable choice of parameters. Moreover, we were able to show that one specific (and very well-motivated) example *does* require $g_{\text{STRING}} \sim 0.5$.

For all cases with $g_{\text{STRING}} < 1$, the compactification scale M_C is above or equal the 4D GUT scale, $M_{\text{GUT}} \sim 3 \times 10^{16}$ GeV. Hence the threshold corrections in these models, which focus the 3 low energy couplings, come predominantly from the contribution of the exotics with mass M_{EX} . While the KK modes contribute the universal power law running

which allows the theory to satisfy the weakly coupled heterotic string boundary condition, Equation (4.7), they also contribute to the differential running in a way which does not focus the 3 gauge couplings. It is the exotic matter at the intermediate scale which furnishes a contribution to the differential running, allowing for $M_C \gtrsim M_{\text{GUT}}$. This result is model dependent and it is possible that in other string models the KK modes alone would be sufficient to both satisfy the weakly coupled heterotic string boundary condition and focus the 3 gauge couplings.

Finally, we commented on extensions of this work to six (and higher) dimensional orbifold GUTs—barring large threshold corrections from somewhere else (i.e., higher dimensional operators), it seems possible to construct models which are consistent with the weak coupling ansatz in six dimensions. However, in going to higher dimensions, it seems likely that one would have to look for models in which some of the compact directions had radii *smaller than* the string length.

Chapter 5

MODULI STABILIZATION IN ORBIFOLD COMPACTIFICATIONS OF THE HETEROtic STRING

5.1 Motivation

In a supersymmetric gauge theory, moduli are scalar fields that have no potentials at tree level. Furthermore, the supersymmetric non-renormalization theorem prevents a potential from being generated for the moduli by radiative corrections. Thus, a modulus can have no potential in a gauge theory with unbroken supersymmetry.

The low energy limit of heterotic string theory compactified on an orbifold is $D = 4, \mathcal{N} = 1$ supergravity (SUGRA) coupled to $E_8 \otimes E_8$ or $SO(32)$ gauge theory. Aside from the gauge bosons, the low energy effective field theory also contains several moduli which parametrize the coupling constant of the gauge theory and the details of the compact dimensions. For example, the Yang-Mills action in the low energy theory actually comes from a dimension five operator:

$$\mathcal{L}_{\text{YM}} \supset \frac{S + \bar{S}}{M_{\text{PL}}} F^{\mu\nu} F_{\mu\nu}. \quad (5.1)$$

S is a modulus, thus it can have no potential if SUSY is unbroken. This corresponds to a gauge theory without a coupling constant, which is clearly unphysical. In order to get realistic phenomenology from our heterotic string compactifications, we must address the issue of moduli stabilization.

One option for stabilizing moduli is to rely on radiative corrections to generate a potential [121], which can (in principle) occur if supersymmetry is broken by some other sector of the theory. If this were possible, one would expect $\langle S \rangle$ to be of order the SUSY breaking scale:

$$\langle S \rangle \sim \Lambda_{\text{SUSY}}. \quad (5.2)$$

Low energy data (see Figure 1.8), together with Equation (5.1) seem to imply that $\langle S \rangle \sim \mathcal{O}(M_{\text{PL}})$. Thus we are left to accept either non-perturbative unification ($g_{\text{GUT}} \gg 1$) or Planck scale supersymmetry breaking, both of which are phenomenologically undesirable.³⁴

There is hope: the SUSY non-renormalization theorems make concrete statements about perturbative physics, and do not apply to non-perturbative effects. Past work to stabilize the dialton in the heterotic string orbifold compactifications [122, 123] has relied on the “Racetrack” mechanism [124]. Because the Yang-Mills coupling is (inversely) proportional to the VEV of S , the competing non-perturbative effects (which always go like e^{1/g^2}) caused when two non-Abelian groups of become strongly coupled at roughly the same scale can generate a potential for S once gravitational corrections are included.³⁵ Multiple gauge groups of “large” rank are common features of the heterotic constructions, however, it was generically found that the moduli either ended up in anti-de Sitter vacua, or that the ranks of the condensing gauge groups needed were too large. While the latter problem suggests that $E_8 \otimes E_8$ or $SO(32)$ are just too small, the former problem requires that one find an additional source of “up-lifting” in the scalar potential.

The problem of stabilizing moduli in anti-de Sitter minima is a generic one in string-derived SUGRA theories, and there have been several attractive mechanisms in the literature which suggest various sources for up-lifting a generic SUGRA scalar potential. In Reference [127], for example, up-lifting was achieved when a $\overline{D3}$ brane was introduced into a IIB background, explicitly breaking SUSY at the Planck scale. A dynamical solution was presented in Reference [128], where the up-lifting came from a dynamically generated mass term, which arose because $F = 0$ and $D = 0$ could not be mutually satisfied. Other examples include Kähler up-lifting, where the leading α' corrections to the IIB [129] and heterotic [130] Kähler potentials were considered, and D Term up-lifting [131, 132], where non-zero D terms provide a positive definite contribution to the scalar potential. In fact, the common theme is that up-lifting and SUSY breaking are always tied together: whatever dynamics gives a positive definite contribution to the vacuum energy must necessarily break supersymmetry.

Thus, aside from the highly non-trivial goals of producing something that has the correct gauge groups, particle content, and Yukawa interactions to be called a proper UV completion of the Standard Model, the aim of the string phenomenologist is two-fold. On the one hand, we would like to understand moduli stabilization within the context of any (semi-) realistic string model. On the other hand, any such model must also contain some interesting dynamics which drive SUSY breaking at an acceptable scale, and provide a

³⁴We expect that the T and U moduli (which are related to the volume and shape of the compact dimensions) are stabilized at $\mathcal{O}(1)$ values as well.

³⁵The size and shape moduli (T and U , respectively) may be stabilized by considering the modular invariance of the underlying string theory, a fact which we will use later [125, 126].

source of up-lifting in the scalar potential to avoid anti-de Sitter vacua. Both issues are vitally important when it comes to understanding what is going on at energy scales that are practically accessible: the moduli fix the coupling constants (among other things) in the low energy theory, and the up-lifting sector breaks SUSY and generates the terms in the soft SUSY breaking lagrangian.

The crucial progress in this work is to demonstrate that this can all be accomplished with ingredients that one can find in a generic heterotic string orbifold compactification, without relying on uncalculable non-perturbative corrections to the Kähler potential. In Section 5.2 we summarize the general structure of the Kähler and superpotential in heterotic orbifold models. The models have a perturbative superpotential satisfying modular invariance constraints, an anomalous $U(1)_A$ gauge symmetry with a dynamically generated Fayet-Iliopoulos D -term and a hidden QCD-like non-Abelian gauge sector generating a non-perturbative superpotential. In Section 5.3 we consider a simple model with a dilaton, S , one volume modulus, T , and three standard model singlets. We obtain a ‘hybrid KKLT’ kind of superpotential that behaves like a single-condensate for the dilaton S , but as a racetrack for the T and, by extension, also for the U moduli. An additional matter F term, driven by the cancelation of an anomalous $U(1)_A$ D -term, is the seed for successful up-lifting. Whereas previous work required multiple condensates, or relied on explicit mass scales [131–140], we find that we can dynamically stabilize all of our moduli with a single non-Abelian hidden sector.³⁶ In Section 5.4 we discuss the other moduli and their stabilization. We conclude that a single gaugino condensate is sufficient to break supersymmetry, stabilize all the moduli and generate a de Sitter vacuum. Finally in Section 5.5 we evaluate the SUSY particle spectrum relevant for the LHC. The main results from this analysis are listed in Tables H.15 and H.16 in Appendix H.

5.2 General structure

In this section we consider the supergravity limit of heterotic orbifold models, focusing on the “mini-landscape” models for definiteness. We discuss the general structure of the Kähler potential, \mathcal{K} , the superpotential, \mathcal{W} , and gauge kinetic function, f_a for generic heterotic orbifold models. The “mini-landscape” models are defined in terms of a \mathbb{Z}_6 -II orbifold of the six internal dimensions of the ten dimensional heterotic string. The orbifold is described by a three dimensional “twist” vector v , which acts on the compact

³⁶It was found that 90% of the models in the mini-landscape survey had a hidden sector gauge group with rank larger than four [38]. A survey of realistic free fermionic models found that roughly 65% had hidden sector gauge groups with rank four or larger [141].

directions. We define the compact directions in terms of complex coordinates:

$$\begin{aligned} Z_1 &\equiv X_4 + iX_5, \\ Z_2 &\equiv X_6 + iX_7, \\ Z_3 &\equiv X_8 + iX_9. \end{aligned} \quad (5.3)$$

The twist is defined by the action $Z_i \rightarrow e^{2\pi i v_i} Z_i$ for $i = 1, 2, 3$, and for \mathbb{Z}_6 -II we have $v = \frac{1}{6}(1, 2, -3)$ or a $(60^\circ, 120^\circ, 180^\circ)$ rotation about the first, second and third torus, respectively. This defines the first twisted sector. The second and fourth twisted sectors are defined by twist vectors $2v$ and $4v$, respectively. Note, the third torus is unaffected by this twist. In addition, for the third twisted sector, generated by the twist vector $3v$, the second torus is unaffected. The fifth twisted sector, given by $5v$ contains the CP conjugate states from the first twisted sector. Twisted sectors with un-rotated tori contain $\mathcal{N} = 2$ supersymmetric spectra, which has consequences for the non-perturbative superpotential discussed in Section 5.2.3. Finally, these models have three bulk volume moduli, T_i , $i = 1, 2, 3$ and one bulk complex structure modulus, U , for the third torus.

5.2.1 Anomalous $U(1)_A$ and Fayet-Illiopoulos D -term

The orbifold limit of the heterotic string has one anomalous $U(1)_A$ symmetry. The dilaton superfield S , in fact, transforms non-trivially under this symmetry. Let V_A , V_a be the gauge superfields with gauge covariant field strengths, W_A^α , W_a^α , of gauge groups, $U(1)_A$, \mathcal{G}_a , respectively. The Lagrangian in the global limit is given in terms of a Kähler potential [63, 64, 142–144]

$$\mathcal{K} = -\log(S + \bar{S} - \delta_{GS}V_A) + \sum_a \left(\bar{Q}_a e^{V_a + 2q_a V_A} Q_a + \bar{\tilde{Q}}_a e^{-V_a + 2\tilde{q}_a V_A} \tilde{Q}_a \right) \quad (5.4)$$

and a gauge kinetic superpotential

$$\mathcal{W} = \frac{1}{2} \left[\frac{S}{4} \left(\sum_a k_a \text{TR} W_a^\alpha W_{\alpha a} + k_A \text{TR} W_A^\alpha W_{\alpha A} \right) + h.c. \right]. \quad (5.5)$$

Note q_a , \tilde{q}_a are the $U(1)_A$ charges of the ‘quark’, Q_a , and ‘anti-quark’, \tilde{Q}_a , supermultiplets transforming under \mathcal{G}_a .

Under a $U(1)_A$ super-gauge transformation with parameter Λ , one has

$$\begin{aligned} \delta_A V_A &= -i(\Lambda - \bar{\Lambda})/2, \\ \delta_A S &= -i\frac{\delta_{GS}}{2}\Lambda, \end{aligned} \quad (5.6)$$

and

$$\delta_A \Phi = iq_\Phi \Lambda \Phi \quad (5.7)$$

for any charged multiplet Φ . The combination

$$S + \bar{S} - \delta_{GS} V_A \quad (5.8)$$

is $U(1)_A$ invariant. δ_{GS} is the Green-Schwarz coefficient given by

$$\delta_{GS} = 4 \frac{\text{TR } Q_A}{192\pi^2} = \frac{(q_a + \tilde{q}_a) N_{f_a}}{4\pi^2} \quad (5.9)$$

where the middle term is for the $U(1)_A$ gravity anomaly and the last term is for the $U(1)_A \times (\mathcal{G}_a)^2$ mixed anomaly.

The existence of an anomalous $U(1)_A$ has several interesting consequences. Due to the form of the Kähler potential (Equation (5.4)) we obtain a Fayet-Illiopoulos D -term given by

$$\xi_A = \frac{\delta_{GS}}{2(S + \bar{S})} = -\frac{1}{2} \delta_{GS} \partial_S \mathcal{K} \quad (5.10)$$

with the D -term contribution to the scalar potential given by

$$V_D = \frac{1}{S + \bar{S}} \left(\sum_a X_a^A \partial_a \mathcal{K} \phi^a + \xi_A \right)^2 \quad (5.11)$$

where X_a^A are Killing vectors for $U(1)_A$. Clearly the perturbative part of the superpotential must be $U(1)_A$ invariant, but $U(1)_A$ invariance constrains the non-perturbative superpotential. In particular, if the dilaton appears in the exponent, the product $e^{q_\Phi S} \Phi^{\delta_{GS}/2}$ is $U(1)_A$ invariant, as it must be.

5.2.2 Target space modular invariance

In this section, we wish to present the modular dependence of the gauge kinetic function, the Kähler potential, and of the superpotential in as general a form as possible. Most studies in the past have worked with a universal T modulus, and neglected the effects of the U moduli altogether. Such a treatment is warranted, for example, in the \mathbb{Z}_3 orbifolds where there are no U moduli. If we want to work in the limit of a stringy orbifold GUT [39] which requires one of the T moduli to be much larger than the others, or in the \mathbb{Z}_6 -II orbifolds, however, it is impossible to treat all of the T and U moduli on the same footing.

Consider the $SL(2, \mathbb{Z})$ modular transformations of T and U given by [145–156]³⁷

$$T \rightarrow \frac{aT - ib}{icT + d}, \quad ad - bc = 1, \quad a, b, c, d \in \mathbb{Z}, \quad (5.12)$$

³⁷For an excellent review with many references, see [157].

and

$$\log(T + \bar{T}) \rightarrow \log\left(\frac{T + \bar{T}}{(icT + d)(-ic\bar{T} + d)}\right). \quad (5.13)$$

The Kähler potential for moduli to zeroth order is given by:

$$\begin{aligned} \mathcal{K} &= -\sum_{i=1}^{h_{(1,1)}} \log(T^i + \bar{T}^i) - \sum_{j=1}^{h_{(2,1)}} \log(U^j + \bar{U}^j) \\ &= -\sum_{i=1}^3 \log(T^i + \bar{T}^i) - \log(U + \bar{U}) \end{aligned} \quad (5.14)$$

where the last line applies to the “mini-landscape” models, since in this case $h_{(1,1)} = 3$, $h_{(2,1)} = 1$. Under the modular group, the Kähler potential transforms as

$$\mathcal{K} \rightarrow \mathcal{K} + \sum_{i=1}^{h_{(1,1)}} \log|ic_i T^i + d_i|^2 + \sum_{j=1}^{h_{(2,1)}} \log|ic_j U^j + d_j|^2. \quad (5.15)$$

The scalar potential V is necessarily modular invariant. We have

$$V = e^{\mathcal{G}} \left(\mathcal{G}_I \mathcal{G}^{I\bar{J}} \mathcal{G}_{\bar{J}} - 3 \right) \quad (5.16)$$

where $\mathcal{G} = \mathcal{K} + \log|\mathcal{W}|^2$. Hence for the scalar potential to be invariant under the modular transformations, the superpotential must also transform as follows:

$$\begin{aligned} \mathcal{W} &\rightarrow \prod_{i=1}^{h_{(1,1)}} \prod_{j=1}^{h_{(2,1)}} (ic_i T^i + d_i)^{-1} (ic_j U^j + d_j)^{-1} \mathcal{W}, \\ \bar{\mathcal{W}} &\rightarrow \prod_{i=1}^{h_{(1,1)}} \prod_{j=1}^{h_{(2,1)}} (-ic_i \bar{T}^i + d_i)^{-1} (-ic_j \bar{U}^j + d_j)^{-1} \bar{\mathcal{W}}. \end{aligned} \quad (5.17)$$

This can be guaranteed by appropriate powers of the Dedekind η function multiplying terms in the superpotential.³⁸ This is due to the fact that under a modular transformation, we have

$$\eta(T) \rightarrow (icT + d)^{1/2} \eta(T), \quad (5.18)$$

up to a phase, where

$$\eta(T) = \exp(-\pi T/12) \prod_{n=1}^{\infty} (1 - e^{-2\pi n T}). \quad (5.19)$$

³⁸These terms arise as a consequence of world-sheet instantons in a string calculation. In fact, world sheet instantons typically result in more general modular functions [150–156].

The transformation of both the matter fields and the superpotential under the modular group fixes the modular dependence of the interactions. A field in the superpotential transforms as

$$\Phi_I \rightarrow \Phi_I \prod_{i=1}^{h_{(1,1)}} \prod_{j=1}^{h_{(2,1)}} (ic_i T^i + d_i)^{-n_I^i} (ic_j U^j + d_j)^{-\ell_I^j}. \quad (5.20)$$

The modular weights n_I^i and ℓ_I^j [75, 100] depend on the localization of the matter fields on the orbifold. For states I in the i th untwisted sector, i.e., those states with internal momentum in the i th torus, we have $n_I^i = \ell_I^i = 1$, otherwise the weights are 0. For twisted sector states, we first define $\vec{\eta}(k)$, which is related to the twisted sector $k (= 1, \dots, N-1)$ and the orbifold twist vector v by

$$\eta_i(k) \equiv kv_i \pmod{1}. \quad (5.21)$$

Further, we require

$$\sum_i \eta_i(k) \equiv 1. \quad (5.22)$$

Then the modular weight of a state in the k th twisted sector is given by

$$\begin{aligned} n_I^i &\equiv (1 - \eta^i(k)) + N^i - \bar{N}^i & \text{for } \eta_i(k) \neq 0 \\ n_I^i &\equiv \quad N^i - \bar{N}^i & \text{for } \eta_i(k) = 0. \end{aligned} \quad (5.23)$$

The N^i (\bar{N}^i) are *integer* oscillator numbers for left-moving oscillators $\tilde{\alpha}^i$ ($\bar{\tilde{\alpha}}^i$), respectively. Similarly,

$$\begin{aligned} \ell_I^i &\equiv (1 - \eta^i(k)) - N^i + \bar{N}^i & \text{for } \eta_i(k) \neq 0 \\ \ell_I^i &\equiv \quad -N^i + \bar{N}^i & \text{for } \eta_i(k) = 0. \end{aligned} \quad (5.24)$$

In general, one can compute the superpotential to arbitrary order in powers of superfields by a straightforward application of the string selection rules [56, 158–160]. One assumes that any term not forbidden by the string selection rules appears with order one coefficient. In practice, even this becomes intractable quickly, and we must cut off the procedure at some low, finite order. More detailed calculations of individual terms give coefficients dependent on volume moduli due to string world sheet instantons. In general the moduli dependence can be obtained using the constraint of target space modular invariance. Consider a superpotential term for the “mini-landscape” models, with three T moduli and one U modulus, of the form:

$$\mathcal{W}_3 = w_{IJK} \Phi_I \Phi_J \Phi_K. \quad (5.25)$$

We assume that the fields $\Phi_{I,J,K}$ transform with modular weights $n_{I,J,K}^i$ and $\ell_{I,J,K}^3$ under T_i , $i = 1, 2, 3$ and U , respectively. Using the (net) transformation property of the superpotential, and the transformation property of $\eta(T)$ under the modular group, we have (for non-universal moduli):

$$w_{IJK} \sim h_{IJK} \prod_{i=1}^3 \eta(T_i)^{\gamma_{T_i}} \eta(U)^{\gamma_U}$$

where $\gamma_{T_i} = -2(1 - n_I^i - n_J^i - n_K^i)$, $\gamma_U = -2(1 - \ell_I^3 - \ell_J^3 - \ell_K^3)$.³⁹ This is easily generalized for higher order interaction terms in the superpotential. We see that the modular dependence of the superpotential is rarely symmetric under interchange of the T_i or U . Note, when minimizing the scalar potential we shall use the approximation $\eta(T)^{\gamma_T} \approx e^{-bT}$ with $b = \pi\gamma_T/12$. (Recall, at large T , we have $\log(\eta(T)) \approx -\pi T/12$.) This approximation misses the physics near the self-dual point in the potential, nevertheless, it is typically a good approximation.

As a final note, Wilson lines break the $\text{SL}(2, \mathbb{Z})$ modular group down to a subgroup [161] (see Appendix F). This has the effect of an additional differentiation of the moduli as they appear in the superpotential. In particular, factors of $\eta(T_i)$ are replaced by factors of $\eta(NT_i)$ or $\eta(T_i/N)$ for Wilson lines in \mathbb{Z}_N . In summary, the different modular dependence of twisted sector fields and the presence of Wilson lines leads quite generally to anisotropic orbifolds [162].

5.2.3 Gauge kinetic function and sigma model anomaly

To one loop, the string-derived gauge kinetic function is given by [76, 99, 100, 163–165]

$$\begin{aligned} f_a(S, T) &= k_a S + \frac{1}{8\pi^2} \sum_{i=1}^{h_{(1,1)}} (\alpha_a^i - k_a \delta_\sigma^i) \log (\eta(T^i))^2 \\ &\quad + \frac{1}{8\pi^2} \sum_{j=1}^{h_{(2,1)}} (\alpha_a^j - k_a \delta_\sigma^j) \log (\eta(U^j))^2 \end{aligned} \quad (5.26)$$

where k_a is the Kač-Moody level of the group, which we will normally take to be 1. The constants α_a^i are model dependent, and are defined as

$$\alpha_a^i \equiv \ell(\text{adj}) - \sum_{\text{rep}_I} \ell_a(\text{rep}_I) (1 + 2n_I^i).$$

$\ell(\text{adj})$ and $\ell_a(\text{rep}_I)$ are the Dynkin indices of the adjoint representation and of the matter representation I of the group \mathcal{G}_a , respectively [61] and n_I^i are modular weights.⁴⁰ The δ_σ^i

³⁹Note, the constants γ_{T_i} , γ_U can quite generally have either sign, depending upon the modular weights of the fields at the particular vertex.

⁴⁰If T_a^r are the generators of the group G_a in the representation r , then we have $\text{Tr}(T_a^r T_b^r) = \ell_a(\text{rep}_r) \delta_{ab}$.

terms are necessary to cancel an anomaly in the underlying σ -model, which induces a transformation in the dilaton field under the modular group:

$$S \rightarrow S + \frac{1}{8\pi^2} \sum_{i=1}^{h_{(1,1)}} \delta_\sigma^i \log (ic_i T_i + d_i) + \frac{1}{8\pi^2} \sum_{j=1}^{h_{(2,1)}} \delta_\sigma^j \log (ic_j U^j + d_j). \quad (5.27)$$

It is important to note that the factor

$$(\alpha_a^i - k_a \delta_\sigma^i) \equiv \frac{b_a^{(\mathcal{N}=2)}(i)}{|D|/|D_i|} \quad (5.28)$$

where $b_a^{(\mathcal{N}=2)}(i)$ is the beta function coefficient for the i th torus. It is non-zero if and only if the k -th twisted sector has an effective $\mathcal{N} = 2$ supersymmetry. Moreover this occurs only when, in the k -th twisted sector, the i th torus is not rotated. The factors $|D|$, $|D_i|$ are the degree of the twist group D and the little group D_i , which does not rotate the i th torus. For example, for the “mini-landscape” models with $D = \mathbb{Z}_6\text{-II}$ we have $|D| = 6$ and $|D_2| = 2$, $|D_3| = 3$ since the little group keeping the second (third) torus fixed is \mathbb{Z}_2 (\mathbb{Z}_3). The first torus is rotated in all twisted sectors. Hence, the gauge kinetic function for the “mini-landscape” models is only a function of T_2 and T_3 .

Taking into account the sigma model anomalies, the heterotic string Kähler potential has the following form, where we have included the loop corrections to the dilaton [76, 163]

$$\begin{aligned} \mathcal{K} = & -\log \left(S + \bar{S} + \frac{1}{8\pi^2} \sum_{i=1}^{h_{(1,1)}} \delta_\sigma^i \log (T^i + \bar{T}^i) + \frac{1}{8\pi^2} \sum_{j=1}^{h_{(2,1)}} \delta_\sigma^j \log (U^j + \bar{U}^j) \right) \\ & - \sum_{i=1}^{h_{(1,1)}} \log (T^i + \bar{T}^i) - \sum_{j=1}^{h_{(2,1)}} \log (U^j + \bar{U}^j). \end{aligned} \quad (5.29)$$

The first line of Equation (5.29) is modular invariant by itself, and one can redefine the dilaton, Y , such that

$$Y \equiv S + \bar{S} + \frac{1}{8\pi^2} \sum_{i=1}^{h_{(1,1)}} \delta_\sigma^i \log (T^i + \bar{T}^i) + \frac{1}{8\pi^2} \sum_{j=1}^{h_{(1,2)}} \delta_\sigma^j \log (U^j + \bar{U}^j), \quad (5.30)$$

where Y is invariant under the modular transformations.

5.2.4 Non-perturbative superpotential

In all “mini-landscape” models [37], and most orbifold heterotic string constructions, there exists a hidden sector with non-Abelian gauge interactions and vector-like matter carrying hidden sector charge. In the “benchmark” models [38] the hidden sector gauge group is $SU(4)$ with chiral matter in the $4 + \bar{4}$ representation.

| | ϕ | χ | Q_1 | Q_2 | \tilde{Q}_1 | \tilde{Q}_2 |
|-----------|--------|----------|-------|-------|---------------|---------------|
| $U(1)_A$ | -1 | q_χ | q_1 | q_2 | \tilde{q}_1 | \tilde{q}_2 |
| $SU(N_1)$ | 1 | 1 | □ | 1 | □ | 1 |
| $SU(N_2)$ | 1 | 1 | 1 | □ | 1 | □ |

Table 5.1: Charge assignments for the fields in a generic hidden sector. Flavor indices are suppressed.

In this section let us consider a generic hidden sector with gauge group $SU(N_1) \otimes SU(N_2) \otimes U(1)_A$, where ‘A’ stands for anomalous. There are N_{f_1} and N_{f_2} flavors of quarks Q_1 and Q_2 in the fundamental representation (along with anti-quarks \tilde{Q}_1 and \tilde{Q}_2 , in the anti-fundamental representations), as well as two singlet fields, called ϕ and χ . The charge assignments are listed in Table 5.1. We assume the existence of two moduli, S and T , which enter the non-perturbative superpotential through the gauge kinetic function, namely $f = f(S, T)$. The model also allows for T dependence in the Yukawa sector.

Non-perturbative effects generate a potential for the S and T moduli. Gaugino condensation will generate a scale Λ_{SQCD} , which is determined purely by the symmetries of the low energy theory:

$$\Lambda_a(S, T) = e^{-\frac{8\pi^2}{\beta_a} f_a(S, T)}, \quad (5.31)$$

where $\beta = 3\ell(\text{adj}) - \sum_I \ell(\text{rep}_I)$ is the one loop beta function coefficient of the theory. At tree level $f_a(S, T) = S$, however, we include the possibility of threshold corrections which introduce a dependence on the T modulus [76, 163]. We also find that $U(1)_A$ and modular invariance together dictate a very specific form for the non-perturbative superpotential.

In the “mini-landscape” analysis the effective mass terms for the vector-like exotics were evaluated. They were given as a polynomial in products of chiral MSSM singlet fields (chiral moduli). It was shown that all vector-like exotics (which carry MSSM quantum numbers) obtain mass⁴¹ when the chiral moduli obtain VEVs at supersymmetric points in moduli space. In our example let us, for simplicity, take couplings between the quarks and the field ϕ to be diagonal in flavor space. Mass terms of the form

$$\mathbb{M}_1(\phi, T) Q_1 \tilde{Q}_1 + \mathbb{M}_2(\phi, T) Q_2 \tilde{Q}_2 \quad (5.32)$$

⁴¹In fact, one of the $SU(4)$ quark- anti-quark pairs remained massless in the two “benchmark” models.

are dynamically generated when ϕ receives a non-zero VEV, which we will discuss below. A key assumption is that those mass terms are larger than the scale of gaugino condensation, so that the quarks and anti-quarks may be consistently integrated out. If this can be accomplished, then one can work in the pure gauge limit [166].⁴²

Before we integrate out the meson fields, the non-perturbative superpotential (plus quark masses) for $N_{f_a} < N_a$ is of the form [167]

$$\mathcal{W}_{\text{NP}} = \sum_{a=1,2} \left[\mathbb{M}_a(\phi, T) Q_a \tilde{Q}_a + (N_a - N_{f_a}) \left(\frac{\Lambda_a^{3N_a - N_{f_a}}}{\det Q_a \tilde{Q}_a} \right)^{\frac{1}{N_a - N_{f_a}}} \right], \quad (5.33)$$

with $\mathbb{M}_a(\phi, T) = c_a e^{-b_a T} \phi^{q_a + \tilde{q}_a}$ where c_a is a constant. Note, given the charges for the fields in Table 5.1 and using Equations (5.6), (5.9) and (5.31), one sees that \mathcal{W}_{NP} is $U(1)_A$ invariant. The Kähler potential for the hidden sector is assumed to be of the form

$$\begin{aligned} \mathcal{K} = & -\log(S + \bar{S}) - 3\log(T + \bar{T}) + \alpha_\phi \bar{\phi} e^{-2V_A} \phi + \alpha_\chi \bar{\chi} e^{2q_\chi V_A} \chi \\ & + \sum_{a=1,2} \alpha_a \left(\bar{Q}_a e^{V_a + 2q_a V_A} Q_a + \bar{\tilde{Q}}_a e^{-V_a + 2\tilde{q}_a V_A} \tilde{Q}_a \right). \end{aligned} \quad (5.34)$$

The quantities $\alpha_\phi, \alpha_\chi, \alpha_i$ are generally functions of the modulus T , where the precise functional dependence is fixed by the modular weights of the fields (see Section 5.2.2). V_i and V_A denote the vector superfields associated with the gauge groups $\mathcal{G}_i = \text{SU}(N_i)$ and $U(1)_A$.

The determinant of the quark mass matrix is given by

$$\det \mathbb{M}_a(\phi, T) = \left(c_a e^{-b_a T} \phi^{q_a + \tilde{q}_a} \right)^{N_{f_a}}. \quad (5.35)$$

We have taken the couplings between ϕ and the quarks to have exponential dependence on the T modulus, an ansatz which is justified by modular invariance (see Section 5.2.2). Inserting the meson equations of motion and Equation (5.35) into Equation (5.33), we have

$$\mathcal{W}_{\text{NP}} = \sum_{a=1,2} \left[N_a \left(c_a e^{-b_a T} \phi^{q_a + \tilde{q}_a} \right)^{\frac{N_{f_a}}{N_a}} (\Lambda_a(S, T))^{\frac{3N_a - N_{f_a}}{N_a}} \right].$$

Note that the transformation of the superpotential under the modular group in Equation (5.17) also requires that the (non-perturbative) superpotential obey

$$\mathcal{W}_{\text{NP}} \rightarrow \prod_{i=1}^{h_{(1,1)}} \prod_{j=1}^{h_{(2,1)}} (ic_i T^i + d_i)^{-1} (ic_j U^j + d_j)^{-1} \mathcal{W}_{\text{NP}}. \quad (5.36)$$

⁴²There is a check on the consistency of this approach: at the end of the day, after calculating the VEVs of the scalars, we can verify that the mass terms for the quarks are indeed of the correct magnitude.

Because the non-perturbative lagrangian must be invariant under all of the symmetries of the underlying string theory, it must be that [122, 123, 125, 164, 168, 169]:

$$\mathcal{W}_{\text{NP}} \equiv A \times e^{-aS} \prod_{i=1}^{h_{(1,1)}} \prod_{j=1}^{h_{(2,1)}} (\eta(T^i))^{-2 + \frac{3}{4\pi^2\beta}\delta_\sigma^i} (\eta(U^j))^{-2 + \frac{3}{4\pi^2\beta}\delta_\sigma^j} \quad (5.37)$$

where $a \equiv \frac{24\pi^2}{\beta}$ and $\beta = 3\ell(\text{adj}) - \sum_I \ell(\text{rep}_I)$ is the one-loop beta function coefficient, and A is generally a function of the chiral matter fields appearing in \mathbb{M} . This, coupled with the one loop gauge kinetic function in Equation (5.26), gives the heterotic generalization of the Racetrack superpotential.

In the following Section 5.3, we construct a simple model using the qualitative features outlined in this section. This model is novel because it requires only one non-Abelian gauge group to stabilize moduli and give a de Sitter vacuum. We have also constructed two condensate models, however, the literature already contains several examples of the “race-track” in regards to stabilization of S and T moduli. Moreover in the “mini-landscape” models, whose features we are seeking to reproduce, there are many examples of hidden sectors containing a single non-Abelian gauge group [37], while there are no examples with multiple hidden sectors.

5.3 Moduli stabilization and supersymmetry breaking in the bulk

In this section we construct a simple, generic heterotic orbifold model which captures many of the features discussed in Section 5.2. In particular, it is a single gaugino condensate model with the following fields - dilaton (S), modulus (T) and MSSM singlets (ϕ_1, ϕ_2, χ). The model has one anomalous $U(1)_A$ with the singlet charges given by ($q_{\phi_1} = -2, q_{\phi_2} = -9, q_\chi = 20$). The Kähler and superpotential are given by⁴³

$$\mathcal{K} = -\log(S + \bar{S}) - 3\log(T + \bar{T}) + \bar{\phi}_1\phi_1 + \bar{\phi}_2\phi_2 + \bar{\chi}\chi \quad (5.38)$$

$$\mathcal{W} = e^{-bT} (w_0 + \chi (\phi_1^{10} + \lambda\phi_1\phi_2^2)) + A \phi_2^p e^{-aS - b_2T}. \quad (5.39)$$

In addition, there is an anomalous $U(1)_A$ D -term given by

$$D_A = 20\bar{\chi}\chi - 2\bar{\phi}_1\phi_1 - 9\bar{\phi}_2\phi_2 - \frac{1}{2}\delta_{GS} \partial_S \mathcal{K} \quad (5.40)$$

with $\delta_{GS} = \frac{(q+\tilde{q})N_f}{4\pi^2} = N_f/(4\pi^2)$.

⁴³The coefficient A (Equation (5.39)) is an implicit function of all other non-vanishing chiral singlet VEVs which would be necessary to satisfy the modular invariance constraints, i.e., $A = A(\langle\phi_I\rangle)$. If one re-scales the $U(1)_A$ charges, $q_{\phi_i}, q_\chi \rightarrow q_{\phi_i}/r, q_\chi/r$, then the $U(1)_A$ constraint is satisfied with $r = 15p$ (assuming no additional singlets in A). Otherwise we may let r and p be independent. This re-scaling does not affect our analysis, since the vacuum value of the ϕ_i, χ term in the superpotential vanishes.

In the absence of the non-perturbative term (with coefficient A) the theory has a supersymmetric minimum with $\langle \chi \rangle = \langle \phi_1 \rangle = 0$ and $\langle \phi_2 \rangle \neq 0$ and arbitrary. This property mirrors the situation in the “mini-landscape” models where supersymmetric vacua have been found in the limit that all non-perturbative effects are neglected. We have also added a constant $w_0 = w_0(\langle \phi_I \rangle)$ which is expected to be generated (in the “mini-landscape” models) at high order in the product of chiral moduli due to the explicit breaking of an accidental R symmetry which exists at lower orders [170].⁴⁴ The T dependence in the superpotential is designed to take into account, in a qualitative way, the modular invariance constraints of Section 5.2.2. We have included only one T modulus, assuming that the others can be stabilized near the self-dual point [125, 126]. Moreover, as argued earlier, the T_i and U moduli enter the superpotential in different ways (see Section 5.2.2). This leads to modular invariant solutions which are typically anisotropic [162].⁴⁵

Note, that the structure, $\mathcal{W} \sim w_0 e^{-bT} + \phi_2 e^{-aS-b_2T}$ gives us the crucial progress⁴⁶

- i.) a ‘hybrid KKLT’ kind of superpotential that behaves like a single-condensate for the dilaton S , but as a racetrack for the T and, by extension, also for the U moduli; and
- ii.) an additional matter F_{ϕ_2} term driven by the cancelation of the anomalous $U(1)_A$ D -term seeds SUSY breaking with successful uplifting.

The constant b is fixed by modular invariance constraints. In general the two terms in the perturbative superpotential would have different T dependence. We have found solutions for this case as well. This is possible since the VEV of the χ term in the superpotential vanishes. The second term (proportional to A) represents the non-perturbative contribution of one gaugino condensate. The constants $a = 24\pi^2/\beta$, b_2 and p depend on the size of the gauge group, the number of flavors and the coefficient of the one-loop beta function for the effective $\mathcal{N} = 2$ supersymmetry of the torus parameterized by T . For the “mini-landscape” models, this would be either T_2 or T_3 . Finally, the coefficient of the exponential factor of the dilaton S is taken to be $A \phi_2^p$. This represents the effective hidden sector quark mass term, which in this case is proportional to a power of the chiral singlet ϕ_2 . In a more general case, it would be a polynomial in powers of chiral moduli.⁴⁷ The exponent p depends in general on the size of the gauge group, the number of flavors and the power that the field ϕ_2 appears in the effective quark mass term.

⁴⁴The fields entering w_0 have string scale mass.

⁴⁵Note, we have chosen to keep the form of the Kähler potential for this single T modulus with the factor of 3, so as to maintain the approximate no-scale behavior.

⁴⁶Note, the constants b , b_2 can have either sign. For the case with b , $b_2 > 0$ the superpotential for T is racetrack-like. However for b , $b_2 < 0$ the scalar potential for T diverges as T goes to zero or infinity and compactification is guaranteed [125, 126].

⁴⁷Holomorphic gauge invariant monomials span the moduli space of supersymmetric vacua. One such monomial is necessary to cancel the Fayet-Illiopoulos D -term (see Appendix E).

We have performed a numerical evaluation of the scalar potential with the following input parameters. We take hidden sector gauge group $SU(N)$ with $N = 5$, $N_f = 3$ and $a = 8\pi^2/N$.⁴⁸ For the other input values we have considered five different possibilities given in Table H.11 on page 160.⁴⁹ We find that supersymmetry breaking, moduli stabilization and up-lifting is a direct consequence of adding the non-perturbative superpotential term.

In our analysis we use the scalar potential V given by

$$V = e^{\mathcal{K}} \left[\sum_{i=1}^5 \sum_{j=1}^5 \left(F_{\Phi_i} \overline{F_{\Phi_j}} \mathcal{K}_{i,j}^{-1} - 3|W|^2 \right) \right] + \frac{D_A^2}{(S + \bar{S})} + \Delta V_{CW} (\Phi_i, \overline{\Phi}_i), \quad (5.41)$$

where $\Phi_{i,j} = \{S, T, \chi, \phi_1, \phi_2\}$ and $F_{\Phi_i} \equiv \partial_{\Phi_i} \mathcal{W} + (\partial_{\Phi_i} \mathcal{K}) \mathcal{W}$. The first two terms are the tree level supergravity potential. The last term is a one loop correction which affects the vacuum energy and D term contribution.

The one loop Coleman-Weinberg [121] potential is in general given by

$$\Delta V_{CW} = \frac{\Lambda^2}{32\pi^2} \text{STR} (\mathbb{M}^2) + \frac{1}{64\pi^2} \text{STR} \left(\mathbb{M}^4 \log \frac{\mathbb{M}^2}{\Lambda^2} \right) \quad (5.42)$$

with the mass matrix \mathbb{M} given by $\mathbb{M} = \mathbb{M}(\Phi_i)$ and Λ is the relevant cut-off in the problem. We take $\Lambda = M_S \sim 10^{17}$ GeV.

We have not evaluated the full one loop correction. Instead we use the approximate formula

$$\Delta V_{CW} (\phi_2, \overline{\phi}_2) = \frac{\lambda^2 F_2^2 |\phi_2|^2}{8\pi^2} \left(\log \left[R (\lambda |\phi_2|^2)^2 \right] + 3/2 \right) + \mathcal{O}(\Lambda^2) \quad (5.43)$$

where $F_2 = \langle F_{\phi_2} \rangle$ is obtained self-consistently and all dimensionful quantities are expressed in Planck units. This one loop expression results from the χ , ϕ_1 contributions to the Coleman-Weinberg formula. The term quadratic in the cut-off is naturally proportional to the number of chiral multiplets in the theory and could be expected to contribute a small amount to the vacuum energy, of order a few percent times $m_{3/2}^2 M_{\text{PL}}^2$. We will discuss this contribution later, after finding the minima of the potential. Finally, note that the parameters λ , R in Table H.11 on page 160 might both be expected to be significantly greater than one when written in Planck units. This is because the scale of the effective higher dimensional operator with coefficient λ in Equation (5.39) is most likely set by some value between M_{PL} and M_S and the cut-off scale for the one loop calculation (which determines the constant R) is the string scale and not M_{PL} .

⁴⁸We have also found solutions for the case with $N = 4$, $N_f = 7$ which is closer to the “mini-landscape” benchmark models. Note, when $N_f > N$ we may still use the same formalism, since we assume that all the Q, \bar{Q} s get mass much above the effective QCD scale.

⁴⁹Note the parameter relation $r = 15p$ in Table H.11 is derived using $U(1)_A$ invariance and the assumption that no other fields with non-vanishing $U(1)_A$ charge enter into the effective mass matrix for hidden sector quarks. We have also allowed for two cases where this relation is not satisfied.

In all cases we find a meta-stable minimum with all (except for two massless modes) fields massive of $\mathcal{O}(\text{TeV})$ or larger. Supersymmetry is broken at the minimum with values given in Table H.12 on page 160. Note $\text{RE}[S] \sim 2.2$ and $\text{RE}[T]$ ranges between 1.1 and 1.6. The moduli χ, ϕ_1 are stabilized at their global minima $\phi_1 = \chi = 0$ with $F_\chi = F_{\phi_1} = 0$ in all cases. The modulus $\sigma = \text{IM}[S]$ is stabilized at $\sigma \approx 1$ in the racetrack cases 1, 2, and 3. This value enforces a relative negative sign between the two terms dependent on $\text{RE}[T]$. We plot the scalar potential V in the $\text{RE}[T]$ direction for case 2 ($b, b_2 > 0$) (Figure 5.1(a)) and for case 4 ($b, b_2 < 0$) (Figure 5.1(b)). Note the potential as a function of $\text{RE}[S]$ is qualitatively the same for both cases (Figure 5.2).

At the meta-stable minimum of the scalar potential we find a vacuum energy which is slightly negative, i.e., of order $(-0.03 \text{ to } -0.01) \times 3m_{3/2}^2 M_{\text{PL}}^2$ (see Table H.12 on page 160). Note, however, one loop radiative corrections to the vacuum energy are of order $(N_T m_{3/2}^2 M_S^2 / 16\pi^2)$, where N_T is the total number of chiral multiplets [171] and we have assumed a cut-off at the string scale M_S . With typical values $N_T \sim \mathcal{O}(300)$ and $M_S/M_{\text{PL}} \sim 0.1$, this can easily lift the vacuum energy the rest of the way to give a small positive effective cosmological constant which is thus a meta-stable local dS minimum. Note that the constants λ, R have also been used to adjust the value of the cosmological constant as well as, and more importantly for LHC phenomenology, the value of D_A (see Figure 5.3).

The two massless fields can be seen as the result of two $U(1)$ symmetries; the first is a $U(1)_R$ symmetry and the second is associated with the anomalous $U(1)_A$. The $U(1)_R$ is likely generic (but approximate), since even the “constant” superpotential term needed to obtain a small cosmological constant necessarily comes with $\eta(T)$ moduli dependence. Since we have approximated $\eta(T) \sim \exp(-\pi T/12)$ by the first term in the series expansion (Equation (5.19)), the symmetry is exact, however, higher order terms in the expansion necessarily break the $U(1)_R$ symmetry. The $U(1)_A$ symmetry is gauged.

One can express the fields S, T , and ϕ_2 in the following basis⁵⁰:

$$\begin{aligned} S &\equiv s + i\sigma, \\ T &\equiv t + i\tau, \\ \phi_2 &\equiv \varphi_2 e^{i\theta_2}. \end{aligned} \tag{5.44}$$

The transformation properties of the fields σ, τ and θ_2 under the two $U(1)$ ’s are given by

$$\begin{aligned} U(1)_R &: \begin{cases} \tau \rightarrow \tau + c \\ \sigma \rightarrow \sigma + \frac{-b_2+b}{a}c \end{cases}, \\ U(1)_A &: \begin{cases} \theta \rightarrow \theta - \frac{9}{r}c' \\ \sigma \rightarrow \sigma - \frac{9p}{a \cdot r}c' \end{cases}, \end{aligned} \tag{5.45}$$

⁵⁰The fields χ and ϕ_1 cannot be expressed in polar coordinates as they receive zero VEV, and cannot be canonically normalized in this basis.

where c, c' are arbitrary constants and for the definition of r see footnote 43. The corresponding Nambu-Goldstone (NG) bosons are given by

$$\begin{aligned}\chi_{\text{NG}}^1 &= \frac{a}{-b_2 + b} \sigma + \tau, \\ \chi_{\text{NG}}^2 &= \tilde{N} \left(-\sigma + \frac{-b_2 + b}{a} \tau \right) + \frac{1}{p} \theta_2,\end{aligned}\quad (5.46)$$

where \tilde{N} is a normalization factor. One can then calculate the mass matrix in the $\sigma - \tau - \theta_2$ basis and find two zero eigenvalues (as expected) and one non-zero eigenvalue. The two NG modes, in all cases, can be shown to be linear combinations of the two eigenvectors of the two massless states. The $U(1)_A$ NG boson is eaten by the $U(1)_A$ gauge boson, while the $U(1)_R$ pseudo-NG boson remains as an “invisible axion” [172]. The $U(1)_R$ symmetry is non-perturbatively broken (by world-sheet instantons) at a scale of order

$$\langle e^{\mathcal{K}/2} \mathcal{W} e^{-\pi T} \rangle \approx m_{3/2} \langle e^{-\pi T} \rangle \sim 0.02 m_{3/2} \quad (5.47)$$

in Planck units, resulting in an “axion” mass of order 10 GeV and decay constant of order M_{PL} .⁵¹

Before we proceed to discussing the stabilization rest of the (chiral singlet) moduli in a more complete string model, or the LHC phenomenology of the mini-version of the mini-landscape models, it is worth comparing our analysis with some previous discussions in the literature.

In a series of two papers by Dvali and Pomarol [134, 174], the authors consider an anomalous $U(1)$ with two charged singlet fields. The D term is given by⁵²

$$D_A = q|\phi_+|^2 - |q_-|^2 + \xi \quad (5.48)$$

The gauge invariant superpotential is

$$\mathcal{W} = m\phi_+\phi_-, \quad (5.49)$$

where m has some charge under $U(1)_A$. They suggest a few different ways to generate m . The first is with some high power of one of the ϕ fields:

$$\mathcal{W} \sim \phi_-^q \phi_+ \Rightarrow m \equiv \langle \phi_- \rangle^{q-1} \quad (5.50)$$

⁵¹In addition, the heterotic orbifold models might very well have the standard invisible axion [173].

⁵²We refer to the anomalous $U(1)$ as $U(1)_A$ and not $U(1)_X$, as in the papers referenced below.

The second is by giving the $\phi_{+,-}$ a coupling to some quarks from a SUSY QCD theory that becomes strongly coupled. The scale, Λ_{SQCD} then serves as the mass term in the superpotential. They do not, however, consider dilaton dependence, and their D term is static, not dynamic. They also work in the global SUSY limit, so they do not consider up-lifting.

In a paper by Binetruy and Dudas [133], the authors assume that S can be stabilized at some finite value S_0 , possibly through some extra S dependent term in the superpotential and they assume that $F_S(S_0) = 0$. In their setup, they have an anomalous $U(1)$, some charged singlets, and some hidden sector SQCD with matter. The singlets couple to matter, and SQCD becomes strongly coupled, generating a scale, just as in our analysis. Since they are working in the global SUSY limit, they are not concerned with up-lifting.

Lalak [135] considers several types of models with an anomalous $U(1)$, some charged singlets, and some coupling to the dilaton S . In the last section, he considers superpotentials with an exponential dependence on S . He then assumes that S_0 is a (globally) supersymmetric minimum of the potential. Also, working in global SUSY, he does not address up-lifting.

In a paper by Dudas and Mambrini [131], the authors consider one modulus, one singlet field, and an $SU(N)$ with one flavor of quarks. The $SU(N)$ becomes strongly coupled, and the superpotential and Kähler potential look like:

$$\mathcal{W} = w_0 + (c/X^2) e^{-aT} + m\phi^q X \quad (5.51)$$

$$\mathcal{K} = -3 \log (T + \bar{T} - |X|^2 - |\phi|^2), \quad (5.52)$$

where X is the meson field and ϕ is the singlet. Note, the modulus appearing in the exponent is T , not S . They find that the only consistent minimum with approximately zero cosmological constant requires $m_{3/2} \sim \xi$. So either the gravitino mass is of order the GUT scale or for the gravitino mass of order a TeV, the meson charge must satisfy $q \sim 10^{-8}$.

In a paper by Dudas et al. [138], the authors consider a single modulus and two singlet fields:

$$D_A = |\phi_+|^2 - |\phi_-|^2 + \xi, \quad (5.53)$$

$$\mathcal{W} = w_0 + m\phi_+\phi_- + a\phi_-^q e^{-bT}. \quad (5.54)$$

They do not discuss the origin of the constant w_0 , and they use an explicit mass scale m , which they suggest might come from non-perturbative effects. Note the latter is crucial, since m affects the up-lifting of the scalar potential. They are also interested in large volume compactifications, as $t \equiv \text{RE}[T] \approx 60$. Given their SUSY breaking scheme, they go on to look at the low energy spectrum, however, they neglect the D term contributions to the soft masses, claiming that there are only two possibilities for the low energy physics:

- Because $\xi > 0$, some SM quarks and leptons carry positive $U(1)_A$ charges. This leads to scalar masses (for them) of around 100 TeV, and may give an unstable low energy spectrum.
- All SM quarks and leptons are neutral under $U(1)_X$. This implies that there should be more matter that is charged under the MSSM and $U(1)_A$, which motivate them to consider gauge mediation.

It seems that they have missed an important possibility, namely that matter in the MSSM appears with $U(1)_A$ charges of both signs. This actually seems to be the generic case, at least in the mini-landscape models (see Table 5.2).

The last paper we consider, by Gallego and Serone [139], contains an analysis which is possibly most similar to that in this paper, however, there are two major differences. If one neglects all non-perturbative dependence on the dilaton and Kähler moduli, then their superpotential is of the form $\mathcal{W} \supset \phi^q \chi$ and the D term is given by $D_A = q|\chi|^2 - |\phi|^2 + \xi$. Thus the model does not have a supersymmetric minimum in the global limit due to a conflict between $F_\chi = 0$ and $D_A = 0$. In our model (Equation 5.39), as in the mini-landscape models, there is a supersymmetric solution when non-perturbative effects are ignored. Finally, the authors were not able to find a supersymmetry breaking solution, like ours, with just one hidden non-Abelian gauge sector.

As an aside, we note that Casas et al. [122] study a similar problem of moduli stabilization and SUSY breaking, but without the anomalous $U(1)$. Their model is very different from ours, but they do include the one loop Coleman-Weinberg corrections.

5.4 Moduli stabilization continued - the twisted sector and blow-up moduli

In our discussion above we considered a simple model which is representative of heterotic orbifold models. Our simple model had only a few moduli, i.e., the dilaton, S , a volume modulus, T , and three chiral singlet ‘moduli’, χ, ϕ_1, ϕ_2 . Any heterotic orbifold construction, on the other hand, will have several volume and complex structure moduli and of order 50 to 100 chiral singlet moduli. The superpotential for the chiral singlet moduli is obtained as a polynomial product of holomorphic gauge invariant monomials which typically contain hundreds of terms at each order (with the number of terms increasing with the order). In the ‘mini-landscape’ analysis, supersymmetric vacua satisfying $F = D = 0$ constraints to sixth order in chiral singlet moduli could be found. Although there are many flat directions in moduli space, the anomalous D -term fixes at least one holomorphic gauge invariant monomial to have a large value. Our simple model expressed this fact with the chiral singlets χ, ϕ_1, ϕ_2 , where the VEVs were fixed by the global SUSY minimum with $\langle \phi_2 \rangle$ fixed by the $U(1)_A$ D -term.

In addition to the non-Abelian hidden gauge sector considered in the simple model, a generic orbifold vacuum also has additional U(1) gauge interactions and vector-like exotics which obtain mass proportional to chiral singlet VEVs. Some of these singlets are assumed to get large VEVs (of order the string scale). These are the ones giving mass to the extra U(1) gauge sector and vector-like exotics. These same VEVs generate non-trivial Yukawa couplings for quarks and leptons. Moreover, there are chiral singlets which get zero VEVs, such as χ and ϕ_1 . For example, in the “mini-landscape” benchmark model 1, the electroweak Higgs μ term is zero in the supersymmetric limit. The question arises as to what happens to all these VEVs once supersymmetry is broken.

We now sketch the fact that the supersymmetry breaking discussed above, ensuing from F -terms, $F_S, F_T, F_{\phi_2} \neq 0$ and driven by the non-perturbative superpotential, inevitably leads to a stabilization of the many singlet ‘moduli’ of the heterotic orbifold vacuum. We shall consider here 3 classes of heterotic MSSM singlets.

5.4.1 Singlets with polynomial Yukawa couplings

Let us first consider singlets having polynomial Yukawa couplings in the superpotential, which in case of a coupling arising among purely untwisted sector fields $\phi_i^{(U)}$ are perturbatively generated, and in the other case involving *at least one* twisted sector field $\phi_i^{(T)}$ are non-perturbatively generated by world-sheet instantons (see Section 5.2.2). The latter case is actually the most common situation. Restricting again for reasons of simplicity to the case of a single scalar field of the type under consideration, we can describe the two cases as follows:

- i)

$$\mathcal{K} = -3 \log \left(T + \bar{T} - \bar{\phi}^{(U)} \phi^{(U)} \right) \quad , \quad \mathcal{W} \supset \lambda \cdot \left(\phi^{(U)} \right)^N , \quad N \geq 3$$

Note that the untwisted sector scalar fields $\phi^{(U)}$, being inherited from the bulk **248** in 10d, appear this way in the Kähler potential.

- ii)

$$\mathcal{K} = -3 \log(T + \bar{T}) + c \bar{\phi}^{(T)} \phi^{(T)} \quad , \quad \mathcal{W} \supset e^{-bT} \left(\phi^{(T)} \right)^N , \quad N \geq 3$$

Here the exponential dependence on T arises from the η -function, which a non-perturbatively generated Yukawa coupling must have for reasons of modular invariance (see Section 5.2.2).

- iii)

$$\mathcal{K} = -3 \log \left(T + \bar{T} - \bar{\phi}^{(U)} \phi^{(U)} \right) + c \bar{\phi}^{(T)} \phi^{(T)}$$

$$\mathcal{W} \supset \lambda e^{-bT} \left(\phi^{(T)} \right)^N + \tilde{\lambda} e^{-\tilde{b}T} \left(\phi^{(T)} \right)^{\tilde{N}} \left(\phi^{(U)} \right)^M \text{ with } M, N, \tilde{N} \geq 2$$

Here, too, the exponential dependence on T from the η -function dependence of a non-perturbatively generated Yukawa coupling.

The calculation in case i) simplifies by the fact that there \mathcal{K} fulfills an extended no-scale relation

$$\begin{aligned} \mathcal{K}_i \mathcal{K}^{i\bar{j}} \mathcal{K}_{\bar{j}} &= 3 \quad \forall i, j = T, \phi^{(U)} \\ \mathcal{K}^i = \mathcal{K}^{i\bar{j}} \mathcal{K}_{\bar{j}} &= -\mathcal{V} \cdot \delta_T^i \quad , \quad \mathcal{V} \equiv \left(T + \bar{T} - \bar{\phi}^{(U)} \phi^{(U)} \right) \end{aligned} \quad (5.55)$$

which implies for the F-term scalar potential a result

$$\begin{aligned} V_F &= e^{\mathcal{K}} \left[\mathcal{K}^{\phi^{(U)} \bar{\phi}^{(U)}} \left(|\partial_{\phi^{(U)}} \mathcal{W}|^2 + \left(\partial_{\phi^{(U)}} \mathcal{W} \cdot \overline{\mathcal{K}_{\phi^{(U)}} \mathcal{W}} + c.c. \right) \right) \right. \\ &\quad \left. + \frac{\mathcal{V}}{3} (T + \bar{T}) |\partial_T \mathcal{W}|^2 + (\mathcal{V} \partial_T \mathcal{W} + c.c.) \right] . \end{aligned} \quad (5.56)$$

It is clear then that one solution to $\partial_{\phi^{(U)}} V_F = 0$ is given by

$$\partial_{\phi^{(U)}} \mathcal{W} = \partial_{\phi^{(U)}} \mathcal{V} = 0 \quad \Rightarrow \quad \langle \phi^{(U)} \rangle = 0 \quad (5.57)$$

because $\partial_{\phi^{(U)}} \partial_T \mathcal{W} \equiv 0 \forall \phi^{(U)}$. This implies that those untwisted sector singlets that were stabilized at the origin in global supersymmetry by a purely untwisted sector Yukawa coupling remain so even in supergravity.

For the twisted sector case ii) we find the scalar potential to be

$$\begin{aligned} V_F &= e^{\mathcal{K}} \left[\mathcal{K}^{\phi^{(T)} \bar{\phi}^{(T)}} |D_{\phi^{(T)}} \mathcal{W}|^2 + \mathcal{K}^{T\bar{T}} \left(|\partial_T \mathcal{W}|^2 + \underbrace{\partial_T \mathcal{W} \overline{\mathcal{K}_T \mathcal{W}}}_{\sim F_T} + c.c. \right) \right] \\ &\sim e^{-2bT} \left(\bar{\phi}^{(T)} \phi^{(T)} \right)^{N-1} - F_T (T + \bar{T}) e^{-bT} \left(\phi^{(T)} \right)^N + c.c. \end{aligned} \quad (5.58)$$

which gives two solutions to $\partial_{\phi^{(T)}} V_F = 0$ as

$$\langle \phi^{(T)} \rangle = 0 \quad \vee \quad \langle \phi^{(T)} \rangle \sim \left(\frac{F_T (T + \bar{T})}{e^{-bT}} \right)^{\frac{1}{N-2}} \sim \left(\frac{m_{3/2}}{e^{-bT}} \right)^{\frac{1}{N-2}} . \quad (5.59)$$

This implies that the $\phi^{(T)}$ get stabilized either at the origin, or at non-zero but small VEVs $\ll 1$. Their value in the latter case approaches $\phi^{(T)} \sim M_{\text{GUT}}$ for non-perturbative Yukawa couplings of order $N \gtrsim 5$ and $m_{3/2} \sim \text{TeV}$ (which can be interesting for phenomenological reasons involving heavy vector-like non-MSSM matter).

Finally, we note that case iii) reduces to case ii). To see this, note, that the structure of \mathcal{K} and \mathcal{W} given in case iii) does not change the arguments given for case i) which implies that in case iii) we still find $\langle \phi_{(U)} \rangle = 0$. This, however, immediately gives us

$$\mathcal{W}|_{\langle \phi_{(U)} \rangle = 0} \supset \lambda e^{-bT} \left(\phi^{(T)} \right)^N \quad (5.60)$$

which is case ii).

5.4.2 Singlet directions which are F - and D -flat in global supersymmetry

There are many directions in singlet field space in our heterotic constructions which are F - and D -flat in global supersymmetry. Let us denote these fields by $\phi_i^{(f)}$, and the remaining set of non-flat directions in field space by χ_i . D -flatness entails that the D -terms do not depend on the $\phi_i^{(f)}$. F -flatness implies that $F_{\phi_i^{(f)}} = \partial_{\phi_i^{(f)}} \mathcal{W}(\phi_i^{(f)}, \chi_i) = \text{const.}$ for all values of $\langle \phi_i^{(f)} \rangle$. Generically this implies that $\langle \chi_i \rangle = 0$.

Simplifying to the case of a single χ , this leads to a consideration of 2 cases

• i)

$$\begin{aligned} F_{\phi_i^{(f)}} &= 0 \quad \forall \phi_i^{(f)} \\ \Rightarrow \mathcal{W} &\supset e^{-bT} \chi \mathfrak{f}(\phi_i) \quad \bigvee \quad \mathcal{W} \supset e^{-bT} \chi^p \mathfrak{f}(\phi_i), \quad p \geq 2 \end{aligned} \quad (5.61)$$

• ii)

$$\begin{aligned} F_{\phi_i^{(f)}} &= \text{const.} \neq 0 \quad \forall \phi_i^{(f)} \\ \Rightarrow \mathcal{W} &\supset \lambda e^{-bT} f(\tilde{\phi}_j) \phi_i^{(f)} \end{aligned} \quad (5.62)$$

where the $\tilde{\phi}_j$ VEVs are assumed fixed by other terms in the superpotential and \mathfrak{f} is an arbitrary function of its argument.

We consider first case i). At the supersymmetric minimum satisfying $\partial_\chi \mathcal{W} = \partial_{\phi_i} \mathcal{W} = 0$, we have $\langle \chi \rangle = 0$ with $\langle \phi_i \rangle$ arbitrary (subject, for the first case only, to the condition $\mathfrak{f}(\phi_i) = 0$). In this example we have $\chi \in \{\chi_i\}$ and $\phi_i \in \{\phi_i^{(f)}\}$. Note the fields $\phi_i^{(f)}$ effectively do not appear in the superpotential at its minimum.

We now argue that the fields $\phi_i^{(f)}$ are stabilized by the corrections from supergravity in the F -term scalar potential. Namely, consider for sake of simplicity the case of a single such field $\phi^{(f)}$ and χ with

$$\begin{aligned} \mathcal{K} &= -3 \log(T + \bar{T}) + c \bar{\phi}^{(f)} \phi^{(f)} + c' \bar{\chi} \chi \\ \partial_\chi \mathcal{W} &= \partial_{\phi^{(f)}} \mathcal{W} \equiv 0 \quad \text{for} \quad \langle \chi \rangle = 0 \end{aligned} \quad (5.63)$$

we get the F-term scalar potential in supergravity to be (for the twisted sector case ii) we find the scalar potential to be

$$\begin{aligned}
V_F &= e^{\mathcal{K}} \left(\mathcal{K}^{\phi(f)\bar{\phi}(f)} |D_{\phi(f)}\mathcal{W}|^2 + \mathcal{K}^{\chi\bar{\chi}} |D_{\chi}\mathcal{W}|^2 + \mathcal{K}^{T\bar{T}} |D_T\mathcal{W}|^2 - 3|\mathcal{W}|^2 \right) \\
&= e^{\mathcal{K}} \left(c\bar{\phi}^{(f)}\phi^{(f)} - \kappa \right) \cdot |\mathcal{W}|^2 \\
&\approx |\mathcal{W}|^2 \cdot \left[-c(\kappa-1)\bar{\phi}^{(f)}\phi^{(f)} - \frac{c^2(\kappa-2)}{2} \left(\bar{\phi}^{(f)}\phi^{(f)} \right)^2 + \right. \\
&\quad \left. - \frac{c^3(\kappa-3)}{6} \left(\bar{\phi}^{(f)}\phi^{(f)} \right)^3 + \frac{c^4(4-\kappa)}{24} \left(\bar{\phi}^{(f)}\phi^{(f)} \right)^4 + \dots \right] \quad (5.64)
\end{aligned}$$

Note, we maintain $\langle \chi \rangle = 0$, $\mathcal{W} \neq 0$ is due to other sectors of the theory and $\kappa = (3 - \mathcal{K}^{T\bar{T}}|D_T\mathcal{W}|^2/|\mathcal{W}|^2) \leq 3$ is a positive semi-definite number of order 3. This scalar potential is unbounded from above at large field values, $\phi^{(f)}$, thus driving the VEV to large-field value. To this order in V_F we find

$$\langle \phi^{(f)} \rangle \sim \frac{1}{\sqrt{c}} \quad . \quad (5.65)$$

This implies that supergravity effects will serve to stabilize all the globally supersymmetric and F - and D -flat singlet fields generically at large values of $\mathcal{O}(1)$. Note, that the non-perturbative effects coming from gaugino-condensation in the hidden sector will add dependence of \mathcal{W} on $\phi^{(f)}$ beyond the global mini-landscape analysis. This may render κ a weak function of ϕ^f such that we may for some of the globally supersymmetric and F - and D -flat fields $\phi^{(f)}$ have $\kappa < 1$ at small $\phi^{(f)}$ while $1 < \kappa < 3$ at larger values of $\phi^{(f)}$. In this situation the involved $\phi^{(f)}$ -type singlets will acquire vacua at both $\langle \phi^{(f)} \rangle = 0$ and $\langle \phi^{(f)} \rangle \sim 1/\sqrt{c}$. The χ -like fields will have their VEVs near the origin, i.e., they may be shifted from the origin by small SUSY breaking effects.

Let us now turn to case ii) of F -flat but *non-supersymmetric* singlet directions and look for vacua stabilizing $\phi^{(f)} \ll 1$ using again

$$\mathcal{K} = -3 \log(T + \bar{T}) + \bar{\phi}^{(f)}\phi^{(f)} + \bar{\chi}\chi \quad . \quad (5.66)$$

The scalar potential is

$$\begin{aligned}
V_F &= e^{\mathcal{K}} \left[\mathcal{K}^{T\bar{T}} \underbrace{\langle D_T\mathcal{W} \rangle \bar{\partial}_T\mathcal{W}}_{=F_T} + c.c. + \mathcal{K}^{\phi(f)\bar{\phi}(f)} |D_{\phi(f)}\mathcal{W}|^2 \right] \\
&\sim \left\{ \mathcal{K}^{T\bar{T}} F_T \cdot b\lambda e^{-bT} f(\chi) \phi^{(f)} + c.c. \right. \\
&\quad \left. + \mathcal{K}^{\phi(f)\bar{\phi}(f)} \left[\lambda e^{-bT} f(\chi) (1 + \bar{\phi}^{(f)}\phi^{(f)}) + \bar{\phi}^{(f)}\langle \mathcal{W} \rangle \right]^2 \right\} \quad . \quad (5.67)
\end{aligned}$$

In the desired regime of $\phi^{(f)} \ll 1$ this gives us two sub-cases:

- iia)

$$\mathcal{K}^{\phi^{(f)} \bar{\phi}^{(f)}} F_{\phi^{(f)}} \ll \mathcal{K}^{T\bar{T}} F_T$$

- iib)

$$\mathcal{K}^{\phi^{(f)} \bar{\phi}^{(f)}} F_{\phi^{(f)}} \gg \mathcal{K}^{T\bar{T}} F_T$$

In case iia) $\phi^{(f)} \ll 1$ implies that $F_{\phi^{(f)}} \equiv \lambda e^{-bT} f(\langle \chi \rangle) \ll \langle \mathcal{W} \rangle$ and thus $\partial_{\phi^{(f)}} V_F = 0$ gives us

$$\langle \phi^{(f)} \rangle \sim \frac{\langle F_{\phi^{(f)}} \rangle}{\langle \mathcal{W} \rangle} \ll 1 \quad (5.68)$$

which is thus a self-consistent vacuum.

In the opposite situation we get $F_{\phi^{(f)}} \equiv \lambda e^{-bT} f(\langle \chi \rangle) \gg \langle \mathcal{W} \rangle, \langle F_T \rangle$. Using again $\phi^{(f)} \ll 1$ this leads to

$$\langle \phi^{(f)} \rangle \sim \frac{\langle F_T \rangle}{\langle F_{\phi^{(f)}} \rangle} \ll 1 \quad . \quad (5.69)$$

Thus, even the F -flat but non-supersymmetric singlet directions of case ii) get stabilized by supersymmetry breaking effects from the bulk moduli stabilization at generically small but non-zero VEVs.

This property, of all F - and D -flat singlet fields generically acquiring non-zero VEVs from supersymmetry breaking in the bulk moduli stabilizing sector through supergravity, dynamically ensures the decoupling of all vector-like non-MSSM matter at low-energies as checked in global supersymmetry for the mini-landscape setup.

Note, that the overall vacuum structure of the F -flat singlet fields implicates a choice of initial conditions. The amount of non-MSSM vector-like extra matter in the mini-landscape constructions which decouples from low energies depends on the choice of the globally F -flat singlets $\phi_i^{(f)}$ placed at their non-zero VEV vacuum instead of their zero VEV vacuum. Thus, the choice of initial conditions in the vacuum distribution among the set of globally F -flat singlet fields characterizes how close to the MSSM one can get when starting from one of the mini-landscape models.

Assuming now that one finds successful eternal inflation occurring somewhere in the mini-landscape, this choice of initial conditions turns into a question of cosmological dynamics. In this situation, all possible initial conditions of the set of globally F -flat singlets were potentially realized in a larger multiverse. The choice of initial conditions on the singlets in the globally F -flat sector would then be amenable to anthropic arguments and might be eventually determined by selection effects.

5.5 SUSY spectrum

Now that we understand how SUSY is broken, we can calculate the spectrum of soft masses. The messenger of SUSY breaking is mostly gravity, however, there are other contributions from gauge and anomaly mediation.

5.5.1 Contributions to the soft terms

At tree level, the general soft terms for gravity mediation are given in References [175–179]. The models described in this paper contain an additional contribution from the F -term of a scalar field ϕ_2 . Following References [175, 176, 179], we define

$$F^I \equiv e^{\mathcal{K}/2} \mathcal{K}^{I\bar{J}} (\bar{\mathcal{W}}_{\bar{J}} + \bar{\mathcal{W}} \mathcal{K}_{\bar{J}}). \quad (5.70)$$

SUGRA effects

The tree level gaugino masses are given by

$$M_a^{(0)} = \frac{g_a^2}{2} F^n \partial_n f_a(S) = \frac{g_a^2}{2} F^S. \quad (5.71)$$

At tree level, the gauge kinetic function in heterotic string theory is linear in the dilaton superfield S , and only dependent on the T modulus at one loop. It is important to note the enhancement of F^S relative to F_S : naively, one might guess that loop corrections to the gaugino masses might be important, however

$$F^S \gg \frac{F^T}{16\pi^2}, \quad (5.72)$$

thus loop corrections will be neglected.

At tree level, the A terms are given by

$$A_{IJK}^{(0)} = F^n \partial_n \mathcal{K} + F^n \partial_n \log \frac{\mathcal{W}_{IJK}}{\kappa_I \kappa_J \kappa_K}, \quad (5.73)$$

where

$$\mathcal{W}_{IJK} \equiv \frac{\partial^3 \mathcal{W}}{\partial \Phi^I \partial \Phi^J \partial \Phi^K} \quad (5.74)$$

and \mathcal{K} is the Kähler potential. Neglecting U dependence, we have

$$\mathcal{K} \supset \Phi_I \bar{\Phi}^I \prod_i (T_i + \bar{T}_i)^{-n_I^i} \Rightarrow \kappa_I \equiv \prod_i (T_i + \bar{T}_i)^{-n_I^i}. \quad (5.75)$$

The κ_I are the Kähler metrics for the chiral multiplets, Φ_I , where the A terms are expressed in terms of canonically normalized fields. As before, the modular weights of the matter field are given by n_I^i .

In general, there are also tree level contributions to A terms proportional to

$$-\frac{F_{\phi_2}}{\langle \phi_2 \rangle} \frac{\partial \log \mathcal{W}_{IJK}}{\partial \log \phi_2}. \quad (5.76)$$

These terms may be dominant, but unfortunately they are highly model dependent. They may give a significant contribution to A_b and A_τ , but in fact we find that the details of the low energy spectrum are not significantly effected.

The tree level scalar masses are given by

$$\left(M_I^{(0)}\right)^2 = m_{3/2}^2 - F^n \bar{F}^{\bar{m}} \partial_n \partial_{\bar{m}} \log \kappa_I + g_{\text{GUT}}^2 f q_A^I \langle D_A \rangle \kappa_I, \quad (5.77)$$

where $g_{\text{GUT}}^2 = 1/\text{RE}[\langle S \rangle]$ and we have implicitly assumed that the Kähler metric is diagonal in the matter fields. The factor f re-scales the $U(1)_A$ charges q_A from the mini-landscape “benchmark” model 1 [38], so they are consistent with the charges q'_A in our mini-version of the mini-landscape model. We have $q'_A = q_A f = q_A \frac{48\pi^2}{\text{TR } Q} \delta_{GS}$ with $\delta_{GS} = \frac{N_f}{4\pi^2}$ (Equation (5.9)) and $\text{TR } Q = \frac{296}{3}$ (Equation E.5, [38]) such that $\frac{\text{TR}(q')}{4\pi^2} = \delta_{GS}$.

Again neglecting U dependence, the Kähler metric for the matter fields depends only on the T moduli, and we find

$$\left(M_I^{(0)}\right)^2 = m_{3/2}^2 - \sum_i \frac{n_I^i |F^{T_i}|^2}{(T_i + \bar{T}_i)^2} + g_{\text{GUT}}^2 \frac{f q_A^I \langle D_A \rangle}{(T + \bar{T})^{n_I^3}}. \quad (5.78)$$

The μ term can come from two different sources:

$$\mathcal{K} \supset Z(T_i + \bar{T}_i, U_j + \bar{U}_j, \dots) \mathbf{H}^u \mathbf{H}^d, \quad \mathcal{W} \supset \tilde{\mu}(\mathbf{s}_I, T_i, U_j, \dots) \mathbf{H}^u \mathbf{H}^d. \quad (5.79)$$

In the orbifold models, Kähler corrections have not been computed, so the function Z is *a priori* unknown. Such a term could contribute to the Giudice-Masiero mechanism [180]. When both $\tilde{\mu}$ and Z vanish, the SUGRA contribution to the $\mu/B\mu$ terms vanish. On the other hand, in the class of models which we consider, we know that vacuum configurations exist such that $\tilde{\mu} = 0$ to a very high order in singlet fields. Moreover $\tilde{\mu} \propto \langle \mathcal{W} \rangle$ which vanishes in the supersymmetric limit, but obtains a value w_0 at higher order in powers of chiral singlets. If μ is generated in this way, there is also likely to be a Peccei-Quinn axion [181, 182]. Finally, supergravity effects will also generate a $B\mu$ term.

Finally, one can consider loop corrections to the tree level expressions in [175, 176, 179]. This was done in References [183, 184], where the complete structure of the soft terms (at one loop) for a generic (heterotic) string model were computed in the effective supergravity

limit. We have applied the results of [183, 184] to our models and find, at most, around a 10% correction to the tree level results of [175, 176, 179].⁵³

Gauge mediation

The “mini-landscape” models generically contain vector-like exotics in the spectrum. Moreover it was shown that such states were necessary for gauge coupling unification [30]. The vector-like exotics obtain mass in the supersymmetric limit by coupling to scalar moduli, thus they may couple to the SUSY breaking field ϕ_2 . We will consider the following light exotics to have couplings linear in the field ϕ_2 :

$$n_3 \times (\mathbf{3}, 1)_{1/3} + n_2 \times (1, \mathbf{2})_0 + n_1 \times (1, 1)_{-1} + \text{h.c.} \quad (5.80)$$

where the constants n_i denote the multiplicity of states and (see Tables H.7 and H.8 in Appendix H)

$$n_3 \leq 4 \text{ and } n_2 \leq 3 \text{ and } n_1 \leq 7. \quad (5.81)$$

The gauge mediated contributions split the gaugino masses by an amount proportional to the gauge coupling:

$$M_3^{(1)}|_{\text{gmsb}} = n_3 \frac{g_3^2}{16\pi^2} \frac{F^{\phi_2}}{\langle \phi_2 \rangle}, \quad (5.82)$$

$$M_2^{(1)}|_{\text{gmsb}} = n_2 \frac{g_2^2}{16\pi^2} \frac{F^{\phi_2}}{\langle \phi_2 \rangle}, \quad (5.83)$$

$$M_1^{(1)}|_{\text{gmsb}} = \frac{n_3 + 3n_1}{10} \frac{g_1^2}{16\pi^2} \frac{F^{\phi_2}}{\langle \phi_2 \rangle}. \quad (5.84)$$

It is interesting to note that this becomes more important as $\langle \phi_2 \rangle$ decreases/ F^{ϕ_2} increases, or if there are a large number of exotics present.

The scalar masses in gauge mediation come in at two loops, and receive corrections proportional to

$$(M_I)^2|_{\text{gmsb}} \sim \left(\frac{1}{16\pi^2} \right)^2 \left(\frac{F_{\phi_2}}{\phi_2} \right)^2. \quad (5.85)$$

Unlike in the case of the gaugino masses, however, the tree level scalar masses are set by the gravitino mass. Typically

$$16\pi^2 m_{3/2} \gg \frac{F_{\phi_2}}{\phi_2}, \quad (5.86)$$

and the gauge mediation contribution gives about a 10% correction to the scalar masses, in our case. We will neglect their contributions in the calculation of the soft masses below.

⁵³In estimating this result, we have assumed that the mass terms of the Pauli-Villars fields do not depend on the SUSY breaking singlet field ϕ_2 , and that the modular weights of the Pauli-Villars fields obey specific properties.

5.5.2 Relevant details from the “mini-landscape”

Given the relative sizes of the F -terms in the SUSY breaking sectors described in this paper, it is very difficult to make model-independent statements. This stems from the fact that F^T plays a dominant role in the SUSY breaking. Because the Kähler metrics for the matter fields have generally different dependences on the T modulus, the dependence of the soft terms on F^T is typically non-universal. Moreover, the couplings of the SUSY breaking singlet field ϕ_2 will necessarily depend on the details of a specific model. Thus, in order to make *any* statements about the phenomenology of these models, we will have to make some assumptions. With the general features of the “mini-landscape” models in mind, we will make the following assumptions:

1. SUSY breaking is dominated by $F_{\phi_2} \neq 0$, $F_{T_3} \neq 0$, $F_S \neq 0$. All other F terms, including those due to the other T and U moduli, are subdominant;
2. the massless spectrum below M_S contains some vector-like exotics;
3. the untwisted sector contains the following Higgs and (3rd generation) matter multiplets: \mathbf{H}_u , \mathbf{H}_d , \mathbf{Q}_3 , \mathbf{U}_3^c , \mathbf{E}_3^c ;
4. the first two families have the same modular weights, see Table 5.2 on page 106;
5. the SUSY breaking field, ϕ_2 , lives in the untwisted, or second or fourth twisted sector, with a modular weight given by $n^3 = 0$; and
6. we neglect possible ϕ_2 dependence of the effective Yukawa terms.

Let us examine these assumptions in some more detail.

In general, gauge coupling unification in the “mini-landscape” models seems to require the existence of light vector-like exotics [30], whose masses can be as small as $\mathcal{O}(10^9 \text{ GeV})$. We further assume that these exotics couple to the SUSY breaking field ϕ_2 , giving a gauge mediated contribution to the gaugino masses above. We will make this contribution to the soft terms explicit in what follows. In assumption 2 we have specialized to the case where only “brane-localized” exotics are present in the model. These are states which come from the first and third twisted sectors of the model, and we refer the reader to [30, 38] for more details.

The top quarks and the up Higgses live in the bulk and the string selection rules allow for the following coupling in the superpotential:

$$\mathcal{W} \supset c \mathbf{Q}_3 \mathbf{H}_u \mathbf{U}_3^c. \quad (5.87)$$

The coupling c is a pure number of $\mathcal{O}(1)$, and is free of any dependence on the moduli. The down and lepton Yukawas are a bit more involved, as they arise at a higher order in

| MSSM particle | Modular Weight \vec{n} | U(1) _A charge |
|------------------|---|--|
| \mathbf{Q}_3 | (0, 1, 0) | 4/3 |
| \mathbf{U}_3^c | (1, 0, 0) | 2/3 |
| \mathbf{D}_3^c | $(\frac{1}{3}, \frac{2}{3}, 0)$ | 8/9 |
| \mathbf{L}_3 | $(\frac{2}{3}, \frac{1}{3}, 0)$ | 4/9 |
| \mathbf{E}_3^c | (1, 0, 0) | 2/3 |
| first two gen. | $(\frac{5}{6}, \frac{2}{3}, \frac{1}{2})$ | $\begin{array}{ll} 7/18 & (\mathbf{10}) \\ -5/18 & (\bar{\mathbf{5}}) \end{array}$ |
| \mathbf{H}_u | (0, 0, 1) | -2 |
| \mathbf{H}_d | (0, 0, 1) | +2 |

Table 5.2: Modular weights of the MSSM states in the “mini-landscape” benchmark model 1A. For the first two generations, the U(1)_A charges differ depending on whether the particle is in the **10** or **5** of $SU(5)$. See [38] for details.

the stringy superpotential. We will take them to be of the following form:

$$\mathcal{W} \supset \eta(T_1)^{p_1} \eta(T_2)^{p_2} \eta(T_3)^{p_3} (f_1(\langle \mathbf{s}_I^5 \rangle) \mathbf{Q}_3 \mathbf{H}_d \mathbf{D}_3^c + f_2(\langle \mathbf{s}_I^5 \rangle) \mathbf{L}_3 \mathbf{H}_d \mathbf{E}_3^c). \quad (5.88)$$

The \mathbf{s}_I are other singlet fields in the model (excluding the SUSY breaking singlet field, ϕ_2 , as per our assumptions), and the numbers p_1, p_2 and p_3 are calculable in principle, given knowledge of the modular weights of the \mathbf{s}_I . As one might expect, the expressions for the A terms explicitly depend on the value of p_3 in such a way that changing its value may result in a significant change in A_b and A_τ at the string scale. The impact on the weak scale observables is much less severe, however, giving a correction of a few percent to the gaugino masses, and leaving the squark and slepton masses virtually unchanged. Motivated by the modular weight assignments in Table 5.2 on page 106, we will choose $p_3 = 0$. Note this choice gives us universal A terms for the third generation.

One of the nice features of the “mini-landscape” models is the incorporation of a discrete (D_4) symmetry between the first two families in the low energy effective field theory. Because of this symmetry, we expect the modular weights of these matter states to be the same [95], see Table 5.2 on page 106. This will turn out to be very beneficial in alleviating the flavor problems that are generic in gravity mediated models of SUSY breaking: the scalar masses (at tree level) are given by a universal contribution (the gravitino mass squared) plus a contribution proportional to the modular weight. If the modular weights are the same between the first two generations, then the leading order prediction is for degenerate squark and slepton masses in the two light generations. Other contributions to the scalar masses come from gauge mediation and anomaly mediation, which do not introduce any new flavor problems into the low energy physics.

5.5.3 Hierarchy of F -terms

Note, in Section 5.3, we find (roughly)

$$F_T \gg F_S \gtrsim F_{\phi_2}, \quad (5.89)$$

for Cases 1, 2 and 3; and

$$F_T \gtrsim F_{\phi_2} \gg F_S, \quad (5.90)$$

for Cases 4 and 5, where

$$F_I \equiv \mathcal{W}_I + \mathcal{W}\mathcal{K}_I. \quad (5.91)$$

When one includes the relevant factors of the Kähler metric, we have (Table H.13 on page 161)

$$F^T > F^S \gg F^{\phi_2} \quad (5.92)$$

for Cases 1, 2 and 3; and

$$F^T \gg F^S \sim F^{\phi_2} \quad (5.93)$$

for Cases 4 and 5. F^S is enhanced by a factor of $\mathcal{K}^{S\bar{S}} \sim (2+2)^2$, while F^{ϕ_2} is decreased by a factor of $\mathcal{K}^{\phi_2\bar{\phi}_2} \sim (2)^{-1/2}$.⁵⁴ This means that although the singlet field ϕ_2 was a dominant source of SUSY breaking, it is the least important when computing the soft terms, given the one condensate hidden sector of the known ‘‘mini-landscape’’ models studied in Section 5.3.⁵⁵ Taking the details of the ‘‘mini-landscape’’ models into account, the soft terms at the string scale are given in Table H.14 on page 161.

In the five chosen Cases, 2, 3 and 4 have a gravitino mass less than 2 TeV. The value of the gravitino mass can be adjusted by varying w_0 . For Cases, 1, 3 (4) the Higgs up (down) mass squared is negative. This is a direct result of the sign of D_A and the $U(1)_A$ charge of the Higgs’ (see Table 5.2 on page 106 for the $U(1)_A$ charges of all the MSSM states).⁵⁶ Note, the first and second generation squarks and sleptons are lighter than the third generation states at the string scale. This is a consequence of the significant T modulus contribution to the first and second generation squark and slepton masses, due to their modular weights,

⁵⁴This is due to the assumed modular weight of the field ϕ_2 (assumption 5 in Section 5.5.2).

⁵⁵In racetrack models F_S is suppressed by more than an order of magnitude. In these cases F_{ϕ_2} is dominant [139].

⁵⁶Note, it is well known that the D -term VEV in supergravity is of order $\langle F^i \rangle^2$ [178, 185]. It is given by the relation

$$\langle D_A \rangle = 2M_A^{-2} \langle F^i \rangle \langle F_j^* \rangle \langle \partial_i \partial^j D_A \rangle. \quad (5.94)$$

Thus the D -term contribution to the vacuum energy is negligible, but its contribution to scalar masses can be significant. Since $|F^S|^2 < |F^T|^2$, F^T is dominant in the above relation. However, the Kähler metric of ϕ_2 which spontaneously breaks $U(1)_A$, in our case, does not include T , i.e., $\langle (\partial_T \partial^T D_A) \rangle = 0$. Hence $\langle D_A \rangle$ is suppressed compared with $|F^T|^2/M_{\text{PL}}^2$, i.e., $\langle D_A \rangle : |F^T|^2/M_{\text{PL}}^2 = |F^S|^2 : |F^T|^2$ where we used $\langle (\partial_S \partial^S D_A) \rangle = (M_A/M_{\text{PL}})^2$, because of the S -dependent FI term. We thank T. Kobayashi, private communication, for this analysis.

Table 5.2 on page 106. Finally we have included the possible gauge mediated SUSY breaking contribution to the gaugino masses, Table H.14 on page 161. This contribution is only significant for Cases 4 and 5, due to the larger value of F_{ϕ_2} in these cases.

5.5.4 Weak scale observables

We do not intend this work to be a comprehensive study of the parameter space of these models, so we will limit our weak scale analysis to the five cases studied in the single condensate model presented in this paper. The points are chosen subject to the following constraints:

- $m_{h^0} \Big|_{\text{LEP}} \gtrsim 114.4 \text{ GeV}$,
- successful electroweak symmetry breaking,
- $m_{\tilde{\chi}^\pm} \gtrsim 94 \text{ GeV}$, and
- the low energy spectrum is free of tachyons.

Note that we take $\text{sgn}(\mu) > 0$ and vary $\tan \beta$, and the number, n_i , of “messenger” exotics. We stay in the region of small to moderate $\tan \beta$ as the “mini-landscape” models do not tend to predict unification of the third family Yukawas. This can be seen from Equations (5.87) and (5.88), for example.

Using `SoftSUSY` (v3.1) [186], we preformed the RGE running from the string scale to the weak scale. We use the current value of the top quark mass [187]

$$m_{top} \Big|_{\text{world avg.}} = 173.1 \text{ GeV} \quad (5.95)$$

and the strong coupling constant at M_Z [14]

$$\alpha_s(M_Z) = 0.1176. \quad (5.96)$$

The μ parameter is obtained under the requirement of radiative electroweak symmetry breaking, and is of order the gravitino mass, as expected. This implies a fine tuning of order

$$\frac{M_Z^2}{m_{3/2}^2} \sim \mathcal{O}(10^{-2}) \text{ to } \mathcal{O}(10^{-4}). \quad (5.97)$$

The results obtained from `SoftSUSY` are presented in Table H.15 on page 162. In this analysis, we have not included any possible gauge mediated SUSY breaking contributions. This assumes that all the vector-like exotics have mass at the string scale. In Case 2 and 3 we have the smallest gravitino masses, so the lightest SUSY partners. $\tan \beta = 25$ in order for the light Higgs mass to be above the LEP bound. Note we assume a $\pm 2 \text{ GeV}$ theoretical uncertainty in the Higgs mass. In all 5 cases the Higgs mass is between the LEP bound

and 121 GeV. All other Higgs masses are of order the gravitino mass. In all 5 cases the gluino mass is less than 1 TeV and of order 600 GeV or less in Cases 2, …, 5. Thus the gluino is very observable at the LHC. In all cases, the lightest MSSM particle is the lightest neutralino. The next-to-lightest neutralino and the lightest chargino are approximately degenerate with mass of order twice the lightest neutralino mass. In Cases 2, 3 and 4 the lightest stop has mass less than 1 TeV. In Cases 2 and 4, the lightest stop is also the lightest squark. Thus in these cases the gluino will predominantly decay into a top - anti-top pair with missing energy (and possibly two energetic leptons). In Case 3, the lightest down squarks of the first two families are lighter than the lightest stop. In these cases gluinos will decay significantly into two light quark jets plus missing energy (and possibly two energetic leptons).

In all cases the lightest MSSM particle is mostly ($\gtrsim 99\%$) bino (see Table H.16 on page 163). We note that this is generically true in the models, even when there are contributions from gauge mediation. The gauge mediated contributions in Equation (5.80) do not appreciably change the composition of the LSP, which one can check with the solutions in Tables H.7 and H.8 in Appendix H.

We have evaluated other low energy observables using `micrOMEGAs` [188]. As expected, the bino LSP overcloses the universe, giving $\Omega_{\text{DM}} >> \Omega_{\text{DM}}^{\text{OBS}} \approx 0.2$. The calculated values for the following observables are given in the last few rows of Table H.15 on page 162. Corrections to the ρ parameter are very small. Corrections to $(g - 2)_\mu$ are significant in Cases 2 and 3 which is not surprising since these are the two cases with the lightest sleptons for the first two families. We also display the results for $BR(b \rightarrow s\gamma)$ and $BR(B_s \rightarrow \mu^+ \mu^-)$. The result for $BR(b \rightarrow s\gamma)$ is within the 2σ experimental bound (see [23] and references therein). Given the small chargino masses and the large values of μ and the squark and CP odd Higgs masses, we obtain a branching ratio $BR(B_s \rightarrow \mu^+ \mu^-)$ consistent with the standard model.

We are not overly concerned about the fact that binos seem to overclose the universe. In some of the heterotic orbifold models the Higgs μ term vanishes in the supersymmetric limit. Hence there is a Peccei-Quinn symmetry. Supersymmetry breaking effects are expected to shift the moduli VEVs and generate a non-vanishing μ term; spontaneously breaking the PQ symmetry and producing the standard invisible axion. In fact, it has been shown that PQ axions may be obtained in heterotic orbifold contractions [173]. In such cases it is possible that the bino decays to an axino + photon leaving an axino dark matter candidate [189–191].

However another, perhaps more important, cosmological effect must be considered. All 5 cases have a gravitino with mass less than 3 TeV. Thus there is most likely a gravitino problem. In addition the lightest moduli mass is of order (Table H.15 on page 162) several 100s GeV. Thus there is also a cosmological moduli problem. But there is hope. The

next lightest massive modulus [nLMM] has, in all cases, a mass above 20 TeV. A detailed cosmological analysis is beyond the scope of this paper. However, it is possible that when cosmological temperatures are of order M_{nLMM} , the universe becomes nLMM dominated. By the time the nLMM decays all matter is diluted and then the universe reheats to temperatures above the scale of big bang nucleosynthesis (for example, see [192]). Thus it is possible that the nLMM solves both the gravitino and light moduli problems. Of course, then the issue of obtaining the correct baryon asymmetry of the universe and the dark matter abundance must be addressed. Both can in principle be obtained via non-thermal processes at low temperature.

In Table H.16 on page 163 we analyze the dependence of our results on the value of $\tan \beta$ and $\text{sgn}(\mu)$ with all other input parameters fixed. We find that only the value of the light Higgs mass is sensitive to varying $\tan \beta$. Note the lowest value of $\tan \beta$ is obtained by the Higgs mass bound, while the largest value of the light Higgs mass is obtained with the largest value of $\tan \beta$ (for both signs of μ). Additionally, at large $\tan \beta$ for $\mu < 0$ the Higgs potential becomes unbounded from below. For $\mu > 0$ we limited the analysis to $\tan \beta \leq 50$. The light Higgs mass does not go above 122 GeV for $\tan \beta \leq 50$.

5.6 Conclusions

As a candidate theory of all fundamental interactions, string theory should admit at least one example of a four-dimensional vacuum which contains particle physics and early universe cosmology consistent with the two standard models. In this context, the recently found “mini-landscape” of heterotic orbifold constructions [34–36, 38, 193] provide us with very promising four-dimensional perturbative heterotic string vacua. Their low-energy effective field theory was shown to resemble that of the MSSM, assuming non-zero VEVs for certain blow-up moduli fields which parametrize resolutions of the orbifold fixed points along F - and D -flat directions in global supersymmetry.

In this paper we have dealt with the task of embedding the globally supersymmetric constructions of the heterotic “mini-landscape” into supergravity and then stabilizing the moduli of these compactifications, including their orbifold fixed point blow-up moduli. The blow-up moduli appear as chiral superfields contained in the twisted sectors of the orbifolded heterotic string theory. They are singlets under all standard model gauge groups, but are charged under several unwanted $U(1)$ gauge symmetries, including the universal anomalous $U(1)_A$ gauge symmetry of the heterotic string. Note, moduli stabilization of string compactifications is a crucial precondition for comparing to low energy data, as well as for analyzing any early universe cosmology, such as inflation, in a given construction.

Section 5.2 served the purpose of reviewing the ingredients and structure of the heterotic 4d $N = 1$ supergravity inherited from orbifold compactifications of the 10d perturbative $E_8 \otimes E_8$ heterotic string theory. The general structure of these compactifications results in:

- i) a standard no-scale Kähler potential for the bulk volume and complex structure moduli, as well as the dilaton, together with
- ii) gaugino condensation in the unbroken sub-group of the hidden E_8 , and
- iii) the fact that the non-perturbative (in the world-sheet instanton sense) Yukawa couplings among the twisted sector singlet fields contain terms explicitly breaking the low-energy $U(1)_R$ -symmetry.

We have shown in Section 5.3 that these three general ingredients, present in all of the “mini-landscape” constructions, effectively realize a KKLT-like setup for moduli stabilization. Here, the existence of terms explicitly breaking the low-energy $U(1)_R$ -symmetry at high order in the twisted sector singlet fields is the source of the effective small term w_0 in the superpotential, which behaves like a constant with respect to the heterotic dilaton [170]. Utilizing this, the presence of just a single condensing gauge group in the hidden sector (in contrast to the racetrack setups in the heterotic literature) suffices to stabilize the bulk volume T (and, by extension, also the bulk complex structure moduli U), as well as the dilaton S at values $\langle \text{Re } T \rangle \sim 1.1 - 1.6$ and $\langle \text{Re } S \rangle \sim 2$. These are the values suitable for perturbative gauge coupling unification into $SU(5)$ - and $SO(10)$ -type GUTs distributed among the orbifold fixed points. Note, we have shown this explicitly for the case one T modulus and a dilaton, however, we believe that all bulk moduli will be stabilized near their self-dual points [125, 126].

At the same time, the near-cancelation of the D -term of the universal anomalous $U(1)_A$ -symmetry stabilizes non-zero VEVs for certain gauge invariant combinations of twisted sector singlet fields charged under the $U(1)_A$. This feature in turn drives non-vanishing F -terms for some of the twisted sector singlet fields. Thus, together with the F -terms of the bulk volume moduli inherited from modular invariance, it is sufficient to uplift the AdS vacuum to near-vanishing cosmological constant.

The structure of the superpotential discussed in this paper, $\mathcal{W} \sim w_0 e^{-bT} + \phi_2 e^{-aS-b_2T}$, behaves like a ‘hybrid KKLT’ with a single-condensate for the dilaton S , but as a racetrack for the T and, by extension, also for U moduli. An additional matter F_{ϕ_2} term driven by the cancelation of the anomalous $U(1)_A$ D -term seeds successful up-lifting.

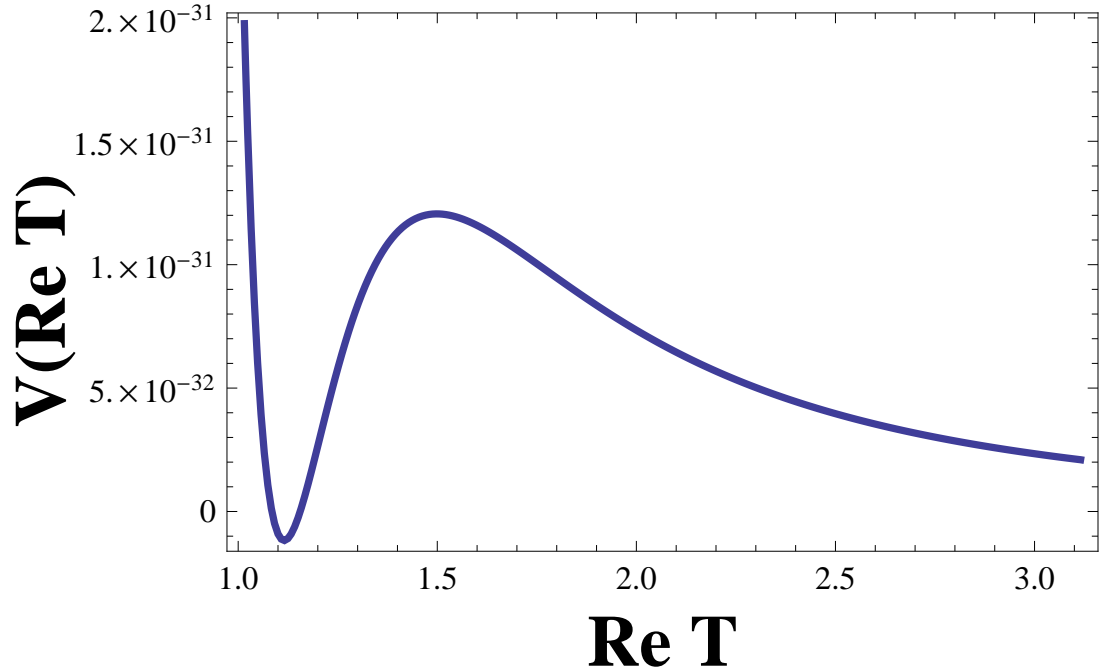
We note the fact that the effective constant term in the superpotential, w_0 , does not arise from a flux superpotential akin to the type IIB case. This leaves open (for the time being) the question of how to eventually fine-tune the vacuum energy to the 10^{-120} -cancelation necessary.

Section 5.4 then serves to demonstrate how the success of stabilizing the bulk moduli and breaking supersymmetry in the F -term sector, driven by the $U(1)_A$ D -term cancellation, transmits itself to the chiral singlet fields from the untwisted and twisted sectors of the orbifold compactification which contain, among others, the blow-up moduli associated with the orbifold fixed points. The effects from the bulk moduli stabilization and supersymmetry breaking, transmitted through supergravity, generically suffice to stabilize all of the twisted sector singlet fields at non-zero VEVs. This property was assumed in the original “mini-landscape” construction in order to decouple the non-MSSM vector-like exotic matter, and our arguments provide the first step towards a self-consistent justification for these assumptions.

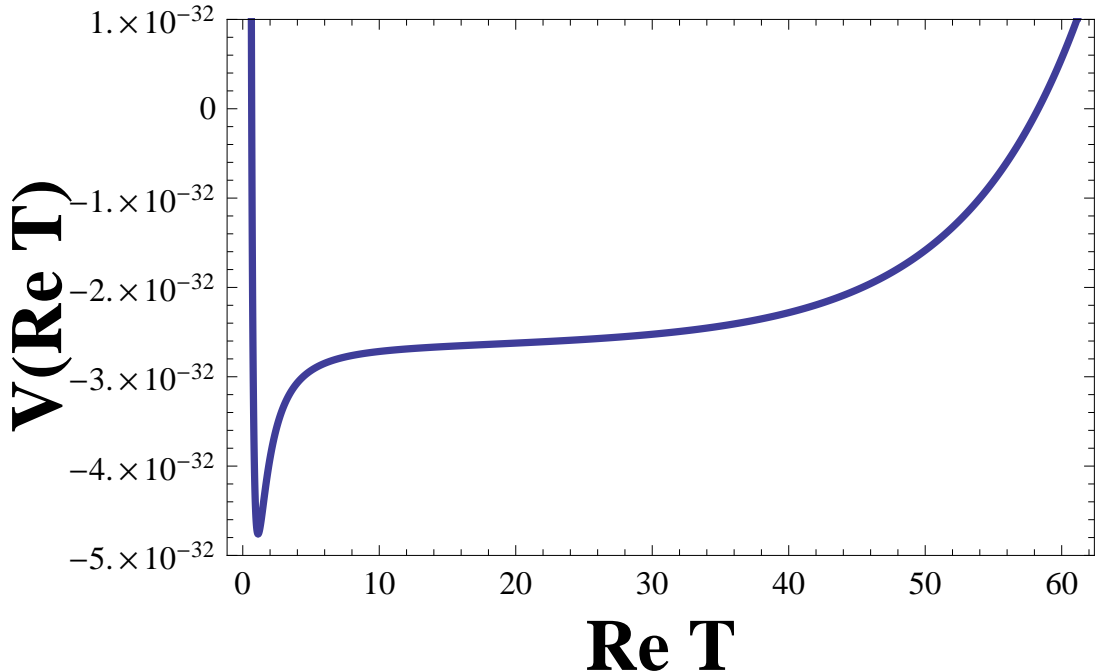
In Section 5.5 we estimate the structure of the soft terms from the moduli sector supersymmetry breaking at the high scale. We find that the contributions from high-scale gauge mediation are subdominant (although not parametrically suppressed) compared to the gravity mediated contributions. Upon RGE running the high-scale soft terms to the weak scale using `softSUSY`, we obtain several benchmark patterns of sparticle and Higgs masses (see Table H.15 162). The low-energy spectrum features an allowed window of $\tan\beta$ values for $m_{3/2} < 5$ TeV. It generically contains a light chargino/ neutralino spectrum and heavy squarks and sleptons. The lightest MSSM partner, in the 5 benchmark cases studied, is given by a bino ($> 99\%$) with mass $\gtrsim 52$ GeV. If this were the LSP, it would yield a dark matter abundance which over closes the universe, however, the “mini-landscape” models offer some possible resolutions. One possibility is that the bino decays into an axino, the partner of the invisible axion responsible for canceling the θ -angle of QCD, which is present in many of the “mini-landscape” setups [173]. We have also considered an alternative possibility that the late decay of the next to lightest massive modulus might ameliorate or solve the cosmological gravitino and moduli problem. This would then dilute the above mentioned cosmological abundance of binos. Of course, the non-thermal production of dark matter and a baryon asymmetry must then be addressed. Note, however, the resolution of these cosmological questions are beyond the scope of the present paper.

Summarizing, we have given a mechanism for moduli stabilization and supersymmetry breaking for the perturbative heterotic orbifold compactifications. It relies on the same variety and number of effective ingredients as the KKLT construction of type IIB flux vacua and thus represents a significant reduction in necessary complexity, compared to the multi-condensate racetrack setups utilized so far. When applied to a simplified analog of the “mini-landscape” heterotic orbifold compactifications, which give the MSSM at low energies, it leads to fully stabilized 4d heterotic vacua with broken supersymmetry and a small positive cosmological constant. Moreover, most of the low energy spectrum could be visible at the LHC.

We leave some important questions like the problem of the full fine-tuning of the vacuum energy to near-vanishing, or the existence of an inflationary cosmology within these stabilized “mini-landscape” constructions for future work. Further study is also warranted with respect to potential cosmological moduli and gravitino problems that may be associated with sub-100 TeV moduli and gravitino mass values (see e.g. [194, 195]). Finally, the numerical evaluation of any particular “mini-landscape” vacuum requires analyzing the supergravity limit with three bulk moduli, T , one bulk complex structure modulus, U , and of order 50 blow-up moduli. A detailed analysis of this more realistic situation would require a much better handle on the moduli space of heterotic orbifold models than is presently available.



(a) The scalar potential in Case 2 for $\text{Re } T$, with $b_i > 0$.



(b) The scalar potential in Case 4 for $\text{Re } T$, with $b_i < 0$.

Figure 5.1: As $\text{RE}[T] \rightarrow \infty$, the potential for $b_i > 0$ mimics a Racetrack, which can be seen from Equation (5.39), for example. In the case where $b_i < 0$, however, the potential exhibits a different asymptotic behavior. As $\text{RE}[T] \rightarrow \infty$ the potential diverges, which means that theory is forced to be compactified [125, 126].

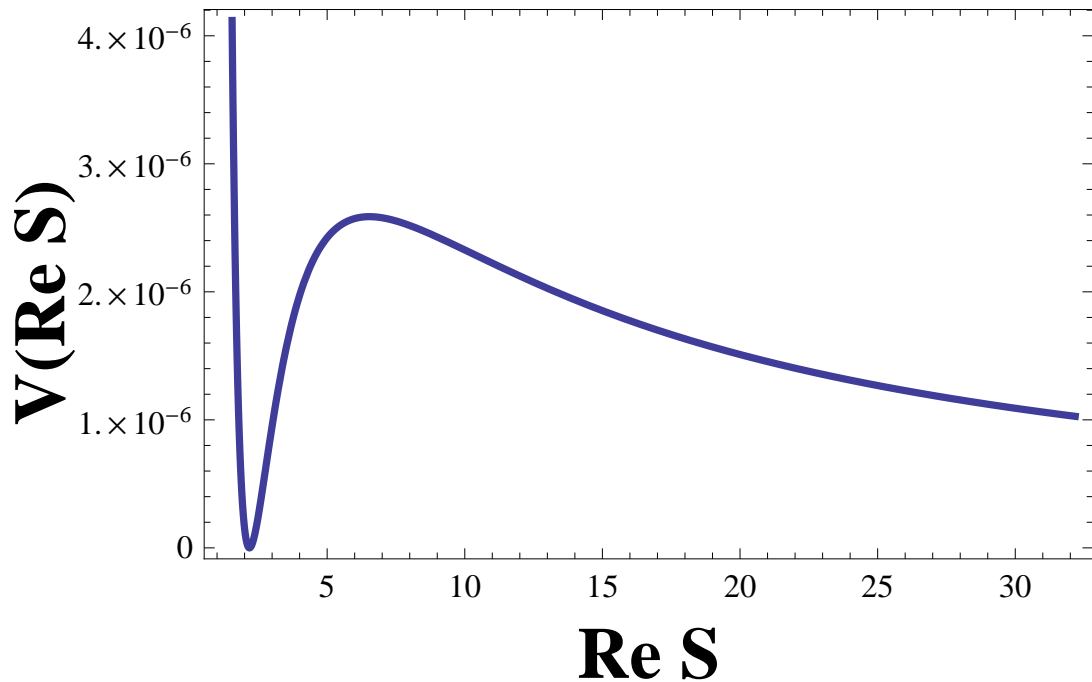


Figure 5.2: The scalar potential in the $\text{Re}[S]$ direction for Case 2.

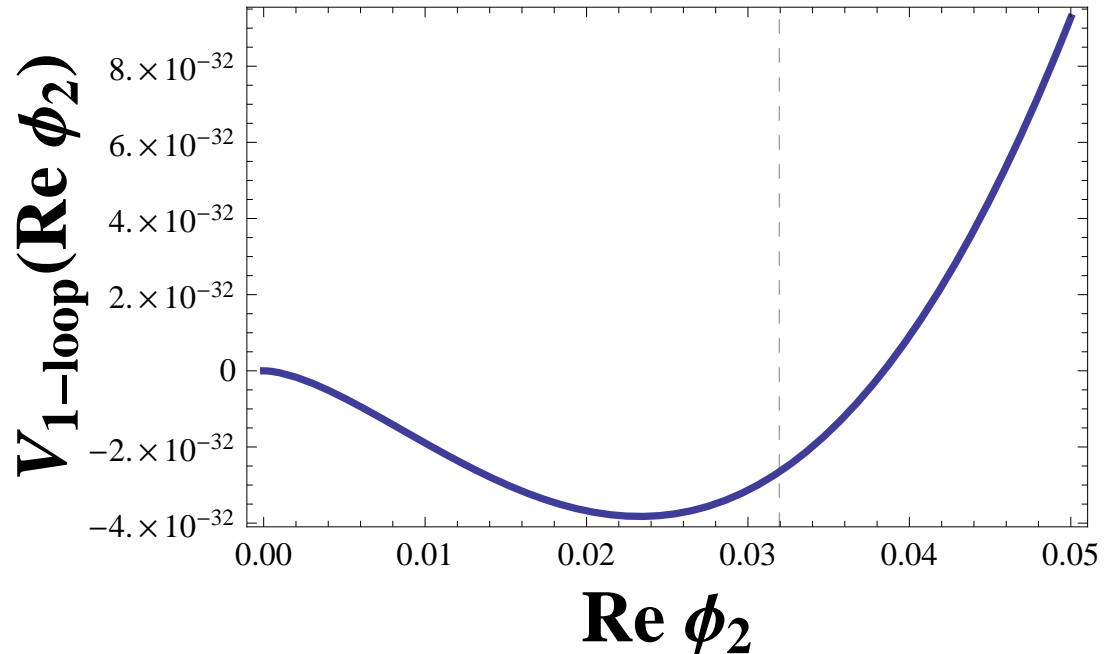


Figure 5.3: The one loop Coleman-Weinberg potential (Case 4) for ϕ_2 . The dashed line represents the VEV of ϕ_2 in the minimum of the *full* potential.

Chapter 6

CONCLUSION

I wonder why. I wonder why.
I wonder why I wonder.
I wonder WHY I wonder why.
I wonder why I wonder!

Richard Feynman

In this Dissertation, we have presented original research in the study of the effective field theories derived from compactifications of the heterotic string on orbifolds, focusing on the “mini-landscape” models [34–38] as an example.

In Chapter 2, we attempted to provide a “How-To” guide for orbifold compactifications of the heterotic string. After a brief discussion of the heterotic string itself, we presented the steps involved in constructing the massless spectrum in the \mathbb{Z}_6 -II compactifications, on which the mini-landscape models are based. The method we use to construct the models is known as the “centralizer” (see [56, 60, 196], for example). Another (equivalent) way to construct the massless spectrum involves the use of generalized GSO projectors, and is outlined in Appendix A of [39]. It is still an open question as to how the two different constructions are related.

In Chapter 3, we addressed the issue of gauge coupling unification in the mini-landscape models. The models admit a “large volume” limit, which gives an effective five dimensional orbifold GUT—of the six compact dimensions, one is slightly larger. The Kaluza-Klein modes of the larger dimension can appear in loops, and furnish a threshold correction to the gauge coupling. We calculate these contributions explicitly in Appendix B. We also include a small set of vector-like exotic matter at an intermediate scale, as the Kaluza-Klein modes of the MSSM states alone do not allow for unification, which we prove in Appendix C. Aside from unification, the structure of the models allow us to place some constraints on the parameter space. In particular, current limits on dimension six proton decay operators constrain the compactification radius, which we show in Appendix D. Chapter 3 concludes with a more detailed analysis of two different vacua, where we

demonstrate that the appearance of an intermediate scale can be made consistent with the requirement that SUSY is not broken by F terms. This is a necessary (but not sufficient) condition: in order to show that SUSY is unbroken in the vacuum, we must also show that $D = 0$ can be satisfied. This proof is completed in Appendix E, where we show the relationship between the holomorphic, gauge invariant monomials and $D = 0$.

Given the “bottom up” approach of Chapter 3, one might wonder about the consistency of our results in regards to the underlying string theory. In Chapter 4, we showed that “top down” constraints limit (but do not invalidate) the results of the previous chapter. We showed that the coupling constant of the underlying string theory, g_{STRING} , is equal to the coupling constant of the gauge theory (α_{GUT}) times the ratio of the string scale to the compactification scale. This allows us to calculate g_{STRING} (which characterizes the underlying string theory) given the parameters of the effective field theory, derived in Chapter 3. Perturbativity of the underlying string theory requires that $g_{\text{STRING}} \lesssim 1$, which proves to be a strict bound, eliminating about half of the models which survived proton decay constraints in Chapter 3. In addition, the dimension six proton decay operator can be written in terms of g_{STRING} , providing an interesting relationship between a macroscopic observable and the microscopic details of the theory. We also commented on the effects of multiple “large” extra dimensions, which tend to require that the underlying string theory be more strongly coupled.

A more fundamental issue to the “top down” consistency of the heterotic string models is that of moduli stabilization, a problem which had stalled progress in the field since the mid 1990’s. We showed how this issue could be addressed in the effective supergravity theory in Chapter 5, which represents the first success in stabilizing all of the moduli of the heterotic orbifold compactifications in Minkowski vacua, without relying on uncalculable non-perturbative corrections to the Kähler potential [130]. To show how this might be accomplished, we wrote down a toy model which satisfied $F = D = 0$ globally, without considering non-perturbative effects. This is the same level at which the mini-landscape models were analyzed in [38]. We then couple the model to a SUSY QCD-like theory (which is a general feature of the mini-landscape models [37]), which generates a (moduli dependent) scale, and embed the model in to supergravity. In addition, we consider the moduli dependence in the superpotential implied by modular invariance of the underlying string theory. For several different sets of parameters, we showed that all the moduli in our model could be stabilized. We concluded the chapter by arguing that all other moduli in the heterotic compactification, including twisted sector states called “blow-up modes”, are stabilized once SUSY is broken.

We motivated dependence on the Kähler and complex structure moduli in the superpotential by modular invariance, inserting appropriate factors of the Dedekind η function to ensure $\text{SL}(2, \mathbb{Z})$ invariance. We know, however, that Wilson lines and even the orbifold

itself may only respect a subgroup of $SL(2, \mathbb{Z})$ [161]. In some cases, for example, the correct transformation properties of the superpotential are ensured by multiplying each term by a linear combination of η functions [197], see Appendix F. Moreover, it has been shown that more generic modular invariant functions (other than η) can appear [126]. Studying the behavior of the superpotential in these cases may give interesting new dynamics, which may include different ratios of F terms, for example.

Given the moduli stabilization mechanism, we showed the types of phenomenology one might expect for LHC physics. While the main contributions to the soft terms come from gravity mediation, we also considered gauge mediation and anomaly mediation contributions. We investigated only a small corner of the parameter space of these models, though some interesting features emerged. For example, at negative μ , an upper limit on $\tan \beta$ exists, beyond which the higgs potential becomes unstable. The models examined tended to prefer a small higgs mass ($\lesssim 115$ GeV), though this bound is not strict. In particular, if the gravitino mass (which is controlled in the microscopic theory by w_0) is much larger, the higgs mass can be pushed higher. This comes at the cost of interesting LHC physics, because the gravitino mass controls all of the soft masses in gravity mediation. The LSP in these models is always the bino, which provides a poor dark matter candidate—in order to evade the WMAP bounds on relic densities, then, we must rely on an axion to fill the role.

One particularly interesting aspect of our SUSY breaking scheme is the appearance of tachyonic masses at the string scale in the soft SUSY breaking lagrangian, \mathcal{L}_{SOFT} [198, 199]. These tachyons resulted from the contribution of the FI D term to the scalar masses, which was generated after SUSY was broken. It seems that this may be a generic situation in the heterotic compactifications: the literature typically assumes that $D = 0$ can always be satisfied, and this is true, until SUSY is broken. When SUSY is broken, D terms are typically generated and obey $D \sim F^2$. Assuming gravity mediation, the soft masses are roughly $m_i^2 \sim m_{3/2}^2 + F^2 + g_{GUT}^2 q_i^A D_A$, where the i th scalar carries charge q_i^A under $U(1)_A$. Because the MSSM matter in heterotic string models generically have q_i^A of both signs, we are left with a situation where one or more scalar masses may be tachyonic at the high scale. While renormalization group evolution can give positive contributions to the masses-squared in the IR, this is not always the case. It would be interesting to understand what the parameter space of these models looks like, with a goal of understanding general patterns of (IR) soft masses. This would be another example of a “bottom up” constraint on the underlying string model.

Appendix A

THE MODE EXPANSION IN THE TWISTED SECTOR

A.1 The Mode Expansion in the Twisted Sector

In the twisted sectors, the states obey different boundary conditions, the equations of motion should be invariant under the symmetries of the orbifold. As before, under the action of the space group S , one has

$$\begin{aligned} Z^a(\sigma_+) \rightarrow Z^a(\tau, \sigma + 2\pi) &= e^{2\pi i k v_a} Z^a(\tau, \sigma) + n_\alpha e_\alpha, \\ Z^{\bar{a}}(\sigma_+) \rightarrow Z^{\bar{a}}(\tau, \sigma + 2\pi) &= e^{-2\pi i k v_a} Z^{\bar{a}}(\tau, \sigma) + n_\alpha e_\alpha. \end{aligned} \quad (\text{A.1})$$

As a function of left-moving coordinates, the $Z^a(\sigma^+)$ are given by

$$Z^a(\sigma_+) = \frac{1}{\sqrt{2}} \left\{ [x^{2a+2} + ix^{2a+3}] + \tau [p^{2a+2} + ip^{2a+3}] + \frac{i}{\sqrt{2}} \sum_n \frac{1}{n} [\tilde{\alpha}_n^{2a+2} + i\tilde{\alpha}_n^{2a+3}] \right\}.$$

with an analogous expression for the right-movers. We define

$$z^a \equiv x^{2a+2} + ix^{2a+3}, \quad (\text{A.2})$$

$$p^a \equiv p^{2a+2} + ip^{2a+3}, \quad (\text{A.3})$$

$$\tilde{\beta}_n^a \equiv \tilde{\alpha}_n^{2a+2} + i\tilde{\alpha}_n^{2a+3}. \quad (\text{A.4})$$

Under these definitions, we have

$$Z^a(\sigma_+) = z^a + \tau p^a + \sum_{m \in ?} \frac{1}{m} \tilde{\beta}_m^a e^{-im\sigma_+} \quad (\text{A.5})$$

Note that we have replaced

$$\sum_{n \in \mathbb{Z} \neq 0} \rightarrow \sum_{m \in ?} . \quad (\text{A.6})$$

For now, we will put no requirement on m —it will turn out that m is not integral, a fact implied by the boundary conditions on the orbifold.

Now, the boundary conditions (A.1) impose

$$z^a \rightarrow z'^a = e^{2\pi i k v_a} z^a + n_\alpha e_\alpha = z^a. \quad (\text{A.7})$$

In other words, z^a is invariant under the action of the orbifold, which is exactly the definition of a fixed point. Next, the momentum transforms as:

$$p^a \rightarrow p'^a = e^{2\pi i k v_a} p^a = p^a. \quad (\text{A.8})$$

The only possible solution to this equation (for generic values of $k v_a$) must be that $p^a = 0$. Physically, z^a is the coordinate of the center of the string, while p^a represents the net momentum of the string. Thus, the strings in the closed sector are localized at various fixed points on the orbifold.

Next, consider the twisted oscillators:

$$\sum_{m \in ?} \frac{1}{m} \tilde{\beta}_m^a e^{-im\sigma_+} \rightarrow \sum_{m \in ?} \frac{1}{m} \tilde{\beta}_m^a e^{-im\sigma_+ - 2\pi i m} = \sum_{m \in ?} \frac{1}{m} \tilde{\beta}_m^a e^{-im\sigma_+ - 2\pi i k v_a}. \quad (\text{A.9})$$

Equating each term, we see that invariance under the action of the twist implies

$$-im\sigma_+ - 2\pi i m = -im\sigma_+ + 2\pi i k v_a, \Rightarrow m = -k v_a \pmod{1}.$$

The “mod 1” appears because of the fact that the above formulae hold in a more general case where we have factors of $1 = e^{2\pi i n}$ floating around. Thus we find that the oscillators are fractionally moded. We can now replace the question mark write (A.5):

$$Z^a(\sigma_+) = z^a + \sum_{n \in \mathbb{Z}} \frac{1}{(n - k v_a)} \tilde{\beta}_{n-k v_a}^a e^{-i(n - k v_a)\sigma_+}. \quad (\text{A.10})$$

Similarly, one can calculate an expression for $Z^{\bar{a}}$, following the same steps. You should see that

$$Z^{\bar{a}}(\sigma_+) = z^{\bar{a}} + \sum_{n \in \mathbb{Z}} \frac{1}{(n + k v_a)} \tilde{\beta}_{n+k v_a}^{\bar{a}} e^{-i(n + k v_a)\sigma_+} \quad (\text{A.11})$$

A.2 Fractionally Moded Oscillators

Equations (A.10) and (A.11) imply that oscillators of twisted sector states may be fractionally moded. When constructing the heterotic string models, it is important to remember that such states are present in the massless spectrum.

Counting the oscillators requires that one know the eigenvalues of the number operator, which requires us to actually construct the number operator.

We now First, consider:

$$\begin{aligned}
[\tilde{\beta}_{n-kv_a}^a, \tilde{\beta}_{m+kv_a}^{\bar{b}}] &= \frac{1}{2} \left[\tilde{\alpha}_{n-kv_a}^{2a+2} + i\tilde{\alpha}_{n-kv_a}^{2a+3}, \tilde{\alpha}_{m+kv_a}^{2b+2} - i\tilde{\alpha}_{m+kv_a}^{2b+3} \right], \\
&= \frac{1}{2} \left\{ \left[\tilde{\alpha}_{n-kv_a}^{2a+2}, \tilde{\alpha}_{m+kv_a}^{2b+2} \right] - i \left(\left[\tilde{\alpha}_{n-kv_a}^{2a+3}, \tilde{\alpha}_{m+kv_a}^{2b+2} \right] - \left[\tilde{\alpha}_{n-kv_a}^{2a+3}, \tilde{\alpha}_{m+kv_a}^{2b+3} \right] \right) \right. \\
&\quad \left. + \left[\tilde{\alpha}_{n-kv_a}^{2a+3}, \tilde{\alpha}_{m+kv_a}^{2b+3} \right] \right\}, \\
&= \frac{1}{2} \left\{ (n - kv_a) \delta_{m+n} \delta^{ab} - i(0 - 0) + (n - kv_a) \delta_{m+n} \delta^{ab} \right\}, \\
\Rightarrow [\tilde{\beta}_{n-kv_a}^a, \tilde{\beta}_{m+kv_a}^{\bar{b}}] &= (n - kv_a) \delta_{m+n} \delta^{ab}. \tag{A.12}
\end{aligned}$$

In the third line above, we get zeros because $2a + 2 \neq 2b + 3$ for $a, b \in \mathbb{Z}$. Also, we have:

$$\begin{aligned}
[\tilde{\beta}_{n-kv_a}^a, \tilde{\beta}_{m-kv_a}^b] &= \frac{1}{2} \left[\tilde{\alpha}_{n-kv_a}^{2a+2} + i\tilde{\alpha}_{n-kv_a}^{2a+3}, \tilde{\alpha}_{m-kv_a}^{2b+2} + i\tilde{\alpha}_{m-kv_a}^{2b+3} \right], \\
&= \frac{1}{2} \left\{ (n - kv_a) \delta_{n+m-2kv_a} + i(0 + 0) - (n - kv_a) \delta_{n+m-2kv_a} \right\}, \\
\Rightarrow [\tilde{\beta}_{n-kv_a}^a, \tilde{\beta}_{m-kv_a}^b] &= 0. \tag{A.13}
\end{aligned}$$

We know enough to build the number operator now. In general, we want something like this:

$$\tilde{N} \equiv \sum_n : \tilde{\beta}_{n-kv_a}^a \tilde{\beta}_{-(n-kv_a)}^{\bar{a}} :. \tag{A.14}$$

Our old friend, the normal ordering operator, is telling us that we have to be careful about writing down an expression for \tilde{N} that we can actually use. There are two cases to worry about.

- $n - kv_a > 0$. In this case, the positively moded operator is $\tilde{\beta}_{n-kv_a}^a$, making it the annihilation operator, so it should act first. Thus

$$\tilde{N} = \sum_{n-kv_a > 0} \tilde{\beta}_{-(n-kv_a)}^{\bar{a}} \tilde{\beta}_{n-kv_a}^a \tag{A.15}$$

- $n - kv_a < 0$. In this case, the annihilation operator is $\tilde{\beta}_{-(n-kv_a)}^{\bar{a}}$. This means the number operator should be

$$\tilde{N} = \sum_{n-kv_a < 0} \tilde{\beta}_{n-kv_a}^a \tilde{\beta}_{-(n-kv_a)}^{\bar{a}}. \tag{A.16}$$

The total number operator is then defined as

$$\Rightarrow \tilde{N} \equiv \sum_{n-kv_a > 0} \tilde{\beta}_{-(n-kv_a)}^{\bar{a}} \tilde{\beta}_{n-kv_a}^a + \sum_{n-kv_a < 0} \tilde{\beta}_{n-kv_a}^a \tilde{\beta}_{-(n-kv_a)}^{\bar{a}}. \tag{A.17}$$

Finally, one can perform the same calculation for the right movers. I will only state the results below, because the derivations follow the same steps as above, with appropriate switching of minus signs and tildes. In general, one has:

$$\bar{Z}^a(\sigma_-) = z^a + \tau q^a + \sum_n \frac{1}{n + kv_a} \beta_{n+kv_a}^a e^{-in\sigma_-}, \quad (\text{A.18})$$

$$[\beta_{n+kv_a}^a, \beta_{m-kv_a}^{\bar{a}}] = (n + kv_a) \delta^{ab} \delta_{m+n}, \quad (\text{A.19})$$

$$\Rightarrow N = \sum_{n+kv_a>0} \beta_{-(n+kv_a)}^{\bar{a}} \beta_{n+kv_a}^a + \sum_{n+kv_a<0} \beta_{n+kv_a}^a \beta_{-(n+kv_a)}^{\bar{a}}. \quad (\text{A.20})$$

A.3 An Explicit Example

Perhaps the best way to see how the calculation proceeds is to work out an example, using the explicit example of the \mathbb{Z}_6 -II orbifold. The goal is to calculate which oscillators are allowed in each of the directions, using our definition of the number operator in Equation (A.17), and the commutators that we derived in Equation (A.12). The main idea here is that consistent states are always eigenvalues of the number operator.

In this case, we will limit ourselves to the first twisted sector ($k = 1$) in the \mathbb{Z}_6 -II orbifold. Let us build two states: $\tilde{\beta}_{-1/6}^1 |\phi\rangle$ and $\tilde{\beta}_{1/6}^1 |\phi\rangle$, where $|\phi\rangle$ is the state with zero momentum and zero oscillators ("vacuum", if you like). We wish to check if these states are both eigenvalues of the number operator in the first twisted sector. Then

$$\begin{aligned} \tilde{N} \tilde{\beta}_{-1/6}^1 |\phi\rangle &= \left\{ \sum_{n-kv_a>0} \tilde{\beta}_{-(n-kv_a)}^{\bar{a}} \tilde{\beta}_{n-kv_a}^a + \sum_{n-kv_a<0} \tilde{\beta}_{n-kv_a}^a \tilde{\beta}_{-(n-kv_a)}^{\bar{a}} \right\} \tilde{\beta}_{-1/6}^1 |\phi\rangle, \\ &= \left\{ \sum_{n-1/6>0} \tilde{\beta}_{-(n-1/6)}^{\bar{1}} \tilde{\beta}_{n-1/6}^1 + \sum_{n-1/6<0} \tilde{\beta}_{n-1/6}^1 \tilde{\beta}_{-(n-1/6)}^{\bar{1}} \right\} \tilde{\beta}_{-1/6}^1 |\phi\rangle \end{aligned} \quad (\text{A.21})$$

Here, we've replaced a with 1, because of the Kronecker deltas in Equation (A.12), and kv_a with $1/6$.

Now consider the first term. We have worked out that $[\tilde{\beta}_{n-1/6}^1, \tilde{\beta}_{-1/6}^1] = 0$ above, so we are free to change the order of operation. Further, we know that $n - 1/6 > 0$ in the first term, which means that we have an annihilation operator acting on the vacuum. So we are

left only to consider the second term. Then,

$$\begin{aligned}
\tilde{N}\tilde{\beta}_{-1/6}^1 |\phi\rangle &= \sum_{n-1/6 < 0} \tilde{\beta}_{n-1/6}^1 \tilde{\beta}_{-(n-1/6)}^1 \tilde{\beta}_{-1/6}^1 |\phi\rangle, \\
&= \sum_{n-1/6 < 0} \tilde{\beta}_{n-1/6}^1 \left\{ \left[\tilde{\beta}_{-(n-1/6)}^1, \tilde{\beta}_{-1/6}^1 \right] + \tilde{\beta}_{-1/6}^1 \tilde{\beta}_{-(n-1/6)}^1 \right\} |\phi\rangle, \\
&= \sum_{n-1/6 < 0} \tilde{\beta}_{n-1/6}^1 \left\{ - \left[\tilde{\beta}_{-1/6}^1, \tilde{\beta}_{-(n-1/6)}^1 \right] + \tilde{\beta}_{-1/6}^1 \tilde{\beta}_{-(n-1/6)}^1 \right\} |\phi\rangle, \\
&= \sum_{n-1/6 < 0} \tilde{\beta}_{n-1/6}^1 \left\{ - \left[\tilde{\beta}_{-1/6}^1, \tilde{\beta}_{-n+1/6}^1 \right] + \tilde{\beta}_{-1/6}^1 \tilde{\beta}_{-(n-1/6)}^1 \right\} |\phi\rangle. \quad (\text{A.22})
\end{aligned}$$

First of all, notice that in the last line I have made a subtle (but crucial!!!) change— $(n - 1/6) \rightarrow -n + 1/6$. In order to use our commutation relations that we derived in Equation (A.12), we *must* write the ladder operator in the barred coordinate in this way. We will see shortly that this isn't always possible. Second of all, the last term here is *again* an annihilation operator acting on the vacuum, so it disappears. Inserting our definition of the commutator, we have, then

$$\begin{aligned}
\tilde{N}\tilde{\beta}_{-1/6}^1 |\phi\rangle &= \sum_{n-1/6 < 0} \tilde{\beta}_{n-1/6}^1 \left\{ - \left[\tilde{\beta}_{-1/6}^1, \tilde{\beta}_{-n+1/6}^1 \right] \right\} |\phi\rangle, \\
&= \sum_{n-1/6 < 0} \tilde{\beta}_{n-1/6}^1 \left\{ - (-1/6) \delta_{-1/6 - n + 1/6} \right\} |\phi\rangle, \\
\Rightarrow \tilde{N}\tilde{\beta}_{-1/6}^1 |\phi\rangle &= \frac{1}{6} \tilde{\beta}_{-1/6}^1 |\phi\rangle \quad (\text{A.23})
\end{aligned}$$

We can follow the same set of steps with the second state:

$$\begin{aligned}
\tilde{N}\tilde{\beta}_{-1/6}^{\bar{1}} |\phi\rangle &= \left\{ \sum_{n-kv_a > 0} \tilde{\beta}_{-(n-kv_a)}^{\bar{a}} \tilde{\beta}_{n-kv_a}^a + \sum_{n-kv_a < 0} \tilde{\beta}_{n-kv_a}^a \tilde{\beta}_{-(n-kv_a)}^{\bar{a}} \right\} \tilde{\beta}_{-1/6}^{\bar{1}} |\phi\rangle, \\
&= \left\{ \sum_{n-1/6 > 0} \tilde{\beta}_{-(n-1/6)}^{\bar{1}} \tilde{\beta}_{n-1/6}^1 + \sum_{n-1/6 < 0} \tilde{\beta}_{n-1/6}^1 \tilde{\beta}_{-(n-1/6)}^{\bar{1}} \right\} \tilde{\beta}_{-1/6}^{\bar{1}} |\phi\rangle \quad (\text{A.24})
\end{aligned}$$

This time, it is the second term which vanishes. Next,

$$\begin{aligned}
\tilde{N}\tilde{\beta}_{-1/6}^{\bar{1}} |\phi\rangle &= \left\{ \sum_{n-1/6 > 0} \tilde{\beta}_{-(n-1/6)}^{\bar{1}} \tilde{\beta}_{n-1/6}^1 \right\} \tilde{\beta}_{-1/6}^{\bar{1}} |\phi\rangle, \\
&= \sum_{n-1/6 > 0} \tilde{\beta}_{-n+1/6}^{\bar{1}} \tilde{\beta}_{n-1/6}^1 \tilde{\beta}_{-1/6}^{\bar{1}} |\phi\rangle, \\
&= \sum_{n-1/6 > 0} \tilde{\beta}_{-n+1/6}^{\bar{1}} \left\{ \left[\tilde{\beta}_{n-1/6}^1, \tilde{\beta}_{-1/6}^{\bar{1}} \right] + \tilde{\beta}_{-1/6}^{\bar{1}} \tilde{\beta}_{n-1/6}^1 \right\} |\phi\rangle. \quad (\text{A.25})
\end{aligned}$$

Notice that there is no way to put this in a form where we can use Equation (A.12)—that is, there is no solution to

$$n + \frac{1}{6} = -\frac{1}{6}, \quad (\text{A.26})$$

for $n \in \mathbb{Z}$. The conclusion that one draws is that *the state $\tilde{\beta}_{-1/6}^{\bar{1}} |\phi\rangle$ is not an eigenstate of the number operator in the first twisted sector*. Stated another way, there is no guarantee that all of the states one possible *could* make should appear in the Hilbert Space of physical states. This means that any oscillator moded states coming from the first twisted sector of $\mathbb{Z}_6\text{-II}$ cannot contain states which contain $\tilde{\beta}_{-1/6}^{\bar{1}}$.

Let's check another case, just for fun. We will work out another example. Consider the fifth twisted sector ($k = 5$) of the $\mathbb{Z}_6\text{-II}$ orbifold. After you calculate a few of these models, you quickly learn that the first and fifth twisted sectors are generally conjugate to each other. One would generally expect, then, that we find the complete opposite results in this calculation.

We will start again with the same states, $\tilde{\beta}_{-1/6}^1 |\phi\rangle$ and $\tilde{\beta}_{1/6}^{\bar{1}} |\phi\rangle$. First,

$$\begin{aligned} \tilde{N} \tilde{\beta}_{-1/6}^1 |\phi\rangle &= \left\{ \sum_{n-5/6>0} \tilde{\beta}_{-(n-5/6)}^{\bar{1}} \tilde{\beta}_{n-5/6}^1 + \sum_{n-5/6<0} \tilde{\beta}_{n-5/6}^1 \tilde{\beta}_{-(n-5/6)}^{\bar{1}} \right\} \tilde{\beta}_{-1/6}^1 |\phi\rangle, \\ &= \sum_{n-5/6<0} \tilde{\beta}_{n-5/6}^1 [\tilde{\beta}_{-(n-5/6)}^{\bar{1}}, \tilde{\beta}_{-1/6}^1] |\phi\rangle. \end{aligned} \quad (\text{A.27})$$

Notice, now, that the commutator cannot be put in the proper form, which we derived in Equation (A.12). But even if one didn't realize this (as I surely didn't the first time I derived it), this is what happens:

$$\tilde{N} \tilde{\beta}_{-1/6}^1 |\phi\rangle = \sum_{n-5/6<0} \tilde{\beta}_{n-5/6}^1 \left(\frac{1}{6} \right) \delta_{-1/6-n+5/6} |\phi\rangle. \quad (\text{A.28})$$

Again, we see that n is forced into an unphysical region ($n = 1/3$), so it *must* be that these states cannot live in our Hilbert space.

Finally we will check the other case.

$$\begin{aligned} \tilde{N} \tilde{\beta}_{-1/6}^{\bar{1}} |\phi\rangle &= \sum_{n-5/6>0} \tilde{\beta}_{-(n-5/6)}^{\bar{1}} \tilde{\beta}_{n-5/6}^1 \tilde{\beta}_{-1/6}^{\bar{1}} |\phi\rangle, \\ &= \sum_{n-5/6>0} \tilde{\beta}_{-(n-5/6)}^{\bar{1}} [\tilde{\beta}_{n-5/6}^1, \tilde{\beta}_{-1/6}^{\bar{1}}] |\phi\rangle, \\ &= \sum_{n-5/6>0} \tilde{\beta}_{-(n-5/6)}^{\bar{1}} \left(n - \frac{5}{6} \right) \delta_{n-5/6-1/6} |\phi\rangle, \\ \Rightarrow \tilde{N} \tilde{\beta}_{-1/6}^{\bar{1}} |\phi\rangle &= \frac{1}{6} \tilde{\beta}_{-1/6}^{\bar{1}} |\phi\rangle. \end{aligned} \quad (\text{A.29})$$

Appendix B

SOME RESULTS FROM 5D FIELD THEORY

This morning I visited the place where the street-cleaners dump the rubbish.
My God, it was beautiful!

Vincent Van Gogh

In this Appendix, we collect some results obtained by studying the compactification of five dimensional field theories. We adhere to the notation that $X_M = (x_\mu, x_5)$, with metric signature $(+ - - -)$. We will compactify our theory on an orbifold, which is defined by two operations: a parity $\mathcal{P} : y \rightarrow -y$ and a translation $\mathcal{T} : y \rightarrow y + 2\pi R$. From these two operations, we define $P \equiv \mathcal{P}$ and $P' \equiv \mathcal{P}\mathcal{T}$. Formally, this corresponds to $S_1/\mathbb{Z}_2 \times \mathbb{Z}'_2$. We demand that the action be invariant under P and P' .

B.1 The Kaluza-Klein Mode Expansion of a Gauge Field

Consider the five dimensional action of $U(1)$ Yang-Mills theory:

$$\mathcal{S} = \frac{-1}{4g^2} \int d^5x F_{MN} F^{MN}. \quad (\text{B.1})$$

As usual, the equations of motion can be found by integrating by parts:

$$\begin{aligned} \mathcal{S} &= \frac{-1}{4g^2} \int d^5x (\partial_M A_N - \partial_N A_M) (\partial^M A^N - \partial^N A^M), \\ \Rightarrow &= \frac{1}{4g^2} \int d^5x \{ A_N \partial_M (\partial^M A^N - \partial^N A^M) - A_M \partial_N (\partial^M A^N - \partial^N A^M) \}, \end{aligned} \quad (\text{B.2})$$

which (after varying the action) gives the familiar Yang-Mills equations of motion:

$$\partial_M F^{MN} = 0. \quad (\text{B.3})$$

This gives us a five dimensional equation of motion for the gauge field A :

$$\partial_M \partial^M A_N = 0. \quad (\text{B.4})$$

We should look at how the five dimensional action decomposes: invariance of the action under the orbifold will dictate how the different components of A_M behave under the parity and translation operations. The five dimensional action decomposes as

$$\mathcal{S} = \frac{-1}{4g^2} \int d^5x F_{MN} F^{MN} = \frac{-1}{4g^2} \int d^5x \{ F_{\mu\nu} F^{\mu\nu} + F_{\mu 5} F^{\mu 5} + F_{5\nu} F^{5\nu} + F_{55} F^{55} \}, \quad (\text{B.5})$$

where $\mu = 0, 1, 2, 3$. The second two terms are identical and the last term vanishes—both of these facts follow from the anti-symmetry of F_{MN} . We are then left with

$$\mathcal{S} = \frac{-1}{4g^2} \int d^5x \{ F_{\mu\nu} F^{\mu\nu} + 2F_{\mu 5} F^{\mu 5} \}. \quad (\text{B.6})$$

The first term says that $A_\mu(x, y)$ can have any of the four boundary conditions. While the first term gives no requirements on the transformation properties of $A_\mu(x, y)$ and $A_5(x, y)$, the second term does.

$$F_{\mu 5} F^{\mu 5} = \partial_\mu A_5 (\partial^\mu A^5 - \partial^5 A^\mu) + \partial_5 A_\mu (\partial^5 A^\mu - \partial^\mu A^5). \quad (\text{B.7})$$

Notice that under the parity transformation \mathcal{P} , $y \rightarrow -y$, $\partial_\mu \rightarrow -\partial_\mu$ and $\partial_5 \rightarrow -\partial_5$. Under the translation transformation \mathcal{T} , $y \rightarrow y + 2\pi R$, $\partial_\mu \rightarrow \partial_\mu$ and $\partial_5 \rightarrow \partial_5$. By construction, we require that our action be invariant under $P \equiv \mathcal{P}$ and $P' \equiv \mathcal{P}\mathcal{T}$, thus it must be that under P we have $A_\mu(x, -y) \rightarrow A_\mu(x, y)$ and $A_5(x, -y) \rightarrow -A_5(x, y)$. Similarly, under the translation \mathcal{T} , $A_\mu(x, y + 2\pi R) \rightarrow A_\mu(x, y)$ and $A_5(x, y + 2\pi R) \rightarrow A_5(x, y)$. Thus the $A_\mu(x, y)$ component of $A_M(x, y)$ *always has* *(++) boundary conditions* and the $A_5(x, y)$ component of $A_M(x, y)$ *always has* *(--) boundary conditions*. This means that the field $A_5(x, y)$ *does not have a zero mode*, while the field $A_\mu(x, y)$ always does.

This all suggests that we use the following Kaluza-Klein mode expansion:

$$\begin{aligned} A_\mu(x, y) &= \sum_{n=0}^{\infty} A_\mu^{(n)}(x) a_{(n)}(y), \\ A_5(x, y) &= \sum_{n=1}^{\infty} A_5^{(n)}(x) b_{(n)}(y) \end{aligned} \quad (\text{B.8})$$

Inserting the mode expansion into the equations of motion, we see

$$\begin{aligned}\partial_\mu \partial^\mu A_\nu &= \partial_\mu \partial^\mu \sum_{n=0}^{\infty} A_\nu^{(n)}(x) a_{(n)}(y) = 0, \\ \Rightarrow &= \sum_n \left\{ a_{(n)}(y) \square A_\nu^{(n)}(x) + A_\nu^{(n)}(x) \partial_5 \partial^5 a_{(n)}(y) \right\} = 0.\end{aligned}\quad (\text{B.9})$$

Also,

$$\begin{aligned}\partial_\mu \partial^\mu A_5 &= \partial_\mu \partial^\mu \sum_{n=0}^{\infty} A_5^{(n)}(x) b_{(n)}(y) = 0, \\ \Rightarrow &= \sum_n \left\{ b_{(n)}(y) \square A_5^{(n)}(x) + A_5^{(n)}(x) \partial_5 \partial^5 b_{(n)}(y) \right\} = 0.\end{aligned}\quad (\text{B.10})$$

This gives us the familiar solutions for $a_{(n)}(y)$ and $b_{(n)}(y)$ as before:

$$\begin{aligned}a_{(n)}(y) &= \cos\left(\frac{ny}{R}\right), \\ b_{(n+1)}(y) &= \sin\left(\frac{(n+1)y}{R}\right).\end{aligned}\quad (\text{B.11})$$

Note that we can *break* the gauge symmetry by introducing a parity operator. In this case, we are explicitly breaking the gauge symmetry in the action by endowing the field $A_\mu(x, y)$ with specific transformation properties. This can be done by writing down an operator which gives $A_\mu(x, y)$ boundary conditions *other than* $(++)$. If this is the case, then we will clearly need a new mode expansion, and one can repeat the calculation in a similar manner and find that

$$a_{(n)}(y) = \begin{cases} \cos\left(\frac{ny}{R}\right) & (++) \\ \cos\left(\frac{(n+\frac{1}{2})y}{R}\right) & (+-) \\ \sin\left(\frac{(n+\frac{1}{2})y}{R}\right) & (-+) \\ \sin\left(\frac{(n+1)y}{R}\right) & (--) \end{cases}.\quad (\text{B.12})$$

B.2 Something Like the Higgs Mechanism

We now examine Equation (B.6) term by term. First, in terms of the five dimensional fields...

$$\begin{aligned}F_{\mu\nu} F^{\mu\nu} &= (\partial_\mu A_\nu - \partial_\nu A_\mu)(\partial^\mu A^\nu - \partial^\nu A^\mu), \\ &= 2(\partial_\mu A_\nu \partial^\mu A^\nu - \partial_\nu A_\mu \partial^\mu A^\nu).\end{aligned}\quad (\text{B.13})$$

Substituting into the first term,

$$\partial_\mu A_\nu(x, y) \partial^\mu A^\nu(x, y) = \sum_{n,m} \cos\left(\frac{ny}{R}\right) \cos\left(\frac{my}{R}\right) \partial_\mu A_\nu^{(n)}(x) \partial^\mu A^\nu{}^{(m)}(x). \quad (\text{B.14})$$

Now we can integrate over the fifth dimension, and see

$$\int_0^{2\pi R} dy \partial_\mu A_\nu(x, y) \partial^\mu A^\nu(x, y) = \sum_{n=0} \left(2^{\delta_{n,0}} \pi R \right) \partial_\mu A_\nu^{(n)}(x) \partial^\mu A^\nu{}^{(n)}(x). \quad (\text{B.15})$$

Renaming the indices gives us the other term in Equation (B.13). Finally, we find

$$\int_0^{2\pi R} dy F_{\mu\nu} F^{\mu\nu} = 2\pi R \left\{ F_{\mu\nu}^{(0)} F^{\mu\nu(0)} + \frac{1}{2} \sum_{n=1} F_{\mu\nu}^{(n)} F^{\mu\nu(n)} \right\}. \quad (\text{B.16})$$

Next, we can look at the $F_{\mu 5} F^{\mu 5}$ term. One must be careful in computing the terms here and take care that the metric is inserted properly. For instance

$$\partial_5 = -\partial^5 \equiv \frac{\partial}{\partial y}, \quad (\text{B.17})$$

$$A_5 = -A^5. \quad (\text{B.18})$$

To make the transformation properties explicit, we write things in terms of A_5 :

$$\begin{aligned} F_{\mu 5} F^{\mu 5} &= \partial_\mu A_5 \partial^\mu A^5 - \partial_\mu A_5 \partial^5 A^\mu - \partial_5 A_\mu \partial^\mu A^5 + \partial_5 A_\mu \partial^5 A^\mu, \\ \Rightarrow F_{\mu 5} F^{\mu 5} &= -\partial_\mu A_5 \partial^\mu A_5 + \partial_\mu A_5 \partial_5 A^\mu + \partial_5 A_\mu \partial^\mu A_5 - \partial_5 A_\mu \partial_5 A^\mu. \end{aligned} \quad (\text{B.19})$$

Substituting in the Kaluza-Klein mode expansion, we find

$$\begin{aligned} F_{\mu 5} F^{\mu 5} &= - \sum_{n,m=1} \sin\left(\frac{ny}{R}\right) \sin\left(\frac{my}{R}\right) \partial_\mu A_5^{(n)}(x) \partial^\mu A_5^{(m)}(x) \\ &\quad - \sum_{n,m=1} \frac{m}{R} \sin\left(\frac{ny}{R}\right) \sin\left(\frac{my}{R}\right) \partial_\mu A_5^{(n)}(x) A^{\mu(m)}(x) \\ &\quad - \sum_{n,m=1} \frac{n}{R} \sin\left(\frac{ny}{R}\right) \sin\left(\frac{my}{R}\right) A_\mu^{(n)}(x) \partial^\mu A_5^{(m)}(x) \\ &\quad - \sum_{n,m=1} \frac{nm}{R^2} \sin\left(\frac{ny}{R}\right) \sin\left(\frac{my}{R}\right) A_\mu^{(n)}(x) A_{(m)}^\mu(x) \end{aligned} \quad (\text{B.20})$$

As before, we integrate out the fifth dimension:

$$\begin{aligned} \int_0^{2\pi R} dy F_{\mu 5} F^{\mu 5} &= - \sum_{n=1} \pi R \left\{ \partial_\mu A_5^{(n)}(x) \partial^\mu A_5^{(n)}(x) + \frac{n^2}{R^2} A_\mu^{(n)}(x) A^{\mu(n)}(x) \right. \\ &\quad \left. + \frac{n}{R} \left(A_\mu^{(n)}(x) \partial^\mu A_5^{(n)}(x) + \partial_\mu A_5^{(n)}(x) A^{\mu(n)}(x) \right) \right\}. \end{aligned} \quad (\text{B.21})$$

Putting everything together, we see that

$$\begin{aligned} \mathcal{S}_{eff} = & \frac{-2\pi R}{4g^2} \int d^4x \left\{ F_{\mu\nu}^{(0)}(x) F^{\mu\nu(0)}(x) + \frac{1}{2} \sum_{n=1} F_{\mu\nu}^{(n)}(x) F^{\mu\nu(n)}(x) \right. \\ & - \sum_{n=1} \left[\partial_\mu A_5^{(n)}(x) \partial^\mu A_5^{(n)}(x) + \frac{n^2}{R^2} A_\mu^{(n)}(x) A^{\mu(n)}(x) \right. \\ & \left. \left. + \frac{n}{R} \left(A_\mu^{(n)}(x) \partial^\mu A_5^{(n)}(x) + \partial_\mu A_5^{(n)}(x) A^{\mu(n)}(x) \right) \right] \right\}. \end{aligned} \quad (B.22)$$

where the effective four dimensional coupling constant is identified:

$$g_{eff}^2 \equiv \frac{g^2}{2\pi R}. \quad (B.23)$$

An interesting point is that the effective coupling constant for the Kaluza-Klein modes is now *larger* by a factor of $\sqrt{2}$. This means that the KK modes couple *more strongly* to the other states in the theory. Other than that, however, Equation (B.22) is *exactly* what we hoped to get—the action of a tower four dimensional vector fields with mass $m_n^2 = \frac{n^2}{R^2}$:

$$\mathcal{S}_{KK} = \frac{-1}{4g_{eff}^2} \int d^4x \frac{1}{2} \sum_{n=1} \left\{ F_{\mu\nu}^{(n)} F^{\mu\nu(n)} - \frac{2n^2}{R^2} A_\mu^{(n)} A^{\mu(n)} \right\}, \quad (B.24)$$

where we have taken a factor of two from the last term. Redefining the fields, we see that

$$\mathcal{S}_{KK} = \sum_{n=1} \int d^4x \left\{ \frac{-1}{4} F_{\mu\nu}^{(n)} F^{\mu\nu(n)} + \frac{1}{2} \frac{n^2}{R^2} A_\mu^{(n)} A^{\mu(n)} \right\}, \quad (B.25)$$

which is indeed the action for a massive gauge boson.

Finally, note that the third polarization of the massive gauge boson is exactly the component along the fifth direction, A_5 —the higgs mechanism happens for each Kaluza-Klein mode. This can be made more explicit by showing that the scalar field A_5 is a gauge artifact, and that it does not appear in the (gauge fixed) theory. First, we will choose to add a gauge-fixing term (for each KK mode) to the lagrangian in Equation (B.22)

$$\mathcal{S}_{g.f.} = -\frac{1}{2} \int d^4x \xi^{-1} \left[\partial_\mu A^\mu + 2\xi \frac{2\pi R}{4g^2} \frac{n}{R} A_5 \right]^2. \quad (B.26)$$

Note that if we take $n = 0$, note that we are left with the typical R_ξ gauge. Multiplying the terms in Equation (B.26), we find

$$\mathcal{S}_{g.f.} = -\frac{1}{2} \int d^4x \xi^{-1} \left[\partial_\mu A^\mu \partial_\nu A^\nu + 4\xi^2 \frac{(2\pi R)^2}{16g^4} \frac{n^2}{R^2} (A_5)^2 + 4\xi \frac{n}{R} \frac{2\pi R}{4g^2} \partial_\mu A^\mu A_5 \right]. \quad (B.27)$$

The last term can be integrated by parts to give

$$\mathcal{S}_{g.f.} = -\frac{1}{2} \int d^4x \left[\xi^{-1} \partial_\mu A^\mu \partial_\nu A^\nu + \xi \frac{(2\pi R)^2}{16g^4} \frac{n^2}{R^2} (A_5)^2 - 4 \frac{n}{R} \frac{2\pi R}{4g^2} A^\mu \partial_\mu A_5 \right]. \quad (\text{B.28})$$

If we add this gauge fixing action to Equation (B.22), we see that the cross term relating the derivative of $A_\mu^{(n)}$ and A_5 cancels. Furthermore, one can choose $\xi \rightarrow \infty$, the so-called “unitary gauge”, and decouple the scalar degree of freedom from the theory—the second term in Equation (B.28) tells us that the scalar degree of freedom gets a mass term proportional to $\sqrt{\xi}$. The analogy with the higgs mechanism is now complete.

B.3 A New Contribution to the Beta Functions

We have shown, in Equation (B.22), that the pure gauge theory in 5 dimensions becomes something much more interesting in four dimensions: a four dimensional (pure gauge) theory coupled to a tower of massive bosons, each of which undergo the higgs mechanism. If we add matter to the theory, a similar story unfolds: the quantization of the fermion field gives a tower of (massive) KK fermions. We know consider corrections to the vacuum polarization of the photon due to this infinite tower of KK fermions. In a straightforward generalization, we may write

$$\Pi_{\mu\nu}(p^2) = \sum_n -e^2 \int \frac{d^4k}{(2\pi)^4} \text{TR} \left\{ \frac{\gamma_\mu (k \cdot \gamma + m_n) \gamma_\nu ((k+p) \cdot \gamma + m_n)}{(k^2 - m_n^2) ((k+p)^2 - m_n^2)} \right\}. \quad (\text{B.29})$$

One then expects, by the Ward Identities, to write

$$\Pi_{\mu\nu}(p^2) = \Pi(p^2) (p^2 g_{\mu\nu} - p_\mu p_\nu) \Rightarrow \Pi(p^2) = \frac{1}{3p^2} g^{\mu\nu} \Pi_{\mu\nu}(p^2). \quad (\text{B.30})$$

In the normal manner (by introducing a Feynman x and changing the integration variables, one finds

$$\Pi(p^2) = \frac{-8e^2}{3p^2} \sum_n \int_0^1 dx \int \frac{d^4\ell}{(2\pi)^4} \frac{-\ell^2 + x(1-x)p^2 + 2m_n^2}{[\ell^2 + p^2x(1-x) - m_n^2]^2}. \quad (\text{B.31})$$

Working with Euclidean momenta, this becomes

$$\Pi(p^2) = \frac{-8e^2}{3p^2} \sum_n \int_0^1 dx \int \frac{d^4\ell}{(2\pi)^4} \frac{\ell^2 - x(1-x)p^2 + 2m_n^2}{[\ell^2 + p^2x(1-x) + m_n^2]^2}. \quad (\text{B.32})$$

If we were working with QED (or, only the zero mode fermion running around the loop), one would now proceed with dimensional regularization as usual. One could proceed in the same manner here, by shifting to $4 - \epsilon$ dimensions and evaluating the Euclidean integral. If one does that, then we end up with a nasty expression, involving an infinite

series of logs. Instead, we can introduce a Schwinger parameter t :

$$\frac{1}{x^2} = \int_0^\infty dt te^{-xt}. \quad (\text{B.33})$$

Then Equation (B.32) can be written as

$$\begin{aligned} \Pi(p^2) &= \frac{-8e^2}{3p^2} \sum_n \int_0^1 dx \int_0^\infty dt te^{-t\{p^2x(1-x)+m_n^2\}} \\ &\quad \times \int \frac{d^4\ell}{(2\pi)^4} e^{-t\ell^2} \{ \ell^2 - x(1-x)p^2 + 2m_n^2 \}, \end{aligned} \quad (\text{B.34})$$

The momentum integrals are now straightforward to evaluate, for example:

$$\int \frac{d^4\ell}{(2\pi)^4} e^{-t\ell^2} = \frac{1}{(2\pi)^4} \int_0^\infty d\ell \ell^3 e^{-t\ell^2} \int d\Omega_4 = \frac{2\pi^2}{(2\pi)^4} \frac{\Gamma(2)}{2t^2} = \frac{1}{16\pi^2 t^2}, \quad (\text{B.35})$$

and one finds

$$\Pi(p^2) = \frac{-e^2}{6\pi^2 p^2} \sum_n \int_0^1 dx \int_0^\infty \frac{dt}{t} e^{-t\{p^2x(1-x)+m_n^2\}} \left\{ \frac{2}{t} + 2m_n^2 - x(1-x)p^2 \right\}. \quad (\text{B.36})$$

The first term can be integrated to give

$$\int_0^\infty \frac{dt}{t^2} e^{-t\{p^2x(1-x)+m_n^2\}} = (-1)^3 \int_0^\infty \frac{dt}{t} \{p^2x(1-x) + m_n^2\} e^{-t\{p^2x(1-x)+m_n^2\}}. \quad (\text{B.37})$$

This gives

$$\begin{aligned} \Pi(p^2) &= \frac{e^2}{2\pi^2} \sum_n \int_0^1 dx x(1-x) \int_0^\infty \frac{dt}{t} e^{-t\{p^2x(1-x)+m_n^2\}}, \\ \Rightarrow \Pi(0) &= \frac{e^2}{12\pi^2} \sum_n \int_0^\infty \frac{dt}{t} e^{-tm_n^2} \end{aligned} \quad (\text{B.38})$$

Luckily for us, we can go a bit further. The Jacobi θ function is defined as

$$\theta_3(t) \equiv \sum_n e^{i\pi n^2 t}. \quad (\text{B.39})$$

Equation (B.38) can be written in terms of the Jacobi θ functions:

$$\Pi(0) = \frac{e^2}{12\pi^2} \int_0^\infty \frac{dt}{t} \theta_3 \left(\frac{it}{\pi R^2} \right) \quad (\text{B.40})$$

In general, this integral gives both UV and IR divergences. In practice, however, this expression is only applicable between the compactification scale, M_C , and the cutoff, M_S —motivated by this, then, we introduce hard UV and IR cutoffs of t , which has units of

energy squared:

$$\Pi(0) = \frac{e^2}{12\pi^2} \int_{M_s^{-2}}^{M_c^{-2}} \frac{dt}{t} \theta_3 \left(\frac{it}{\pi R^2} \right). \quad (\text{B.41})$$

Notice that this expression reduces to the familiar result from QED (coupling renormalization) when we set $n = 0$ in Equation (B.38). This makes the θ_3 function equal to unity, and the integral in Equation (B.41) evaluates to a logarithm of the ratio of UV to IR scales.

Using the approximation

$$\theta_3 \left(\frac{it}{\pi R^2} \right) \cong \sqrt{\frac{\pi}{t}} R, \quad (\text{B.42})$$

we find after integrating

$$\Pi(0) \sim R t^{-1/2} \Big|_{M_s^{-2}}^{M_c^{-2}}, \quad (\text{B.43})$$

where we identify $R = M_c^{-1}$. Finally,

$$\Rightarrow \Pi(0) \sim \left(\frac{M_s}{M_c} - 1 \right). \quad (\text{B.44})$$

This implies that the KK tower gives a new contribution to the running of the coupling constant, for $\mu < M_c$:

$$\alpha^{-1}(\mu) \sim \left(\frac{M_s}{M_c} - 1 \right) + \log \frac{M_s}{\mu}, \quad (\text{B.45})$$

where the log term is due to the states that contribute to the gauge coupling evolution below the compactification scale. Thus, the prediction is that the gauge couplings receive power law corrections between the compactification scale and the cutoff due to the presence of virtual Kaluza-Klein fermions.

Thusfar, this treatment has been similar to that of [43], with Kaluza-Klein states there were taken to have mass $m_n = n/R$ as is the case when the fifth dimension is compactified on a circle. In our orbifold case, we found four sets of Kaluza-Klein modes in Equation (B.12): $(\pm\pm)$ and $(\pm\mp)$. The masses of these modes are given by

$$\begin{aligned} (++) \quad m_n^2 &= \frac{n^2}{R^2} \\ (\pm\mp) \quad m_n^2 &= \frac{(n+1/2)^2}{R^2} \\ (--) \quad m_n^2 &= \frac{(n+1)^2}{R^2}. \end{aligned} \quad (\text{B.46})$$

We must now modify the above expressions to take into account the new spectrum of Kaluza-Klein modes. To do this, we start with Equation (B.38), except substitute our new

Kaluza-Klein masses:

$$\begin{aligned}
\Pi(0) &= \frac{e^2}{12\pi^2} \sum_n \int_0^\infty \frac{dt}{t} e^{-tm_n^2}, \\
\Rightarrow \Pi(0) &= \frac{\alpha}{4\pi} \sum_{n=1} \left\{ (b_{++} + b_{--}) \int \frac{dt}{t} e^{-t\frac{n^2}{R^2}} + (b_{+-} + b_{-+}) \int \frac{dt}{t} e^{-t\frac{(n+1/2)^2}{R^2}} \right\} \\
&\quad + \frac{\alpha}{4\pi} b_{++} \int \frac{dt}{t},
\end{aligned} \tag{B.47}$$

where the last line is the zero mode contribution. We can define another theta function as

$$\theta_2(t) \equiv \sum_{n=-\infty}^{\infty} e^{i\pi t(n+1/2)^2}. \tag{B.48}$$

Substituting this definition, along with the definition (B.39) into Equation (B.47), we find

$$\begin{aligned}
\Pi(0) &= \frac{\alpha}{4\pi} \left\{ (b_{++} + b_{--}) \int_{rM_s^{-2}}^{rM_c^{-2}} \frac{dt}{t} \frac{1}{2} \left[\theta_3 \left(\frac{it}{\pi R^2} \right) - 1 \right] \right. \\
&\quad \left. + (b_{+-} + b_{-+}) \int_{rM_s^{-2}}^{rM_c^{-2}} \frac{dt}{t} \frac{1}{2} \theta_2 \left(\frac{it}{\pi R^2} \right) \right\} + \frac{\alpha}{4\pi} b_{++} \int_{rM_s^{-2}}^{rM_c^{-2}} \frac{dt}{t}.
\end{aligned} \tag{B.49}$$

This result is exact, however, we can make an approximation to the theta functions in the limit where $t/R^2 \ll 1$:

$$\theta_3 \left(\frac{it}{\pi R^2} \right) \simeq \theta_2 \left(\frac{it}{\pi R^2} \right) \simeq \sqrt{\frac{\pi}{t}} R. \tag{B.50}$$

This gives us, finally,

$$\begin{aligned}
\Pi(0) &= \frac{\alpha}{4\pi} \left\{ b^G \int_{rM_s^{-2}}^{rM_c^{-2}} \frac{dt}{t} \sqrt{\frac{\pi}{t}} R - \frac{1}{2} (b_{++} + b_{--}) \int_{rM_s^{-2}}^{rM_c^{-2}} \frac{dt}{t} \right. \\
&\quad \left. + b_{++} \int_{rM_s^{-2}}^{rM_c^{-2}} \frac{dt}{t} \right\},
\end{aligned} \tag{B.51}$$

where $b^G \equiv b_{++} + b_{+-} + b_{-+} + b_{--}$. We can perform the integrals and find

$$\Pi(0) = \frac{\alpha}{4\pi} \left\{ b^G \left(\frac{M_s}{M_c} - 1 \right) - \frac{1}{2} (b_{++} + b_{--}) \log \frac{M_s}{M_c} + b_{++} \log \frac{M_s}{M_c} \right\}. \tag{B.52}$$

As before, the zero modes (given only by states with $++$ boundary conditions) contribute logarithmically between the compactification scale and the cutoff, and the full set of Kaluza-Klein fermions furnish a power law correction. What was lacking before is the contributions of the $++$ and $--$ modes to an *additional* logarithmic correction.

One may argue that the approximation we have used is not valid. This is a legitimate concern, but it was shown in [42, 43] that the approximation is reasonably good even for moderate t/R^2 . Further, as $M_C \rightarrow M_S$, we recover a pure logarithmic running, as we would expect from no large extra dimensions. So, if the ratio between the compactification scale and string scale is nearly one, then the effect due to extra dimensions is small. As the ratio between the two scales increases, the approximation becomes better and better.

Appendix C

COMPARING TWO $SU(6)$ ORBIFOLD GUTS

The $SU(6)$ orbifold GUTs considered in this paper satisfy the special property of gauge-Higgs unification. This is also a property of the 5D $SU(6)$ orbifold GUT discussed in Reference [93]. It is instructive to compare this $SU(6)$ model to one without gauge-Higgs unification, in particular the 5D $SU(5)$ orbifold GUT discussed in Reference [85].

In the models with gauge-Higgs unification, the Higgs multiplets come from the 5D *vector* multiplet (V, Φ), both in the adjoint representation of $SU(6)$. V is the 4D gauge multiplet and the 4D chiral multiplet Φ contains the Higgs doublets. These states transform as follows under the orbifold parities ($P P'$):

$$V : \left(\begin{array}{ccc|cc|c} (++) & (++) & (++) & (+-) & (+-) & (-+) \\ (++) & (++) & (++) & (+-) & (+-) & (-+) \\ (++) & (++) & (++) & (+-) & (+-) & (-+) \\ \hline (+-) & (+-) & (+-) & (++) & (++) & (--) \\ (+-) & (+-) & (+-) & (++) & (++) & (--) \\ \hline (-+) & (-+) & (-+) & (--) & (--) & (++) \end{array} \right) \quad (C.1)$$

$$\Phi : \left(\begin{array}{ccc|cc|c} (--) & (--) & (--) & (-+) & (-+) & (+-) \\ (--) & (--) & (--) & (-+) & (-+) & (+-) \\ (--) & (--) & (--) & (-+) & (-+) & (+-) \\ \hline (-+) & (-+) & (-+) & (--) & (--) & (++) \\ (-+) & (-+) & (-+) & (--) & (--) & (++) \\ \hline (+-) & (+-) & (+-) & (++) & (++) & (--) \end{array} \right) . \quad (C.2)$$

Note the appearance of the MSSM Higgs multiplets in Φ with $(++)$ boundary conditions, and its partner in V with $(--)$ boundary conditions. These massive KK states contribute

to a logarithmic running of the gauge couplings with a term of the form

$$\alpha_i^{-1} \supset -\frac{1}{4\pi} (b_i^{++} + b_i^{--}) \log \frac{M_S}{M_C}. \quad (\text{C.3})$$

We find for the model of Reference [93] (including just V, Φ above)

$$\vec{b}^{++} = (-9, -5, 3/5), \quad \vec{b}^{--} = (3, -1, -9/5), \quad \vec{b}^{++} + \vec{b}^{--} = (-6, -6, -6/5). \quad (\text{C.4})$$

(These numbers can be calculated using the values in Table H.) Again we stress that the only difference between the models presented in this paper and that of Reference [93] is that the third family lives in the bulk in our constructions, which will only change these numbers by a universal contribution. Indeed, one can check by comparing Equation (C.4) with (3.9) that the only difference is a family universal contribution.

This can then be compared to an SU(5) model without gauge-Higgs unification [85]. In this case the 5D gauge multiplet includes the states, with their transformation under the orbifold parities ($P P'$):

$$V : \left(\begin{array}{ccc|cc} (++) & (++) & (++) & (+-) & (+-) \\ (++) & (++) & (++) & (+-) & (+-) \\ (++) & (++) & (++) & (+-) & (+-) \\ \hline (+-) & (+-) & (+-) & (++) & (++) \\ (+-) & (+-) & (+-) & (++) & (++) \end{array} \right) \quad (\text{C.5})$$

$$\Phi : \left(\begin{array}{ccc|cc} (--) & (--) & (--) & (-+) & (-+) \\ (--) & (--) & (--) & (-+) & (-+) \\ (--) & (--) & (--) & (-+) & (-+) \\ \hline (-+) & (-+) & (-+) & (--) & (--) \\ (-+) & (-+) & (-+) & (--) & (--) \end{array} \right). \quad (\text{C.6})$$

The Higgs multiplets are contained in the chiral multiplets, $H_5 + H_5^c$ and $H_{\bar{5}} + H_{\bar{5}}^c$, with parities

$$H_5, H_{\bar{5}} : \left(\begin{array}{c} (+-) \\ (+-) \\ \hline (+-) \\ (++) \\ (++) \end{array} \right). \quad (\text{C.7})$$

$$H_5^c, H_{\bar{5}}^c : \begin{pmatrix} (+-) \\ (-+) \\ (-+) \\ \hline (- -) \\ (- -) \end{pmatrix}. \quad (C.8)$$

In this case, the $(--)$ partners of the Higgs doublets appear in chiral multiplets *not the gauge multiplet* as before. Thus we now find the beta function coefficients given by

$$\vec{b}^{++} = (-9, -5, 3/5), \quad \vec{b}^{--} = (3, 3, 3/5), \quad \vec{b}^{++} + \vec{b}^{--} = (-6, -2, 6/5). \quad (C.9)$$

To get relationships between the cutoff (M_s) and the compactification scale (M_c), we can compare $5\alpha_1^{-1}(M_c) - 3\alpha_2^{-1}(M_c) - 2\alpha_3^{-1}(M_c)$ and $\alpha_3^{-1}(M_c) - \alpha_2^{-1}(M_c)$ in the orbifold GUT and in the MSSM. Including the threshold correction in Equation (3.3) we find (for gauge-Higgs unification)

$$\begin{aligned} \log \frac{M_{\text{GUT}}}{M_c} &= \frac{2}{3} \log \frac{M_s}{M_c} + \frac{1}{3}, \\ \log \frac{M_s}{M_{\text{GUT}}} &= -\frac{3}{2} \end{aligned} \quad (C.10)$$

The factors of $\frac{1}{3}$ and $-\frac{3}{2}$ come from the threshold correction applied at M_{GUT} . These equations implicitly assume the relation $M_c \leq M_{\text{GUT}}, M_s$, however, the solution to the equation gives the unphysical relation $M_c > M_{\text{GUT}} > M_s$. This is the main reason we need to rely on “light” exotics. On the other hand, for the SU(5) orbifold GUT we find

$$\begin{aligned} \log \frac{M_{\text{GUT}}}{M_c} &= \frac{2}{3} \log \frac{M_s}{M_c} + \frac{1}{3}, \\ \log \frac{M_{\text{GUT}}}{M_c} &= \frac{1}{2} \log \frac{M_s}{M_c} + \frac{3}{2} \end{aligned} \quad (C.11)$$

which gives the physically acceptable solution $\log \frac{M_s}{M_{\text{GUT}}} = 2$ and $\log \frac{M_{\text{GUT}}}{M_c} = 5$. We thus conclude that simple gauge-Higgs unification in 5D SU(6) is not viable.

In Reference [93] an $N = 2$ model with gauge-Higgs unification in 6D (or $N = 4$ in 4D) was also considered. In this case the Higgs multiplet and its $(--)$ partners are contained in chiral adjoints. Gauge coupling unification works in this model. Unfortunately, we do not know how to obtain such a model from the heterotic string.

Of course, the additional problem concerning gauge coupling unification in the context of the heterotic string is the need to match the low energy values of the coupling constants given values of M_c and M_s . In particular, we must satisfy the relation

$$\alpha_{\text{STRING}}^{-1} = \frac{1}{8} \left(\frac{M_{\text{PL}}}{M_s} \right)^2. \quad (C.12)$$

In most cases, with $M_C \leq M_{\text{GUT}} < M_S$, the power law running due to the KK modes is required, i.e.

$$\alpha_i^{-1}(M_C) \supset \alpha_{\text{STRING}}^{-1} + \frac{b^G}{2\pi} \left(\frac{M_S}{M_C} - 1 \right) + \text{Log terms} \sim \mathcal{O}(10). \quad (\text{C.13})$$

Appendix D

SOME (UPDATED) CONSTRAINTS ON PROTON DECAY IN ORBIFOLD GUTS

D.1 Dimension 6 Operators

The gauge bosons in GUTs can mediate proton decay via effective dimension 6 operators. The best bounds on proton decay come from the channel $p \rightarrow e^+ + \pi^0$, and current (published) experimental limits are[29]

$$\tau(p \rightarrow e^+ + \pi^0) > 8.2 \times 10^{33} \text{ yr.} \quad (\text{D.1})$$

In this paper, we are looking at an $SU(6)$ GUT in five dimensions, which is broken to either $SU(5)$ or $SU(4) \times SU(2)$ on the branes. The dangerous operators come from $SU(5)$ gauge boson (\mathbf{X}) exchange and have been calculated in Reference [200]. In a 4-d $SU(5)$ GUT, the effective lagrangian leading to proton decay from \mathbf{X} boson exchange is given by

$$\mathcal{L}_{\text{eff}} = \frac{g_{\text{GUT}}^2}{2M_{\mathbf{X}}^2} J^\mu J_\mu^*, \quad (\text{D.2})$$

where

$$J^\mu = -(l)^* \bar{\sigma}^\mu d^c + (u^c)^* \bar{\sigma}^\mu q + (q)^* \bar{\sigma}^\mu e^c + \text{h.c.} \quad (\text{D.3})$$

The operators which lead to proton decay are given by

$$\mathcal{L}_{\text{eff}} = -\frac{g_{\text{GUT}}^2}{2M_{\mathbf{X}}^2} \sum_{i,j} [(q_i^* \bar{\sigma}^\mu u_i^c)(\ell^* \bar{\sigma}_\mu d_j^c) + (q_i^* \bar{\sigma}^\mu e_i^c)(q_j^* \bar{\sigma}_\mu u_j^c)]. \quad (\text{D.4})$$

The decay rate of $p \rightarrow \pi^0 e^+$ in the 4-d theory is given by

$$\Gamma(p \rightarrow \pi^0 e^+) = \frac{(m_p^2 - m_\pi^2)^2}{64\pi m_p^3 f_\pi^2} \beta_{\text{LAT}}^2 A^2 \frac{g_{\text{GUT}}^4}{M_{\mathbf{X}}^4} (1 + D + F)^2 \left[(1 + |V_{ud}|^2)^2 + 1 \right]. \quad (\text{D.5})$$

These formulae will receive modifications in our model, based on the fact that there is a relationship between the string scale, the Planck scale and the coupling constant (see Equation (3.2)), and that the whole tower of KK modes associated with the SU(5) gauge bosons will contribute to the decay rate.

Explicitly, the decay rate goes like g_{GUT}^4 . We replace this by

$$g_{\text{GUT}}^4 \rightarrow (4\pi)^2 \alpha_{\text{STRING}}^2 = 64 \times (4\pi)^2 \times \left(\frac{M_s}{M_{\text{PL}}}\right)^4. \quad (\text{D.6})$$

Next, we should consider the relationship between the compactification scale and the \mathbf{X} boson mass. The SU(5) gauge bosons have $(+-)$ boundary conditions, and masses of $m_n = (n + \frac{1}{2}) M_c$. Proton decay can proceed by exchange of any of the tower of KK modes, which suggests we take

$$\frac{1}{M_{\mathbf{X}}^2} \rightarrow 2 \times \frac{1}{M_c^2} \sum_{n=0}^{\infty} \frac{1}{(n + \frac{1}{2})^2} = \frac{\pi^2}{M_c^2}. \quad (\text{D.7})$$

The factor of two comes from the fact that the KK modes of the gauge bosons are normalized differently than the zero modes [85].⁵⁷ Including all corrections, we make the replacement

$$\frac{g_{\text{GUT}}^4}{M_{\mathbf{X}}^4} \rightarrow 64 \times (4\pi)^2 \times \left(\frac{M_s}{M_{\text{PL}}}\right)^4 \times \frac{\pi^4}{M_c^4} \quad (\text{D.8})$$

In our 5-d orbifold GUT, we find

$$\Gamma(p \rightarrow \pi^0 e^+) \cong 4.00 \times 10^{-73} \left(\frac{M_s}{M_c}\right)^4 \text{ GeV}. \quad (\text{D.9})$$

where we have used $A = 3.4$, $D = 0.80$ and $F = 0.44$, and $\beta_{\text{LAT}} \simeq 0.011 \text{ GeV}^3$ [201]. For the proton lifetime, we find

$$\tau(p \rightarrow \pi^0 e^+) \cong 5.21 \times 10^{40} \left(\frac{M_c}{M_s}\right)^4 \text{ yr}. \quad (\text{D.10})$$

This corresponds to an upper limit on the ratio between the string scale and the compactification scale of

$$\frac{M_s}{M_c} \lesssim 64. \quad (\text{D.11})$$

Alternatively, given a (typical) string scale of about $5 \times 10^{17} \text{ GeV}$, this corresponds to

$$M_c \gtrsim 7.8 \times 10^{15} \text{ GeV}. \quad (\text{D.12})$$

⁵⁷Equivalently, one can understand this factor as the Kaluza-Klein tower of gauge bosons coupling *more strongly* to the fermions by a factor of $\sqrt{2}$, which corresponds to rescaling $g_{\text{GUT}} \rightarrow \sqrt{2}g_{\text{GUT}}$.

An interesting difference between this result and the result one typically finds in an orbifold GUT (see for example Reference [202]) is that the proton lifetime no longer scales like the compactification scale directly, but as a ratio of scales. This means that the compactification scale can be smaller than $M_C \sim 7.8 \times 10^{15}$ GeV if the string scale is sufficiently small, which means that the underlying GUT is very weakly coupled ($\alpha_{\text{GUT}} \ll 1$).⁵⁸ We note that this is an additional constraint that has no analogy in typical orbifold GUT model building, imposed by the relationship between the coupling constant, Newton's constant, and α' . Finally, in the interesting limit that $M_C \rightarrow M_S$, we find the upper bound on proton lifetime in this class of models: $\tau(p \rightarrow \pi^0 e^+) \lesssim 5.21 \times 10^{40}$ yr.

D.2 Dimension 5 Operators

In supersymmetric theories, the proton may decay via dimension five operators as well. In the mini-landscape models [38], the $(\mathbf{3}, 1)_{-2/3, -2/3} + (\bar{\mathbf{3}}, 1)_{2/3, 2/3}$ states, called δ and $\bar{\delta}$, can mediate proton decay via dimension five operators—they have the same gauge quantum numbers as color triplet Higgses. It was shown in Reference [72] that the effective mass of the color triplet Higgsino $M_{\tilde{H}} \sim 10^{18} - 10^{21}$ GeV has to be much larger than the (four dimensional) GUT scale in order to evade bounds on $p \rightarrow K^+ \bar{\nu}$, depending on the soft SUSY breaking parameters.

The δ particles have the same quantum numbers as color triplet Higgses, thus we expect similar bounds for them (assuming they couple to quarks and leptons with small effective Yukawa couplings). Unfortunately, to make matters worse, it was found in Reference [38] that the δ states have tree level coupling to the quarks in the superpotential, and so the coupling is naturally of order one, i.e. *not* suppressed by Yukawa factors as they are in the typical dimension five proton decay operator. However, by carefully adjusting the singlet VEVs that describe the $\delta, \bar{\delta}$, interactions, this problem can be avoided, but currently, we are lacking a mechanism that would naturally suppress this decay channel for the proton.

⁵⁸This may correspond to a region where the string coupling constant $g_{\text{STRING}} \sim e^\phi$ (where ϕ is the dilaton field) is no longer small. This is undesirable, as we wish to embed these models in the weakly coupled heterotic string.

Appendix E

THE ROLE OF HOLOMORPHIC GAUGE INVARIANT MONOMIALS

In Chapter 3, we showed, by working in the orbifold GUT limit of the Heterotic string, how one could accommodate gauge coupling unification in the “mini-landscape” models of References [34–38]. Furthermore, we showed how one of the solutions we found was consistent with the decoupling of other exotics and $F = 0$. In this appendix, we will show that this solution is also consistent with $D = 0$.

For simplicity, and without loss of generality, we will consider a $U(1)_A \times U(1)_B$ gauge theory. We will further consider N fields Φ_i charged under both $U(1)$ s, where each Φ_i has charge q_i^A under the first $U(1)$, and charge q_i^B under the second $U(1)$. If we turn the superpotential off, unbroken supersymmetry (SUSY) requires

$$D_A \equiv \sum_{i=1}^N q_i^A |\Phi_i|^2 = 0 \quad (E.1)$$

$$D_B \equiv \sum_{i=1}^N q_i^B |\Phi_i|^2 = 0. \quad (E.2)$$

It is well known that the moduli space of $D = 0$ is spanned by a basis of holomorphic, gauge invariant monomials (HIMs) [203]. Quite generally, the dimension of the moduli space \mathcal{M} of some gauge group \mathcal{G} is given by the number of fields charged under \mathcal{G} minus the number of constraints coming from $V_D = 0$:

$$\dim \mathcal{M} = N - \dim \mathcal{G}. \quad (E.3)$$

The HIMs can be represented as vectors \vec{x} in the $U(1)_A \times U(1)_B$ charge space. That is, if we define the charge matrix \mathbb{Q} as

$$\mathbb{Q} \equiv \begin{pmatrix} q_1^A & q_2^A & \cdots & q_N^A \\ q_1^B & q_2^B & \cdots & q_N^B \end{pmatrix}, \quad (E.4)$$

then the set of HIMs are defined as the solutions to

$$\mathbb{Q} \cdot \vec{x} = 0. \quad (\text{E.5})$$

The requirement that the monomials be holomorphic is a non-trivial constraint—effectively, this means that the entries in \vec{x} be positive semi-definite integers.⁵⁹

In general, a HIM is given by

$$M_\alpha = \Phi_1^{x_1^\alpha} \Phi_2^{x_2^\alpha} \cdots \Phi_N^{x_N^\alpha}, \quad (\text{E.6})$$

where $\mathbb{Q} \cdot \vec{x}^\alpha = 0$. We can guarantee solutions to $V_D = 0$ if we demand that

$$|\Phi_i|^2 = \Phi_i \frac{\partial}{\partial \Phi_i} \sum_{\alpha}^{\dim \mathcal{M}} a_\alpha M_\alpha. \quad (\text{E.7})$$

In general, one must choose the constants a_α such that all of the phases on the right hand side of Equation (E.7) cancel. A substitution into Equations (E.1) and (E.2) shows that we do indeed satisfy $D = 0$.

Next, consider the case where we turn on a superpotential, \mathcal{W} . The superpotential is an arbitrary function of the holomorphic, gauge invariant monomials. The requirement that $F = 0$ can be stated as follows:

$$\Phi_i \frac{\partial}{\partial \Phi_i} \mathcal{W}(M_\alpha) = 0. \quad (\text{E.8})$$

Expanding \mathcal{W} in powers of M_α , one has:

$$\Phi_i \frac{\partial}{\partial \Phi_i} \mathcal{W}(M_\alpha) = \sum_{\alpha} b_\alpha x_\alpha^i M_\alpha + \sum_{\alpha\beta} c_{\alpha\beta} (x_\alpha^i + x_\beta^i) M_\alpha M_\beta + \cdots = 0, \quad (\text{E.9})$$

This only tells us something that we already knew—the superpotential only constrains combinations of the holomorphic, gauge invariant monomials M_α , not the fields themselves.⁶⁰ We can solve these constraints explicitly for the M_α , and then express $|\Phi_i|^2$ in terms of a linear combination of the M_α (as before), with arbitrary a_α . Thus we see that it is *always* possible to satisfy $D = 0$ when given a solution to $F = 0$.⁶¹

Finally we consider the (relevant) case where the “ A ” in $U(1)_A \times U(1)_B$ stands for “anomalous”. In this case, Equation (E.1) is modified slightly. We must now cancel a

⁵⁹Here we will note that it is entirely possible that the null space of the charge matrix Q is empty—that is, it could very well be that there exists no holomorphic, gauge invariant monomials. This corresponds to a situation where SUSY is broken spontaneously *everywhere* in moduli space by D terms, except possibly at the origin where one would expect an enhanced gauge symmetry.

⁶⁰See Chapter VIII in Reference [204], for example.

⁶¹A different argument was made by Luty and Taylor [205].

Fayet-Iliopoulos (FI) term if we wish to keep SUSY unbroken:

$$D_A = \sum_i |\Phi_i|^2 + |\xi| = 0. \quad (\text{E.10})$$

In order to ensure that there exists a direction in moduli space along which this constraint can be satisfied, we seek at least one HIM which has a net negative charge under $U(1)_A$. This will ensure that we can cancel the (negative) FI term.

We now turn to the issue which we would like to address, namely proving $D = 0$ for the solution presented in Section 4 of Reference [30], wherein we showed $F = 0$ for one of the models, and neglected the issue of $D = 0$. We consider Model 1A in Reference [38], where it was shown that solutions to $F = D = 0$ existed for arbitrary (string scale) vevs for some subset of the non-Abelian singlet fields—see Equation (5.3) of [38]. We require two fields, called s_1 and s_{25} , to have intermediate scale (M_{EX}) vevs, while several other fields are required to have vevs of order the string scale. There are also several other non-Abelian singlet fields which we require to get zero vevs. (The complete list of fields, along with their charges are listed in Appendix E of Reference [38].)

Using the arguments above, we note that the proof of $D = 0$ for our solution is straightforward. One only need check that there are enough HIMs to saturate the dimension of the moduli space, and that there exists at least one holomorphic monomial which has a negative charge under the $U(1)_A$. We have verified that this is the case.

In closing, we will note that simply taking s_1 and s_{25} out of the charge matrix \mathbb{Q} produces a null result for $\mathbb{Q} \cdot \vec{x} = 0$, meaning that there are no vectors \vec{x} which satisfy the above equation if we set the vevs of $s_1 = s_{25} = 0$. In other words, SUSY is broken by D terms at the string scale at a generic point in moduli space.⁶²

Doing this, however, puts one in a different vacuum of the theory entirely. That is, one cannot scale a zero vev to a non-zero quantity, no matter how clever the choice of a_α ! We point out that the solution to $F = 0$ does require one engineer a cancellation on the order $M_{\text{EX}}/M_s \sim 10^{-8}$ among the other vevs. We should expect, then, that a tuning in the coefficients a_α is required to this order as well. While this is aesthetically unappealing, it is nonetheless possible, as the relationship in Equation (E.7) only constrains the phases of the a_α s and not their magnitudes.

⁶²The trivial result, with all fields having zero vevs, remains, and is a point of enhanced symmetry in moduli space. This point in moduli space is interesting in its own right, but is not useful for getting good phenomenology.

Appendix F

A DIFFERENT RACETRACK

The form of the gaugino condensate, given in Eqn. (5.37), ensures that the non-perturbative part of the superpotential is invariant under the modular group $SL(2, \mathbb{Z})$. In deriving the form of \mathcal{W}_{NP} , however, we have neglected the fact that the presence of discrete Wilson lines often break the modular group $SL(2, \mathbb{Z})$ to one of its subgroups. It has been noted [161] that turning on one or more Wilson lines breaks the modular group $SL(2, \mathbb{Z})$ down to one of its subgroups. Define the subgroup $\Gamma_0(p) \subset SL(2, \mathbb{Z})$. The subgroup is defined as the set of 2×2 matrices such that⁶³

$$\mathcal{M} \equiv \begin{pmatrix} a & b \\ c & d \end{pmatrix}, \quad (F.1)$$

$$ad - cb = 1, \quad (F.2)$$

$$a, b, c, d \in \mathbb{Z}, \quad (F.3)$$

$$c \equiv 0 \pmod{p}, \quad p \in \mathbb{P}, \quad (F.4)$$

where \mathbb{P} is the set of prime integers. Under this subgroup, then, the invariant function is a linear combination of Dedekind η functions:

$$f_p(\tau) = \frac{1}{p} \sum_{\lambda=0}^{p-1} \eta\left(\frac{\tau + \lambda}{p}\right). \quad (F.5)$$

⁶³A detailed mathematical treatment of the modular functions can be found in Reference [197].

Appendix G

SOME TRICKS FOR MINIMIZING POTENTIALS USING MATHEMATICA

I can see you're really upset about this. I honestly think you ought to sit down calmly, take a stress pill and think things over. I know I've made some very poor decisions recently, but I can give you my complete assurance that my work will be back to normal. I've still got the greatest enthusiasm and confidence in the mission. And I want to help you.

H.A.L.

`Mathematica` can be infuriating. But it is also one of the most useful pieces of software that a physicist (that isn't interested in building everything from scratch using C++) can master. In all parts of this Dissertation, we have relied heavily on `Mathematica` to do numerical work, especially in Chapter 5 to minimize complicated potentials. In this Appendix, we endeavor to provide a few of the tricks which were developed to deal with `Mathematica` and its results. We list this "bag of tricks" here in the hopes that someone will find something useful. Finally, appropriate credit must be given where it is due: some of these ideas were developed originally by Alex Westphal and Konstantin Bobkov.

G.1 My Potential has Spurious Imaginary Parts

Let's consider a simple problem: given some superpotential \mathcal{W} and some Kähler potential \mathcal{K} , we want to calculate the scalar potential as a function of real fields. The algorithm seems straightforward: calculate the Kähler metric, calculate the F terms, write down the scalar potential, then express everything in terms of (canonically normalized) real fields. The scalar potential will be a manifestly real function of the real-valued fields, which can then be minimized.

The trouble comes in because `Mathematica` is not this smart. `Mathematica` will make no *a priori* assumptions, and we have to trick it into believing that the potential (which is, after all, a complicated function of complex variables) is indeed real valued.

There are several ways to do this, here we describe a fool-proof method that should work every time. This comes at the cost of performance, though below we will give one way to deal with these issues.

We will assume a theory of the following form:

$$\mathcal{W} = \mathcal{W}(S, \Phi), \quad \mathcal{K} = \mathcal{K}(S, \bar{S}, \Phi, \bar{\Phi}). \quad (\text{G.1})$$

The first step is to calculate the F terms and the scalar potential in terms of the complex fields. The trick here is to treat S and \bar{S} as different fields. This can all be done symbolically, and all parameters in \mathcal{W} can be left arbitrary, for now.

The next step is to define real fields. We define

$$\begin{aligned} S &\equiv s + i\sigma, \\ \bar{S} &\equiv s - i\sigma, \\ \Phi &\equiv \varphi e^{i\theta}, \\ \bar{\Phi} &\equiv \varphi e^{-i\theta}. \end{aligned} \quad (\text{G.2})$$

Here, one can also use `$Assumptions` to define all of the parameters to be real:

$$\begin{aligned} \$Assumptions &= s > 0 \wedge \sigma > 0 \wedge \sigma \leq 2\pi \wedge \text{Arg}[s] == 0 \wedge \text{Arg}[\sigma] == 0 \\ &\wedge s \in \text{Reals} \wedge \sigma \in \text{Reals} \wedge \dots \end{aligned} \quad (\text{G.3})$$

Keep in mind that the more rules you give `Mathematica` the more likely it is that it will perform as expected.

Next, we use the `ComplexExpand` command to expand the F terms, explicitly defining the arguments of the complex phases. For example:

$$\begin{aligned} \text{FSsimp} &= \text{Simplify}[\text{ComplexExpand}[FS]] / . \text{Arg}[e^{i\theta}] \rightarrow \theta; \\ \text{FSBsimp} &= \text{Simplify}[\text{ComplexExpand}[FSbar]] / . \text{Arg}[e^{-i\theta}] \rightarrow -\theta; \end{aligned} \quad (\text{G.4})$$

The complex phases give `Mathematica` some trouble, and explicitly defining a rule for their replacement ensures that the result does not depend on $\text{Arg}[e^{i\theta}]$. We should note, however, that each rule increases the time it takes to execute the above commands, so some experimentation is required if there are many fields Φ_i —rules may not be needed for *all* fields θ , but rules will probably needed for *some* fields θ .

We can now explicitly separate the F terms into their real and imaginary parts in the usual manner:

$$\text{ReFS} = \text{Simplify} \left[\text{ComplexExpand} \left[\frac{\text{FSsimp} + \text{FSBsimp}}{2} \right] \right], \quad (\text{G.5})$$

with a similar expression for the imaginary part of F_S . Finally, the scalar potential can be expressed in terms of the real fields:

$$V(s, \sigma, \varphi, \theta) = |F_S|^2 \mathcal{K}^{S\bar{S}} + \dots, \quad (\text{G.6})$$

Note that `Mathematica` will automatically use the definitions above, in Equation (G.2).

Performance-wise, this entire procedure took 15-20 minutes to complete on a MacBook Pro, running a 2 GHz Intel Core 2 Duo processor with 4 GB of RAM, using the potentials from Chapter 5. In order to limit the number of times the full notebook must be run, it is convenient to use the `Save` command. The files only need to be built when the functional form of \mathcal{W} or \mathcal{K} is altered, not when the parameters are changed. Loading the saved files can be accomplished with `<<''Filename''`.

G.2 `Mathematica` Fails to Find a Minimum

In our models, an anomalous D term was generated at the string scale, and was canceled when some singlet fields took on VEVs, breaking the anomalous $U(1)$ symmetry. The F terms, on the other hand, were generated by gaugino condensates well below the string scale, leading to a mis-match in scales by several orders of magnitude. This leads to a potential which is computationally very tricky to handle: the D term potential dominates the full scalar potential, however, the true minimum requires us to consider the F term potential as well.

A common approach in the literature is to simply *assume* that $D_A = 0$ is satisfied, and surely it is, to leading order. But as the results of Chapter 5 indicate, a very tiny shift in the VEV of the field which cancels the D_A can result in disastrous consequences for the soft masses—this is indeed the generic case in the heterotic string models. Thus, in order to understand low energy physics, we should have a very good understanding of how to minimize the full potential.

In the following, all of the root finding routines require an initial guess. One can get a reasonably good initial guess by simply assuming $D_A = 0$, which will set the initial value of some of the fields. One can then substitute this into the full potential, and minimize V_F . The resulting set of field VEVs provides a suitable initial guess for the true minimum of the potential *in most cases*. In our analysis, the T modulus sometimes received large shifts from very tiny shifts in the other field VEVs.

G.2.1 The Konstantin Trick: Invent Something Small

Let us consider a potential of the following form:

$$V(\phi) = V_F(\phi) + V_D(\phi). \quad (\text{G.7})$$

where ϕ are just some real fields. Numerically, we can minimize V_F and V_D rather easily if we do it independently. The trouble is that the characteristic scales of the two potentials are wildly different:

$$V_F(\phi_0 + \epsilon) \sim \mathcal{O}(10^{-30}), \quad (G.8)$$

$$V_D(\phi_0 + \epsilon) \sim \mathcal{O}(10^{-6}). \quad (G.9)$$

ϕ_0 is the location of the true minimum, and ϵ is some small shift away from the minimum: one potential is very steep, while the other is very smooth.

One way to deal with this is to define

$$V_K(\phi, \delta_K) = V_F(\phi) + \delta_K V_D(\phi). \quad (G.10)$$

One can then set δ_K to something tiny ($\mathcal{O}(10^{-20})$, or so), and use `Mathematica`'s minimization routines. Once a minimum is found, one can then increment δ_K and minimize again, using the previous result as an initial guess. Typically, the more accurate the initial guess in the numerical minimization routines, the better the performance. We have listed an excerpt from our `Mathematica` notebook, suitably modified, in Equation (G.11) to demonstrate our point.

```
While[k > 0,
  {For[j = 1, j < 10, j++,
    {Δ = j 10-k,
     loopSoln = FindRoot[∂φV[φ, Δ] == 0, {φ, φtemp}],
     φtemp = Rationalize[φ/.loopSoln, 10-1000] }],
   k = k - 1}]]
```

(G.11)

We would like to point out a few features of the above code. First, we have used the `FindRoot` routine. This does not guarantee a minimum, and the mass matrix needs to be checked to ensure that we are not sitting at a local maximum. It is possible that `NMinimize` will work better in some cases. Indeed, sometimes it is much faster. Secondly, we have used the `Rationalize` command to ensure that we have 1000 digits of accuracy⁶⁴. This is overkill to be sure, but it is best to work with many more digits of precision than are needed—on most processors, the user will not notice the performance loss due to

⁶⁴We thank Steve Avery for pointing out that the `SetPrecision` command also works for this.

additional overhead. If speed does become an issue, one can always define global options:

```
PRES = 250;
MAXIT = 500;
SetOptions[FindRoot, WorkingPrecision -> 2*PRES,
Compiled -> False, MaxIterations -> MAXIT]; (G.12)
```

G.2.2 The Alex Trick: Step, Step, Decrease, Repeat

When the above trick work, it works very well. Convergence is quick, and we have control over how many times the loops are evaluated. However, this method does not always work, and it is nice to have some other tricks to rely on in this case.

The “trick of last resort” is basically a steepest descent method in one dimension. We will shift notation slightly in what follows: our full potential is given by $V(s, \phi_1, \dots, \phi_N)$. We do not provide a code example for this trick, as the actual implementation is a bit long (but still manageable). The algorithm is loosely as follows:

1. Set $V_D = 0$ and minimize V_F . This provides the initial guess: $\{\langle s \rangle_0, \langle \phi_1 \rangle_0, \dots, \langle \phi_N \rangle_0\}$.
2. Pick a field, which we denote with s . Check the derivative of the *full* potential with respect to s at $\{\langle s \rangle_0, \langle \phi_1 \rangle_0, \dots, \langle \phi_N \rangle_0\}$.
3. Define a small parameter ϵ . If the derivative was positive, then $\epsilon < 0$, if it was negative, $\epsilon > 0$. ϵ is the stepping parameter.
4. Define $\langle s \rangle_1 \equiv \langle s \rangle_0 + \epsilon$
5. Eliminate the field’s dependence in V : $V(\langle s \rangle_1, \phi_1, \dots, \phi_N)$.
6. Minimize the full potential using `NMinimize`, `FindRoot`, or `FindMinimum`. This defines a new set of field VEVs, $\{\langle s \rangle_1, \langle \phi_1 \rangle_1, \dots, \langle \phi_N \rangle_1\}$.
7. Check the derivative again with respect to s at the new set of VEVs. If the derivative changes sign, step back and decrease ϵ . Then repeat.
8. If the derivative does not change sign, step again in the same direction.

One can continue in this manner until the desired tolerance (which can be made arbitrarily small) in the derivative with respect to s is achieved.

G.3 Using the UNIX Terminal from **Mathematica**

The final trick we have come across is using **Mathematica** to access the UNIX terminal. For readers familiar with C++, this is the equivalent of the `system()` function in

the standard C library, `stdlib.h`. For example, if one wanted to run `SoftSUSY`, the `Mathematica` code looks like:

```
<< " !/.../softpoint.x leshouches < /.../input.dat >
/.../output.dat"                                     (G.13)
```

Note the `!`. This command runs a single point in parameter space (`softpoint.x`) using the boundary conditions in `input.dat`, and storing the result in `output.dat`. We refer the reader to the `SoftSUSY` documentation for more information [186].

Appendix H

MISCELLANY

| U | | T_3 | | T_5 | | | |
|--|------|--|---|--|---|---|---|
| $1 \times (\mathbf{3}, \mathbf{2})_{1/3, 1/3}$ | bulk | $4 \times (\mathbf{1}, \mathbf{1})_{1, 3}$ | ▲ | $1 \times (\mathbf{3}, \mathbf{2})_{1/3, 1/3}$ | ★ | $1 \times (\mathbf{1}, \mathbf{1})_{-1, 3}$ | ■ |
| $1 \times (\bar{\mathbf{3}}, \mathbf{1})_{-4/3, -1/3}$ | bulk | $4 \times (\mathbf{1}, \mathbf{1})_{-1, -3}$ | ▲ | $1 \times (\mathbf{3}, \mathbf{2})_{1/3, 1/3}$ | ● | $1 \times (\mathbf{1}, \mathbf{1})_{1, -3}$ | ▲ |
| $1 \times (\mathbf{1}, \mathbf{2})_{1, 0}$ | bulk | $4 \times (\mathbf{1}, \mathbf{1})_{1, 3}$ | ■ | $1 \times (\bar{\mathbf{3}}, \mathbf{1})_{-4/3, -1/3}$ | ★ | $1 \times (\mathbf{1}, \mathbf{1})_{1, 3}$ | ▲ |
| $1 \times (\mathbf{1}, \mathbf{2})_{-1, 0}$ | bulk | $4 \times (\mathbf{1}, \mathbf{1})_{-1, -3}$ | ■ | $1 \times (\bar{\mathbf{3}}, \mathbf{1})_{-4/3, -1/3}$ | ● | $1 \times (\mathbf{1}, \mathbf{1})_{1, 3}$ | ■ |
| $1 \times (\mathbf{1}, \mathbf{1})_{2, 1}$ | bulk | $2 \times (\mathbf{1}, \mathbf{1})_{1, 2}$ | ▲ | $1 \times (\bar{\mathbf{3}}, \mathbf{1})_{2/3, -1/3}$ | ★ | $1 \times (\mathbf{1}, \mathbf{1})_{1, -3}$ | ■ |
| $4 \times (\mathbf{1}, \mathbf{1})_{0, -1}$ | bulk | $2 \times (\mathbf{1}, \mathbf{1})_{-1, -2}$ | ▲ | $1 \times (\bar{\mathbf{3}}, \mathbf{1})_{2/3, -1/3}$ | ● | $2 \times (\mathbf{1}, \mathbf{1})_{1, -2}$ | ▲ |
| $5 \times (\mathbf{1}, \mathbf{1})_{0, 1}$ | bulk | $2 \times (\mathbf{1}, \mathbf{1})_{1, 2}$ | ■ | $1 \times (\bar{\mathbf{3}}, \mathbf{1})_{-1/3, 8/3}$ | ▲ | $2 \times (\mathbf{1}, \mathbf{1})_{-1, 2}$ | ▲ |
| $2 \times (\mathbf{1}, \mathbf{1})_{0, 0}$ | bulk | $2 \times (\mathbf{1}, \mathbf{1})_{-1, -2}$ | ■ | $1 \times (\mathbf{3}, \mathbf{1})_{1/3, 8/3}$ | ▲ | $2 \times (\mathbf{1}, \mathbf{1})_{1, -2}$ | ■ |
| T_2 | | $1 \times (\mathbf{1}, \mathbf{1})_{1, 2}$ | ▲ | $1 \times (\bar{\mathbf{3}}, \mathbf{1})_{-1/3, 8/3}$ | ■ | $2 \times (\mathbf{1}, \mathbf{1})_{-1, 2}$ | ■ |
| $3 \times (\bar{\mathbf{3}}, \mathbf{1})_{2/3, 2/3}$ | bulk | $1 \times (\mathbf{1}, \mathbf{1})_{1, -2}$ | ▲ | $1 \times (\mathbf{3}, \mathbf{1})_{1/3, -8/3}$ | ■ | $1 \times (\mathbf{1}, \mathbf{1})_{0, 5}$ | ★ |
| $3 \times (\mathbf{3}, \mathbf{1})_{-2/3, -2/3}$ | bulk | $1 \times (\mathbf{1}, \mathbf{1})_{1, -2}$ | ■ | $1 \times (\mathbf{1}, \mathbf{2})_{-1, -1}$ | ★ | $1 \times (\mathbf{1}, \mathbf{1})_{0, -5}$ | ★ |
| $2 \times (\bar{\mathbf{3}}, \mathbf{1})_{2/3, -1/3}$ | bulk | $1 \times (\mathbf{1}, \mathbf{1})_{-1, 2}$ | ■ | $1 \times (\mathbf{1}, \mathbf{2})_{-1, -1}$ | ● | $1 \times (\mathbf{1}, \mathbf{1})_{0, 5}$ | ● |
| $1 \times (\mathbf{1}, \mathbf{2})_{1, 1}$ | bulk | $1 \times (\mathbf{1}, \mathbf{1})_{0, 6}$ | ★ | $1 \times (\mathbf{1}, \mathbf{2})_{0, -3}$ | ▲ | $1 \times (\mathbf{1}, \mathbf{1})_{0, -5}$ | ● |
| $3 \times (\mathbf{1}, \mathbf{1})_{0, 5}$ | bulk | $1 \times (\mathbf{1}, \mathbf{1})_{0, -6}$ | ★ | $1 \times (\mathbf{1}, \mathbf{2})_{0, 3}$ | ▲ | $2 \times (\mathbf{1}, \mathbf{1})_{0, 3}$ | ★ |
| $6 \times (\mathbf{1}, \mathbf{1})_{0, 3}$ | bulk | $1 \times (\mathbf{1}, \mathbf{1})_{0, 6}$ | ● | $1 \times (\mathbf{1}, \mathbf{2})_{0, 3}$ | ■ | $2 \times (\mathbf{1}, \mathbf{1})_{0, -3}$ | ★ |
| $4 \times (\mathbf{1}, \mathbf{1})_{0, 2}$ | bulk | $1 \times (\mathbf{1}, \mathbf{1})_{0, -6}$ | ● | $1 \times (\mathbf{1}, \mathbf{2})_{0, -3}$ | ■ | $2 \times (\mathbf{1}, \mathbf{1})_{0, 3}$ | ● |
| $4 \times (\mathbf{1}, \mathbf{1})_{0, -2}$ | bulk | $2 \times (\mathbf{1}, \mathbf{1})_{0, -2}$ | ★ | $1 \times (\mathbf{1}, \mathbf{2})_{0, 2}$ | ▲ | $2 \times (\mathbf{1}, \mathbf{1})_{0, -3}$ | ● |
| $5 \times (\mathbf{1}, \mathbf{1})_{0, 1}$ | bulk | $2 \times (\mathbf{1}, \mathbf{1})_{0, 2}$ | ★ | $1 \times (\mathbf{1}, \mathbf{2})_{0, -2}$ | ▲ | $1 \times (\mathbf{1}, \mathbf{1})_{0, -1}$ | ★ |
| $2 \times (\mathbf{1}, \mathbf{1})_{0, -1}$ | bulk | $2 \times (\mathbf{1}, \mathbf{1})_{0, -2}$ | ● | $1 \times (\mathbf{1}, \mathbf{2})_{0, 2}$ | ■ | $1 \times (\mathbf{1}, \mathbf{1})_{0, -1}$ | ● |
| $21 \times (\mathbf{1}, \mathbf{1})_{0, 0}$ | bulk | $2 \times (\mathbf{1}, \mathbf{1})_{0, 2}$ | ● | $1 \times (\mathbf{1}, \mathbf{2})_{0, -2}$ | ■ | $1 \times (\mathbf{1}, \mathbf{1})_{0, 1}$ | ★ |
| T_4 | | | | $2 \times (\mathbf{1}, \mathbf{2})_{0, 0}$ | ▲ | $1 \times (\mathbf{1}, \mathbf{1})_{0, 1}$ | ★ |
| $3 \times (\bar{\mathbf{3}}, \mathbf{1})_{2/3, 2/3}$ | bulk | | | $2 \times (\mathbf{1}, \mathbf{2})_{0, 0}$ | ■ | $1 \times (\mathbf{1}, \mathbf{1})_{0, 1}$ | ● |
| $3 \times (\mathbf{3}, \mathbf{1})_{-2/3, -2/3}$ | bulk | | | $1 \times (\mathbf{1}, \mathbf{1})_{2, 1}$ | ★ | $1 \times (\mathbf{1}, \mathbf{1})_{0, 1}$ | ● |
| $1 \times (\bar{\mathbf{3}}, \mathbf{1})_{-2/3, 1/3}$ | bulk | | | $1 \times (\mathbf{1}, \mathbf{1})_{2, 1}$ | ● | $8 \times (\mathbf{1}, \mathbf{1})_{0, 0}$ | ★ |
| $2 \times (\mathbf{1}, \mathbf{2})_{-1, -1}$ | bulk | | | $1 \times (\mathbf{1}, \mathbf{1})_{-1, -3}$ | ▲ | $8 \times (\mathbf{1}, \mathbf{1})_{0, 0}$ | ★ |
| $3 \times (\mathbf{1}, \mathbf{1})_{0, -5}$ | bulk | | | $1 \times (\mathbf{1}, \mathbf{1})_{-1, 3}$ | ▲ | $6 \times (\mathbf{1}, \mathbf{1})_{0, 0}$ | ● |
| $6 \times (\mathbf{1}, \mathbf{1})_{0, -3}$ | bulk | | | $1 \times (\mathbf{1}, \mathbf{1})_{-1, 3}$ | ■ | $6 \times (\mathbf{1}, \mathbf{1})_{0, 0}$ | ● |
| $2 \times (\mathbf{1}, \mathbf{1})_{0, -2}$ | bulk | | | | | | |
| $2 \times (\mathbf{1}, \mathbf{1})_{0, 2}$ | bulk | | | | | | |
| $1 \times (\mathbf{1}, \mathbf{1})_{0, 1}$ | bulk | | | | | | |
| $4 \times (\mathbf{1}, \mathbf{1})_{0, -1}$ | bulk | | | | | | |
| $21 \times (\mathbf{1}, \mathbf{1})_{0, 0}$ | bulk | | | | | | |

Table H.1: Spectrum of Model 1 of the mini-landscape search [38]. From the viewpoint of the 5-dimensional theory, all states that are not localize in the $\text{SO}(4)$ torus (U, T_2, T_4) are bulk modes. The symbols $\bullet, \star, \blacksquare, \blacktriangle$ indicate the localization of the brane modes in the $\text{SO}(4)$ torus, compare Figure 3.1 on page 54.

| U | | T_3 | | T_5 | | | |
|--|------|---|---|--|---|--|---|
| $1 \times (\mathbf{3}, \mathbf{2})_{1/3, 1/3}$ | bulk | $1 \times (\mathbf{3}, \mathbf{1})_{1/3, -8/3}$ | ▲ | $1 \times (\mathbf{3}, \mathbf{2})_{1/3, 1/3}$ | ★ | $2 \times (\mathbf{1}, \mathbf{1})_{-1, -2}$ | ■ |
| $1 \times (\bar{\mathbf{3}}, \mathbf{1})_{-4/3, -1/3}$ | bulk | $1 \times (\bar{\mathbf{3}}, \mathbf{1})_{-1/3, 8/3}$ | ▲ | $1 \times (\mathbf{3}, \mathbf{2})_{1/3, 1/3}$ | ● | $2 \times (\mathbf{1}, \mathbf{1})_{1, 1}$ | ▲ |
| $1 \times (\mathbf{1}, \mathbf{2})_{1, 0}$ | bulk | $1 \times (\mathbf{3}, \mathbf{1})_{1/3, -8/3}$ | ■ | $1 \times (\bar{\mathbf{3}}, \mathbf{1})_{-4/3, -1/3}$ | ★ | $2 \times (\mathbf{1}, \mathbf{1})_{1, -1}$ | ▲ |
| $1 \times (\mathbf{1}, \mathbf{2})_{-1, 0}$ | bulk | $1 \times (\bar{\mathbf{3}}, \mathbf{1})_{-1/3, 8/3}$ | ■ | $1 \times (\bar{\mathbf{3}}, \mathbf{1})_{-4/3, -1/3}$ | ● | $2 \times (\mathbf{1}, \mathbf{1})_{-1, 1}$ | ▲ |
| $1 \times (\mathbf{1}, \mathbf{1})_{2, 1}$ | bulk | $3 \times (\mathbf{1}, \mathbf{1})_{1, 3}$ | ▲ | $1 \times (\bar{\mathbf{3}}, \mathbf{1})_{2/3, -1/3}$ | ★ | $2 \times (\mathbf{1}, \mathbf{1})_{-1, -1}$ | ▲ |
| $1 \times (\mathbf{1}, \mathbf{1})_{0, -2}$ | bulk | $3 \times (\mathbf{1}, \mathbf{1})_{-1, 3}$ | ▲ | $1 \times (\bar{\mathbf{3}}, \mathbf{1})_{2/3, -1/3}$ | ● | $2 \times (\mathbf{1}, \mathbf{1})_{1, -1}$ | ■ |
| $1 \times (\mathbf{1}, \mathbf{1})_{0, 2}$ | bulk | $3 \times (\mathbf{1}, \mathbf{1})_{1, 3}$ | ■ | $1 \times (\bar{\mathbf{3}}, \mathbf{1})_{-1/3, 5/3}$ | ▲ | $2 \times (\mathbf{1}, \mathbf{1})_{1, 1}$ | ■ |
| $8 \times (\mathbf{1}, \mathbf{1})_{0, 1/2}$ | bulk | $3 \times (\mathbf{1}, \mathbf{1})_{-1, 3}$ | ■ | $1 \times (\mathbf{3}, \mathbf{1})_{1/3, -5/3}$ | ▲ | $2 \times (\mathbf{1}, \mathbf{1})_{-1, 1}$ | ■ |
| $1 \times (\mathbf{1}, \mathbf{1})_{0, 0}$ | bulk | $1 \times (\mathbf{1}, \mathbf{1})_{1, -2}$ | ▲ | $1 \times (\bar{\mathbf{3}}, \mathbf{1})_{-1/3, 5/3}$ | ■ | $2 \times (\mathbf{1}, \mathbf{1})_{-1, -1}$ | ■ |
| T_2 | | $1 \times (\mathbf{1}, \mathbf{1})_{-1, 2}$ | ▲ | $1 \times (\mathbf{3}, \mathbf{1})_{1/3, -5/3}$ | ■ | $1 \times (\mathbf{1}, \mathbf{1})_{1, 0}$ | ▲ |
| $3 \times (\mathbf{3}, \mathbf{1})_{-2/3, -2/3}$ | bulk | $1 \times (\mathbf{1}, \mathbf{1})_{1, -2}$ | ■ | $1 \times (\mathbf{1}, \mathbf{2})_{-1, -1}$ | ★ | $1 \times (\mathbf{1}, \mathbf{1})_{-1, 0}$ | ▲ |
| $1 \times (\mathbf{3}, \mathbf{1})_{-2/3, 1/3}$ | bulk | $1 \times (\mathbf{1}, \mathbf{1})_{-1, 2}$ | ■ | $1 \times (\mathbf{1}, \mathbf{2})_{-1, -1}$ | ● | $1 \times (\mathbf{1}, \mathbf{1})_{1, 0}$ | ■ |
| $2 \times (\mathbf{1}, \mathbf{2})_{-1, -1}$ | bulk | $1 \times (\mathbf{1}, \mathbf{1})_{0, 3}$ | ★ | $1 \times (\mathbf{1}, \mathbf{2})_{0, -1}$ | ▲ | $1 \times (\mathbf{1}, \mathbf{1})_{-1, 0}$ | ■ |
| $3 \times (\mathbf{1}, \mathbf{2})_{-1, 0}$ | bulk | $1 \times (\mathbf{1}, \mathbf{1})_{0, -3}$ | ★ | $1 \times (\mathbf{1}, \mathbf{2})_{0, 1}$ | ▲ | $1 \times (\mathbf{1}, \mathbf{1})_{0, 3}$ | ★ |
| $6 \times (\mathbf{1}, \mathbf{1})_{0, 2}$ | bulk | $1 \times (\mathbf{1}, \mathbf{1})_{0, 3}$ | ● | $1 \times (\mathbf{1}, \mathbf{2})_{0, 1}$ | ■ | $1 \times (\mathbf{1}, \mathbf{1})_{0, -3}$ | ★ |
| $6 \times (\mathbf{1}, \mathbf{1})_{0, -2}$ | bulk | $1 \times (\mathbf{1}, \mathbf{1})_{0, -3}$ | ● | $1 \times (\mathbf{1}, \mathbf{2})_{0, -1}$ | ■ | $1 \times (\mathbf{1}, \mathbf{1})_{0, -3}$ | ● |
| $6 \times (\mathbf{1}, \mathbf{1})_{0, -1}$ | bulk | $2 \times (\mathbf{1}, \mathbf{1})_{0, -2}$ | ★ | $2 \times (\mathbf{1}, \mathbf{2})_{0, 0}$ | ▲ | $1 \times (\mathbf{1}, \mathbf{1})_{0, 3}$ | ● |
| $5 \times (\mathbf{1}, \mathbf{1})_{0, 1}$ | bulk | $2 \times (\mathbf{1}, \mathbf{1})_{0, 2}$ | ★ | $2 \times (\mathbf{1}, \mathbf{2})_{0, 0}$ | ■ | $2 \times (\mathbf{1}, \mathbf{1})_{0, -2}$ | ★ |
| $16 \times (\mathbf{1}, \mathbf{1})_{0, -1/2}$ | bulk | $2 \times (\mathbf{1}, \mathbf{1})_{0, -2}$ | ● | $1 \times (\mathbf{1}, \mathbf{1})_{2, 1}$ | ★ | $2 \times (\mathbf{1}, \mathbf{1})_{0, 2}$ | ★ |
| $21 \times (\mathbf{1}, \mathbf{1})_{0, 0}$ | bulk | $2 \times (\mathbf{1}, \mathbf{1})_{0, 2}$ | ● | $1 \times (\mathbf{1}, \mathbf{1})_{2, 1}$ | ● | $2 \times (\mathbf{1}, \mathbf{1})_{0, 2}$ | ● |
| T_4 | | | | $1 \times (\mathbf{1}, \mathbf{1})_{1, -2}$ | ▲ | $2 \times (\mathbf{1}, \mathbf{1})_{0, -2}$ | ● |
| $3 \times (\bar{\mathbf{3}}, \mathbf{1})_{2/3, 2/3}$ | bulk | | | $2 \times (\mathbf{1}, \mathbf{1})_{1, 2}$ | ▲ | $3 \times (\mathbf{1}, \mathbf{1})_{0, 1}$ | ★ |
| $2 \times (\bar{\mathbf{3}}, \mathbf{1})_{2/3, -1/3}$ | bulk | | | $2 \times (\mathbf{1}, \mathbf{1})_{-1, -2}$ | ▲ | $2 \times (\mathbf{1}, \mathbf{1})_{0, -1}$ | ★ |
| $1 \times (\mathbf{1}, \mathbf{2})_{1, 1}$ | bulk | | | $1 \times (\mathbf{1}, \mathbf{1})_{-1, 2}$ | ▲ | $2 \times (\mathbf{1}, \mathbf{1})_{0, -1}$ | ● |
| $3 \times (\mathbf{1}, \mathbf{2})_{1, 0}$ | bulk | | | $2 \times (\mathbf{1}, \mathbf{1})_{1, 2}$ | ■ | $3 \times (\mathbf{1}, \mathbf{1})_{0, 1}$ | ● |
| $6 \times (\mathbf{1}, \mathbf{1})_{0, 2}$ | bulk | | | $1 \times (\mathbf{1}, \mathbf{1})_{1, -2}$ | ■ | $12 \times (\mathbf{1}, \mathbf{1})_{0, 0}$ | ★ |
| $6 \times (\mathbf{1}, \mathbf{1})_{0, -2}$ | bulk | | | $1 \times (\mathbf{1}, \mathbf{1})_{-1, 2}$ | ■ | $12 \times (\mathbf{1}, \mathbf{1})_{0, 0}$ | ● |
| $4 \times (\mathbf{1}, \mathbf{1})_{0, -1}$ | bulk | | | | | | |
| $6 \times (\mathbf{1}, \mathbf{1})_{0, 1}$ | bulk | | | | | | |
| $8 \times (\mathbf{1}, \mathbf{1})_{0, 1/2}$ | bulk | | | | | | |
| $12 \times (\mathbf{1}, \mathbf{1})_{0, 0}$ | bulk | | | | | | |

Table H.2: Spectrum of Model 2 of the mini-landscape search [38]. From the viewpoint of the 5-dimensional theory, all states that are not localize in the $SO(4)$ torus (U, T_2, T_4) are bulk modes. The symbols \bullet , \star , \blacksquare , \blacktriangle indicate the localization of the brane modes in the $SO(4)$ torus, compare Figure 3.1 on page 54.

| Multiplet Type | Representation | Number |
|----------------|---|---|
| tensor | singlet | 1 |
| vector | $(\mathbf{35}, 1, 1) \oplus (1, \mathbf{28}, 1)$ $\oplus (1, 1, \mathbf{8}) \oplus 5 \times (1, 1, 1)$ | $35 + 28$ $8 + 5$ |
| hyper | $(\mathbf{20}, 1, 1) \oplus (1, \mathbf{8}_{v+c+s}, 1) \oplus 4 \times (1, 1, 1)$ $\oplus 9 \times \{(\mathbf{6}, 1, 1) \oplus (\bar{\mathbf{6}}, 1, 1)\}$ $\oplus 9 \times \{(1, 1, \mathbf{3}) \oplus (1, 1, \bar{\mathbf{3}})\}$ $\oplus 3 \times (1, \mathbf{8}_{v+c+s}, 1)$ $\oplus 36 \times (1, 1, 1)$ SUGRA singlets | $20+24+4$ 108 54 72 36 2 |

Table H.3: The full (five dimensional) spectrum of the models that we analyze [36]. Note that $\mathbf{8}_{v+c+s} \equiv \mathbf{8}_v + \mathbf{8}_c + \mathbf{8}_s$. In five dimensions, both Model 1 and Model 2 have the gauge group $SU(6) \times [SO(8) \times SU(3)]'$. Note that states are written in the language of $D = 5, N = 1$, and that the spectrum of these models are identical to those examined by Reference [206].

| Model | Hidden Sector | | Exotic Matter Irrep | Name |
|-------|----------------------|---------------|--|--|
| 1 A/B | $SU(4) \times SU(2)$ | brane exotics | $2 \times [(\mathbf{3}, 1; 1, 1)_{1/3,2/3} + (\bar{\mathbf{3}}, 1; 1, 1)_{-1/3,-2/3}]$ $4 \times [(1, \mathbf{2}; 1, 1)_{0,*} + (1, \mathbf{2}; 1, 1)_{0,*}]$ $1 \times [(1, \mathbf{2}; 1, \mathbf{2})_{0,0} + (1, \mathbf{2}; 1, \mathbf{2})_{0,0}]$ $2 \times [(1, 1; \mathbf{4}, 1)_{1,1} + (1, 1; \bar{\mathbf{4}}, 1)_{-1,-1}]$ $14 \times [(1, 1; 1, 1)_{1,*} + (1, 1; 1, 1)_{-1,*}]$ | $v + \bar{v}$ $m + m$ $y + y$ $f^+ + \bar{f}^-$ $s^+ + s^-$ |
| | | bulk exotics | $6 \times [(\mathbf{3}, 1; 1, 1)_{-2/3,-2/3} + (\bar{\mathbf{3}}, 1; 1, 1)_{2/3,2/3}]$ $1 \times [(\mathbf{3}, 1; 1, 1)_{-2/3,-1/3} + (\bar{\mathbf{3}}, 1; 1, 1)_{2/3,1/3}]$ $1 \times [(1, \mathbf{2}; 1, 1)_{-1,-1} + (1, \mathbf{2}; 1, 1)_{1,1}]$ | $\delta + \bar{\delta}$ $d + \bar{d}$ $\ell + \bar{\ell}$ |
| 2 | $SO(8) \times SU(2)$ | brane exotics | $4 \times [(\mathbf{3}, 1; 1, 1)_{1/3,*} + (\bar{\mathbf{3}}, 1; 1, 1)_{-1/3,*}]$ $2 \times [(1, \mathbf{2}; 1, 1)_{0,*} + (1, \mathbf{2}; 1, 1)_{0,*}]$ $1 \times [(1, \mathbf{2}; 1, \mathbf{2})_{0,0} + (1, \mathbf{2}; 1, \mathbf{2})_{0,0}]$ $2 \times [(1, 1; 1, \mathbf{2})_{1,1} + (1, 1; 1, \mathbf{2})_{-1,-1}]$ $20 \times [(1, 1; 1, 1)_{1,*} + (1, 1; 1, 1)_{-1,*}]$ | $v + \bar{v}$ $m + m$ $y + y$ $x^+ + x^-$ $s^+ + s^-$ |
| | | bulk exotics | $3 \times [(\mathbf{3}, 1; 1, 1)_{-2/3,-2/3} + (\bar{\mathbf{3}}, 1; 1, 1)_{2/3,2/3}]$ $1 \times [(\mathbf{3}, 1; 1, 1)_{-2/3,2/3} + (\bar{\mathbf{3}}, 1; 1, 1)_{2/3,-2/3}]$ $1 \times [(1, \mathbf{2}; 1, 1)_{-1,-1} + (1, \mathbf{2}; 1, 1)_{1,1}]$ $3 \times [(1, \mathbf{2}; 1, 1)_{-1,0} + (1, \mathbf{2}; 1, 1)_{1,0}]$ | $\delta + \bar{\delta}$ $d + \bar{d}$ $\ell + \bar{\ell}$ $\phi + \bar{\phi}$ |

Table H.4: Exotic matter content in Models 1A/B and 2 from [38]. Listed are the states' quantum numbers under the MSSM and hidden sector gauge groups, with the hypercharge denoted in the subscript. The brane localized exotic matter in Model 1 is a subset of that in Model 2.

| irrep | Mult (Model 2) | b_3 | b_2 | b_Y |
|--|----------------|-------|-------|-------|
| $(\mathbf{3}, 1)_{1/3} + (\bar{\mathbf{3}}, 1)_{-1/3}$ | 4 | 1 | 0 | 1/10 |
| $(1, \mathbf{2})_0 + (1, \mathbf{2})_0$ | 4 | 0 | 1 | 0 |
| $(1, 1)_1 + (1, 1)_{-1}$ | 24 | 0 | 0 | 3/10 |

Table H.5: Values of the β -function coefficients for the *brane-localized* exotic matter. These states do not have zero modes, and come from the T^3 and T^1/T^5 sectors of the theory.

| SU(6) rep | | irrep | b_3^{++} | b_2^{++} | b_Y^{++} | | irrep | b_3^{--} | b_2^{--} | b_Y^{--} |
|---------------------------------|---|--|------------|------------|------------|---|---|------------|------------|------------|
| 35 | V | $(\mathbf{8}, 1)_0$ | -9 | 0 | 0 | C | $(\mathbf{8}, 1)_0$ | 3 | 0 | 0 |
| | V | $(1, \mathbf{3})_0$ | 0 | -6 | 0 | C | $(1, \mathbf{3})_0$ | 0 | 2 | 0 |
| | C | $(1, \mathbf{2})_1$ | 0 | 1/2 | 3/10 | V | $(1, \mathbf{2})_{-1}$ | 0 | -3/2 | -9/10 |
| | C | $(1, \mathbf{2})_{-1}$ | 0 | 1/2 | 3/10 | V | $(1, \mathbf{2})_1$ | 0 | -3/2 | -9/10 |
| 20 | C | $(\bar{\mathbf{3}}, \mathbf{2})_{1/3}$ | 1 | 3/2 | 1/10 | C | $(\bar{\mathbf{3}}, \mathbf{2})_{-1/3}$ | 1 | 3/2 | 1/10 |
| | C | $(\bar{\mathbf{3}}, 1)_{-4/3}$ | 1/2 | 0 | 4/5 | C | $(\mathbf{3}, 1)_{4/3}$ | 1/2 | 0 | 4/5 |
| | C | $(1, 1)_2$ | 0 | 0 | 3/5 | C | $(1, 1)_{-2}$ | 0 | 0 | 3/5 |
| 6 + $\bar{6}$ | C | $(1, \mathbf{2})_{-1}$ | 0 | 1/2 | 3/10 | C | $(1, \mathbf{2})_1$ | 0 | 1/2 | 3/10 |
| | C | $(\bar{\mathbf{3}}, 1)_{2/3}$ | 1/2 | 0 | 1/5 | C | $(\mathbf{3}, 1)_{-2/3}$ | 1/2 | 0 | 1/5 |

Table H.6: Values of the β -function coefficients for matter living in the bulk, along with their embeddings into SU(6). (The group branching rules for $SU(6) \rightarrow SU(5) \times U(1)$ can be found in Reference [61].) It is important to distinguish whether these are vector (V) or chiral (C) multiplets.

| \vec{n} | M_{STRING} in GeV | M_C in GeV | M_{EX} in GeV | $\tau(p \rightarrow e^+ \pi^0)$ in yr |
|------------------|---|---|--------------------------------------|---|
| (2, 1, 0) | 9.18×10^{17} | 2.22×10^{17} | 2.60×10^9 | 1.77×10^{38} |
| (4, 2, 0) | 9.18×10^{17} | 2.22×10^{17} | 4.88×10^{13} | 1.77×10^{38} |
| (3, 2, 3) | 9.88×10^{17} | 2.22×10^{17} | 2.08×10^9 | 1.32×10^{38} |
| (4, 3, 6) | 1.08×10^{18} | 2.22×10^{17} | 1.59×10^9 | 9.23×10^{37} |
| (4, 2, 1) | 8.26×10^{17} | 6.65×10^{16} | 5.43×10^{13} | 2.19×10^{36} |
| (4, 2, 2) | 6.87×10^{17} | 2.19×10^{16} | 6.52×10^{13} | 5.34×10^{34} |
| (2, 1, 1) | 6.87×10^{17} | 2.19×10^{16} | 6.18×10^9 | 5.34×10^{34} |
| (3, 2, 4) | 7.07×10^{17} | 2.16×10^{16} | 5.68×10^9 | 4.52×10^{34} |
| (4, 3, 7) | 7.28×10^{17} | 2.13×10^{16} | 5.21×10^9 | 3.79×10^{34} |
| (3, 1, 0) | 5.43×10^{17} | 8.20×10^{15} | 8.25×10^{13} | 2.70×10^{33} |
| (4, 2, 3) | 5.47×10^{17} | 8.15×10^{15} | 8.19×10^{13} | 2.57×10^{33} |

Table H.7: Comparison of proton lifetime to M_S , M_C , and M_{EX} , in the case where no exotic matter lives in the bulk. In general, an intermediate scale is needed to fit the low energy data and the proton decay constraints. We have used $\beta_{\text{LATTICE}} \simeq 0.011$ [201]. We note the solutions which will also work for Model 1A in **bold**. Note that \vec{n} refers to *brane localized* exotics only, and is defined in Equation (3.8).

| Bulk Exotics | \vec{n} | M_{STRING} in GeV | M_C in GeV | M_{EX} in GeV | $\tau(p \rightarrow e^+ \pi^0)$ in yr |
|--|--|---|---|--------------------------------------|---|
| $[(\mathbf{3}, 1)_{2/3,*} + (\bar{\mathbf{3}}, 1)_{-2/3,*})]^{++} +$ $[(1, \mathbf{2})_{1,*} + (1, \mathbf{2})_{-1,*})]^{--}$ | (4, 3, 1) | 9.96×10^{17} | 7.74×10^{17} | 4.50×10^{13} | 1.90×10^{40} |
| | (4, 3, 2) | 9.73×10^{17} | 2.22×10^{17} | 4.61×10^{13} | 1.40×10^{38} |
| | $\Rightarrow (\mathbf{2}, \mathbf{2}, \mathbf{2})$ | 1.01×10^{18} | 2.22×10^{17} | 1.92×10^9 | 1.19×10^{38} |
| | (3, 3, 5) | 1.12×10^{18} | 2.22×10^{17} | 1.43×10^9 | 7.97×10^{37} |
| | (4, 4, 8) | 1.28×10^{18} | 2.22×10^{17} | 9.64×10^8 | 4.73×10^{37} |
| | (3, 2, 0) | 8.79×10^{17} | 6.55×10^{16} | 5.10×10^{13} | 1.61×10^{36} |
| | (4, 3, 3) | 9.06×10^{17} | 6.50×10^{16} | 4.95×10^{13} | 1.38×10^{36} |
| | (3, 2, 1) | 7.67×10^{17} | 2.07×10^{16} | 5.84×10^{13} | 2.77×10^{34} |
| | (1, 1, 0) | 7.67×10^{17} | 2.07×10^{16} | 4.45×10^9 | 2.77×10^{34} |
| | (4, 3, 4) | 7.82×10^{17} | 2.05×10^{16} | 5.73×10^{13} | 2.47×10^{34} |
| | (2, 2, 3) | 7.97×10^{17} | 2.03×10^{16} | 3.96×10^9 | 2.20×10^{34} |
| | (3, 3, 6) | 8.31×10^{17} | 1.99×10^{16} | 3.50×10^9 | 1.71×10^{34} |
| | (4, 4, 9) | 8.69×10^{17} | 1.95×10^{16} | 3.06×10^9 | 1.31×10^{34} |
| | (4, 2, 0) | 6.69×10^{17} | 1.03×10^{16} | 1.44×10^{15} | 2.92×10^{33} |
| $[(\mathbf{3}, 1)_{2/3,*} + (\bar{\mathbf{3}}, 1)_{-2/3,*})]^{--} +$ $[(1, \mathbf{2})_{1,*} + (1, \mathbf{2})_{-1,*})]^{++}$ | (3, 1, 1) | 1.01×10^{18} | 2.22×10^{17} | 1.92×10^9 | 1.19×10^{38} |
| | (4, 2, 4) | 1.12×10^{18} | 2.22×10^{17} | 1.43×10^9 | 7.97×10^{37} |
| | (4, 1, 0) | 7.67×10^{17} | 2.07×10^{16} | 5.84×10^{13} | 2.77×10^{34} |
| | (3, 1, 2) | 7.97×10^{17} | 2.03×10^{16} | 3.96×10^9 | 2.20×10^{34} |
| | (4, 2, 5) | 8.31×10^{17} | 1.99×10^{16} | 3.50×10^9 | 1.71×10^{34} |
| $[(\mathbf{3}, 1)_{2/3,*} + (\bar{\mathbf{3}}, 1)_{-2/3,*})]^{++} +$ $[(1, \mathbf{2})_{1,*} + (1, \mathbf{2})_{-1,*})]^{++}$ | (2, 1, 0) | 1.01×10^{18} | 2.22×10^{17} | 1.92×10^9 | 1.19×10^{38} |
| | (3, 2, 3) | 1.12×10^{18} | 2.22×10^{17} | 1.43×10^9 | 7.97×10^{37} |
| | (4, 2, 0) | 9.73×10^{17} | 2.22×10^{17} | 4.61×10^{13} | 1.40×10^{38} |
| | (4, 3, 6) | 1.28×10^{18} | 2.22×10^{17} | 9.64×10^8 | 4.73×10^{37} |
| | (4, 2, 1) | 9.06×10^{17} | 6.50×10^{16} | 4.95×10^{13} | 1.38×10^{36} |
| | (4, 2, 2) | 7.82×10^{17} | 2.05×10^{16} | 5.73×10^{13} | 2.47×10^{34} |
| | (2, 1, 1) | 7.97×10^{17} | 2.03×10^{16} | 3.96×10^9 | 2.20×10^{34} |
| | (3, 2, 4) | 8.31×10^{17} | 1.99×10^{16} | 3.50×10^9 | 1.71×10^{34} |
| | (4, 3, 7) | 8.69×10^{17} | 1.95×10^{16} | 3.06×10^9 | 1.31×10^{34} |
| $[(\mathbf{3}, 1)_{2/3,*} + (\bar{\mathbf{3}}, 1)_{-2/3,*})]^{--} +$ $[(1, \mathbf{2})_{1,*} + (1, \mathbf{2})_{-1,*})]^{--}$ | (2, 1, 0) | 9.36×10^{17} | 2.22×10^{17} | 2.45×10^9 | 1.64×10^{38} |
| | (4, 2, 0) | 9.36×10^{17} | 2.22×10^{17} | 4.79×10^{13} | 1.64×10^{38} |
| | (3, 2, 3) | 1.01×10^{18} | 2.22×10^{17} | 1.92×10^9 | 1.19×10^{38} |
| | (4, 3, 6) | 1.12×10^{18} | 2.22×10^{17} | 1.43×10^9 | 7.97×10^{37} |
| | (4, 2, 1) | 8.79×10^{17} | 6.55×10^{16} | 5.10×10^{13} | 1.61×10^{36} |
| | (2, 1, 1) | 7.67×10^{17} | 2.07×10^{16} | 4.45×10^9 | 2.77×10^{34} |
| | (4, 2, 2) | 7.67×10^{17} | 2.07×10^{16} | 5.84×10^{13} | 2.77×10^{34} |
| | (3, 2, 4) | 7.97×10^{17} | 2.03×10^{16} | 3.96×10^9 | 2.20×10^{34} |
| | (4, 3, 7) | 8.31×10^{17} | 1.99×10^{16} | 3.50×10^9 | 1.71×10^{34} |

Table H.8: Comparison of proton lifetime to M_S , M_C , and M_{EX} . In general, an intermediate scale is needed to fit the low energy data and the proton decay constraints. We have used $\beta_{\text{LATTICE}} \simeq 0.011$ [201]. Note that \vec{n} refers to *brane localized* exotics only, and is defined in Equation (3.8). For details on the solution marked with an arrow (\Rightarrow), see Section 3.4. We note the solutions which will also work for Model 1A in **bold**.

| Bulk Exotics | \vec{n} | M_{STRING} in GeV | M_{C} in GeV | M_{EX} in GeV | $\tau(p \rightarrow e^+ \pi^0)$ in yr |
|--|-------------------------------------|---|---|---|---|
| None | (4, 2, 3) (3, 1, 0) (4, 2, 2) | 5.47×10^{17} 5.43×10^{17} 6.87×10^{17} | 8.15×10^{15} 8.20×10^{15} 2.19×10^{16} | 8.19×10^{13} 8.25×10^{13} 6.52×10^{13} | 2.57×10^{33} 2.70×10^{33} 5.34×10^{34} |
| $[(\mathbf{3}, 1)_{2/3,*} + (\bar{\mathbf{3}}, 1)_{-2/3,*})]^{++} +$ $[(1, \mathbf{2})_{1,*} + (1, \mathbf{2})_{-1,*})]^{--}$ | (4, 2, 0) (4, 3, 4) (3, 2, 1) | 6.69×10^{17} 7.82×10^{17} 7.67×10^{17} | 1.03×10^{16} 2.05×10^{16} 2.07×10^{16} | 1.44×10^{15} 5.73×10^{13} 5.84×10^{13} | 2.92×10^{33} 2.47×10^{34} 2.77×10^{34} |
| $[(\mathbf{3}, 1)_{2/3,*} + (\bar{\mathbf{3}}, 1)_{-2/3,*})]^{--} +$ $[(1, \mathbf{2})_{1,*} + (1, \mathbf{2})_{-1,*})]^{++}$ | (4, 1, 0) | 7.67×10^{17} | 2.07×10^{16} | 5.84×10^{13} | 2.77×10^{34} |
| $[(\mathbf{3}, 1)_{2/3,*} + (\bar{\mathbf{3}}, 1)_{-2/3,*})]^{++} +$ $[(1, \mathbf{2})_1 + (1, \mathbf{2})_{-1})]^{++}$ | (4, 2, 2) | 7.82×10^{17} | 2.05×10^{16} | 5.73×10^{13} | 2.47×10^{34} |
| $[(\mathbf{3}, 1)_{2/3,*} + (\bar{\mathbf{3}}, 1)_{-2/3,*})]^{--} +$ $[(1, \mathbf{2})_1 + (1, \mathbf{2})_{-1})]^{--}$ | (4, 2, 2) | 7.67×10^{17} | 2.07×10^{16} | 5.84×10^{13} | 2.77×10^{34} |

Table H.9: Subset of models listed in Tables H.7 and H.8 which exhibit moderate hierarchies between all of the scales in the problem, as pictured in Figure 3.4, in the red box. Note that none of these results can be accommodated in Model 1A.

| Bulk Exotics | \vec{n} | M_s in GeV | M_c in GeV | M_{ex} in GeV | $\tau(p \rightarrow e^+\pi^0)$ in yr | g_{string} | α_{GUT}^{-1} |
|--|---|---|---|---|---|--|--|
| None | (4, 2, 0) (2, 1, 0) (3, 2, 3) (4, 3, 6) (4, 2, 1) (4, 2, 2) (2, 1, 1) (3, 2, 4) (4, 3, 7) | 9.18×10^{17} 9.18×10^{17} 9.88×10^{17} 1.08×10^{18} 8.26×10^{17} 6.87×10^{17} 6.87×10^{17} 7.07×10^{17} 7.28×10^{17} | 2.22×10^{17} 2.22×10^{17} 2.22×10^{17} 2.22×10^{17} 6.65×10^{16} 2.19×10^{16} 2.19×10^{16} 2.16×10^{16} 2.13×10^{16} | 4.88×10^{13} 2.60×10^9 2.08×10^9 1.59×10^9 5.43×10^{13} 6.52×10^{13} 6.18×10^9 5.68×10^9 5.21×10^9 | 1.77×10^{38} 1.77×10^{38} 1.32×10^{38} 9.23×10^{37} 2.19×10^{36} 5.34×10^{34} 5.34×10^{34} 4.52×10^{34} 3.79×10^{34} | 0.43 0.43 0.48 0.55 0.67 0.89 0.89 0.94 0.99 | 22 22 19 16 27 39 39 37 35 |
| $[(\mathbf{3}, 1)_{2/3, *} + (\bar{\mathbf{3}}, 1)_{-2/3, *})]^{++} +$ $[(1, \mathbf{2})_{1, *} + (1, \mathbf{2})_{-1, *})]^{--}$ | (4, 3, 1) (4, 3, 2) (2, 2, 2) (3, 3, 5) (4, 4, 8) (3, 2, 0) (4, 3, 3) | 9.96×10^{17} 9.73×10^{17} 2.22×10^{17} 2.22×10^{17} 2.22×10^{17} 8.79×10^{17} 9.06×10^{17} | 7.74×10^{17} 4.61×10^{13} 1.92×10^9 1.43×10^9 9.64×10^8 5.10×10^{13} 4.95×10^{13} | 4.50×10^{13} 1.40×10^{38} 1.19×10^{38} 7.97×10^{37} 4.73×10^{37} 1.61×10^{36} 1.38×10^{36} | 0.26 0.47 0.5 0.58 0.71 0.75 0.78 | 19 20 18 15 11 24 23 | |
| $[(\mathbf{3}, 1)_{2/3, *} + (\bar{\mathbf{3}}, 1)_{-2/3, *})]^{--} +$ $[(1, \mathbf{2})_{1, *} + (1, \mathbf{2})_{-1, *})]^{++}$ | (3, 1, 1) (4, 2, 4) (4, 2, 0) (2, 1, 0) (3, 2, 3) (4, 3, 6) (4, 2, 1) | 1.01×10^{18} 1.12×10^{18} 9.73×10^{17} 1.01×10^{18} 1.12×10^{18} 1.28×10^{18} 9.06×10^{17} | 2.22×10^{17} 2.22×10^{17} 2.22×10^{17} 2.22×10^{17} 2.22×10^{17} 2.22×10^{17} 6.50×10^{16} | 1.92×10^9 1.43×10^9 4.61×10^{13} 1.92×10^9 1.43×10^9 9.64×10^8 4.95×10^{13} | 1.19×10^{38} 7.97×10^{37} 1.40×10^{38} 1.19×10^{38} 7.97×10^{37} 4.73×10^{37} 1.38×10^{36} | 0.5 0.58 0.47 0.5 0.58 0.71 0.78 | 18 15 20 18 15 11 23 |
| $[(\mathbf{3}, 1)_{2/3, *} + (\bar{\mathbf{3}}, 1)_{-2/3, *})]^{--} +$ $[(1, \mathbf{2})_1 + (1, \mathbf{2})_{-1})]^{++}$ | (2, 1, 0) (4, 2, 0) (3, 2, 3) (4, 3, 6) (4, 2, 1) | 9.36×10^{17} 9.36×10^{17} 2.22×10^{17} 2.22×10^{17} 6.55×10^{16} | 2.22×10^{17} 4.79×10^{13} 1.92×10^9 1.43×10^9 5.10×10^{13} | 2.45×10^9 1.64×10^{38} 1.19×10^{38} 7.97×10^{37} 1.61×10^{36} | 0.45×10^{38} 0.45×10^{38} 0.5 0.58 0.75 | 21 21 18 15 24 | |

Table H.10: Subset of models listed in Reference [30] which exhibit $g_{\text{string}} \lesssim 1$.

| Case | b | b_2 | λ | R | p | r | A | w_0 |
|------|------------|------------|-----------|-----|-----|--------|--------|----------------------|
| 1 | $\pi/50$ | $3\pi/2$ | 33 | 10 | 2/5 | $15p$ | 160 | 8×10^{-15} |
| 2 | $8/125$ | $3\pi/2$ | 0 | 5 | 2/5 | $15p$ | 30 | 42×10^{-16} |
| 3 | $1/16$ | $29\pi/20$ | 38 | 10 | 2/5 | $15p$ | 90 | 6×10^{-15} |
| 4 | $-\pi/120$ | $-\pi/40$ | 40 | 64 | 2/3 | 1 | $1/10$ | -5×10^{-15} |
| 5 | $-\pi/250$ | $-\pi/100$ | 25 | 16 | 1 | $10/3$ | $7/5$ | -7×10^{-15} |

Table H.11: Input values for the superpotential parameters for three different cases. Case 2 has a vanishing one loop correction for ϕ_2 .

| | Case 1 | Case 2 | Case 3 | Case 4 | Case 5 |
|--------------------------|------------------------|------------------------|------------------------|------------------------|------------------------|
| $\langle s \rangle$ | 2.2 | 2.2 | 2.1 | 2.1 | 2.2 |
| $\langle t \rangle$ | 1.2 | 1.1 | 1.6 | 1.1 | 1.1 |
| $\langle \sigma \rangle$ | 1.0 | 1.0 | 1.0 | 0.0 | 0.0 |
| $\langle \phi_2 \rangle$ | 0.08 | 0.08 | 0.08 | 0.03 | 0.06 |
| F_S | 2.8×10^{-16} | 1.3×10^{-16} | 2.7×10^{-16} | 1.1×10^{-16} | 8.0×10^{-17} |
| F_T | -8.7×10^{-15} | -5.1×10^{-15} | -5.0×10^{-15} | 6.7×10^{-15} | 9.1×10^{-15} |
| F_{ϕ_2} | -9.2×10^{-17} | -4.5×10^{-17} | -8.9×10^{-17} | 1.3×10^{-15} | 1.3×10^{-15} |
| D_A | 4.4×10^{-31} | 1.0×10^{-32} | 5.9×10^{-31} | -3.8×10^{-31} | -4.8×10^{-32} |
| $D_A/m_{3/2}^2$ | 0.6 | 0.03 | 2.7 | -0.7 | -0.05 |
| $V_0/(3m_{3/2}^2)$ | -0.02 | -0.01 | -0.02 | -0.03 | -0.02 |
| $m_{3/2}$ | 2.2 TeV | 1.4 TeV | 1.1 TeV | 1.8 TeV | 2.4 TeV |

Table H.12: The values for field VEVs and soft SUSY breaking parameters at the minimum of the scalar potential. Note $F_\Phi \equiv \partial_\Phi \mathcal{W} + (\partial_\Phi \mathcal{K}) \mathcal{W}$.

| | Case 1 | Case 2 | Case 3 | Case 4 | Case 5 |
|--------------|------------------------|------------------------|------------------------|-----------------------|-----------------------|
| F^S | 6.6×10^{-16} | 3.7×10^{-16} | 4.2×10^{-16} | 2.7×10^{-16} | 2.1×10^{-16} |
| F^T | -2.2×10^{-15} | -1.2×10^{-15} | -1.4×10^{-15} | 1.6×10^{-15} | 2.2×10^{-15} |
| F^{ϕ_2} | -1.1×10^{-17} | -6.5×10^{-18} | -7.7×10^{-18} | 1.9×10^{-16} | 1.8×10^{-16} |

Table H.13: The hierarchy of F terms in the five examples of the single condensate model we studied. Note that F^Φ is defined in Eqn. (5.70). All of the F terms contribute to the soft masses, as they are all within an order of magnitude.

| All Masses in GeV | | | | | | | | | | |
|--------------------|-------------------------|--------------|-------------------------|--------|-------------------------|--------------|----------------------|--------------|---------------------|--------|
| Parameter | Case S2 | | Case A3 | | Case A4 | | Case A5b | | Case A6 | |
| $m_{3/2}$ | 2159 | | 1350 | | 1133 | | 1808 | | 2375 | |
| m_{H_u} | | 238 <i>i</i> | | 181 | | 372 <i>i</i> | | 546 | | 355 |
| m_{H_d} | | 537 | | 205 | | 495 | | 228 <i>i</i> | | 290 |
| M_1 | $362 - 0.3n_1 - 0.1n_3$ | | $206 - 0.2n_1 - 0.1n_3$ | | $243 - 0.2n_1 - 0.1n_3$ | | $158 + 13n_1 + 4n_3$ | | $118 + 7n_1 + 2n_3$ | |
| M_2 | $362 - 1n_2$ | | $206 + 1n_2$ | | $243 - 1n_2$ | | $158 + 45n_2$ | | $118 + 23n_2$ | |
| M_3 | $362 - 1n_3$ | | $206 + 1n_3$ | | $243 - 1n_3$ | | $158 + 45n_3$ | | $118 + 23n_3$ | |
| A_t | 3901 | | 2466 | | 1974 | | -3690 | | -4798 | |
| A_b | 3901 | | 2466 | | 1974 | | -3690 | | -4798 | |
| A_τ | 3901 | | 2466 | | 1974 | | -3690 | | -4798 | |
| $m_{\tilde{q}}$ | Gen. 1,2 | Gen. 3 | Gen. 1,2 | Gen. 3 | Gen. 1,2 | Gen. 3 | Gen. 1,2 | Gen. 3 | Gen. 1,2 | Gen. 3 |
| | 1580 | 2225 | 966 | 1353 | 895 | 1299 | 1262 | 1734 | 1691 | 2368 |
| $m_{\tilde{u}^c}$ | 1580 | 2192 | 966 | 1352 | 895 | 1219 | 1262 | 1771 | 1691 | 2371 |
| $m_{\tilde{d}^c}$ | 1521 | 2203 | 964 | 1352 | 757 | 1246 | 1330 | 1759 | 1697 | 2370 |
| $m_{\tilde{\ell}}$ | 1580 | 2181 | 964 | 1351 | 757 | 1191 | 1330 | 1784 | 1697 | 2372 |
| $m_{\tilde{e}^c}$ | 1580 | 2192 | 966 | 1352 | 895 | 1219 | 1262 | 1771 | 1691 | 2371 |

Table H.14: Boundary conditions at the string scale. n_3, n_2, n_1 refer to possible intermediate mass vector-like exotics which couple to the SUSY breaking field ϕ_2 , see Eqn. (5.80).

All Masses in GeV (defined at $M_W \approx 80$ GeV, unless otherwise noted.)

| | Observable | Case 1 | Case 2 | Case 3 | Case 4 | Case 5 | | | |
|------------------------|-----------------------------------|-----------------------|-----------------------|-----------------------|-----------------------|-----------------------|--------|----------|--------|
| Inputs | $m_{3/2}$ | 2159 | 1350 | 1133 | 1808 | 2375 | | | |
| | $\tan \beta$ | 10 | 25 | 25 | 10 | 4 | | | |
| | $\text{sgn}(\mu)$ | + | + | + | + | + | | | |
| | n_1, n_2, n_3 | 0,0,0 | 0,0,0 | 0,0,0 | 0,0,0 | 0,0,0 | | | |
| EWSB | $\mu(M_{\text{SUSY}})$ | 2163 | 1315 | 1216 | 1913 | 2642 | | | |
| | m_{h^0} | 115.7 | 113.3 | 112.9 | 121.0 | 116.7 | | | |
| | m_{H^0} | 2205 | 1157 | 1185 | 1848 | 2728 | | | |
| | m_{A^0} | 2209 | 1169 | 1193 | 1844 | 2725 | | | |
| | m_{H^+} | 2211 | 1172 | 1196 | 1846 | 2726 | | | |
| $M_a(M_{\text{SUSY}})$ | M_1 | 151 | 83 | 99 | 69 | 53 | | | |
| | M_2 | 277 | 155 | 184 | 128 | 100 | | | |
| | M_3 | 774 | 457 | 540 | 368 | 279 | | | |
| | $m_{\tilde{g}}$ | 914 | 545 | 630 | 456 | 365 | | | |
| Neut./Charg. | $m_{\tilde{\chi}_1^0}$ | 150 | 83 | 99 | 68 | 52 | | | |
| | $m_{\tilde{\chi}_2^0}$ | 293 | 164 | 194 | 136 | 104 | | | |
| | $m_{\tilde{\chi}_3^0}$ | -2146 | -1303 | -1209 | -1899 | -2622 | | | |
| | $m_{\tilde{\chi}_4^0}$ | 2148 | 1305 | 1210 | 1901 | 2624 | | | |
| | $m_{\tilde{\chi}_1^\pm}$ | 293 | 164 | 194 | 137 | 104 | | | |
| | $m_{\tilde{\chi}_2^\pm}$ | 2156 | 1310 | 1216 | 1904 | 2628 | | | |
| Squarks/Sleptons | | Gen. 1,2 | Gen. 3 | Gen. 1,2 | Gen. 3 | Gen. 1,2 | Gen. 3 | Gen. 1,2 | Gen. 3 |
| | $m_{\tilde{u}_1}$ | 1713 | 1512 | 1040 | 920 | 1015 | 925 | 1282 | 779 |
| | $m_{\tilde{u}_2}$ | 1706 | 1977 | 1038 | 1161 | 1009 | 1198 | 1286 | 1350 |
| | $m_{\tilde{d}_1}$ | 1715 | 1972 | 1043 | 1147 | 1018 | 1183 | 1284 | 1318 |
| | $m_{\tilde{d}_2}$ | 1652 | 2280 | 1036 | 1340 | 890 | 1281 | 1351 | 1752 |
| | $m_{\tilde{e}_1}$ | 1533 | 2163 | 970 | 1226 | 770 | 1113 | 1332 | 1734 |
| | $m_{\tilde{e}_2}$ | 1584 | 2181 | 968 | 1304 | 900 | 1164 | 1259 | 1775 |
| | $m_{\tilde{\nu}}$ | 1531 | 2175 | 967 | 1295 | 766 | 1149 | 1330 | 1769 |
| Other Obs. | $\delta\rho$ | 9.0×10^{-6} | 3.0×10^{-5} | 2.9×10^{-5} | 1.4×10^{-5} | 7.0×10^{-6} | | | |
| | $\delta(g-2)_\mu$ | 6.1×10^{-11} | 4.0×10^{-10} | 5.9×10^{-10} | 6.8×10^{-11} | 1.2×10^{-11} | | | |
| | $BR(b \rightarrow s\gamma)$ | 3.7×10^{-4} | 3.9×10^{-4} | 3.9×10^{-4} | 3.6×10^{-4} | 3.7×10^{-4} | | | |
| | $BR(B_s \rightarrow \mu^+ \mu^-)$ | 3.1×10^{-9} | 2.7×10^{-9} | 2.8×10^{-9} | 3.1×10^{-9} | 3.1×10^{-9} | | | |
| | m_{LMM} | 272 | 175 | 138 | 531 | 487 | | | |
| | m_{nLMM} | 41659 | 25694 | 22745 | 27231 | 36795 | | | |

Table H.15: Weak scale observables, with no contribution from gauge mediation: $n_3 = n_2 = n_1 = 0$, see Eqn. 5.80. We have listed the mass eigenstates of the squarks and sleptons. Note that for light generations, $m_{\tilde{u}_1} \approx m_{\tilde{u}_L}$, etc. The last two rows give the lightest massive modulus (m_{LMM}) [mostly Kähler modulus ($\text{RE}[T]$)] and the *next to* lightest massive modulus (m_{nLMM}) [mostly the dilaton ($\text{RE}[S]$)]. All other moduli have mass $\gtrsim 100$ TeV.

| Case | 1 | | 2 | | 3 | | 4 | | 5 | | |
|-----------------------------------|----------------|----------------|----------------|----------------|----------------|----------------|----------------|----------------|----------------|----------------|-------|
| | $\mu < 0$ | $\mu > 0$ | |
| $\tan \beta$ | lo | 5 | 6 | 8 | 12 | 12 | 15 | 6 | 4 | 5 | 3 |
| | hi | 37 | 50 | 36 | 50 | 36 | 50 | 34 | 50 | 39 | 50 |
| m_{h^0} | lo | 113.4 | 113.0 | 112.4 | 112.4 | 112.4 | 112.4 | 114.5 | 116.0 | 113.5 | 112.4 |
| | hi | 117.3 | 117.1 | 113.7 | 113.4 | 113.0 | 113.0 | 120.1 | 121.4 | 120.8 | 121.9 |
| Neut. comp. | bino | |
| | $\gtrsim 99\%$ | |
| $m_{\tilde{\chi}_1^0}$ (GeV) | lo | 149.1 | 148.4 | 82.5 | 82.0 | 98.5 | 98.0 | 69.0 | 67.3 | 53.6 | 51.5 |
| | hi | 151.0 | 149.8 | 84.0 | 82.9 | 99.4 | 98.5 | 69.8 | 70.6 | 55.1 | 55.9 |
| $m_{\tilde{\chi}_1^\pm}$ (GeV) | lo | 290.5 | 291.1 | 162.3 | 162.3 | 193.5 | 193.0 | 139.6 | 134.4 | 110.3 | 103.3 |
| | hi | 298.5 | 293.5 | 167.1 | 163.7 | 196.5 | 193.9 | 141.7 | 142.1 | 113.9 | 114.6 |

Table H.16: Scan over $\tan \beta$ and $\text{sgn}(\mu)$.

BIBLIOGRAPHY

- [1] P. A. M. Dirac, "The Quantum theory of electron," *Proc. Roy. Soc. Lond.* **A117** (1928) 610–624.
- [2] P. A. M. Dirac, "The Quantum theory of electron. 2," *Proc. Roy. Soc. Lond.* **A118** (1928) 351.
- [3] C. D. Anderson, "The positive electron," *Phys. Rev.* **43** (1933) 491–494.
- [4] W. Pauli, "The Desparate Solution." Letter to the Federal Institute of Technology, Zürich, December, 1930.
- [5] F. Reines and C. L. Cowan, "Detection of the free neutrino," *Phys. Rev.* **92** (1953) 830–831.
- [6] S. L. Glashow, J. Iliopoulos, and L. Maiani, "Weak Interactions with Lepton-Hadron Symmetry," *Phys. Rev.* **D2** (1970) 1285–1292.
- [7] **E598** Collaboration, J. J. Aubert *et al.*, "Experimental Observation of a Heavy Particle J," *Phys. Rev. Lett.* **33** (1974) 1404–1406.
- [8] **SLAC-SP-017** Collaboration, J. E. Augustin *et al.*, "Discovery of a Narrow Resonance in e+ e- Annihilation," *Phys. Rev. Lett.* **33** (1974) 1406–1408.
- [9] S. L. Glashow, "Partial Symmetries of Weak Interactions," *Nucl. Phys.* **22** (1961) 579–588.
- [10] S. Weinberg, "A Model of Leptons," *Phys. Rev. Lett.* **19** (1967) 1264–1266.
- [11] J. Goldstone, A. Salam, and S. Weinberg, "Broken Symmetries," *Phys. Rev.* **127** (1962) 965–970.
- [12] **UA1** Collaboration, G. Arnison *et al.*, "Experimental observation of lepton pairs of invariant mass around 95-GeV/c**2 at the CERN SPS collider," *Phys. Lett.* **B126** (1983) 398–410.

- [13] **UA2** Collaboration, P. Bagnaia *et al.*, “Evidence for $Z^0 \rightarrow e^+ e^-$ at the CERN anti-p p collider,” *Phys. Lett.* **B129** (1983) 130–140.
- [14] **Particle Data Group** Collaboration, C. Amsler *et al.*, “Review of particle physics,” *Phys. Lett.* **B667** (2008) 1.
- [15] D. Binosi and L. Theussl, “JaxoDraw: A graphical user interface for drawing Feynman diagrams,” *Comput. Phys. Commun.* **161** (2004) 76–86, hep-ph/0309015.
- [16] E. Fermi, “An attempt of a theory of beta radiation. 1,” *Z. Phys.* **88** (1934) 161–177.
- [17] **CHARM-II** Collaboration, P. Vilain *et al.*, “A Precise measurement of the cross-section of the inverse muon decay muon-neutrino + e⁻ → mu⁻ + electron-neutrino,” *Phys. Lett.* **B364** (1995) 121–126.
- [18] Y. A. Golfand and E. P. Likhtman, “Extension of the algebra of Poincaré group generators and violation of p invariance,” *JETP Lett.* **13** (1971) 323–326.
- [19] J.-L. Gervais and B. Sakita, “Field theory interpretation of supergauges in dual models,” *Nucl. Phys.* **B34** (1971) 632–639.
- [20] D. V. Volkov and V. P. Akulov, “Possible universal neutrino interaction,” *JETP Lett.* **16** (1972) 438–440.
- [21] J. Wess and B. Zumino, “Supergauge transformations in four dimensions,” *Nucl. Phys.* **B70** (1974) 39–50.
- [22] **Belle** Collaboration, A. Limosani *et al.*, “Measurement of Inclusive Radiative B-meson Decays with a Photon Energy Threshold of 1.7 GeV,” *Phys. Rev. Lett.* **103** (2009) 241801, 0907.1384.
- [23] M. Misiak, “ $B \rightarrow X_s \gamma$ - Current Status,” *Acta Phys. Polon.* **B40** (2009) 2987–2996, 0911.1651.
- [24] D. J. Gross and F. Wilczek, “Ultraviolet behavior of non-Abelian gauge theories,” *Phys. Rev. Lett.* **30** (1973) 1343–1346.
- [25] H. D. Politzer, “Reliable perturbative results for strong interactions?,” *Phys. Rev. Lett.* **30** (1973) 1346–1349.
- [26] H. Georgi and S. L. Glashow, “Unity of All Elementary Particle Forces,” *Phys. Rev. Lett.* **32** (1974) 438–441.
- [27] S. Dimopoulos, S. A. Raby, and F. Wilczek, “Unification of couplings,” *Phys. Today* **44N10** (1991) 25–33.

[28] C.-N. Yang and R. L. Mills, “Conservation of isotopic spin and isotopic gauge invariance,” *Phys. Rev.* **96** (1954) 191–195.

[29] **Super-Kamiokande** Collaboration, H. Nishino *et al.*, “Search for Proton Decay via $p \rightarrow e^+ \pi^0$ and $p \rightarrow \mu^+ \pi^0$ in a Large Water Cherenkov Detector,” *Phys. Rev. Lett.* **102** (2009) 141801, 0903.0676.

[30] B. Dundee, S. Raby, and A. Wingerter, “Reconciling Grand Unification with Strings by Anisotropic Compactifications,” *Phys. Rev.* **D78** (2008) 066006, 0805.4186.

[31] B. Dundee, S. Raby, and A. Wingerter, “Addendum to “reconciling grand unification with strings by anisotropic compactifications”,” *Phys. Rev. D* **79** (2009), no. 4, 047901, 0811.4026.

[32] B. Dundee and S. Raby, “On the string coupling in a class of stringy orbifold GUTs,” 0808.0992.

[33] B. Dundee, S. Raby, and A. Westphal, “Moduli stabilization and SUSY breaking in heterotic orbifold string models,” 1002.1081.

[34] W. Buchmüller, K. Hamaguchi, O. Lebedev, and M. Ratz, “Supersymmetric standard model from the heterotic string,” *Phys. Rev. Lett.* **96** (2006) 121602, hep-ph/0511035.

[35] W. Buchmüller, K. Hamaguchi, O. Lebedev, and M. Ratz, “Supersymmetric standard model from the heterotic string. II,” *Nucl. Phys.* **B785** (2007) 149–209, hep-th/0606187.

[36] O. Lebedev *et al.*, “A mini-landscape of exact MSSM spectra in heterotic orbifolds,” *Phys. Lett.* **B645** (2007) 88–94, hep-th/0611095.

[37] O. Lebedev *et al.*, “Low Energy Supersymmetry from the Heterotic Landscape,” *Phys. Rev. Lett.* **98** (2007) 181602, hep-th/0611203.

[38] O. Lebedev *et al.*, “The Heterotic Road to the MSSM with R parity,” *Phys. Rev.* **D77** (2008) 046013, 0708.2691.

[39] T. Kobayashi, S. Raby, and R.-J. Zhang, “Searching for realistic 4d string models with a Pati-Salam symmetry: Orbifold grand unified theories from heterotic string compactification on a Z(6) orbifold,” *Nucl. Phys.* **B704** (2005) 3–55, hep-ph/0409098.

[40] S. Forste, H. P. Nilles, P. K. S. Vaudrevange, and A. Wingerter, “Heterotic brane world,” *Phys. Rev.* **D70** (2004) 106008, hep-th/0406208.

- [41] T. Kobayashi, S. Raby, and R.-J. Zhang, “Constructing 5d orbifold grand unified theories from heterotic strings,” *Phys. Lett.* **B593** (2004) 262–270, [hep-ph/0403065](#).
- [42] K. R. Dienes, E. Dudas, and T. Gherghetta, “Extra spacetime dimensions and unification,” *Phys. Lett.* **B436** (1998) 55–65, [hep-ph/9803466](#).
- [43] K. R. Dienes, E. Dudas, and T. Gherghetta, “Grand unification at intermediate mass scales through extra dimensions,” *Nucl. Phys.* **B537** (1999) 47–108, [hep-ph/9806292](#).
- [44] S. Kaluza, “Zum unitatsproblem in der physik (on the problem of unity in physics),” *Sitzungsber. Preuss. Akad. Wiss. Berlin. (Math. Phys.)* (1921) 966–972.
- [45] O. Klein, “Quantum theory and the five-dimensional theory of relativity,” *Z. Phys* **37** (1926) 895–906.
- [46] D. J. Gross, J. A. Harvey, E. J. Martinec, and R. Rohm, “The Heterotic String,” *Phys. Rev. Lett.* **54** (1985) 502–505.
- [47] D. J. Gross, J. A. Harvey, E. J. Martinec, and R. Rohm, “Heterotic String Theory. 1. The Free Heterotic String,” *Nucl. Phys.* **B256** (1985) 253.
- [48] M. B. Green, J. H. Schwarz, and E. Witten, “Superstring Theory Vol. 1: Introduction,”. Cambridge, Uk: Univ. Pr. (1987) 469 P. (Cambridge Monographs On Mathematical Physics).
- [49] M. B. Green, J. H. Schwarz, and E. Witten, “Superstring Theory Vol. 2: Loop Amplitudes, Anomalies, and Phenomenology,”. Cambridge, Uk: Univ. Pr. (1987) 596 P. (Cambridge Monographs On Mathematical Physics).
- [50] D. Lüst and S. Theisen, *Lectures on String Theory*. Berlin, Germany: Springer-Verlag (1989) 346 P.
- [51] J. Polchinski, “String theory. Vol. 1: An introduction to the bosonic string,”. Cambridge, UK: Univ. Pr. (1998) 402 p.
- [52] J. Polchinski, “String theory. Vol. 2: Superstring theory and beyond,”. Cambridge, UK: Univ. Pr. (1998) 531 p.
- [53] L. J. Dixon, J. A. Harvey, C. Vafa, and E. Witten, “Strings on Orbifolds,” *Nucl. Phys.* **B261** (1985) 678–686.
- [54] A. Font, L. E. Ibanez, and F. Quevedo, “ $Z(N) \times Z(M)$ Orbifolds and Discrete Torsion,” *Phys. Lett.* **B217** (1989) 272.

- [55] T. Kobayashi and N. Ohtsubo, “Geometrical aspects of Z(N) orbifold phenomenology,” *Int. J. Mod. Phys. A* **9** (1994) 87–126.
- [56] P. Vaudrevange, *Grand Unification in the Heterotic Braneworld*. PhD thesis, Universität Bonn, 2008. <http://www.th.physik.uni-bonn.de/nilles/db/thesis/>.
- [57] L. J. Dixon, J. A. Harvey, C. Vafa, and E. Witten, “Strings on Orbifolds. 2,” *Nucl. Phys.* **B274** (1986) 285–314.
- [58] K. S. Narain, “New Heterotic String Theories in Uncompactified Dimensions ≥ 10 ,” *Phys. Lett.* **B169** (1986) 41.
- [59] K. S. Narain, M. H. Sarmadi, and E. Witten, “A Note on Toroidal Compactification of Heterotic String Theory,” *Nucl. Phys.* **B279** (1987) 369.
- [60] P. Vaudrevange, “Geometrical Aspects of Heterotic Orbifolds,” Master’s thesis, Universität Bonn, 2004.
- [61] R. Slansky, “Group Theory for Unified Model Building,” *Phys. Rept.* **79** (1981) 1–128.
- [62] H. Esmaeli, N. Mahdavi-Amiri, and E. Spedicato, “A class of abs algorithms for diophantine linear systems,” *Numerische Mathematik* **90** (2001), no. 1, 101–115.
- [63] M. B. Green and J. H. Schwarz, “Anomaly Cancellation in Supersymmetric D=10 Gauge Theory and Superstring Theory,” *Phys. Lett.* **B149** (1984) 117–122.
- [64] M. Dine, N. Seiberg, and E. Witten, “Fayet-Iliopoulos Terms in String Theory,” *Nucl. Phys.* **B289** (1987) 589.
- [65] S. N. Ramos-Sánchez, *Towards Low Energy Physics from the Heterotic String*. PhD thesis, Universität Bonn, 2008. <http://www.th.physik.uni-bonn.de/nilles/db/thesis/>.
- [66] S. Dimopoulos, S. Raby, and F. Wilczek, “Supersymmetry and the Scale of Unification,” *Phys. Rev.* **D24** (1981) 1681–1683.
- [67] S. Dimopoulos and H. Georgi, “Softly Broken Supersymmetry and SU(5),” *Nucl. Phys.* **B193** (1981) 150.
- [68] L. E. Ibanez and G. G. Ross, “Low-Energy Predictions in Supersymmetric Grand Unified Theories,” *Phys. Lett.* **B105** (1981) 439.
- [69] N. Sakai, “Naturalness in Supersymmetric Guts,” *Zeit. Phys.* **C11** (1981) 153.
- [70] M. B. Einhorn and D. R. T. Jones, “The Weak Mixing Angle and Unification Mass in Supersymmetric SU(5),” *Nucl. Phys.* **B196** (1982) 475.

[71] W. J. Marciano and G. Senjanovic, “Predictions of Supersymmetric Grand Unified Theories,” *Phys. Rev.* **D25** (1982) 3092.

[72] R. Dermisek, A. Mafi, and S. Raby, “SUSY GUTs under siege: Proton decay,” *Phys. Rev.* **D63** (2001) 035001, [hep-ph/0007213](#).

[73] H. Murayama and A. Pierce, “Not even decoupling can save minimal supersymmetric $SU(5)$,” *Phys. Rev.* **D65** (2002) 055009, [hep-ph/0108104](#).

[74] V. S. Kaplunovsky, “One Loop Threshold Effects in String Unification,” *Nucl. Phys.* **B307** (1988) 145, [hep-th/9205068](#).

[75] L. J. Dixon, V. Kaplunovsky, and J. Louis, “On Effective Field Theories Describing (2,2) Vacua of the Heterotic String,” *Nucl. Phys.* **B329** (1990) 27–82.

[76] L. J. Dixon, V. Kaplunovsky, and J. Louis, “Moduli dependence of string loop corrections to gauge coupling constants,” *Nucl. Phys.* **B355** (1991) 649–688.

[77] K. R. Dienes, “String Theory and the Path to Unification: A Review of Recent Developments,” *Phys. Rept.* **287** (1997) 447–525, [hep-th/9602045](#).

[78] J. D. Breit, B. A. Ovrut, and G. C. Segre, “E(6) Symmetry Breaking in the Superstring Theory,” *Phys. Lett.* **B158** (1985) 33.

[79] L. E. Ibanez, J. E. Kim, H. P. Nilles, and F. Quevedo, “Orbifold Compactifications with Three Families of $SU(3) \times SU(2) \times U(1)^{**n}$,” *Phys. Lett.* **B191** (1987) 282–286.

[80] L. E. Ibanez, H. P. Nilles, and F. Quevedo, “Orbifolds and Wilson Lines,” *Phys. Lett.* **B187** (1987) 25–32.

[81] L. E. Ibanez, H. P. Nilles, and F. Quevedo, “Reducing the Rank of the Gauge Group in Orbifold Compactifications of the Heterotic String,” *Phys. Lett.* **B192** (1987) 332.

[82] J. A. Casas and C. Munoz, “Three Generation $SU(3) \times SU(2) \times U(1)$ -Y Models from Orbifolds,” *Phys. Lett.* **B214** (1988) 63.

[83] J. A. Casas, E. K. Katehou, and C. Munoz, “ $U(1)$ Charges in Orbifolds: Anomaly Cancellation and Phenomenological Consequences,” *Nucl. Phys.* **B317** (1989) 171.

[84] Y. Kawamura, “Triplet-doublet splitting, proton stability and extra dimension,” *Prog. Theor. Phys.* **105** (2001) 999–1006, [hep-ph/0012125](#).

[85] L. J. Hall and Y. Nomura, “Gauge unification in higher dimensions,” *Phys. Rev.* **D64** (2001) 055003, [hep-ph/0103125](#).

[86] T. Asaka, W. Buchmuller, and L. Covi, “Gauge unification in six dimensions,” *Phys. Lett.* **B523** (2001) 199–204, hep-ph/0108021.

[87] R. Contino, L. Pilo, R. Rattazzi, and E. Trincherini, “Running and matching from 5 to 4 dimensions,” *Nucl. Phys.* **B622** (2002) 227–239, hep-ph/0108102.

[88] R. Dermisek and A. Mafi, “SO(10) grand unification in five dimensions: Proton decay and the mu problem,” *Phys. Rev.* **D65** (2002) 055002, hep-ph/0108139.

[89] L. J. Hall and Y. Nomura, “Grand unification in higher dimensions,” *Annals Phys.* **306** (2003) 132–156, hep-ph/0212134.

[90] H. D. Kim and S. Raby, “Unification in 5D SO(10),” *JHEP* **01** (2003) 056, hep-ph/0212348.

[91] H. M. Lee, “Gauge Coupling Unification in a 6D SO(10) Orbifold GUT,” *Phys. Lett.* **B643** (2006) 136–140, hep-ph/0609064.

[92] J. E. Kim and B. Kyae, “Kaluza-Klein masses in nonprime orbifolds: Z(12-I) compactification and threshold correction,” *Phys. Rev.* **D77** (2008) 106008, 0712.1596.

[93] L. J. Hall, Y. Nomura, and D. Tucker-Smith, “Gauge-Higgs unification in higher dimensions,” *Nucl. Phys.* **B639** (2002) 307–330, hep-ph/0107331.

[94] T. Kobayashi, H. P. Nilles, F. Ploger, S. Raby, and M. Ratz, “Stringy origin of non-Abelian discrete flavor symmetries,” *Nucl. Phys.* **B768** (2007) 135–156, hep-ph/0611020.

[95] P. Ko, T. Kobayashi, J.-h. Park, and S. Raby, “String-derived D4 flavor symmetry and phenomenological implications,” *Phys. Rev.* **D76** (2007) 035005, 0704.2807.

[96] E. Witten, “Some Properties of O(32) Superstrings,” *Phys. Lett.* **B149** (1984) 351–356.

[97] A. Sagnotti, “A Note on the Green-Schwarz mechanism in open string theories,” *Phys. Lett.* **B294** (1992) 196–203, hep-th/9210127.

[98] M. Berkooz *et al.*, “Anomalies, Dualities, and Topology of D=6 N=1 Superstring Vacua,” *Nucl. Phys.* **B475** (1996) 115–148, hep-th/9605184.

[99] L. E. Ibanez, D. Lust, and G. G. Ross, “Gauge coupling running in minimal $SU(3) \times SU(2) \times U(1)$ superstring unification,” *Phys. Lett.* **B272** (1991) 251–260, hep-th/9109053.

- [100] Ibañez, Luis E. and Lüst, Dieter, “Duality anomaly cancellation, minimal string unification and the effective low-energy Lagrangian of 4-D strings,” *Nucl. Phys.* **B382** (1992) 305–364, [hep-th/9202046](#).
- [101] A. Hebecker and M. Trapletti, “Gauge unification in highly anisotropic string compactifications,” *Nucl. Phys.* **B713** (2005) 173–203, [hep-th/0411131](#).
- [102] J. Perkins *et al.*, “Stringent Phenomenological Investigation into Heterotic String Optical Unification,” *Phys. Rev.* **D75** (2007) 026007, [hep-ph/0510141](#).
- [103] J. Giedt, “Optical unification,” *Mod. Phys. Lett.* **A18** (2003) 1625–1633, [hep-ph/0205224](#).
- [104] P. Horava and E. Witten, “Eleven-Dimensional Supergravity on a Manifold with Boundary,” *Nucl. Phys.* **B475** (1996) 94–114, [hep-th/9603142](#).
- [105] K. R. Dienes and A. E. Faraggi, “Making ends meet: String unification and low-energy data,” *Phys. Rev. Lett.* **75** (1995) 2646–2649, [hep-th/9505018](#).
- [106] K. R. Dienes and A. E. Faraggi, “Gauge coupling unification in realistic free fermionic string models,” *Nucl. Phys.* **B457** (1995) 409–483, [hep-th/9505046](#).
- [107] K. R. Dienes, A. E. Faraggi, and J. March-Russell, “String Unification, Higher Level Gauge Symmetries, and Exotic Hypercharge Normalizations,” *Nucl. Phys.* **B467** (1996) 44–99, [hep-th/9510223](#).
- [108] L. E. Ibanez, “Gauge coupling unification: Strings versus SUSY GUTs,” *Phys. Lett.* **B318** (1993) 73–76, [hep-ph/9308365](#).
- [109] P. Mayr, H. P. Nilles, and S. Stieberger, “String unification and threshold corrections,” *Phys. Lett.* **B317** (1993) 53–59, [hep-th/9307171](#).
- [110] A. Font, L. E. Ibanez, and F. Quevedo, “HIGHER LEVEL KAč-MOODY STRING MODELS AND THEIR PHENOMENOLOGICAL IMPLICATIONS,” *Nucl. Phys.* **B345** (1990) 389–430.
- [111] D. C. Lewellen, “Embedding Higher Level Kac-Moody Algebras in Heterotic String Models,” *Nucl. Phys.* **B337** (1990) 61.
- [112] S. Weinberg, “Effective Gauge Theories,” *Phys. Lett.* **B91** (1980) 51.
- [113] L. J. Hall, “Grand Unification of Effective Gauge Theories,” *Nucl. Phys.* **B178** (1981) 75.

- [114] D. R. T. Jones, “The Two Loop beta Function for a $G(1) \times G(2)$ Gauge Theory,” *Phys. Rev.* **D25** (1982) 581.
- [115] D. M. Ghilencea and S. Groot Nibbelink, “String corrections to gauge couplings from a field theory approach,” *Class. Quant. Grav.* **20** (2003) S495–S500, hep-ph/0212197.
- [116] O. Lebedev *et al.*, “Minilandscape tables.” Available publicly at www.th.physik.uni-bonn.de/nilles/Z6IIorbifold/.
- [117] M. Bershadsky *et al.*, “Geometric singularities and enhanced gauge symmetries,” *Nucl. Phys.* **B481** (1996) 215–252, hep-th/9605200.
- [118] G. G. Ross, “Wilson line breaking and gauge coupling unification,” hep-ph/0411057.
- [119] E. Witten, “Strong Coupling Expansion Of Calabi-Yau Compactification,” *Nucl. Phys.* **B471** (1996) 135–158, hep-th/9602070.
- [120] D. M. Ghilencea and S. Groot Nibbelink, “String threshold corrections from field theory,” *Nucl. Phys.* **B641** (2002) 35–60, hep-th/0204094.
- [121] S. R. Coleman and E. J. Weinberg, “Radiative Corrections as the Origin of Spontaneous Symmetry Breaking,” *Phys. Rev.* **D7** (1973) 1888–1910.
- [122] J. A. Casas, Z. Lalak, C. Munoz, and G. G. Ross, “Hierarchical Supersymmetry Breaking and Dynamical Determination of Compactification Parameters by Non-Perturbative Effects,” *Nucl. Phys.* **B347** (1990) 243–269.
- [123] B. de Carlos, J. A. Casas, and C. Munoz, “Supersymmetry breaking and determination of the unification gauge coupling constant in string theories,” *Nucl. Phys.* **B399** (1993) 623–653, hep-th/9204012.
- [124] N. V. Krasnikov, “On Supersymmetry Breaking in Superstring Theories,” *Phys. Lett.* **B193** (1987) 37–40.
- [125] A. Font, L. E. Ibanez, D. Lust, and F. Quevedo, “Supersymmetry Breaking from Duality Invariant Gaugino Condensation,” *Phys. Lett.* **B245** (1990) 401–408.
- [126] M. Cvetic, A. Font, L. E. Ibanez, D. Lust, and F. Quevedo, “Target space duality, supersymmetry breaking and the stability of classical string vacua,” *Nucl. Phys.* **B361** (1991) 194–232.
- [127] S. Kachru, R. Kallosh, A. Linde, and S. P. Trivedi, “De Sitter vacua in string theory,” *Phys. Rev.* **D68** (2003) 046005, hep-th/0301240.

- [128] M. Serone and A. Westphal, “Moduli Stabilization in Meta-Stable Heterotic Supergravity Vacua,” *JHEP* **08** (2007) 080, 0707.0497.
- [129] A. Westphal, “de Sitter String Vacua from Kahler Uplifting,” *JHEP* **03** (2007) 102, hep-th/0611332.
- [130] M. K. Gaillard and B. D. Nelson, “Kaehler stabilized, modular invariant heterotic string models,” *Int. J. Mod. Phys. A* **22** (2007) 1451, hep-th/0703227.
- [131] E. Dudas and Y. Mambrini, “Moduli stabilization with positive vacuum energy,” *JHEP* **10** (2006) 044, hep-th/0607077.
- [132] Z. Lalak, O. J. Eytom-Williams, and R. Matyszkiewicz, “F-term uplifting via consistent D-terms,” *JHEP* **05** (2007) 085, hep-th/0702026.
- [133] P. Binetruy and E. Dudas, “Gaugino condensation and the anomalous U(1),” *Phys. Lett.* **B389** (1996) 503–509, hep-th/9607172.
- [134] G. R. Dvali and A. Pomarol, “Anomalous U(1), gauge-mediated supersymmetry breaking and Higgs as pseudo-Goldstone bosons,” *Nucl. Phys.* **B522** (1998) 3–19, hep-ph/9708364.
- [135] Z. Lalak, “Anomalous D-term, dynamical supersymmetry breaking and dynamical gauge couplings,” *Nucl. Phys.* **B521** (1998) 37–57, hep-ph/9708410.
- [136] B. de Carlos, S. Gurrieri, A. Lukas, and A. Micu, “Moduli stabilisation in heterotic string compactifications,” *JHEP* **03** (2006) 005, hep-th/0507173.
- [137] K. Choi and K. S. Jeong, “Supersymmetry breaking and moduli stabilization with anomalous U(1) gauge symmetry,” *JHEP* **08** (2006) 007, hep-th/0605108.
- [138] E. Dudas, Y. Mambrini, S. Pokorski, and A. Romagnoni, “Moduli stabilization with Fayet-Iliopoulos uplift,” *JHEP* **04** (2008) 015, 0711.4934.
- [139] D. Gallego and M. Serone, “Moduli Stabilization in non-Supersymmetric Minkowski Vacua with Anomalous U(1) Symmetry,” *JHEP* **08** (2008) 025, 0807.0190.
- [140] E. Dudas, Y. Mambrini, S. Pokorski, A. Romagnoni, and M. Trapletti, “Gauge vs. Gravity mediation in models with anomalous U(1)’s,” *JHEP* **03** (2009) 011, 0809.5064.
- [141] K. R. Dienes and M. Lennek, “Fighting the floating correlations: Expectations and complications in extracting statistical correlations from the string theory landscape,” *Phys. Rev.* **D75** (2007) 026008, hep-th/0610319.

- [142] P. Fayet and J. Iliopoulos, “Spontaneously Broken Supergauge Symmetries and Goldstone Spinors,” *Phys. Lett.* **B51** (1974) 461–464.
- [143] J. J. Atick, L. J. Dixon, and A. Sen, “String Calculation of Fayet-Iliopoulos d Terms in Arbitrary Supersymmetric Compactifications,” *Nucl. Phys.* **B292** (1987) 109–149.
- [144] M. Dine, I. Ichinose, and N. Seiberg, “F Terms and d Terms in String Theory,” *Nucl. Phys.* **B293** (1987) 253.
- [145] E. Witten, “Dimensional Reduction of Superstring Models,” *Phys. Lett.* **B155** (1985) 151.
- [146] S. Ferrara, C. Kounnas, and M. Petraki, “General Dimensional Reduction of Ten-Dimensional Supergravity and Superstring,” *Phys. Lett.* **B181** (1986) 263.
- [147] M. Cvetic, J. Louis, and B. A. Ovrut, “A String Calculation of the Kahler Potentials for Moduli of Z(N) Orbifolds,” *Phys. Lett.* **B206** (1988) 227.
- [148] A. D. Shapere and F. Wilczek, “Selfdual Models with Theta Terms,” *Nucl. Phys.* **B320** (1989) 669.
- [149] S. Ferrara, D. Lust, A. D. Shapere, and S. Theisen, “Modular Invariance in Supersymmetric Field Theories,” *Phys. Lett.* **B225** (1989) 363.
- [150] J. Lauer, J. Mas, and H. P. Nilles, “DUALITY AND THE ROLE OF NONPERTURBATIVE EFFECTS ON THE WORLD SHEET,” *Phys. Lett.* **B226** (1989) 251.
- [151] E. J. Chun, J. Mas, J. Lauer, and H. P. Nilles, “DUALITY AND LANDAU-GINZBURG MODELS,” *Phys. Lett.* **B233** (1989) 141.
- [152] S. Ferrara, . D. Lust, and S. Theisen, “Target Space Modular Invariance and Low-Energy Couplings in Orbifold Compactifications,” *Phys. Lett.* **B233** (1989) 147.
- [153] J. Lauer, J. Mas, and H. P. Nilles, “Twisted sector representations of discrete background symmetries for two-dimensional orbifolds,” *Nucl. Phys.* **B351** (1991) 353–424.
- [154] J. Erler, D. Jungnickel, and H. P. Nilles, “Space duality and quantized Wilson lines,” *Phys. Lett.* **B276** (1992) 303–310.
- [155] J. Erler, D. Jungnickel, J. Lauer, and J. Mas, “String emission from twisted sectors: cocycle operators and modular background symmetries,” *Ann. Phys.* **217** (1992) 318–363.

[156] S. Stieberger, D. Jungnickel, J. Lauer, and M. Spalinski, “Yukawa couplings for bosonic $Z(N)$ orbifolds: Their moduli and twisted sector dependence,” *Mod. Phys. Lett.* **A7** (1992) 3059–3070, [hep-th/9204037](#).

[157] D. Bailin and A. Love, “Orbifold compactifications of string theory,” *Phys. Rept.* **315** (1999) 285–408.

[158] S. Hamidi and C. Vafa, “Interactions on Orbifolds,” *Nucl. Phys.* **B279** (1987) 465.

[159] J. A. Casas, F. Gomez, and C. Munoz, “Complete structure of $Z(n)$ Yukawa couplings,” *Int. J. Mod. Phys.* **A8** (1993) 455–506, [hep-th/9110060](#).

[160] J. Erler, D. Jungnickel, M. Spalinski, and S. Stieberger, “Higher twisted sector couplings of $Z(N)$ orbifolds,” *Nucl. Phys.* **B397** (1993) 379–416, [hep-th/9207049](#).

[161] A. Love and S. Todd, “Modular symmetries of threshold corrections for Abelian orbifolds with discrete Wilson lines,” *Nucl. Phys.* **B481** (1996) 253–288, [hep-th/9606161](#).

[162] D. Bailin, A. Love, W. A. Sabra, and S. Thomas, “Anisotropic solutions for orbifold moduli from duality invariant gaugino condensates,” *Mod. Phys. Lett.* **A9** (1994) 2543–2555, [hep-th/9405031](#).

[163] J. P. Derendinger, S. Ferrara, C. Kounnas, and F. Zwirner, “On loop corrections to string effective field theories: Field dependent gauge couplings and sigma model anomalies,” *Nucl. Phys.* **B372** (1992) 145–188.

[164] D. Lust and C. Munoz, “Duality invariant gaugino condensation and one loop corrected Kahler potentials in string theory,” *Phys. Lett.* **B279** (1992) 272–280, [hep-th/9201047](#).

[165] V. Kaplunovsky and J. Louis, “On gauge couplings in string theory,” *Nucl. Phys.* **B444** (1995) 191–244, [hep-th/9502077](#).

[166] B. de Carlos, J. A. Casas, and C. Munoz, “Massive hidden matter and gaugino condensation,” *Phys. Lett.* **B263** (1991) 248–254.

[167] I. Affleck, M. Dine, and N. Seiberg, “Dynamical Supersymmetry Breaking in Supersymmetric QCD,” *Nucl. Phys.* **B241** (1984) 493–534.

[168] S. Ferrara, N. Magnoli, T. R. Taylor, and G. Veneziano, “Duality and supersymmetry breaking in string theory,” *Phys. Lett.* **B245** (1990) 409–416.

[169] H. P. Nilles and M. Olechowski, “Gaugino Condensation and Duality Invariance,” *Phys. Lett.* **B248** (1990) 268–272.

- [170] R. Kappl *et al.*, “Large hierarchies from approximate R symmetries,” 0812.2120.
- [171] S. Ferrara, C. Kounnas, and F. Zwirner, “Mass formulae and natural hierarchy in string effective supergravities,” *Nucl. Phys.* **B429** (1994) 589–625, hep-th/9405188.
- [172] H. P. Nilles and S. Raby, “SUPERSYMMETRY AND THE STRONG CP PROBLEM,” *Nucl. Phys.* **B198** (1982) 102.
- [173] K.-S. Choi, H. P. Nilles, S. Ramos-Sanchez, and P. K. S. Vaudrevange, “Actions,” *Phys. Lett.* **B675** (2009) 381, 0902.3070.
- [174] G. R. Dvali and A. Pomarol, “Anomalous U(1) as a mediator of supersymmetry breaking,” *Phys. Rev. Lett.* **77** (1996) 3728–3731, hep-ph/9607383.
- [175] A. Brignole, L. E. Ibanez, and C. Munoz, “Towards a theory of soft terms for the supersymmetric Standard Model,” *Nucl. Phys.* **B422** (1994) 125–171, hep-ph/9308271.
- [176] A. Brignole, L. E. Ibanez, C. Munoz, and C. Scheich, “Some issues in soft SUSY breaking terms from dilaton / moduli sectors,” *Z. Phys.* **C74** (1997) 157–170, hep-ph/9508258.
- [177] Y. Kawamura and T. Kobayashi, “Soft Scalar Masses in String Models with Anomalous $U(1)$ symmetry,” *Phys. Lett.* **B375** (1996) 141–148, hep-ph/9601365.
- [178] Y. Kawamura and T. Kobayashi, “Generic formula of soft scalar masses in string models,” *Phys. Rev.* **D56** (1997) 3844–3859, hep-ph/9608233.
- [179] A. Brignole, L. E. Ibanez, and C. Munoz, “Soft supersymmetry-breaking terms from supergravity and superstring models,” hep-ph/9707209.
- [180] G. F. Giudice and A. Masiero, “A Natural Solution to the mu Problem in Supergravity Theories,” *Phys. Lett.* **B206** (1988) 480–484.
- [181] J. E. Kim and H. P. Nilles, “The mu Problem and the Strong CP Problem,” *Phys. Lett.* **B138** (1984) 150.
- [182] J. E. Kim and H. P. Nilles, “Symmetry principles toward solutions of the mu problem,” *Mod. Phys. Lett.* **A9** (1994) 3575–3584, hep-ph/9406296.
- [183] P. Binetruy, M. K. Gaillard, and B. D. Nelson, “One loop soft supersymmetry breaking terms in superstring effective theories,” *Nucl. Phys.* **B604** (2001) 32–74, hep-ph/0011081.

[184] P. Binetruy, A. Birkedal-Hansen, Y. Mambrini, and B. D. Nelson, “Phenomenological aspects of heterotic orbifold models at one loop,” *Eur. Phys. J.* **C47** (2006) 481–505, [hep-ph/0308047](#).

[185] Y. Kawamura, “On Low-Energy Theory from General Supergravity,” *Prog. Theor. Phys. Suppl.* **123** (1996) 421–430, [hep-ph/9511334](#).

[186] B. C. Allanach, “SOFTSUSY: A C++ program for calculating supersymmetric spectra,” *Comput. Phys. Commun.* **143** (2002) 305–331, [hep-ph/0104145](#).

[187] **Tevatron Electroweak Working Group** Collaboration, “Combination of CDF and D0 Results on the Mass of the Top Quark,” [0903.2503](#).

[188] G. Belanger, F. Boudjema, A. Pukhov, and A. Semenov, “Dark matter direct detection rate in a generic model with micrOMEGAs2.1,” *Comput. Phys. Commun.* **180** (2009) 747–767, [0803.2360](#).

[189] K. Rajagopal, M. S. Turner, and F. Wilczek, “Cosmological implications of axinos,” *Nucl. Phys.* **B358** (1991) 447–470.

[190] L. Covi, J. E. Kim, and L. Roszkowski, “Axinos as cold dark matter,” *Phys. Rev. Lett.* **82** (1999) 4180–4183, [hep-ph/9905212](#).

[191] L. Covi, H.-B. Kim, J. E. Kim, and L. Roszkowski, “Axinos as dark matter,” *JHEP* **05** (2001) 033, [hep-ph/0101009](#).

[192] B. S. Acharya *et al.*, “Non-thermal Dark Matter and the Moduli Problem in String Frameworks,” *JHEP* **06** (2008) 064, [0804.0863](#).

[193] O. Lebedev, H. P. Nilles, S. Ramos-Sanchez, M. Ratz, and P. K. S. Vaudrevange, “Heterotic mini-landscape (II): completing the search for MSSM vacua in a \mathbb{Z}_6 orbifold,” *Phys. Lett.* **B668** (2008) 331–335, [0807.4384](#).

[194] M. Endo, K. Hamaguchi, and F. Takahashi, “Moduli-induced gravitino problem,” *Phys. Rev. Lett.* **96** (2006) 211301, [hep-ph/0602061](#).

[195] S. Nakamura and M. Yamaguchi, “Gravitino production from heavy moduli decay and cosmological moduli problem revived,” *Phys. Lett.* **B638** (2006) 389–395, [hep-ph/0602081](#).

[196] A. Wingerter, *Aspects of Grand Unification in Higher Dimensions*. PhD thesis, Universität Bonn, 2005.
<http://www.th.physik.uni-bonn.de/nilles/db/thesis/>.

- [197] T. M. Apostol, *Modular functions and Dirichlet series in number theory*. Springer-Verlag, New York, 1976.
- [198] R. Dermisek, H. D. Kim, and I.-W. Kim, “Mediation of supersymmetry breaking in gauge messenger models,” *JHEP* **10** (2006) 001, hep-ph/0607169.
- [199] R. Dermisek and H. D. Kim, “Radiatively generated maximal mixing scenario for the Higgs mass and the least fine tuned minimal supersymmetric standard model,” *Phys. Rev. Lett.* **96** (2006) 211803, hep-ph/0601036.
- [200] J. Hisano, “Proton decay in the supersymmetric grand unified models,” hep-ph/0004266.
- [201] Y. Aoki, C. Dawson, J. Noaki, and A. Soni, “Proton decay matrix elements with domain-wall fermions,” *Phys. Rev.* **D75** (2007) 014507, hep-lat/0607002.
- [202] M. L. Alciati, F. Feruglio, Y. Lin, and A. Varagnolo, “Proton lifetime from SU(5) unification in extra dimensions,” *JHEP* **03** (2005) 054, hep-ph/0501086.
- [203] G. Cleaver, M. Cvetic, J. R. Espinosa, L. L. Everett, and P. Langacker, “Classification of flat directions in perturbative heterotic superstring vacua with anomalous U(1),” *Nucl. Phys.* **B525** (1998) 3–26, hep-th/9711178.
- [204] J. Wess and J. Bagger, *Supersymmetry and Supergravity*. Princeton University Press, Princeton, NJ, second ed., 1992.
- [205] M. A. Luty and W. Taylor, “Varieties of vacua in classical supersymmetric gauge theories,” *Phys. Rev.* **D53** (1996) 3399–3405, hep-th/9506098.
- [206] W. Buchmuller, C. Ludeling, and J. Schmidt, “Local SU(5) Unification from the Heterotic String,” *JHEP* **09** (2007) 113, 0707.1651.